MODULATION OF THE NF-KAPPA B SIGNALING PATHWAY BY THE BACTERIAL TYPE III SECRETION SYSTEM EFFECTORS

By

Xiaofei Gao

Submitted to the graduate degree program in Microbiology, Molecular Genetics and Immunology and the Graduate Faculty of the University of Kansas in partial fulfillment of the requirements for the degree of Doctor of Philosophy.

Dissertation Committee:

_____

Philip R. Hardwidge, Ph.D., Chairperson

_____

Indranil Biswas, Ph.D.

_____

Grace Guo, Ph.D.

_____

Joe Lutkenhaus, Ph.D.

_____

Thomas Yankee, Pharm. D., Ph.D.

Date Defended: 05-14-2012

The Dissertation Committee for Xiaofei Gao

certifies that this is the approved version of the following dissertation:

MODULATION OF THE NF-KAPPA B SIGNALING PATHWAY BY THE BACTERIAL TYPE III SECRETION SYSTEM EFFECTORS

_____

Philip R. Hardwidge, Ph.D., Chairperson

Date approved: 05-14-2012

Abstract

The type III secretion system (T3SS) is a bacterial injection system expressed by many Gram-negative bacteria. During the last two decades, the repertoire of T3SS effectors has been greatly explored, and several mechanisms of these effectors have been discovered. The identified host targets of T3SS effectors are involved in different biological events including cytoskeleton rearrangement, cellular signaling, transcription and protein degradation. A/E (attaching and effacing) pathogens including EHEC (Enterohaemorrhaigic *E. coli*), EPEC (Enteropathogenic *E. coli*) and *C. rodentium* (*Citrobacter rodentium*), a pathogen of mice, inhibit NF-κB transcriptional activity by employing unidentified T3SS effectors. However, the identity of these effector(s) was unknown. In this thesis, my goals were to identify T3SS effectors from attaching and effacing (A/E) pathogens responsible for modulating NF-κB activation and reveal the working mechanism of these identified effectors.

In the first project, NleH1 and NleH2, which share C-termini similarity with the *S. flexneri* T3SS effector OspG, were studied. OspG targets ubiquitin-conjugating enzyme UbcH5 to prevent IκBα degredation, which results in the inhibition of NF-κB activation. We discovered that both NleH1 and NleH2 interact with the N-terminus of ribosomal protein S3 (RPS3) after their translocation into host cells. RPS3 is a non-Rel NF-κB subunit which promotes the DNA binding affinity of NF-κB. We found that NleH1, but not NleH2, blocks the nuclear translocation of RPS3 stimulated by TNF and by bacterial infection. By this process, NleH1 selectively attenuates RPS3-mediated NF-κB dependent gene transcription. In addition, we discovered NleH proteins as Ser/Thr kinases and that kinase activity is critical for the effect of NleH1 on RPS3.

By collaborating with Dr. Lenardo's group in National Institute of Allergy and Infectious Diseases (NIAID), we discovered that RPS3 is inducibly associated with and phosphorylated by IKKβ at serine 209 (S209) and that NleH1 efficiently blocks this phosphorylation. Moreover, by using a gnotobiotic pig model, we found piglets infected with wild-type *E. coli* O157:H7 exhibits diffuse and low intensity phospho-RPS3 staining. Surprisingly, although infection by *ΔnleH1* EHEC causes mild diarrhea and displays significantly reduced bacterial colonization in piglets, this mutant becomes hypervirulent to the host, as infected piglets die more rapidly and develop systemic intoxication compared to infection with the wild-type strain. Therefore, our data suggests a complex role for NleH1 in mediating bacterial virulence in the host to maximize bacterial survival and growth.

In the second project, we identified NleB, another T3SS effector known to target NF-κB activation, as an O-GlcNAc (O-linked N-acetylglucosamine) transferase. We found NleB directly interacts with host glycolytic protein GAPDH (Glyceraldehyde 3-phosphate dehydrogenase) and O-GlcNAcylates GAPDH during infection. GAPDH has many nonglycolytic roles and is involved in a broad range of biological events, such as transcription, cell signaling, membrane integrity and cell survivial. In our study, we demonstrated an essential role for GAPDH in NF-κB activation. We found that GAPDH serves as a co-activator of TRAF2 (TNF receptor-associated factor 2) and promotes TRAF2 polyubiquitination under stress conditions. Targeting the catalytic site C150 of GAPDH by a chemical inhibitor or by site-directed mutagenesis specifically impairs TNF-induced TRAF2 polyubiquitination and NF-κB activation. This function is unrelated to glycolysis, as targeting the rate-limiting glycolytic enzymes does not imipair TRAF2 activation and only leads to a moderate inhibition on NF-κB activation, which is likely due to an unrelated mechanism. Moreover, O-GlcNAcylated GAPDH

fails to interact with TRAF2 resulting in the attenuation of TRAF2 polyubiquitination. Eliminating the O-GlcNAc transferase activity of NleB by mutating its catalytic sites or by deleting the nucleotide sugar-binding domain abolishes the effect of NleB on NF-κB activation and reduces bacteria colonization of mice. Taken together, our studies suggest an integral role of the metabolic protein GAPDH in the NF-κB signaling pathway and that the T3SS effector NleB O-GlcNAcylates GAPDH to prevent the participation of GAPDH in NF-κB signaling.

ACKNOWLEDGEMENTS

Foremost, I am deeply grateful to my mentor Dr. Philip Hardwidge for his patience, continuous support and guidance of my research these years. His knowledge and his logical way of thinking are invaluable for my studies. I also want to thank him for continuously encouraging me and pushing me to my limits to complete this thesis.

I also want to take this opportunity to thank the previous and current members in Hardwidge lab for their help. I especially thank Dr. Leigh Ann Feuerbacher, Dr. Thanh Pham and Dr. Xiaogang Wang for those days and nights we were working together. I also thank Dr. Michael Lenardo from National Institute of Allergy and Infectious Diseases and Dr. Fengyi Wan from Johns Hopkins for their help and very insightful suggestions.

I thank Drs. Indranil Biswas, Grace Guo, Joe Lutkenhaus and Thomas Yankee for serving on my thesis committee and their valuable advices.

Lastly, I want to acknowledge my parents and my wife for their support and encouragement throughout my studies.

Table of Contents

List of Figures

List of Tables

Abbreviations

A/E: Attaching and effacing

ATEC: Atypical enteropathogenic *E. coli*

ATPase: Adenosine triphosphatase

BI-1*:* Bax inhibitor-1

Esc*: E.coli* secretion complex

EAEC: Enteroaggregative *E. coli*

EHEC: Enterohaemorrhaigic *E. coli*

EIEC: Enteroinvasive *E. coli*

EPEC: Enteropathogenic *E. coli*

ETEC: Enterotoxigenic *E. coli*

Esp: *E.coli* secreted protein

C. rodentium: *Citrobacter rodentium*

DAEC: Diffusely adhering *E. coli*

GAPDH : Glyceraldehyde 3-phosphate dehydrogenase

HUS: Haemolytic uremic syndrome

IFN: Interferon

IκB: Inhibitor of NF-kappaB

IKK: Inhibitor of NF-kappaB kinase

IL: Interleukin

JNK: c-Jun N-terminal kinases

LEE: Locus of enterocyte effacement

LPS: Liposaccharides

Map: Mitochondrial associated proteins

MAPK: Mitogen-activated protein kinase

MyD88: Myeloid differentiation primary response 88

Nck: Non-catalytic region of tyrosine kinase

NEMO: NF-kappa-B essential modulator

NF-κB: Nuclear factor-kappaB

NLS: Nuclear localization signal

Nle: Non-LEE-encoded effectors

O-GlcNAc: O-linked N-acetylglucosamine

OspG: Outer *Shigella* protein G

PAMPs: Pathogen associated molecular patterns

PRRs: Pattern recognition receptors

PI: Phosphoinositide

RING: Really Interesting New Gene

RPS3: Ribosomal protein subunit 3

Stx: Shiga toxins

TAK1: Transforming growth factor-activated protein kinase 1

Tir: Translocated Intimin Receptor

TLRs: Toll-like receptors

TRADD: TNF receptor-associated death domain

TRAF: TNF receptor-associated factor

TNF: Tumor necrosis factor

TRIF: TIR domain-containing adaptor gene inducing IFN-β

T3SS: Type III secretion system

UPEC: uropathogenic *E. coli*

VirA: Virulence gene A

YopJ: *Yersinia* outer protein J

NMEC: Neonatal meningitis/sepsis-causing *E.coli*

Chapter I: Introduction

Attaching and Effacing *Escherichia coli*

Escherichia coli (*E.coli*) is one of the most studied microorganism. It has been used as a model organism for a variety of biological purposes. Recent studies showed that *E. coli* is an extremely versatile organism with high genome plasticity (Hacker et al., 1997). Studies in *E.coli* K12 strains demonstrated that bacterial genome contains mobile genetic elements such as phages, transposons and plasmids (Blattner et al., 1997). These elements are responsible for acquisition or loss of pathogenicity islands and have diverse pathogenic consequences. Therefore, pathogenic *E. coli* is believed to have evolved from non-pathogenic strains by horizontal DNA transfer among different bacterial strains.

Non-pathogenic *E.coli* includes bacterial strains such as commensal *E.coli* in gut flora and engineered strains used in the laboratories or industries. Pathogenic *E.coli* strains are those causing certain diseases such as diarrhea, meningitis, sepsis or urinary tract infection (Yamamoto et al., 1990). Pathogenic *E. coli* are catagorized by serogroups (O antigens) or serotypes (O or H antigens). Recently, some strains have also been profiled by virulence factors contributing to specific types of diseases (Pupo et al., 1997). Currently, there are at least nine types of pathogenic *E.coli* identified including uropathogenic (UPEC) or neonatal meningitis/sepsis-causing *E.coli* (NMEC). The other seven are enteropathogenic *E. coli* (EPEC), enterohaemorrhaigic *E. coli* (EHEC), enterotoxigenic *E. coli* (ETEC), enteroinvasive *E. coli* (EIEC), enteroaggregative *E. coli* (EAEC), atypical enteropathogenic *E. coli* (aEPEC or ATEC) and diffusely adhering *E. coli* (DAEC), which are all intestinal pathogens and cause diarrhea (Kaper et al., 2004).

Recent studies have defined a group of pathogenic *E.coli* strains as Attaching and Effacing (A/E) *Escherichia coli*, including the human pathogens EPEC, shiga-producing *E.coli* strains such as EHEC, and the mouse-specific strain *Citrobacter rodentium* (*C. rodentium*) (Mundy et al., 2005; Schmidt, 2010). This group of bacteria induces signal transduction pathways leading to the rearrangement of cytoskeleton and causes A/E lesions (Kodama, 2002). A/E lesions result from localized intestinal microvilli destruction and the subsequent formation of a pedestal-like projection in the gut mucosa of human and animal hosts (Schmidt, 2010) . A/E lesions normally contain cytoskeletal components from host cells such as actin, ezrin, myosin light chain and molecules associated with polymerized actin structures (Fig. 1) (Finlay et al., 1992; Yuhan et al., 1997). This pedestal-like projection pushes bacteria slightly above the cell's surface (Fig. 1). All factors from bacteria contributing to the formation of A/E lesion are found in the pathogenic island locus of enterocyte effacement (LEE), which encodes over 20 proteins including type III secretion system (T3SS) proteins, intimin, gene regulators and chaperons (Tobe et al., 1999). As most A/E strains are extracellular bacteria, they often subvert host intracellular signaling cascades to facilitate their survival in the host.

Similar strategies are employed by EPEC and EHEC to colonize the host, although the pathogenical consequences are variable. EPEC were first isolated in 1940 and experimentally demonstrated as intestinal pathogens in 1978 by using EPEC O127:H6 strain E2348/69 (Spears et al., 2006). EHEC were isolated from individual patients in 1982. Since then, EHEC have emerged as a global health threat. The main sources of EPEC and EHEC transmission are food, dairy products, animal contact and water (Kaper et al., 2004). EPEC cause diarrhea and

Fig. 1. A/E pathogens induce cytoskeleton rearrangement to form pedestal-like projection. A: steps of EPEC adherence. 1. Initial adhesion; 2. Translocation of bacterial proteins by T3SS; 3. Pedestal formation.

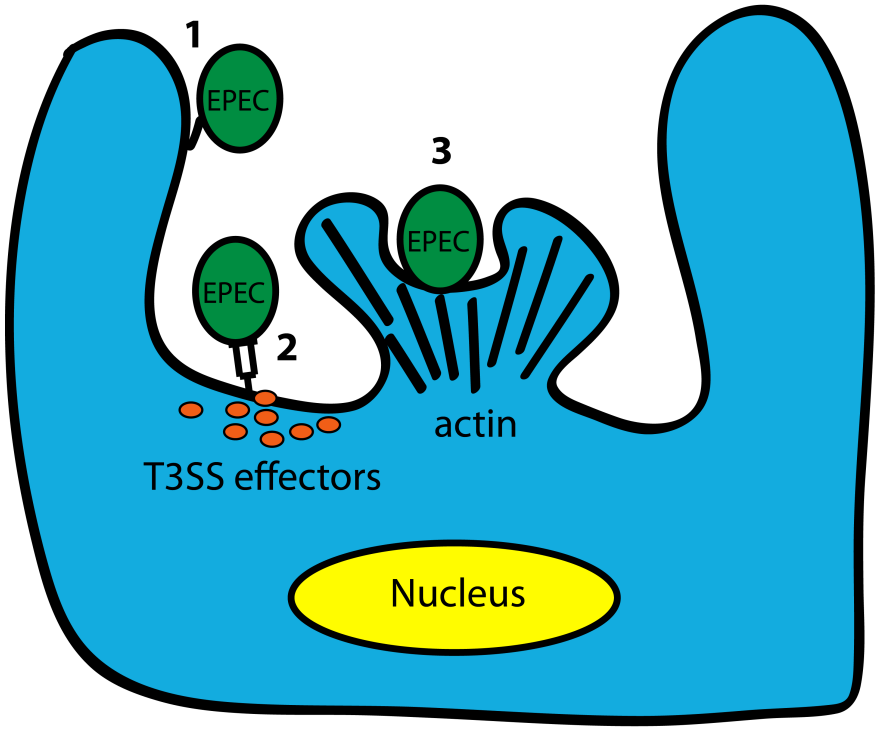
1
EPEC
3
EPEC
EPEC
2
actin
T3SS effectors
Nucleus

gastroenteritis in infants in developing countries, whereas the infection of EHEC results in the development of bloody diarrhea and diarrhea-associated haemolytic uraemic syndrome (HUS). EPEC and EHEC are typical bacteria inducing A/E lesions in concert with pedestal formation. The colonization factors from these two strains include adhesins, flagella and T3SS. However, EPEC may encode more types of fimbrial adhesins compared to EHEC (Johnson and Nolan, 2009). Many EPEC strains contain a plasmid called *E. coli* adherence factor (EAF), which has an operon encoding the type IV bundle-forming pilus (BFP) (Stone et al., 1996). BFP, which is regulated by a transcriptional activator called plasmid encoded regulator (Per), is important for EPEC binding to the host cells. BFP may not be important for initial bacterial binding to host cells, but rather for the interaction between bacteria. It has been found BFP is important for the formation of bacterial aggregates at the late stage of infection (Hicks et al., 1998). The functional BFP is critical for EPEC virulence as a mutation in the *bfpF* gene severely impairs EPEC's abilities to cause diarrhea *in vivo* (Bieber et al., 1998). In contrast, EHEC do not carry the EAF plasmid and do not express Bfp. However, EHEC have two fimbriae operons *lpf* and *lpfA*, which are similar with the long polar fimbriae (LPF) of *Salmonella* but not found in EPEC (Baumler et al., 1996).

The type of EHEC is usually defined by their O (LPS, Liposaccharides) and H (flagella) antigens. After gastrointestinal infection with EHEC, patients develop HUS and thrombotic thrombocytopenic purpura (TTP) (Karmali, 1989). HUS, characterized by microvascular thrombi and swollen endothelial cells, is caused by Shiga toxins (Stx) (O'Brien et al., 1992). Therefore, EHEC are also called Stx-producing *E.coli*. In EHEC O157 strains, they are two different Shiga toxins, Stx1 and Stx2. Shiga toxins are A_1B_5 toxins, consisting of a 32 kDa catalytic A subunit and five 7.7 kDa binding B subunits (Ling et al., 1998). Stx B subunits bind with their receptor

glycosphingolipid globotriaosylceramid (Gb3) on the surface of host cells. Gb3 is expressed more abundantly on glomerular endothelial cells and tubular epithelial cells in human kidney than other types of cells (Meyers and Kaplan, 2000). The expression level of Gb3 varies in cells, which might contribute to their different susceptibility to Stx (Louise and Obrig, 1991). Once Stx is internalized by clathrin-dependent endocytosis, the toxins are transported to the endoplasmic reticulum (ER) and Golgi apparatus (Sandvig et al., 1992). In the cytoplasm, the Stx A subunit specifically targets 28S eukaryotic rRNA by its N-glycosidase activity and inhibits protein synthesis in host cells (Saxena et al., 1989). This leads to a ribotoxic-stress response, which can cause intestinal and endothelial cell apoptosis and death. The cell death will in turn induce inflammation and leads to severe tissue damage in the host.

Different serotypes of EHEC also contain a highly conserved protein named hemolysin (Brunder et al., 1999). Although the role of hemolysin in pathogenesis is not entirely clear, studies suggest hemolysin can facilitate bacterial growth in the gut by promoting iron metabolism (Law and Kelly, 1995). Of note, the homolog of EHEC hemolysin is the RTX (repeats in the structural toxin) family of pore-forming toxins, which are widely present in Gram-negative bacteria (Schmidt et al., 1995; Welch, 1991).

C. rodentium is a mouse pathogen inducing A/E lesion formation during infection (Mundy et al., 2005). *C. rodentium* infects the lumen of the intestine and results in the colonic hyperplasia. *C. rodentium* encodes similar genes as EPEC and EHEC inducing A/E lesions such as LEE pathogenicity island (Garmendia et al., 2005). The entire life cycle of *C.rodentium* in the host is around 21-28 days post infection (pi) followed by host-mediated clearance. The mechanism of this clearance is not well understood; however, it is related to the host adaptive immunity (Vallance et al., 2002). The pathogenesis of *C. rodentium* in different genetic background of

mice varies significantly (Mundy et al., 2005). While C3H/HeJ strain shows high colonic hyperplasia and high mortality, some other strains such as C57BL/6, NIH Swiss and Balb/c strains generally show limited or no mortality (Mundy et al., 2005). The convenience of manipulating both bacteria and host make *C.rodentium* an excellent model for studying the interaction between A/E pathogens and host.

Type III Secretion System

Since its discovery in the early of 1990s, T3SS has been found to be widely present in Gram-negative pathogens (Rosqvist et al., 1994). T3SS is a molecular syringe, which secretes effector proteins from the bacterial cytoplasm into host cells (Erhardt et al., 2010). All A/E pathogens contain T3SS, which is important for the pathogenicity (Schmidt, 2010). According to studies completed in *Salmonella*, the overall structure of T3SS apparatus is similar to the bacterial flagellum (Fig. 2) (Cornelis, 2006; Tampakaki et al., 2004). The basal structure of T3SS apparatus consists of a pair of pentameric rings on both the inner and outer membranes of bacteria composed of over twenty proteins (Cornelis, 2006). The extracellular portion of T3SS apparatus is a needle-like structure and the length varies in different bacterial families (Cornelis, 2006). There are tip proteins at the top of T3SS needle responsible for forming a pore in eukaryotic cell membranes, which allows T3SS effectors to be delivered into the host cells (Kimbrough and Miller, 2002).

The repertoire of T3SS effectors has been greatly expanded in the past two decades. In A/E pathogens, it is clear that the T3SS and several effectors are encoded on a pathogenicity island termed the 'locus of enterocyte effacement' (LEE), whose genomic structure, function, and regulation are well conserved among all the characterized A/E pathogens (McDaniel et al., 1995). In addition, over 20 other secreted proteins (non-LEE-encoded effectors; Nles) encoded

by genes in multiple pathogenicity islands located throughout the EHEC genome have also been described (Deng et al., 2004). A bioinformatics study recently employed homology searches against other bacterial effectors to identify 39 secreted/translocated effectors encoded in the EHEC Sakai genome (Tobe et al., 2006). In addition, several studies have reported the importance of Nles to virulence (Wong et al., 2011).

Translocators

In EPEC and EHEC, the LEE island encodes over 40 proteins important for the T3SS secretion system such as Esp (*E.coli* secreted protein) A, EspB and EspD proteins; effectors such as EspF, EspG, EspH and Map (Mitochondrial associated proteins); a bacterial outer membrane adhesin known as intimin and its receptor Tir (Translocated Intimin Receptor); regulatory proteins Ler (LEE-encoded regulator) and GrlA/GrlR (Wong et al., 2011). EspA, a highly secreted protein with a molecular weight of 25 KD, is a major structural component of T3SS needle complex (Kenny et al., 1996). EspA is a homopolymer and can form sheath-like filaments, which directly interact with the needle-forming protein EscF directly (Daniell et al., 2001; Sekiya et al., 2001). Remarkably, the architecture of EspA filaments are almost identical with *Salmonella* flagellar filaments (Daniell et al., 2001). Although highly secreted, EspA is not detected in host cells (Kenny et al., 1997). Therefore, EspA filaments provide a molecular link between the bacteria and the host cell. Mutation in the *espA* gene impairs T3SS and renders bacteria avirulent in vivo (Abe et al., 1998).

EspB as well as EspD are both T3SS translocator proteins that induce A/E lesion formation during infection (Lai et al., 1997; Taylor et al., 1998). Neither of them is a component of EspA filaments (Knutton et al., 1998). EspB localizes between the cell membrane and cytoplasm of host

Fig. 2: EPEC type III secretion apparatus. The apparatus includes inner and outer membrane rings, a connector form by *E.coli* secretion complex (Esc) proteins, an EspA-formed filamentous tube and pores on host cell membranes formed by EspB and EspD. Tir is inserted into host membrane, where it will interact with bacterial outer membrane protein intimin. Type III effectors are translocated into cytoplasm through the apparatus.

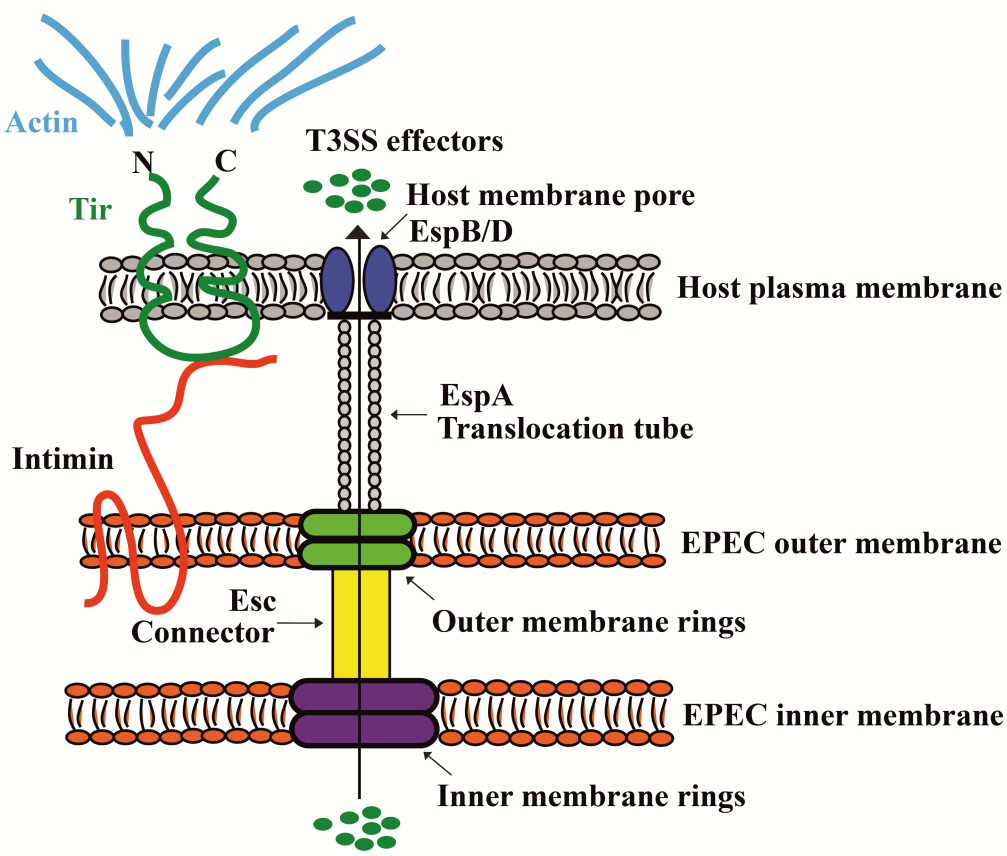
Actin
T3SS effectors
N
C
Tir
Host membrane pore
EspB/D
Host plasma membrane
EspA
Translocation tube
Intimin
EPEC outer membrane
Esc
Connector
Outer membrane rings
EPEC inner membrane
Inner membrane rings

cells (Knutton et al., 1998). The function of EspB has been demonstrated in different studies, although mechanisms are still not clear. Overexpression of EspB in HeLa cells disrupts filamentous actin distribution (Taylor et al., 1998). In addition, EspB is involved in forming a pore in the host membrane to support delivery of other T3SS effectors (Kenny and Finlay, 1995). EspB is critical for A/E pathogen pathogenesis, as deletion of the *espB* gene eliminates their ability to form A/E lesions and cause diseases (Abe et al., 1998). Unlike EspB, EspD is secreted into the extracellular milieu and is inserted into host cell membrane but is not found in the host cytoplasm (Wachter et al., 1999). Recently, EspD was demonstrated to be a homodimer and also forms a pore on host membrane (Dasanayake et al., 2011). Although a detailed mechanism of EspD is not clear, EspD is essential for A/E lesion formation on intestinal cells (Lai et al., 1997).

EscN is known to function as a T3SS ATPase with chaperones to release their secretion substrate (Akeda and Galan, 2005). Structure analysis showed that EscN shares a structural homology with the α/β-subunit of F_1-ATPase (Zarivach et al., 2007). Deletion of *escN* from bacteria results in hypersecretion of T3SS effectors (Deng et al., 2004).

Adherence and cytoskeleton rearrangement

The intimate adherence of A/E pathogens is mediated by the outer membrane adhesin knon as intimin (Jerse et al., 1990). Intimin is encoded by the *eae* gene in the LEE island (Jerse et al., 1990). Mutation or deletion of intimin in A/E pathogenic strains significantly reduces A/E pathogen adherence ability, induces immature A/E lesion formation and attenuates bacterial virulence in both human and animal models (Dean-Nystrom et al., 1998; Donnenberg et al., 1993; McKee and O'Brien, 1995). Intimin interacts with T3SS effector Tir, which localizes on the tip of the A/E lesion and links the bacteria and host cells together (Kenny et al., 1997). Before translocating into the host cell, Tir is an unphosphorylated protein with a molecular weight of 78

kD. However, once inserted into the host membrane, Tir becomes tyrosine phosphorylated and its molecule weight shifts to 90 kD (DeVinney et al., 1999a). In EPEC, this phosphorylation is mediated by eukaryotic Src-family kinase c-Fyn at tyrosine 474 (Phillips et al., 2004). The phosphorylated Tir binds cellular protein Nck (non-catalytic region of tyrosine kinase) and trigger actin polymerization by activating the Nck-WASP (Wiskott-Aldrich syndrome protein) - Arp (Actin-related proteins) 2/3 cascade (Phillips et al., 2004). However, studies from EHEC showed that although the Tir-intimin interaction is required for EHEC adherence to epithelial cells, Tir does not undergo tyrosine phosphorylation (DeVinney et al., 1999b). Therefore, the role of Tir phosphorylation in A/E pathogen-induced pathogenesis is still unclear.

In addition to the interaction with intimin and triggering actin rearrangement, Tir is also involved in the phosphoinositide (PI) metabolism (Sason et al., 2009). Tir catalyzes the exchange between phosphtidylinositol 4,5-bisphophate [$PI(4,5)P_2$] and phosphtidylinositol 3,4,5-bisphophate [$PI(3,4,5)P_3$] through recruiting host phosphoinositide-3-kinase (PI3K) and/or inositol-5-phosphatase SHIP2. The role of Tir-mediated phosphoinositide metabolism in EPEC/EHEC pathogenesis has not yet been identified.

Besides Tir, other T3SS effectors also induce host cell cytoskeleton rearrangement. EPEC EspF or EHEC EspFu (a homolog of EspF in EHEC) recruits and activates the actin polymerization regulator N-WASP (Cheng et al., 2008; Sallee et al., 2008). Interestingly, EspF is also suggested to be a multifunctional protein involved in different biological events such as apoptosis, mitochondria dysfunction and membrane remodeling (Dean and Kenny, 2009).

The function of EspG/EspG2 on the cytoskeleton was predicted by its homology with *Shigella* T3SS effector VirA (Virulence gene A) (Yoshida et al., 2006). It has been shown that VirA can interact with microtubules and destabilize the microtubules by its cysteine protease activity both

in vitro and *in vivo* (Yoshida et al., 2002). Although EspG interacts with microtubules, the destabilization of microtubules by EspG/EspG2 is controversial (Hardwidge et al., 2005; Matsuzawa et al., 2004; Selyunin et al., 2011). However, EspG interacts with Arf GTPases (ADP ribosylation factor Guanosine-5'-triphosphatases) and p21-activated kinases (PAKs) (Selyunin et al., 2011). The interaction between EspG and Arf GTPases results in the blockage of GTPase hydrolysis on Arf GTPases, which is essential for golgi vesicle trafficking (Selyunin et al., 2011). In contrast, EspG activates PAK kinase activity and regulates different signaling pathways. Therefore, EspG is suggested to act like a catalytic scaffold and regulate endomembrane trafficking.

Anti-phagocytosis

Phagocytosis is the process by which bacteria are engulfed by host cell membrane and destroyed in the internal phagosome of immune cells. Phagocytosis is a multi-step process initiated by surface receptors and driven by remodeling of the cytoskeleton. There are two well-characterized receptors, complement receptor 3 (CR3) which binds with complement fragment C3bi and Fc gamma receptors (FcγR) which binds with IgG (Griffin, 1981). Several EPEC/EHEC T3SS effectors are suggested to play roles in blocking internalization of IgG-opsonized particles (Celli et al., 2001). In EPEC, the N-termini of EspF is required for inhibiting PI3K-mediated phagocytosis into macrophage and M cells (Martinez-Argudo et al., 2007; Quitard et al., 2006). EspJ inhibits both CR3- and IgG-mediated phagocytosis (Marches et al., 2008). Interestingly, EspF is required for inhibition of phagocytosis as only deletion of *espf* but not *espJ* in EPEC abolishes the inhibitory effect (Marches et al., 2008). Other effectors also contribute to anti-phagocytosis of A/E pathogens. EspH inhibits phagocytosis in both epithelial cells and macrophage (Dong et al., 2010). EspH binds with multiple RhoGEFs DH-PH domains

and prevents Rho activation, which subsequently leads to the interruption of actin local reorganization and inhibits phagocytosis. Recently, EspB was shown to interact with myosin and interrupt myosin and actin interaction (Iizumi et al., 2007). The myosin-binding region on EspB is required for EPEC-mediated phagocytosis suppression but is not essential for T3SS function and its induction of actin polymerization.

Cell survival and apoptosis

Infection by EPEC and EHEC induces apoptosis of epithelial cells (Abul-Milh et al., 2001). EPEC strains lacking *espA*, *espB* or *espD* fail to kill cells, likely due to their inability to adhere to host cells (Crane et al., 2001). Translocated EspF, but not secreted EspF induces apoptosis in host cells (Crane et al., 2001; Holmes et al., 2010). Deletion of *espF* in EPEC results in a similar deficiency in inducing apoptosis compared to T3SS deficient strains. The mechanism of EspF-induced apoptosis is still unknown but it might be related to its function on mitochondria. Mitochondrial associated protein (Map) contains mitochondrial targeting sequence and is imported into mitochondria (Kenny and Jepson, 2000). Map import is regulated by the mitochondrial outer membrane translocase (Tom) and the matrix chaperone, mtHsp70 (Papatheodorou et al., 2006) of host cells. Imported Map disrupts mitochondrial membrane potential and induces cell death.

Several T3SS effectors from EPEC and EHEC also have anti-apoptotic functions, which are believed to promote overall bacterial survival and colonization. A Δ*espZ* EPEC strain induces a strong cytotoxic effect on epithelial cells and shows a marked reduction in colonization (Shames et al., 2010). EspZ appears to interact with CD98 (Cluster of Differentiation 98), which can activate focal adhesion kinase (FAK) signaling and increase host cell survival. NleH1 and NleH2 interact with the anti-apoptotic protein Bax inhibitor-1 (BI-1) and block multiple apoptotic

pathways (Hemrajani et al., 2010). Deletion of *nleh1* and *nleh2* from EPEC induces strong apoptosis in epithelial cells. In addition, the PDZ (PSD-95/Discs-large/ZO-1) domain of NHERF2 (Na+/H+ exchanger regulatory factor 2) interacts with NleH proteins and blocks their anti-apoptotic function (Martinez et al., 2010).

NF-κB transcription factors

In the past three decades, NF-κB (nuclear factor-kappaB) has been the most extensively studied transcriptional factor family (Hayden and Ghosh, 2008). NF-κB is involved in a broad range of biological events such as development, inflammation and immunity. NF-κB transcription factors are evolutionarily conserved. In mammals, there are five members in the NF-κB family: RelA (p65), p50, p52, RelB and c-Rel (Ghosh et al., 1998). In Drosophila, the NF-κB family includes two proteins dorsal and DIF, which are functionally similar to p65, and the NF-κB precursor protein named Relish respectively (Huguet et al., 1997). Each factor can form either homo- or heterodimers with other members through a C-terminal dimerization domain (DD) (Huang et al., 1997; Huang et al., 2005). The dimerization results in the formation of fifteen different dimers with distinct stabilities and functions (Gilmore, 2006). For instance, p50:RelA heterodimer is more stable than the p50 or RelA homodimer. Moreover, these combinations of dimers also have cell type or tissue specificities, and therefore contribute to distinct roles of NF-κB in different cells and tissues (Hagemann et al., 2008; Lenardo and Baltimore, 1989).

Under normal conditions, NF-κB is usually sequestered by its inhibitor IκB (inhibitor of NF-kappaB) in the cytoplasm by the formation of IκB: NF-κB complexes (Whiteside et al., 1997). The classical IκB proteins include three proteins: IκBα, IκBβ and IκBε (Beg and Baldwin, 1993). The most clear mechanism of IκB is from studies of IκBα. IκBα inhibits NF-κB activity by

binding with p50:RelA heterodimer, mainly to mask the NLS (nuclear localization signal) region on RelA (Jacobs and Harrison, 1998). In addition, the binding of IκBα also converts RelA into a conformation unfavorable to DNA binding. Although both IκBβ and IκBε can also bind with RelA and some other NF-κB members, the mechanism is not clear and will not be addressed here (Li and Nabel, 1997; Malek et al., 2003).

After receiving activation signals, serines 32 and 36 of IκBα are phosphorylated by the upstream IKK (inhibitor of NF-kappaB kinase) kinase complexes (Brown et al., 1995). The phosphorylated IκBα will be recognized by $SCF^{\beta\text{-}TrCP}$ (Skp1-Cul1-F-box protein $^{\text{F-box/WD repeat-containing protein}}$) E3 ligase, which catalyes the polyubiquitination of IκBα leading to IκBα degradation by the 26S proteasome (Chen, 2005). Free NF-κB will enter into the nucleus and bind with κB DNA sites in thousands of gene promoters and enhancer regions (Fig. 3) (Pahl, 1999). The κB DNA sites usually contain 9 to 11 nucleotides with the consensus sequence: 5'-GGGRNWYYCC-3' (where R=A/G; N=A/C/G/T; W=A/T; Y=C/T). NF-κB recognizes 5'-GG or –GGG sequence and the N-terminal domain (NTD) of NF-κB binds with acidic DNA (Sen and Baltimore, 1986). Binding of NF-κB with DNA requires post-translational modification of NF-κB proteins. Monomethylation of Lysine (K) 37 on RelA is required for RelA:DNA binding in response to TNF (tumor necrosis factor) and IL(Interleukin)-1 stimulation (Ea and Baltimore, 2009). The phosphorylation of Serine 276 on RelA by host kinases such as PKA (Protein Kinase A) is also essential for NF-κB activation as mutating serine to alanine significantly attenuates NF-κB activity (Reber et al., 2009; Vermeulen et al., 2003). In addition to post-translational modification, recent studies showed that the binding of NF-κB:DNA is also mediated by other proteins. RPS3 (ribosomal protein subunit 3) interacts with RelA via its KH (K Homology) domain and specifies p50:RelA:DNA binding (Wan et al., 2007). In fact, the phosphorylation of

RelA at Ser276 also recruits acetytransferase CBP/p300, which can regulate NF-κB activity (Zhong et al., 1998).

Interplays between NF-κB and microbes

Bacteria are known to cause inflammation in the host due to aberrant activation of the host immune system. Despite the fact that many of inflammatory cytokines are regulated by NF-κB, the role of NF-κB in controlling pathogen infection and preventing the host from pathogen-induced acute intestinal injury has been demonstrated. Transplantation of RelA-deficient fetal liver cells to lethally irradiated mice significantly increases the host susceptibility to leishmania infection (Mise-Omata et al., 2009). Macrophages in transplanted mice fail to be activated and therefore can not be recruited to infection sites or secrete anti-bacterial cytokines. In another study, overexpression of RelA by an adenoviral vector in wild-type but not in *tnf*$^{-/-}$ mice promotes their resistance to *Pseudomonas aeruginosa* infection, which is due to the role of RelA in regulating TNF expression (Sadikot et al., 2006).

Mice deficient in p50 have been widely used in innate host defense studies as they do not show abnormalities in phenotype compared to the wild-type mice (Sha et al., 1995). Infections of *p50*$^{-/-}$ mice with *Listeria monocytogenes* and *Streptococcus pneumoniae* result in greater bacterial colonization, wider systemic distribution of bacteria and more severe inflammation in the host (Sha et al., 1995). Similarly, infection of *p50*$^{-/-}$ mice with *Mycobacterium tuberculosis* causes multifocal necrotic pulmonary lesions or lobar pneumonia. Expression of genes regulated by NF-κB and important for controlling *M. tuberculosis* infection such as IL-2, IFN (Interferon)-γ and TNF is significantly down-regulated in *p50*$^{-/-}$ mice (Yamada et al., 2001). Finally, infection of *p50*$^{-/-}$ mice with *C. rodentium* exhibits a greater bacterial burden and a longer infection cycle

in the intestine (Dennis et al., 2008). This is likely due to the defect of leukocyte recruitment to the infection site in *p50*$^{-/-}$ mice.

Other NF-κB members also contribute to the host defense against bacterial infection. Mice lacking c-Rel fail to produce TNF in response to *L. monocytogenes* infection, which is due to the inactivation of macrophages (Mason et al., 2002). Neutrophils in *RelB*$^{-/-}$ mice infected by *L. monocytogenes* can not be recruited to infection sites and are therefore highly susceptible to the bacterial infection (Weih et al., 1995). In addition, *RelB*$^{-/-}$ mice fail to produce IFN-γ to activate natural killer cell and become susceptible to *Toxoplasma gondii* infection (Caamano et al., 1999)

Besides its role in preventing pathogen infection, NF-κB is also critical for keeping gut homeostasis by maintaining the balance between commensal bacteria and the host. The mammalian gastrointestinal tract is colonized by over 10^{13} microbial organisms (Kau et al., 2011). As the intestine is the central organ in keeping host nutrition and energy balance, gut microbes as well as intestinal pathogens have the potential to disrupt normal function in intestine and cause damage in other organs (Littman and Pamer, 2011). Conditional knockout of NEMO (NF-kappa-B essential modulator) in young mice, in which NF-κB function is only abolished in intestinal epithelial cells, induces strong apoptosis in these cells and disrupts epithelial barriers (Nenci et al., 2007). This leads to the translocation of gut commensal bacteria into the mucosa and circulatory system, which contribute to sustaining inflammation and severe colitis. A similar phenotype has also been observed in mice lacking both IKKα and IKKβ (Egan et al., 2004). These data indicate the importance of NF-κB in keeping intestinal homeostasis under normal resting condition.

NF-κB signaling pathways

During the past two decades, the knowledge of innate immunity has been expanded (Medzhitov and Janeway, 2000b). It is now clear that the innate immune system is the first line of host defense and induces rapid, non-specific responses against pathogen infection. The central idea in innate immunity is the pattern recognition theory, which can partially explain how host cells detect pathogen products and initiate immune responses (Medzhitov and Janeway, 2000a). The recognition of pathogen products known as PAMPs (pathogen associated molecular patterns) including LPS (liposaccharides) and flagellin is mediated by pattern recognition receptors (PRRs) including TLRs (Toll-like receptors), NLRs (NOD-like receptors) and RLRs (RIG-I-like receptors) (Kabelitz and Medzhitov, 2007). Once these PRRs bind with their ligands, multiple signaling pathways will be activated, which result in the induction of cytokines or anti-microbial peptides. Secreted cytokines including TNF and IL-1 can subsequently bind with their receptors such as TNFR and IL-1R, which further enhance the innate immune response. Transcription of many cytokines and anti-microbial peptide are regulated by NF-κB transcriptional factors indicating that the NF-κB family is essential for innate immune response. There are classical and alternative NF-κB pathways (Karin, 1999). Activation of classical NF-κB pathway is usually mediated via TLRs, TNFR or IL-1R. The signaling induces IKKβ phosphorylation, which can catalyze IκBα degradation and release RelA/p50 heterodimer into nucleus. The alternative pathway can be triggered by receptors including CD40, LTbR (Lymphotoxin beta receptor) and BAFF-R (B cell-activating factor-receptor). In this pathway, NIK (Nck Interacting Kinase) and IKKα will be activated and subsequently catalyze the NF-κB precursor protein p100 processing into p52, which will translocate to nucleus with RelB as heterodimers (Demchenko et al., 2010). We will focus on the classic pathway in this dissertation due to our research interests and space limitation.

Activation of NF-κB by TLRs and IL-1R is dependent on the signaling of MyD88 (myeloid differentiation primary response 88) and TRIF (TIR domain-containing adaptor gene inducing IFN-β) (Fig. 3). So far, only TLR3 has been suggested to utilize TRIF to activate NF-κB, while other TLRs appear to be dependent on MyD88 (Fitzgerald et al., 2003; McWhirter et al., 2004; Yamamoto et al., 2002). The cytoplasmic portion of TLRs contains Toll/IL-1R (TIR) homology domain, which can interact with MyD88 and TRIF (Akira, 2003; Kaisho and Akira, 2001). MyD88 and TRIF signaling also require another critical protein family the TNF receptor-associated factor (TRAF) family (Gohda et al., 2004). Seven TRAF proteins (TRAF1-7) have been identified in this family (Xu et al., 2004). Except for TRAF1, the N-termini of TRAFs contain a conserved RING (Really Interesting New Gene) finger domain, which is responsible for TRAF protein self-ubiquitination and E3 ligase activity (Li et al., 2002). The C-termini of TRAFs also contain a conserved TRAF domain responsible for binding with multiple proteins including receptors, adaptor proteins and kinases (Pineda et al., 2007). MyD88 and TRIF recruit TRAF6, which binds with IRAK (IL-1 receptor associated kinase). Recruited TRAF6 will undergo self-ubiquitination and promote phosphorylation of TAK1 (transforming growth factor-activated protein kinase 1) and polyubiquitination of IKKγ/NEMO. TAK1 normally binds with its cofactors TAB (TAK1-binding proteins) 1 and TAB 2 (Wang et al., 2001). It has been known that TAK1/TAB 1/TAB 2 complex is able to activate IKK in the presence of TRAF6 and Ubc 13 (Ubiquitin carrier protein 13). Recently, several studies showed that free K63 polyubiquitin chains generated by TRAF6 directly activate TAK1 by binding with TAB2 (Xia et al., 2009). Interestingly, the free K63 polyubiquitin chains also can activate IKK complex through direct binding with NEMO, whereas autoubiquitinated TRAF6 is unable to do so. Similar results were also reported in cells stimulated by IL-1β but not by TNF (Xu et al., 2009). Activated TAK1

Fig.3. The TLRs/IL-1R- and TNF-NF-κB signaling pathways.

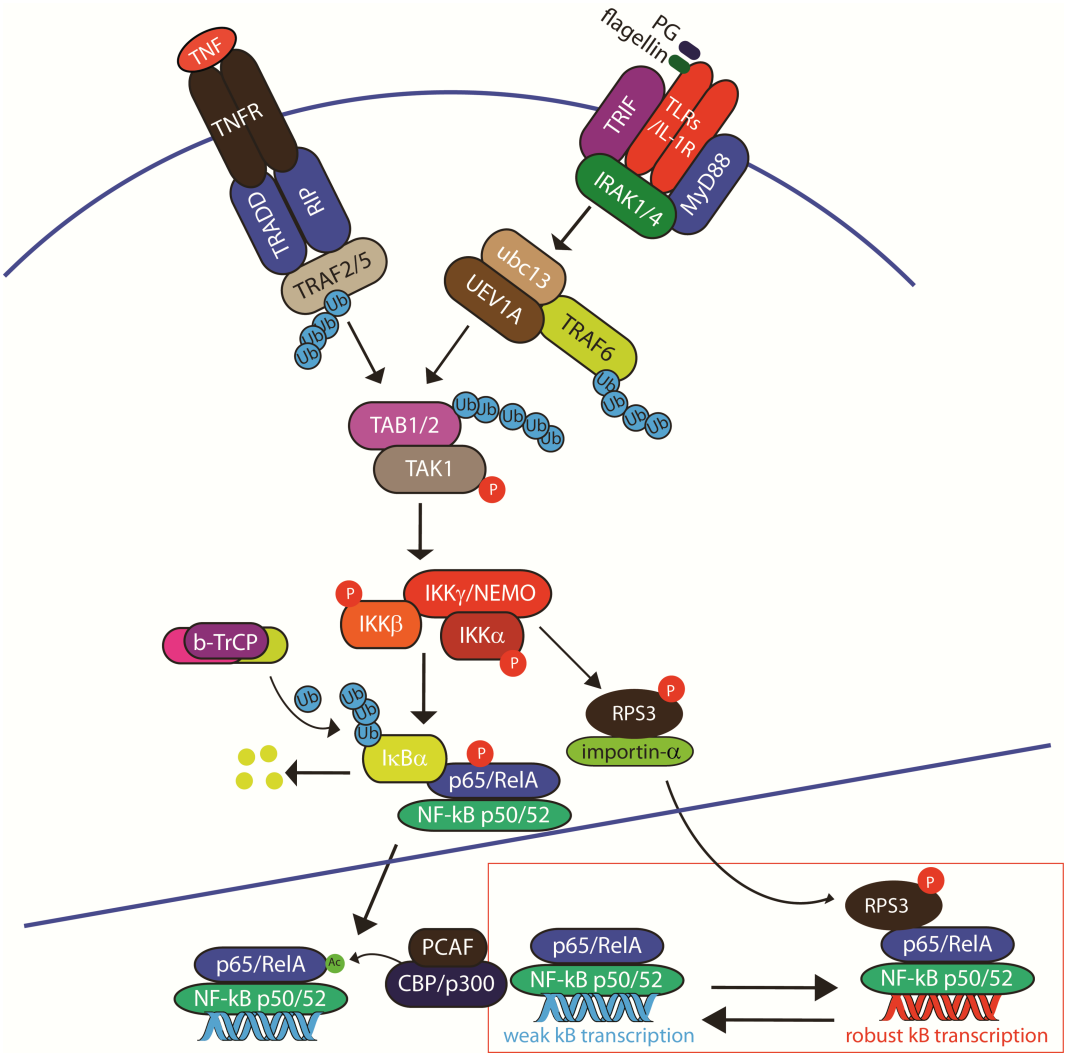
TNF
TNFR
TRADD
RIP
TRAF2/5
Ub
PG
flagellin
TRIF
TLRs
/IL-1R
IRAK1/4
MyD88
ubc13
UEV1A
TRAF6
TAB1/2
TAK1
P
IKKγ/NEMO
IKKβ
IKKα
b-TrCP
RPS3
importin-α
IκBα
p65/RelA
NF-kB p50/52
PCAF
CBP/p300
Ac
weak kB transcription
robust kB transcription

subsequently phosphorylates IKKα at Ser 176 and 180 or IKKβ at Ser 177 and 181, which are residues positioned in the activation loop of IKKs (Ninomiya-Tsuji et al., 1999; Wang et al., 2001). The exact function of NEMO in NF-κB activation is still not clear and studies have shown NEMO lacks catalytic properties to activate NF-κB (Legarda-Addison et al., 2009). It has been suggested polyubiquitination of NEMO might recruit the TAK1 complex to the IKK complex and allow TAK1 to phosphorylate IKK kinases (Xia et al., 2009). In addition, a NEMO deficient cell line fails to activate NF-κB upon stimulation indicating NEMO is important for NF-κB activation.

TNF is another major mediator of NF-κB activation. TNF belongs to a family with more than twenty homologues such as lymphotoxin α, CD40 ligand and Fas ligand (Darnay and Aggarwal, 1999). There are also more than forty members in the TNF receptor superfamily, which includes TNF-R1, TNF-R2, Fas, CD30, CD40, TRAIL (TNF-related apoptosis-inducing ligand) receptors and RNAK (Receptor activator of nuclear factor kappa-B). Many of TNF receptors have their own ligands, while TNF-R1 and TNF-R2 share TNF. Both TNF-R1 and TNF-R2 contain domains responsible for binding intracellular adaptor proteins, which can link the TNF stimulation to the activation of downstream signaling pathways (Rickert et al., 2011). However, TNF-R1 contains a unique death domain (DD) of approximately 80 amino acids. The DD is associated with multiple proteins involved in cell death and therefore activation of TNF-R1 mediated signaling pathway strongly induces cell death (Jiang et al., 1999).

After the engagement with ligands, TNF receptors recruit TRAF2 and/or TRAF5 protein(s) and form multiple protein complexes (Fig. 3). Current studies suggest only TNF-R1 binds TRAF2 through its adaptor protein TNF receptor-associated death domain (TRADD), whereas other TNF receptors bind TRAF2 directly (Hsu et al., 1995). Like TRAF6, TRAF2 also

undergoes self-ubiquitination and can recruit other signaling molecules such as RIP1 (receptor-interacting protein 1) kinase and cIAPs (inhibitor of apoptosis). Both TRAF2 and cIAP are able to polyubiquitinate RIP1 (Receptor-interacting protein 1) kinase at Lys 377 residue, which might be required for binding with TAB 2 Zinc finger to recruit the TAK1/TAB 1/TAB 2 complex (Xu et al., 2009). The activated TAK1 will in turn phosphorylate IKKβ and activates downstream IκBα:NF-κB complex.

Modulation of NF-κB by T3SS effectors

As mentioned before, pathogens have developed multiple strategies to inhibit host defense. Inhibition of NF-κB has been revealed as a powerful way for pathogens to attenuate the pro-inflammatory response. T3SS is a main strategy utilized by Gram-negative bacteria to modulate NF-κB activation. One of the earliest studies was of the YopJ (*Yersinia* outer protein J) protein of *Yersinia pestis*, which now is categorized in the YopJ superfamily including *Salmonella* AvrA (avirulence protein A), *Vibrio* VopJ (*Vibrio* outer protein J), *Aeromonas* AopP (avirulence outer protein P) and *Pseudomonas* HopZ family (Ma et al., 2006). Although initially considered as a cysteine protease, YopJ is an acetyltransferase and inhibits activation of both NF-κB and MAPK (mitogen-activated protein kinase) signaling pathways (Orth et al., 1999). YopJ utilizes an acetyl group from the metabolite acetyl-CoA to cause the acetylation on Ser/Thr residues located in the activation loop of MKKs and IKKβ kinases (Mukherjee et al., 2006). This acetylation prevents Ser/Thr phosphorylation, which results in the inhibition of MAPK and NF-κB signaling pathway activation. In addition, YopJ also targets other signaling molecules in the NF-κB pathway. YopJ is a deubiquitinating enzyme and removes both K48 and K63-linked ubiquitin chains from TRAF2 and TRAF6 to prevent NF-κB activation from TLR signaling (Zhou et al., 2005). Mutation of predicted protease catalytic residue cysteine 172 to alanine abolishes YopJ's

deubiquitinating enzyme activity. Interestingly, YopJ's inhibitory effect is also required to activate host NLRP3 (NLR family, pyrin domain containing 3)/ASC (apoptosis-associated speck-like protein containing a CARD)/caspase-1 inflammasome and induce apoptosis in macrophage (Zheng et al., 2011). In addition, hypersecretion of YopJ in *Y. pseudotuberculosis* attenuates bacterial virulence in mice (Brodsky and Medzhitov, 2008). These data indicate a complex system in pathogens to control their cytotoxicity to the host during infection in order to reach their maximal virulence.

Other members in the YopJ superfamily also target NF-κB. *Salmonella* AvrA also acetylates MAPKKs to inhibit JNK (c-Jun N-terminal kinases) and NF-κB signaling pathways (Jones et al., 2008). While it is clear that the acetylation of MAPKKs tends to inhibit the activation of JNK pathway, how this acetylation contributes to AvrA-mediated inhibition of NF-κB activation is still not clear. However, AvrA is demonstrated to be a deubiquitylase and removes ubiquitin from IκBα to inhibit NF-κB pathway activation (Collier-Hyams et al., 2002). VopA from Vibrio parahemeolyticus acetylates a conserved lysine residue in the catalytic loop of MAPKKs, which blocks ATP (adenosine triphosphate) binding to the kinases and results in the inactivation of MAPKKs (Trosky et al., 2007).

T3SS effectors from enteropathogenic bacteria also target the NF-κB pathway. *S. flexneri* OspG (outer *Shigella* protein G) binds ubiquitin-conjugating enzymes (E2s) to prevent ubiquitination and degradation of IκBα (Kim et al., 2005a). *S. flexneri* OspF is a dually specific phosphatase and dephosphorylates MAPK kinases in the nucleus. The dephosphorylated MAPK fails to phosphorylate histone H3 at Ser10, which is important for the recruitment of NF-κB to the chromatin (Arbibe et al., 2007). Consequently, OspF inhibits NF-κB mediated gene expression and attenuates the host innate immune response. *S. flexneri* IpaH9.8 (Invasion

plasmid antigen H 9.8) possesses E3 ligase activity and interacts with NEMO and ABIN-1 (Ashida et al., 2010). ABIN-1 (A20 binding and inhibitor of NF-κB) is a ubiquitin-binding adaptor protein and normally binds NEMO. Through ABIN-1, IpaH9.8 promotes NEMO ubiquitination and degradation, thus leading to the inactivation of the NF-κB signaling pathway.

T3SS effectors from A/E pathogens targeting NF-κB signaling pathway have also been demonstrated. NleE from EPEC/EHEC has been suggested to inhibit IκBα degradation by preventing IKKβ activation (Nadler et al., 2010; Newton et al., 2010). The most current studies have shown that NleE is a methyltransferase that specifically methylates zinc-coordinating cysteines 673/692 in Npl4 zinc finger (NZF) domains of TAB2/TAB3 (Zhang et al., 2012). The methylated NZF domains of TAB2/3 show a deficiency in binding with zinc ions as well as binding with ubiquitin chains to impair the signaling of NF-κB pathway. NleB is suggested to block TNF-induced NF-κB activation without detailed mechanism (Nadler et al., 2010). NleC is a Zn-dependent protease that specifically cleaves the N-termini of RelA and inhibits RelA nuclear translocation upon stimulation (Baruch et al., 2011; Yen et al., 2010). NleC efficiently inhibits TNF-induced IL-8 secretion and cooperates with other effectors such as NleE and NleD to inhibi the host innate immune response. Interestingly, the Tir protein of EPEC is associated with TRAF2 and induces its degradation independent from the host ubiquitin-26S proteasome system (Ruchaud-Sparagano et al., 2011). This study also suggested Tir plays a minor role in inhibition of NF-κB activation.

In this thesis, I studied the functions of T3SS effectors NleH (NleH1 and NleH2) and NleB during bacterial infection. I demonstrated that NleH1 but not NleH2 is a virulence factor contributing to bacterial colonization *in vivo*. By performing proteomic screens, I demonstrated while both NleH proteins are able to interact with NF-κB non-Rel subunit RPS3, only NleH1

inhibits RPS3 nuclear translocation induced by TNF stimulation or bacterial infection. The prevention of RPS3 nuclear translocation by NleH1 specifically attenuates the NF-κB activation. Furthermore, NleH1 specifically blocks IKKβ-mediated RPS3 phosphorylation at Ser 209, which is required for RPS3 nuclear translocation. Deletion of *nleH1* from *E.coli* O157:H7 produces a hypervirulent phenotype in a gnotobiotic piglet model of Shiga toxin-producing *E. coli* infection, which indicates a complex mechanism utilized by bacteria to colonize the host.

I also elucidated the mechanism of another effector NleB, which has been shown to target the NF-κB pathway. I demonstrated that NleB is an O-GlcNAc transferase and utilizes UDP-GlcNAc sugar from the hexamine biosysthesis pathway to O-GlcNAcylate the host glycolytic protein GAPDH (Glyceraldehyde 3-phosphate dehydrogenase). I further identified that GAPDH directly interacts with TRAF2 and serves as a co-activator to promote TRAF2 polyubiquitination in response to stress stimulation. NleB-mediated GAPDH O-GlcNAcylation prevents the interaction of GAPDH with TRAF2 and inhibits TRAF2 polyubiquitination, which subsequently leads to the attenuation of NF-κB activation. These studies indicated several novel mechanisms for bacterial manipulation of the NF-κB signaling pathway to dampen the host immune response.

Chapter II: Bacterial Effector Binding to Ribosomal Protein S3 Subverts NF-κB Function

Abstract

Enteric bacterial pathogens cause food borne disease, which constitutes an enormous economic and health burden. Enterohemorrhagic *Escherichia coli* (EHEC) causes a severe bloody diarrhea following transmission to humans through various means, including contaminated beef and vegetable products, water, or through contact with animals. EHEC also causes a potentially fatal kidney disease (hemolytic uremic syndrome) for which there is no effective treatment or prophylaxis. EHEC and other enteric pathogens (e.g., enteropathogenic *E. coli* (EPEC), *Salmonella*, *Shigella*, *Yersinia*) utilize a type III secretion system (T3SS) to inject virulence proteins (effectors) into host cells. While it is known that T3SS effectors subvert host cell function to promote diarrheal disease and bacterial transmission, in many cases, the mechanisms by which these effectors bind to host proteins and disrupt the normal function of intestinal epithelial cells have not been completely characterized. In this study, we present evidence that the *E. coli* O157:H7 *nleH1* and *nleH2* genes encode T3SS effectors that bind to the human ribosomal protein S3 (RPS3), a subunit of nuclear factor kappa-light-chain-enhancer of activated B cells (NF-κB) transcriptional complexes. NleH1 and NleH2 co-localized with RPS3 in the cytoplasm, but not in cell nuclei. The N-terminal region of both NleH1 and NleH2 was required for binding to the N-terminus of RPS3. NleH1 and NleH2 are autophosphorylated Ser/Thr protein kinases, but their binding to RPS3 is independent of kinase activity. NleH1, but not NleH2, reduced the nuclear abundance of RPS3 without altering the p50 or p65 NF-κB subunits or affecting the phosphorylation state or abundance of the inhibitory NF-κB chaperone IκBα NleH1 repressed the transcription of a RPS3/NF-κB-dependent reporter plasmid, but did

not inhibit the transcription of RPS3-independent reporters. In contrast, NleH2 stimulated RPS3-dependent transcription, as well as an AP-1-dependent reporter. We identified a region of NleH1 (N40-K45) that is at least partially responsible for the inhibitory activity of NleH1 toward RPS3. Deleting *nleH1* from *E. coli* O157:H7 produced a hypervirulent phenotype in a gnotobiotic piglet model of Shiga toxin-producing *E. coli* infection. We suggest that NleH may disrupt host innate immune responses by binding to a cofactor of host transcriptional complexes.

Introduction

Diarrheal disease caused by enteric bacteria is an important endemic health threat and a major source of food borne disease (Clarke, 2001). Over 76 million cases of diarrheal disease and 5,000 deaths result from food borne illness in the United States annually (Centers for Disease Control and Prevention). Diarrheagenic strains of *E. coli* contribute greatly to the enormous economic and health burden of food borne disease. Enteropathogenic *E. coli* (EPEC) is a frequent cause of infantile diarrhea, while enterohemorrhagic *E. coli* (EHEC) has emerged as an important cause of hemorrhagic colitis in developed countries (Garmendia et al., 2005). Often transmitted to humans through consumption of fruit juice, raw/undercooked meat, and vegetables contaminated with manure, EHEC is especially important because it is the leading cause of pediatric renal failure (hemolytic uremic syndrome; HUS).

EHEC adheres to intestinal enterocytes and produces a characteristic attaching/effacing (A/E) lesion resulting from localized intestinal microvilli destruction and the formation of a pedestal-like projection composed of epithelial-derived cytoskeletal components (Donnenberg et al., 1997). EHEC virulence proteins (effectors) are translocated directly into intestinal epithelial cells through a type III secretion system (T3SS;(Hueck, 1998)). The T3SS is a molecular syringe, widely conserved among animal and plant pathogens, that directs the active transport of effectors into host cells. The EHEC T3SS and several effectors are encoded on a pathogenicity island termed the 'locus of enterocyte effacement' (LEE;(Hueck, 1998)), whose genomic structure, function, and regulation are well conserved among the characterized A/E pathogens (i.e. EHEC, EPEC, *Citrobacter rodentium*). Over 20 other secreted proteins (non-LEE-encoded effectors; Nles) encoded by genes in multiple pathogenicity islands located throughout the EHEC genome have also been described (Deng et al., 2004). A bioinformatics study recently employed

homology searches against other bacterial effectors to identify 39 secreted/translocated effectors encoded in the EHEC Sakai genome (Tobe et al., 2006). Several studies have reported the importance of Nles to virulence (Campellone et al., 2004; Deng et al., 2004; Echtenkamp et al., 2008; Gruenheid et al., 2004; Marches et al., 2008; Marches et al., 2003; Marches et al., 2005).

Intestinal epithelial cells have evolved mechanisms to prevent infection by pathogens by inhibiting bacterial colonization and by interacting with the underlying immune system (Oswald, 2006). Paneth cells located at the base of intestinal crypts produce proinflammatory cytokines and express Toll-like receptors (TLRs) and nucleotide-binding oligomerization domain (NOD) proteins. NOD proteins recognize pathogen-associated molecular patterns (PAMPs) and promote activation of host proinflammatory signaling pathways (Abreu et al., 2005), many of which are regulated by the nuclear factor kappa-light-chain-enhancer of activated B cells (NF-κB). PAMP detection typically initiates a signal transduction cascade that promotes polyubiquitination of the inhibitor of NF-κB (IκB)-kinase-γ complex (NEMO), ultimately leading to NF-κB activation through the degradation of the inhibitory NF-κB chaperone IκBα. IκBα masks the nuclear localization signal (NLS) of p65, yet leaves the p50 nuclear localization signal exposed, permitting flux of IκBα/NF-κB complexes between the nucleus and the cytoplasm (Ghosh and Karin, 2002). IκBα degradation shifts the balance to favor increased nuclear localization of NF-κB.

NF-κB homo- and hetero-dimers (typically composed of the p50 and p65 subunits) bind to DNA (κB sites) within target gene promoters and regulate transcription by recruiting co-activator/repressor molecules (Wan et al., 2007). It is not completely clear how diverse stimuli generate unique transcriptional responses in different cells and tissues (Hayden and Ghosh, 2008). However, the recent discovery of a non-Rel NF-κB subunit, RPS3, which guides NF-κB

to specific κB sites after specific cellular stimuli, has shed some light on this issue. RPS3 was detected as a major co-purifying molecule with the p65 NF-κB subunit (Wan et al., 2007). The N-terminal region of RPS3, notably the KH domain, is required for binding to the N-terminal portion of p65 (Wan et al., 2007). RPS3 forms a complex with p65 that significantly increases the affinity of NF-κB complexes for a subset of target genes and provides a mechanism by which selected promoters could be activated in response to specific stimuli (Wan et al., 2007).

The identity and underlying mechanism of action of *E. coli* PAMPs and effector proteins that respectively stimulate vs. repress host innate immunity have been incompletely characterized. *E. coli* flagellin induces secretion of interleukin (IL)-8 from intestinal epithelial cells (Ruchaud-Sparagano et al., 2007). However, IL-8 secretion is inhibited relatively early during infection by the delivery of one or more unidentified T3SS effectors (Khan et al., 2008; Ruchaud-Sparagano et al., 2007). These effectors are believed to function by preventing the degradation of IκBα, to reduce NF-κB translocation into the nucleus (Ruchaud-Sparagano et al., 2007). That the nuclear abundance of NF-κB and its affinity for DNA are increased at early stages of infection, without concomitant increases in IL-8 expression (Hauf and Chakraborty, 2003; Ruchaud-Sparagano et al., 2007; Savkovic et al., 1997), may also suggest effector-mediated inhibition of innate responses. Despite significant effort, how T3SS effectors coordinate their activities to suppress the potent host inflammatory response normally induced by flagellin and other PAMPs remains incompletely characterized.

E. coli O157:H7 EDL933 contains two copies of the nleH gene, designated nleH1 (Z0989) and nleH2 (Z6021). Each gene encodes predicted protein products with significant sequence similarity to Shigella OspG (Garcia-Angulo et al., 2008; Hemrajani et al., 2008; Tobe et al., 2006) , a protein known to interfere with NF-κB activation (Kim et al., 2005a). C. rodentium, a

pathogen of mice that shares many pathogenic strategies with EHEC, rapidly induces the nuclear translocation of NF-κB in host cells (Khan et al., 2006). *C. rodentium* NleH has been shown to play an important role in the colonization of animal hosts and in altering NF-κB activity (Hemrajani et al., 2008). We therefore undertook a biochemical analysis of the host binding partners and mechanism of action of the *E. coli* O157:H7 effectors NleH1 and NleH2 to understand better how bacterial effectors modulate host innate immunity. In this study we show that the E. coli O157:H7 NleH proteins play an important role in host-pathogen interactions by binding to the human ribosomal protein S3 (RPS3), a newly identified subunit of NF-κB (Wan et al., 2007). Our results suggest a potentially novel mechanism for bacterial effector-mediated disruption of host innate responses to infection.

Results

NleH1 and NleH2 are injected into host cells by the T3SS. Recent proteomic (Deng et al., 2003) and bioinformatic (Tobe et al., 2006) screens identified a repertoire of novel T3SS-effectors encoded on pathogenicity islands throughout EHEC genomes in non-locus of enterocyte effacement pathogenicity islands. Among these, E. coli O157:H7 strain EDL933 contains two copies of the nleH gene, designated nleH1 (Z0989) and nleH2 (Z6021), which are predicted to encode T3SS substrates (Deng et al., 2003). NleH1 (293 amino acids) and NleH2 (303 amino acids) are 84% identical and encoded on distinct, non-LEE pathogenicity islands (O-islands 36 and 71, respectively) from which other T3SS-effectors with proven roles in bacterial virulence (e.g. NleA, NleD) are expressed (Kim et al., 2007; Marches et al., 2005). Others have noted NleH sequence similarity to *Shigella flexneri* OspG and serine/threonine protein kinases of Yersinia spp (Tobe et al., 2006).

Both NleH1 and NleH2 contain a lysine residue (K159 and K169, respectively) present in a

Ser/Thr protein kinase domain that based on homology to Shigella OspG, may function as the catalytic site of kinase activity. Despite 84% shared identity, NleH1 differs from NleH2 in that NleH1 lacks a 10 amino acid insertion containing putative SH2 and PKA-interaction domains (Figure 1A). NleH1 also possesses several potential Ser/Thr phosphorylation sites lacking in NleH2.

Other A/E pathogens also encode multiple copies of nleH. The EHEC Sakai strain encodes nleH1 and nleH2 (Tobe et al., 2006). The recently sequenced EPEC 2348/69 encodes three copies of nleH, one of which may be a pseudogene (Iguchi et al., 2009). *nleH* genes are present in other EPEC genomes, including B171 and E22 (Iguchi et al., 2009; Rasko et al., 2008). NleH1 and NleH2 are also 83% identical to NleH encoded by C. rodentium (Hemrajani et al., 2008). Only one copy of NleH is present in C. rodentium (Garcia-Angulo et al., 2008). This copy of NleH appears to be more similar to EHEC NleH1 than to NleH2, as it lacks the 10 amino-acid insertion that is present in EHEC NleH2, but absent in NleH1(Garcia-Angulo et al., 2008).

To determine if EHEC NleH1 and/or NleH2 are translocated into host cells by the *E. coli* T3SS, we constructed fusions to the TEM-1 β-lactamase. This reporter system has proven robust for assaying effector translocation into host cells (Charpentier and Oswald, 2004). These constructs were introduced into both wild type and ΔescN EPEC, a strain deficient in T3SS function that is commonly used to evaluate the dependence of A/E pathogen effector translocation on the T3SS. These strains were used to infect HeLa cells loaded with the CCF2/AM substrate. We used a fluorescence microplate reader to quantify β-lactamase activity in host cells after a 4 h infection. While NleH1- and NleH2-TEM were expressed at similar levels in both wild type and ΔescN EPEC (Figure 1B), the proteins were detectably translocated into mammalian cells only by wild type ($p<0.001$, ANOVA), indicating, as predicted from

studies of C. rodentium NleH (Garcia-Angulo et al., 2008), that both EHEC NleH1 and NleH2 are translocated into host cells by the T3SS (Figure 1C).

To validate these data and begin to determine the subcellular localization of NleH1 and NleH2, we constructed fusions to the FLAG epitope in pFLAG-CTC, expressed these plasmids in EHEC, and infected HeLa cells. After 4 h, we removed the extracellular bacteria and subjected the cell lysates to immunoblotting. The expected distribution of calnexin and tubulin validated the integrity of membrane and cytoplasmic fractions, respectively. NleH1 and NleH2 were detected in both the host cytoplasmic and membrane fractions (Figure 2A). We obtained similar data after we fractionated host cells infected with EPEC strains expressing FLAG fusions to NleH1 and NleH2 (Figure 1D). We also employed immunofluorescence microscopy to assess the intracellular localization of NleH1 and NleH2 by infecting HeLa cells with EHEC strains expressing either NleH1 or NleH2 fused to the FLAG epitope. NleH1 and NleH2 both localized to the cell periphery and around, but not in, the host nucleus (Figure 2B).

NleH1 and NleH2 bind the human RPS3. To identify eukaryotic cell binding partners of NleH, we used purified His-NleH1 to isolate mammalian proteins that bind to this effector. We incubated His-NleH1 with HeLa cell lysates and captured His-NleH1 and any co-purifying host proteins through passage over Ni-NTA agarose resin (Figure 3A). Using mass spectrometry, we identified a protein with an apparent molecular mass of ~28 kDa that selectively eluted with NleH1 in affinity purification experiments as RPS3, a nucleic acid- binding KH domain protein implicated in DNA repair (Yacoub et al., 1996), and the regulation of NF-κB-dependent transcription (Wan et al., 2007).

To verify that RPS3 interacts with NleH1 (Figure 4A), we used an α-RPS3 antibody to immunoprecipitate RPS3 from cell lysates obtained after infection with EPEC UMD207 [eae-/

Fig.4. NleH amino acid sequences and T3SS-dependent translocation. A. *E. coli* EDL933 NleH1 (Z0989) and NleH2 (Z6021) amino acid sequences. Asterisks indicate identical residues. Amino acids differing between NleH1 and NleH2 are indicated in red. The lysine residue implicated in autophosphorylation activity is depicted in blue. B. Immunoblotting of bacterial lysates for NleH1- and NleH2-TEM expression in wild type (wt) or T3SS-deficient Δ*escN* EPEC (T3SS). Blots were probed with α-TEM antibody. C. β-lactamase activity (arbitrary units) in HeLa cells loaded with CCF2/AM substrate and infected for 4 h with wt or Δ*escN* EPEC (T3SS) strains expressing NleH1- or NleH2-TEM fusions. Asterisks indicate significantly different β-lactamase activity compared with uninfected samples ($p<0.05$, ANOVA). D. Immunoblot analysis of cytoplasmic and membrane HeLa cell fractions following infection with EPEC strains expressing NleH1- or NleH2-FLAG. Blots were probed with α-FLAG, α-tubulin, and α-calnexin antibodies.

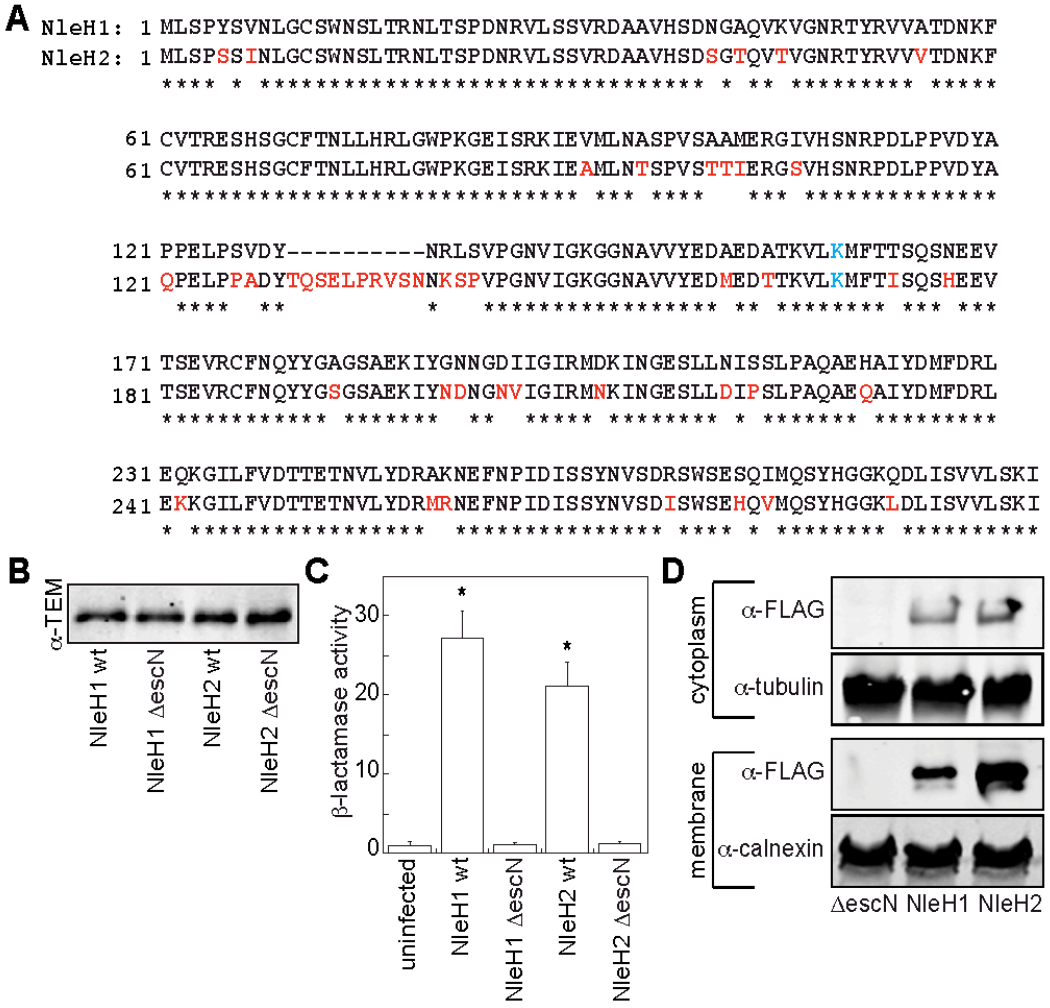
A
NleH1: 1 MLSPYSVNLGCSWNSLTRNLTSPDNRVLSSVRDAAVHSDNGAQVKVGNRTYRVVATDNKF
NleH2: 1 MLSPSSINLGCSWNSLTRNLTSPDNRVLSSVRDAAVHSDSGTQVTVGNRTYRVVVTDNKF
61 CVTRESHSGCFTNLLHRLGWPKGEISRKIEVMLNASPVSAAMERGIVHSNRPDLPPVDYA
61 CVTRESHSGCFTNLLHRLGWPKGEISRKIEAMLNTSPVSTTIERGSVHSNRPDLPPVDYA
121 PPELPSVDY----------NRLSVPGNVIGKGGNAVVYEDAEDATKVLKMFTTSQSNEEV
121 QPELPPADYTQSELPRVSNNKSPVPGNVIGKGGNAVVYEDMEDTTKVLKMFTISQSHEEV
171 TSEVRCFNQYYGAGSAEKIYGNNGDIIGIRMDKINGESLLNISSLPAQAEHAIYDMFDRL
181 TSEVRCFNQYYGSGSAEKIYNDNGNVIGIRMNKINGESLLDIPSLPAQAEQAIYDMFDRL
231 EQKGILFVDTTETNVLYDRAKNEFNPIDISSYNVSDRSWSESQIMQSYHGGKQDLISVVLSKI
241 EKKGILFVDTTETNVLYDRMRNEFNPIDISSYNVSDISWSEHQVMQSYHGGKLDLISVVLSKI
B
α-TEM
NleH1 wt
NleH1 ΔescN
NleH2 wt
NleH2 ΔescN
C
β-lactamase activity
30
20
10
0
uninfected
NleH1 wt
NleH1 ΔescN
NleH2 wt
NleH2 ΔescN
D
cytoplasm
α-FLAG
α-tubulin
membrane
α-FLAG
α-calnexin
ΔescN NleH1 NleH2

Fig. 5. Translocation of NleH proteins. A. Immunoblot analysis of cytoplasmic and membrane HeLa cell fractions following infection with EHEC strains expressing NleH1- or NleH2-FLAG fusions. Blots were probed with α-FLAG, α-tubulin, and α-calnexin antibodies. B. Immunofluorescence microscopy analysis of NleH localization. HeLa cells were infected with EHEC Δ*escN* (left), EHEC/p*nleH1*-FLAG (middle), or EHEC/p*nleH2*-FLAG (right) and stained with DAPI (blue) and an α-FLAG monoclonal antibody (green).

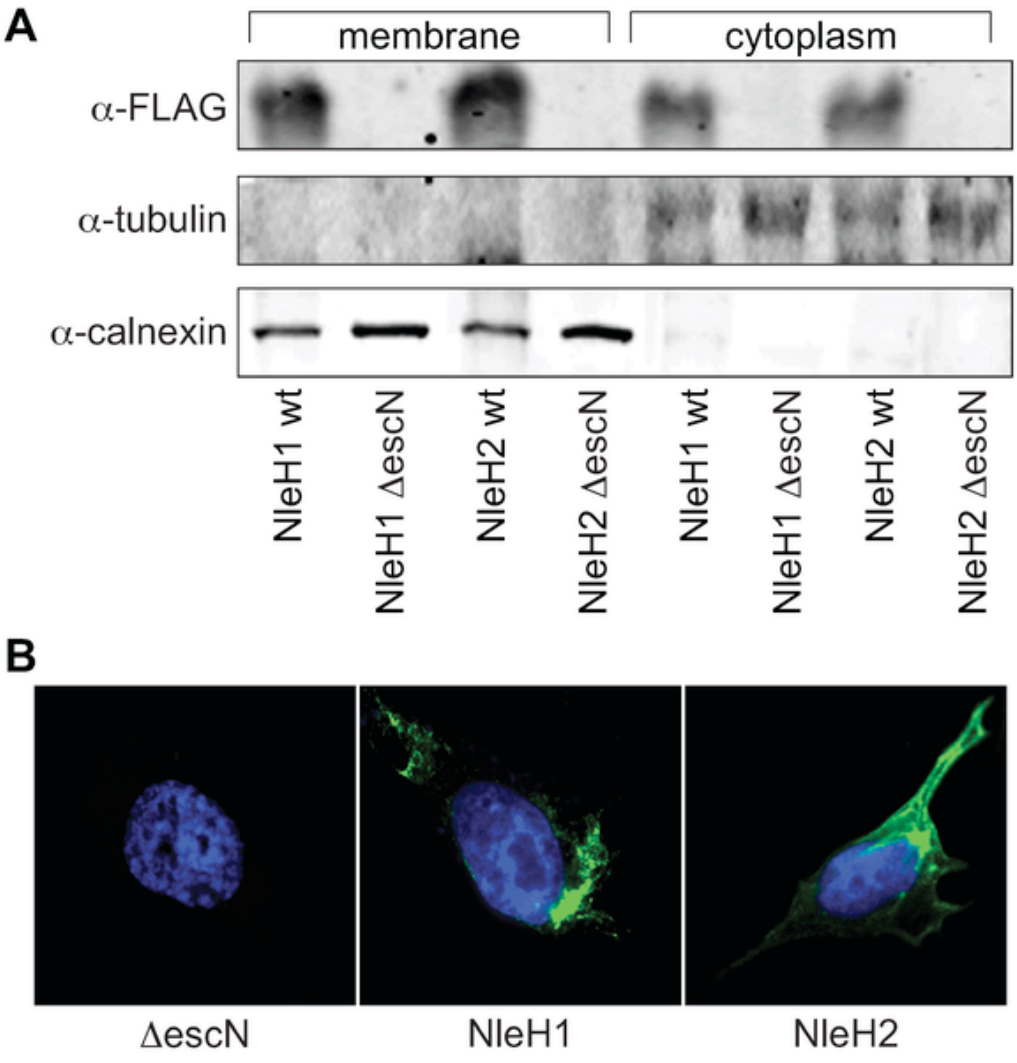
A
membrane
cytoplasm
α-FLAG
α-tubulin
α-calnexin
NleH1 wt
NleH1 ΔescN
NleH2 wt
NleH2 ΔescN
NleH1 wt
NleH1 ΔescN
NleH2 wt
NleH2 ΔescN
B
ΔescN
NleH1
NleH2

Fig. 6. Binding specificity of NleH. A. Affinity enrichment of HeLa proteins with affinity for His-NleH1. HeLa cell lysates were incubated with purified His-NleH1 pre-bound to Ni-NTA agarose, eluted with imidazole, and analyzed by SDS-PAGE. Samples included HeLa lysate + His-NleH1 (lane 1), His-NleH1 (lane 2), and HeLa lysate (lane 3). Bands identified by mass spectrometry as NleH1 and RPS3 are indicated. B. NleH does not bind RPS16. HeLa cells were infected with EPEC expressing NleH1-FLAG and immunoprecipitated with α-RPS3 (left) or α-RPS16 (right) antibodies. The top and middle panels depict the abundance of RPS3 and RPS16 in the cell lysate, whereas the bottom panel depicts an α-FLAG immunoblot of the immunoprecipitated samples. Similar results were obtained with NleH2-FLAG. C. NleF does not bind RPS3. HeLa cells were infected with EPEC expressing FLAG (left) or NleF-FLAG (right) and immunoprecipitated with α-RPS3 antibody. The top panel depicts RPS3 in the cell lysates whereas the middle and bottom panels depict samples immunoprecipitated with α-FLAG antibody and subsequently immunoblotted for FLAG and RPS3, respectively.

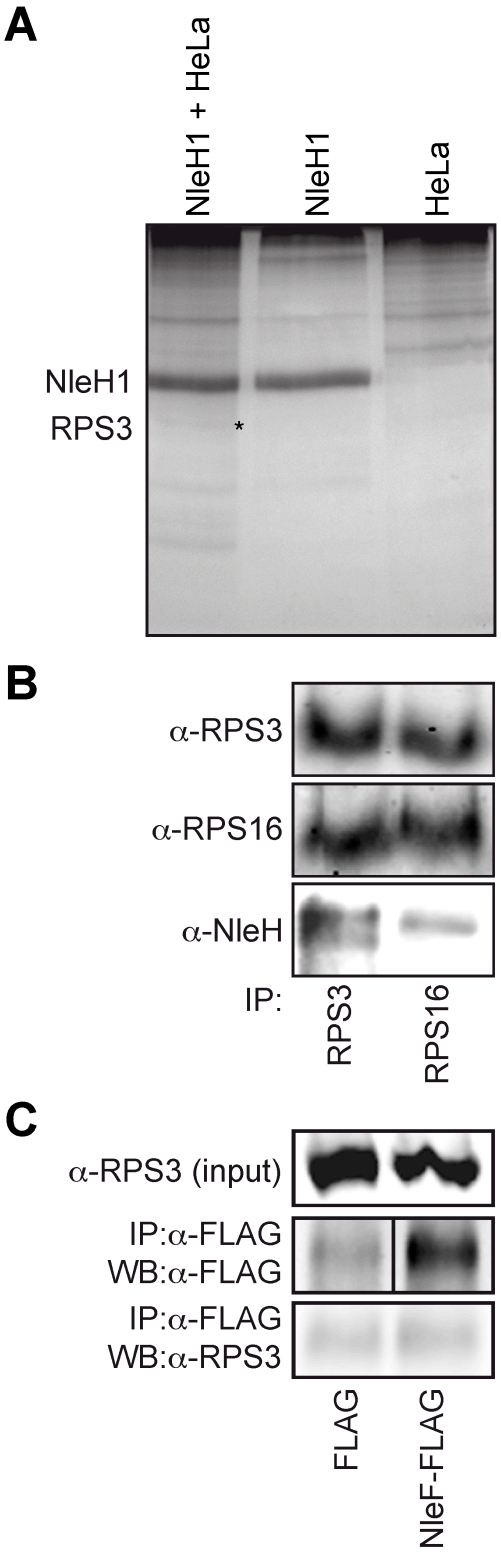
A
NleH1 + HeLa
NleH1
HeLa
NleH1
RPS3
*
B
α-RPS3
α-RPS16
α-NleH
IP:
RPS3
RPS16
C
α-RPS3 (input)
IP:α-FLAG
WB:α-FLAG
IP:α-FLAG
WB:α-RPS3
FLAG
NleF-FLAG

bfp-;(Anantha et al., 1998)] strains expressing FLAG-tagged NleH1, NleH2, or a control FLAG epitope. We used this strain because it lacks both the intimin protein and the bundle-forming pilus (BFP), thus facilitating removal of the bacteria after infection, to reduce potential contamination of translocated, immunoprecipitated NleH with bacterial proteins. Both NleH1 and NleH2 co-immunoprecipitated RPS3, supporting the affinity purification data (Figure 4B). Likewise, immunoprecipitated RPS3 selectively enriched for translocated NleH1 and NleH2 (Figure 4C).

To provide additional evidence for the specificity of NleH-RPS3 binding, we assessed the ability of NleH1 to bind to a different ribosomal protein, RPS16. We determined that NleH1 did not significantly bind to RPS16 (Figure 3B). Similarly, we assessed the ability of a different EHEC effector protein, NleF (Echtenkamp et al., 2008), to interact with RPS3. We determined that NleF could not effectively immunoprecipitate RPS3 following its translocation into host cells (Figure 3C).

RPS3 binds directly to the p65 NF-κB subunit (Wan et al., 2007). We therefore tested whether NleH associated with other NF-κB proteins through RPS3 interaction. Immunoprecipitation of NleH1 and NleH2 also enriched for the NF-κB subunits p50 and p65 (Figure 4D). We also performed experiments by depleting RPS3 from cell lysates using an a-RPS3 antibody. When these RPS3-depleted cell lysates were immunoprecipitated for NleH, we were no longer able to detect either p50 or p65 (data not shown), further substantiating that NleH interacts indirectly with NF-κB via binding to RPS3.

Because of the homology between NleH and Shigella OspG, a protein that binds ubiquitin-conjugating enzymes (E2s), including UbcH5 and UbcH7 (Kim et al., 2005a), we also tested if NleH interacted with the host ubiquitin machinery. To do this we immunoprecipitated NleH1

from cell lysates and performed immunoblotting experiments to detect ubiquitination of NleH1 or its binding to Ub-associated proteins. We did not obtain evidence of such interactions (data not shown). Taken together, these biochemical data suggest that NleH1 and NleH2 possess a novel host substrate, RPS3, a protein that interacts with NF-κB to regulate mammalian transcription.

BiFC analysis of NleH-RPS3 interaction. We next sought to confirm immunoprecipitation data with an additional protein interaction assay, bimolecular fluorescence complementation (BiFC). BiFC assays are based on the reconstitution of two fragments of the enhanced yellow fluorescent protein (eYFP) when they are brought in close proximity by an interaction between proteins fused to the YFP fragments (Figure 5A; (Hu et al., 2002; Hu and Kerppola, 2003)). Protein-protein interactions generate a fluorescent signal at the site of the protein complex, permitting quantification or direct visualization of the interaction.

We based our design of NleH and RPS3 BiFC constructs on the BiFC assay originally developed by Hu et al. (Hu et al., 2005, 2006). This design utilizes Venus, an enhanced yellow fluorescent protein (eYFP) variant, which emits strong fluorescence (Hu et al., 2002) without requiring significant protein over-expression (Kerppola, 2006). We generated protein chimeras with split N- and C-terminal fragments (VN and VC, respectively), of eYFP. Then we designed plasmids to contain a linker region between the eYFP fragment and a multi-cloning site. HA epitope tags were added to facilitate detection with immunoblotting. We also constructed fusions to actin, a protein often used as a positive control in BiFC assays, as well as fusions to RPS3 and NleH1 and NleH2 (Figure 5B). These constructs were transfected into HeLa cells and analyzed 48 h post-transfection.

The reconstitution of eYFP mediated by interaction between the N- and C-termini of actin

Fig.7. NleH1 and NleH2 bind to the host RPS3. A. RPS3 amino acid sequence. Tryptic peptides identified by mass spectrometry are indicated in red. B. Immunoprecipitation of RPS3 from HeLa cells by translocated NleH1- and NleH2-FLAG following infection with EPEC UMD207. Samples were immunoprecipitated with α-FLAG antibody and immunoblotted for RPS3. The lower panel indicates the RPS3 abundance in the cell lysates. C. Immunoprecipitation of NleH1- and NleH2-FLAG from HeLa cells by RPS3 following infection with EPEC UMD207. Samples were immunoprecipitated with α-RPS3 antibody and immunoblotted for FLAG to detect NleH. The lower panel demonstrates the equal enrichment of RPS3 among samples following α-RPS3 immunoprecipitation. D. Enrichment of the p50 and p65 NF-κB subunits by NleH1 and NleH2. Samples were immunoprecipitated with α-FLAG antibody and immunoblotted for p50 (top) and p65 (bottom).

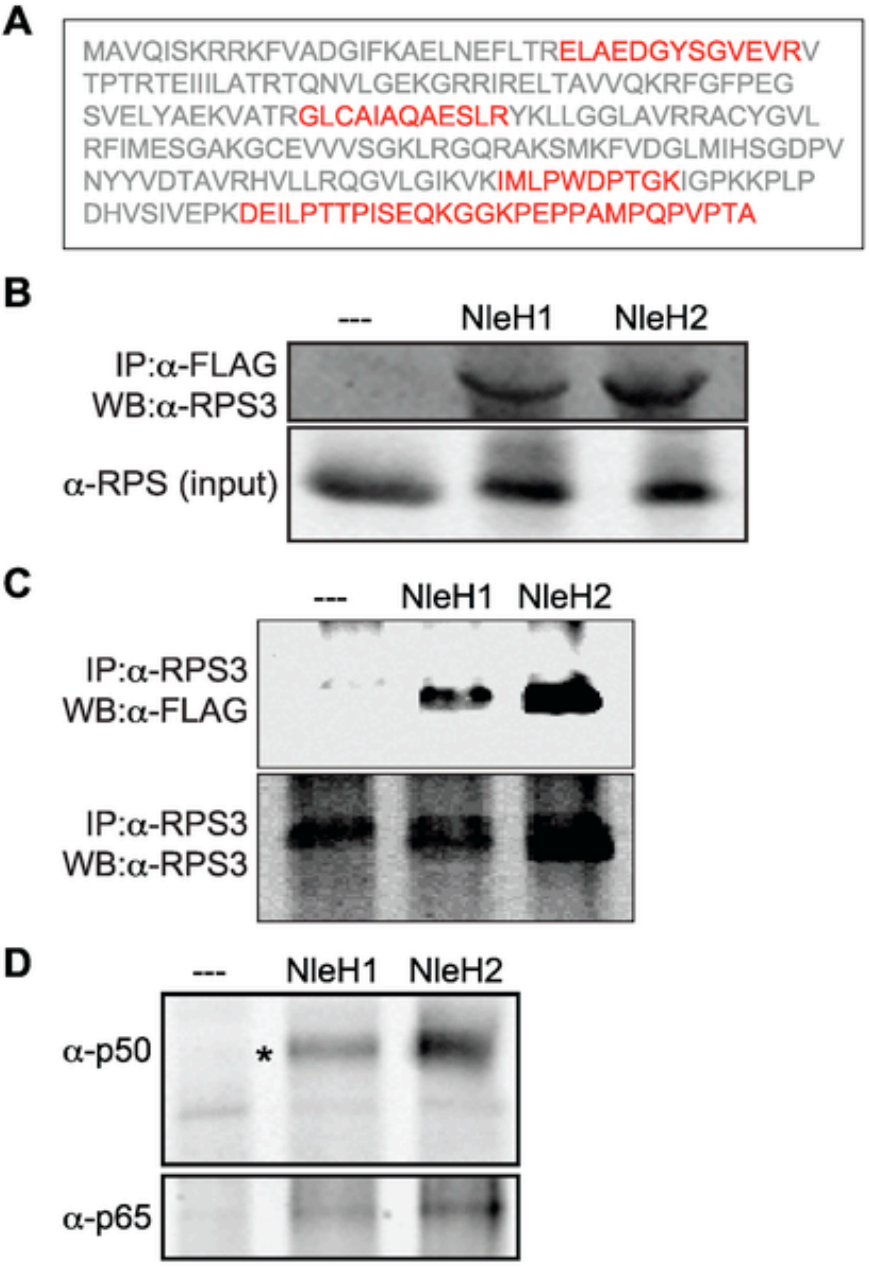
A
MAVQISKRRKFVADGIFKAELNEFLTRELAEDGYSGVEVRV
TPTRTEIIILATRTQNVLGEKGRRIRELTAVVQKRFGFPEG
SVELYAEKVATRGLCAIAQAESLRYKLLGGLAVRRACYGVL
RFIMESGAKGCEVVVSGKLRGQRAKSMKFVDGLMIHSGDPV
NYYVDTAVRHVLLRQGVLGIKVKIMLPWDPTGKIGPKKPLP
DHVSIVEPKDEILPTTPISEQKGGKPEPPAMPQPVPTA
B

NleH1
NleH2
IP:α-FLAG
WB:α-RPS3
α-RPS (input)
C

NleH1
NleH2
IP:α-RPS3
WB:α-FLAG
IP:α-RPS3
WB:α-RPS3
D

NleH1
NleH2
α-p50
*
α-p65

generated intense fluorescence (Figure 5C). In contrast, the expression of individual constructs or constructs lacking both actin fragments did not generate significant fluorescence. We then examined the potential for interaction between RPS3 and NleH1 or NleH2. The co-expression of eYFP chimeras of RPS3 and both NleH1 and NleH2 also reconstituted YFP fluorescence ($p<0.001$, ANOVA), whereas transfection of individual plasmids did not (Figure 5C), suggesting that both NleH1 and NleH2 bind RPS3 in mammalian cells. Similar data were obtained irrespective of the position of the eYFP fusion relative to NleH or RPS3 (e.g. compare Figure 5C, lanes G–H and K–L). In addition, we used confocal immunofluorescence microscopy after infecting cells with EPEC strains expressing NleH1- or NleH2-FLAG to determine that both NleH1 and NleH2 co-localize with endogenous RPS3 in the cytoplasm (Figure 5D). These microscopy data support the previously described biochemical analyses that showed an interaction between NleH and RPS3.

NleH N-termini bind to the N-terminus of RPS3. To map the binding domain of RPS3 on NleH1 and NleH2, we carried out a structure-function study with deletions of RPS3 that encompass the known functional domains of this protein (Figure 6A). Co-immunoprecipitation experiments revealed that the region of RPS3 (AAs 1–41) N-terminal to the KH domain is required for RPS3 binding to both NleH1 and NleH2 (Figure 6B). A similar analysis revealed that the N-termini of NleH1 and NleH2 (AAs 1–139 and 1–149, respectively) were required for binding to RPS3 (Figure 6C).

NleH1 and NleH2 are autophosphorylated Ser/Thr protein kinases. Given the sequence conservation between NleH and a domain implicated in the autophosphorylation and kinase activities of Shigella OspG (Kim et al., 2005a; Tobe et al., 2006), we examined if NleH1 and NleH2 are also Ser/Thr protein kinases. We purified His-NleH1 and NleH2, as well as NleH site-

directed mutants in which a lysine residue was mutated to alanine [NleH1(K159A) and NleH2(K169A)]. By performing Pro-Q staining of purified proteins, we determined that, similar to OspG, both NleH1 and NleH2 are autophosphorylated (Figure 7A). We also used these proteins to assay for phosphorylation of the myelin basic protein (MBP), a commonly used substrate in protein phosphorylation assays. Both wild-type NleH1 and NleH2, but not the site directed mutants [NleH1(K159A) or NleH2(K169A)], phosphorylated MBP in vitro (Figure 7B), suggesting that NleH1 and NleH2 possess kinase activity.

RPS3 is phosphorylated by the extracellular signal-regulated kinase 1 (ERK1) on T42 (Kim et al., 2005b). This event is necessary for RPS3 nuclear translocation in response to DNA damage (Yadavilli et al., 2007) and may play a role in the transcriptional activities of RPS3 (Wan et al., 2007). The non-ribosomal fraction of RPS3 is also phosphorylated by PKCδ on S6 and T221 to promote its nuclear translocation (Kim et al., 2009). To determine if NleH kinase activity is essential to RPS3 binding, we immunoprecipitated RPS3 and interrogated the samples for the presence of wild type or kinase-deficient NleH1/NleH2. We observed that NleH-RPS3 binding was independent of NleH kinase activity (Figure 6D).

To determine if NleH could phosphorylate RPS3, we conducted in vitro kinase assays with NleH and RPR3 and analyzed the results by immunoblotting with an α-phospho-Ser/Thr-specific antibody (the utility of which for RPS3 phosphorylation studies has been documented previously (Kim et al., 2009), following separation by SDS-PAGE. We determined that while NleH1 and NleH2 could phosphorylate MBP, and ERK1 could phosphorylate RPS3, NleH1 and NleH2 had no detectable ability to phosphorylate RPS3 (data not shown). Overall, these data suggest that the NleH-RPS3 interaction is independent of NleH kinase activity. Further, they leave open the possibility that NleH effectors may be multifunctional proteins with the capacity to target

Fig. 8 Bimolecular fluorescence complementation analysis of NleH-RPS3 interaction. A. BiFC schematic. Protein-protein interaction promotes the reconstitution of a functional fluorophore, measured as an increase in the YFP:CFP emission ratio. B. Experimental design of NleH- and RPS3-eYFP fusions. VN, N-terminus (AAs 1–173) of Venus fluorescence protein; VC, C-terminus (AAs 155–238) of Venus fluorescence protein. C. Relative fluorescence intensity resulting from the co-transfection of the indicated NleH- and RPS3-eYFP plasmid combinations (n = 3). Asterisks indicate significantly different fluorescence intensity compared with uninfected samples ($p<0.05$, ANOVA). D. Confocal immunofluorescence microscopy analysis of NleH and RPS3 co-localization. HeLa cells were infected with EPEC strains expressing NleH1- or NleH2-FLAG and stained with DAPI (blue), α-FLAG (green), and α-RPS3 (red) antibodies. Two representative cells are shown for each infection condition.

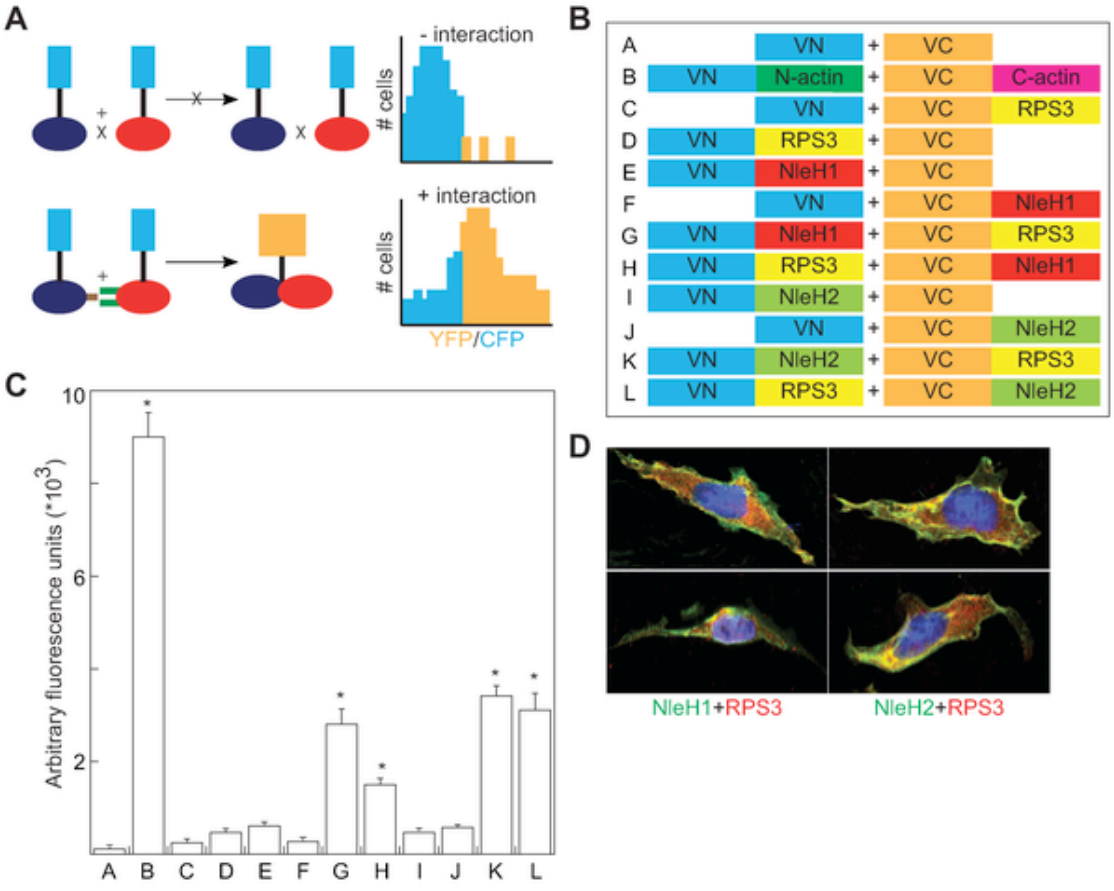
A
- interaction
cells
+ interaction
# cells
YFP/CFP
B
A VN + VC
B VN N-actin + VC C-actin
C VN + VC RPS3
D VN RPS3 + VC
E VN NleH1 + VC
F VN + VC NleH1
G VN NleH1 + VC RPS3
H VN RPS3 + VC NleH1
I VN NleH2 + VC
J VN + VC NleH2
K VN NleH2 + VC RPS3
L VN RPS3 + VC NleH2
C
Arbitrary fluorescence units (*10^3)
10
6
2
A B C D E F G H I J K L
D
NleH1+RPS3
NleH2+RPS3

Fig. 9. N-termini of NleH1 and NleH2 bind to the N-terminus of RPS3. A. Design of RPS3 and NleH protein truncations. The amino acids present in each truncation are indicated to the left of the figure. The death (pink), KH (green), and DNA-repair (blue) domains of RPS3 are indicated. The white box depicts the 10 amino acids lacking in NleH1 but present in NleH2. B. Co-immunoprecipitation of NleH1- (top) and NleH2-HA (middle) with RPS3-FLAG truncations. Samples were immunoprecipitated with α-FLAG antibody to capture RPS3 and immunoblotted for HA to detect NleH. The bottom panel depicts the expression levels of the RPS3-FLAG truncations. C. Co-immunoprecipitation of RPS3-FLAG with NleH1- and NleH2-HA truncations. Samples were immunoprecipitated with α-HA antibody to capture NleH and immunoblotted for FLAG to detect RPS3. The lower panel depicts the expression levels of the NleH truncations. D. Immunoprecipitation of RPS3-FLAG with NleH1(K159A)-HA and NleH2(K169A)-HA. Samples were immunoprecipitated with α-HA antibody to capture NleH and immunoblotted for FLAG to detect RPS3. The lower panel depicts the expression levels of RPS3 in cell lysates.

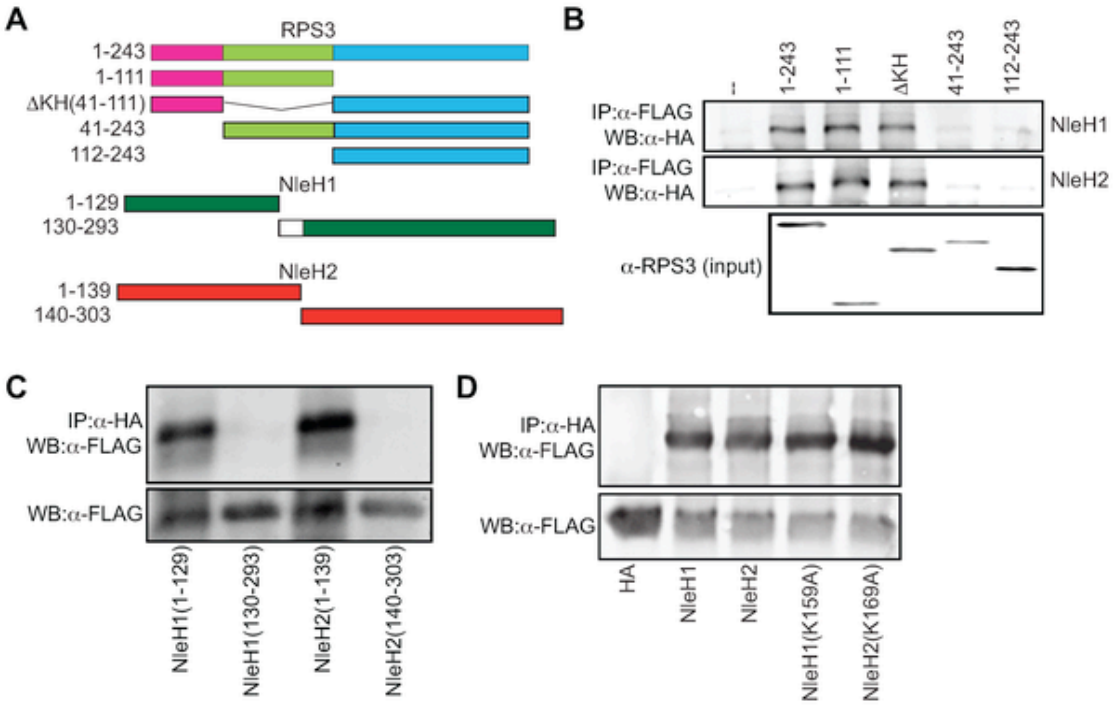
A
RPS3
1-243
1-111
ΔKH(41-111)
41-243
112-243
NleH1
1-129
130-293
NleH2
1-139
140-303
B
-
1-243
1-111
ΔKH
41-243
112-243
IP:α-FLAG
WB:α-HA
NleH1
IP:α-FLAG
WB:α-HA
NleH2
α-RPS3 (input)
C
IP:α-HA
WB:α-FLAG
WB:α-FLAG
NleH1(1-129)
NleH1(130-293)
NleH2(1-139)
NleH2(140-303)
D
IP:α-HA
WB:α-FLAG
WB:α-FLAG
HA
NleH1
NleH2
NleH1(K159A)
NleH2(K169A)

multiple host regulatory pathways.

NleH1 reduces the nuclear abundance of RPS3. RPS3 translocates to the nucleus after stimulation with tumor necrosis factor-alpha (TNF-α). NleH1 and NleH2 bind to the N-terminus of RPS3, potentially masking its putative nuclear localization signal. To determine if NleH binding to RPS3 inhibits translocation of RPS3 into the nucleus, we first used immunofluorescence microscopy to evaluate the relative abundance of nuclear vs. cytoplasmic RPS3. The percentage of cells containing predominantly nuclear RPS3 was significantly reduced in cells infected with wild type (8±3%) vs. ΔescN EHEC (36±10%; $p = 0.01$, t-test), suggesting an EHEC T3SS effector alters RPS3 nuclear abundance (Figure 8A-B).

We evaluated the relative abundance of nuclear vs. cytoplasmic RPS3 in 293T cells in the presence or absence of transfected NleH1- and NleH2-HA with or without 1 h stimulation with 100 ng/µl TNF-α. We subsequently fractionated the cells to separate nuclear from cytoplasmic components. We quantified poly(ADP-ribose) polymerase (PARP) and tubulin abundance to normalize the concentrations of nuclear and cytoplasmic subcellular protein fractions. The lack of PARP in the cytoplasmic fraction and the lack of tubulin in the nuclear fraction demonstrated 52the absence of cross-contamination between the fractions (Figure 9A). As expected from previous reports utilizing similar treatment conditions (Wan et al., 2007), the nuclear abundance of both RPS3 and p65 significantly increased after stimulation with TNF-α. Most notably, the nuclear abundance of RPS3 was significantly reduced in samples containing NleH1, while nuclear p65 and cytoplasmic concentrations of both RPS3 and p65 were unchanged. NleH1 and NleH2 were expressed equally among all samples, but were detected only in the cytoplasm, rather than the nuclear fraction (Figure 9A), consistent with immunofluorescence microscopy data.

Quantitative analysis of RPS3 abundance (based on densitometry analysis of immunoblots) revealed that NleH1 significantly reduced (~65%) the relative abundance of nuclear RPS3 (Figure 9B, $p<0.001$, ANOVA) after stimulation with TNF-α. In contrast, NleH2 transfection did not significantly alter RPS3 nuclear abundance. Neither protein altered the nuclear abundance of the NF-κB p65 subunit (Figure 10A). The nuclear abundance of p50 was also unchanged as a function of NleH expression (data not shown), indicating that NleH1 activity is specific to RPS3. The kinase activity of NleH1 was important for its ability to reduce RPS3 nuclear abundance, as the effect of transfecting NleH1(K159A) was not significantly different from that of transfecting the HA control plasmid (Figure 9B).

Immunofluorescence microscopy analyses support these biochemical data. We observed that RPS3 translocated into the nuclei of HeLa cells after TNF-α stimulation. The nuclear translocation of RPS3 was inhibited in cells infected with EPEC expressing NleH1-FLAG, but not NleH2-FLAG, relative to uninfected controls (Figure 10B). We also used an α-p65 antibody for immunoprecipitation of nuclear extracts to validate further that the impact of NleH1 on reducing RPS3 nuclear abundance would alter the nuclear association of RPS3 with p65. Our analysis of immunoprecipitated nuclear p65 samples indicated a reduced abundance of RPS3 in samples co-transfected with NleH1, but not NleH2, relative to an HA epitope control (Figure 10C), also suggesting that NleH1 could interfere with RPS3-p65 interactions by reducing RPS3 nuclear abundance.

To test further the hypothesis that NleH1 reduces RPS3 nuclear abundance, we also quantified changes in nuclear RPS3 after infecting HeLa cells with EHEC strains possessing or lacking nleH1 and/or nleH2 constructed using lambda Red mutagenesis (Datsenko and Wanner, 2000). After 3 h of infection, bacteria were killed with antibiotics and TNF-α was added at 100 ng/ml

Fig. 10. NleH1 and NleH2 are autophosphorylated Ser/Thr protein kinases. A. Autophosphorylation assay of His-NleH1 and NleH2, and site-directed mutants NleH1(K159A) and NleH2(K169A). Blots were stained with Pro-Q. B. Phosphorylation of myelin basic protein (MBP) by wild-type NleH1 and NleH2, but not the site-directed mutants NleH1(K159A) and NleH2(K169A). Blots were probed with α-His and α-phospho-Ser/Thr antibodies.

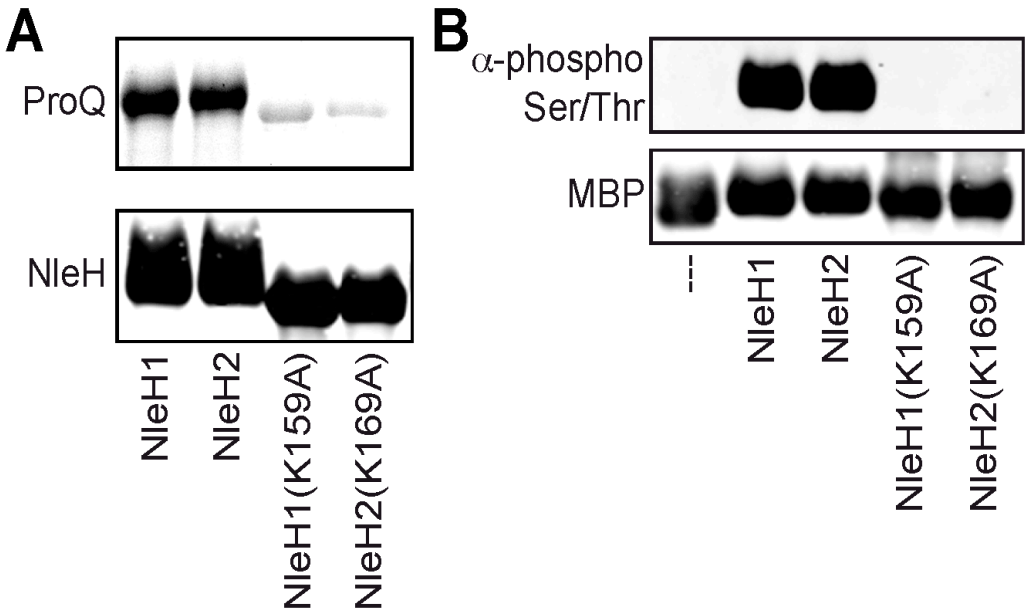
A
ProQ
NleH
NleH1
NleH2
NleH1(K159A)
NleH2(K169A)
B
α-phospho Ser/Thr
MBP

NleH1
NleH2
NleH1(K159A)
NleH2(K169A)

Fig.11. T3SS effector(s) inhibit RPS3 nuclear translocation. A. Immunofluorescence microscopy analysis of RPS3 nuclear abundance in HeLa cells infected with wild type (wt) or Δ*escN* EHEC. B. Quantification of the % of cells containing predominantly nuclear RPS3 (n = 100 cells). Asterisks indicate significantly different compared with wild-type infection ($p<0.05$, t-test).

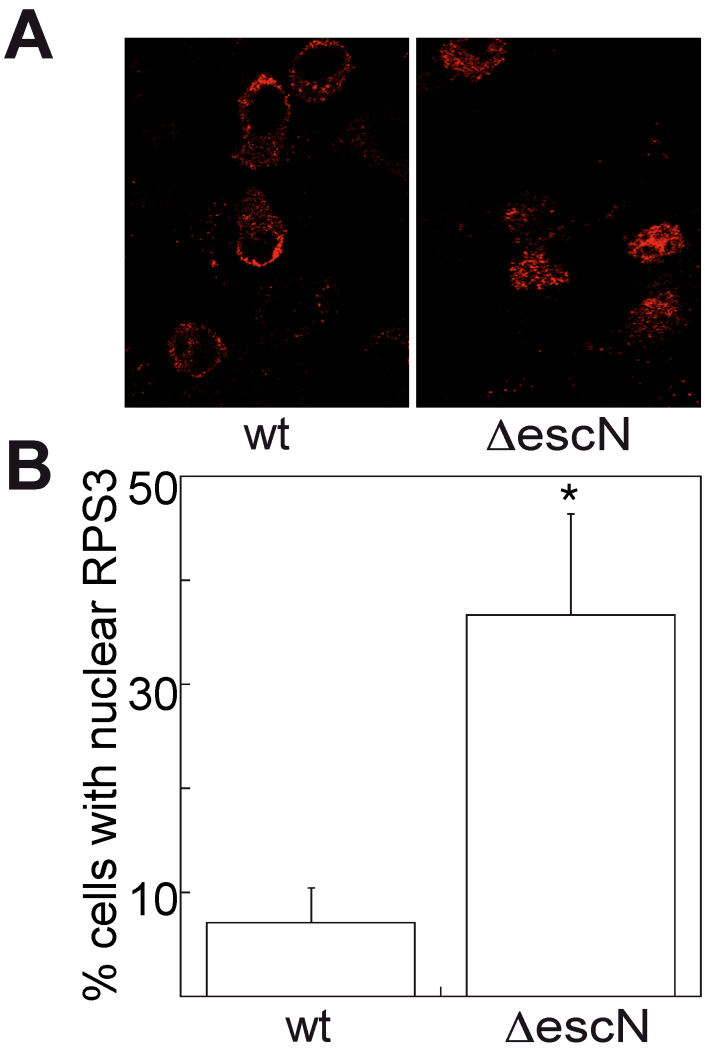
A
wt
ΔescN
B
% cells with nuclear RPS3
50
30
10
*
wt
ΔescN

Fig. 12. NleH1 reduces the nuclear abundance of RPS3. **A.** Immunoblot analysis of cytoplasmic and nuclear fractions of 293T cells transfected with NleH1, NleH2, or an HA-epitope control, in the presence or absence of TNF-α (100 ng/ml) stimulation for 1 h. Blots were probed with α-RPS3, α-p65, α-HA, α-tubulin, and α-PARP monoclonal antibodies. **B.** Quantification ($n \geq 4$) of the fold-increase in nuclear RPS3 as assessed by densitometry analysis of immunoblots in the absence (open bars) or presence (black bars) of TNF-α stimulation. RPS3 signal intensity was normalized to tubulin (cytoplasmic) and PARP (nuclear). Asterisks indicate significantly different compared with HA transfection ($p<0.05$, ANOVA). **C.** Quantification of the fold-increase in nuclear RPS3 following a 3 h infection of HeLa cells with *E. coli* O157:H7 EDL933 strains possessing or lacking *nleH1* and/or *nleH2*, as well as with strains complemented with the indicated NleH plasmids ($n = 3$). Asterisks indicate significantly different compared with wild-type infection ($p<0.05$, ANOVA). **D.** Immunoblot analysis of IκBα phosphorylation induced by TNF-α (left) or PMA (right), and total IκBα, in the presence or absence of NleH. **E.** Immunoblot analysis of the impact of *C. rodentium* NleH and EHEC NleH1 truncations and site-directed mutants on RPS3 nuclear abundance. Blots were probed with α-HA (top), α-RPS (middle), and α-PARP (bottom) monoclonal antibodies. The HA-input panel depicts the expression levels of the indicated constructs. The α-RPS panel depicts the nuclear abundance of RPS3 after stimulation with TNF-α in 293T cells transfected with the indicated constructs. The α-PARP signal was used for normalization of immunoblot signal intensities. **F.** Quantification ($n = 3$) of the fold-increase in nuclear RPS3 as assessed by immunoblotting in the presence of the indicated NleH expression plasmids. Asterisks indicate significantly different compared with NleH1 transfection ($p<0.05$, ANOVA).

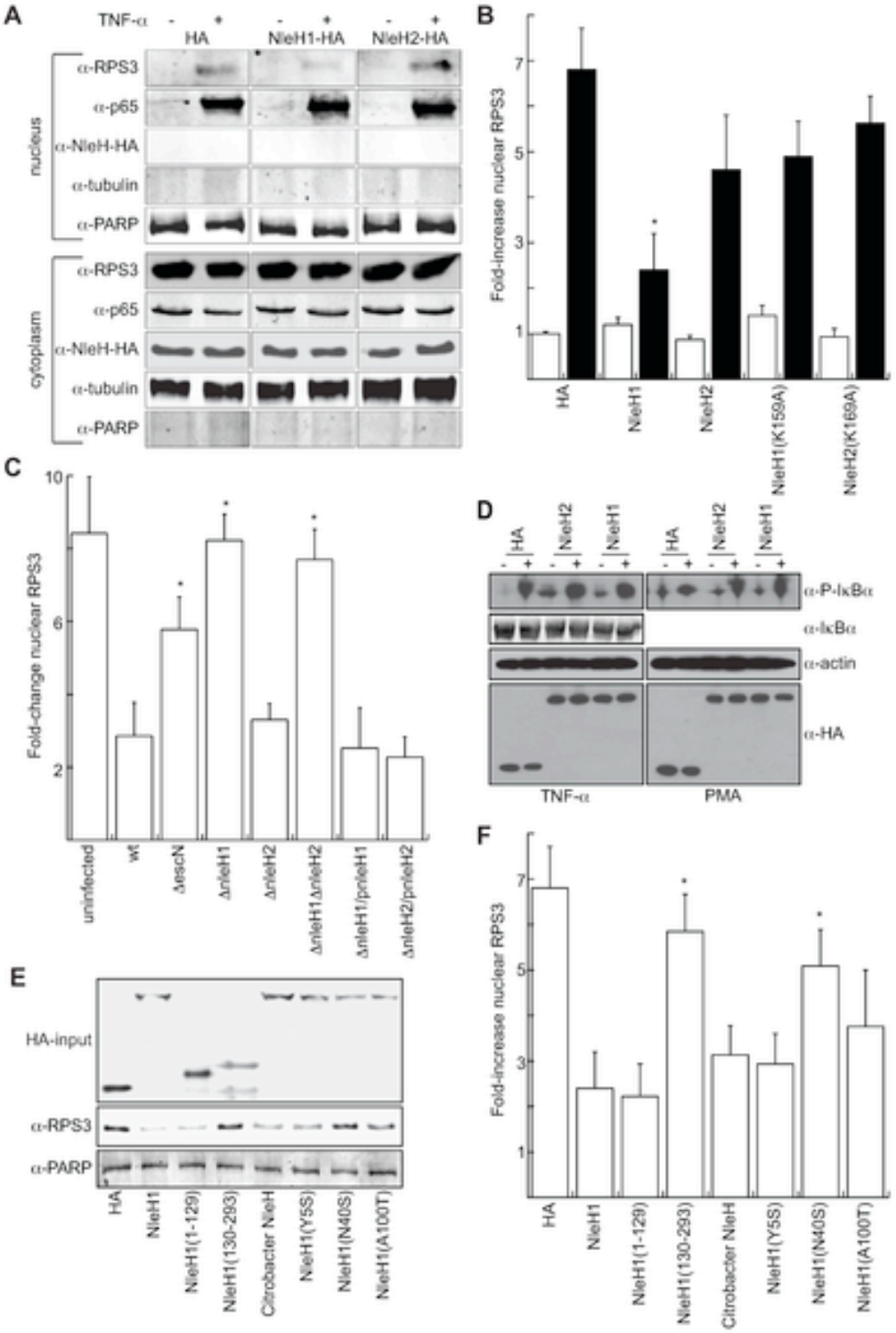
A
TNF-α
HA
NleH1-HA
NleH2-HA
nucleus
cytoplasm
α-RPS3
α-p65
α-NleH-HA
α-tubulin
α-PARP
B
Fold-increase nuclear RPS3
HA
NleH1
NleH2
NleH1(K159A)
NleH2(K169A)
C
Fold-change nuclear RPS3
uninfected
wt
ΔescN
ΔnleH1
ΔnleH2
ΔnleH1ΔnleH2
ΔnleH1/pnleH1
ΔnleH2/pnleH2
D
α-P-IκBα
α-IκBα
α-actin
α-HA
TNF-α
PMA
E
HA-input
α-RPS3
α-PARP
HA
NleH1
NleH1(1-129)
NleH1(130-293)
Citrobacter NleH
NleH1(Y5S)
NleH1(N40S)
NleH1(A100T)
F
Fold-increase nuclear RPS3
HA
NleH1
NleH1(1-129)
NleH1(130-293)
Citrobacter NleH
NleH1(Y5S)
NleH1(N40S)
NleH1(A100T)

Fig. 13. NleH1 reduces the nuclear abundance of RPS3. A. Quantification (n = 4) of the fold-increase in nuclear p65 as assessed from immunoblotting, in the absence (open bars) or presence (black bars) of TNF-α stimulation. p65 signal intensity was normalized to PARP. B. Immunofluorescence microscopy analysis of NleH and RPS3 localization as a function of TNF-α stimulation. HeLa cells were infected for 3 h with EPEC strains expressing NleH1- or NleH2-FLAG, treated with TNF-α (100 ng/ml) for 1 h, and stained with DAPI (blue), a-FLAG (green), and a-RPS3 (red) monoclonal antibodies. C. Immunoprecipitation of nuclear extracts with α-p65 antibody. Immunoprecipitated samples were immunoblotted for p65 and RPS3 in samples transfected with the indicated plasmids, in the absence or presence of TNF-α stimulation. The numbers below the gel indicate the relative RPS3 signal intensity (normalized to PARP). D. Immunoprecipitation of RPS3 with C. rodentium NleH and EHEC NleH1 site-directed mutants. 293T cells were transfected with the indicated plasmids for 48 h and immunoprecipitated with an α-HA antibody. Immunoprecipitated samples were immunoblotted for RPS3 and HA. The top panel indicates immunoprecipitated RPS3 as a function of plasmid transfection (N.S. is a non-specific band, used for normalization of sample loading). The middle and bottom panels indicate RPS3 and HA abundance in the cell lysates, respectively.

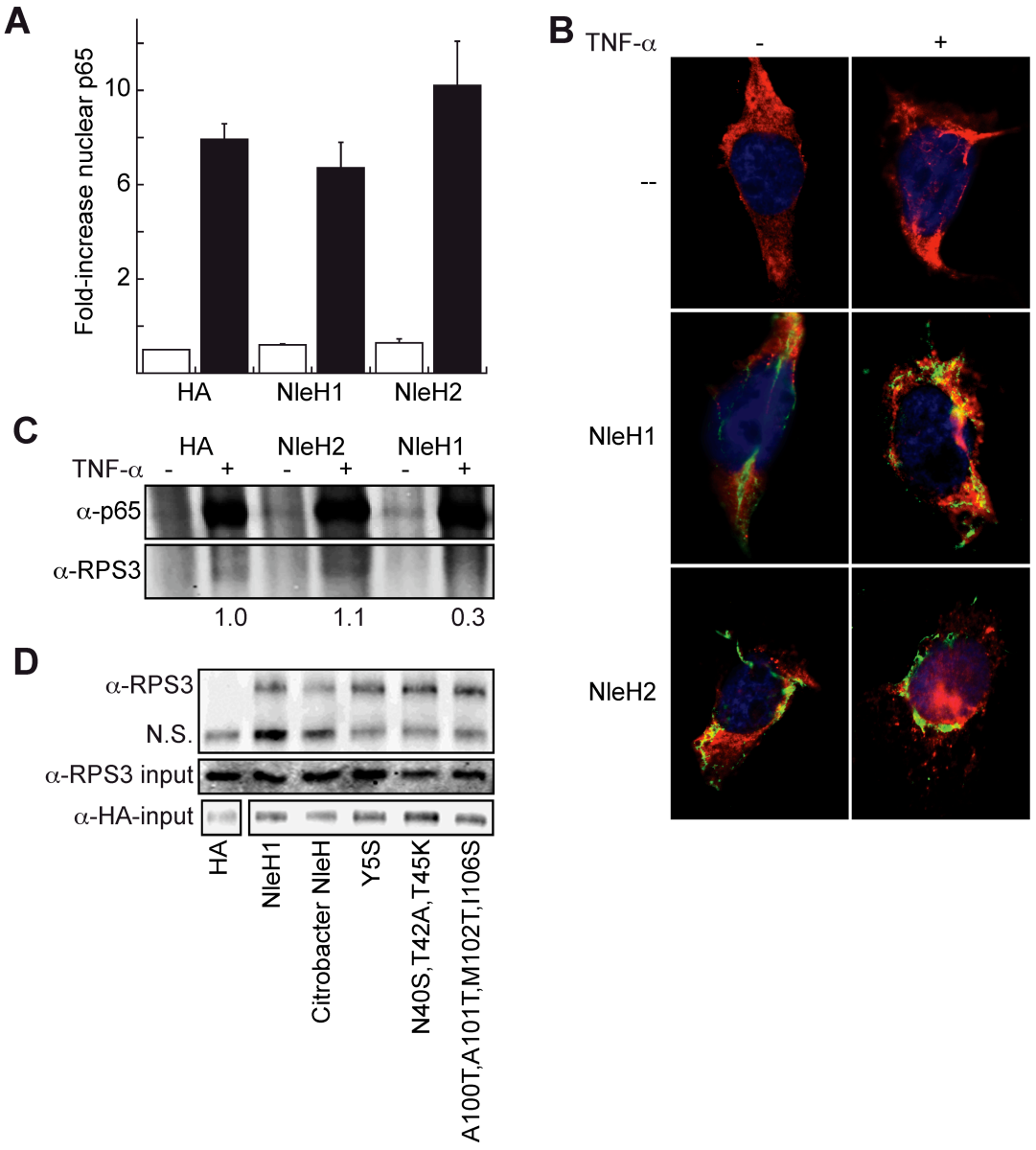
A
Fold-increase nuclear p65
10
6
2
HA
NleH1
NleH2
B
TNF-α
-
+
--
NleH1
NleH2
C
HA
NleH2
NleH1
TNF-α - + - + - +
α-p65
α-RPS3
1.0
1.1
0.3
D
α-RPS3
N.S.
α-RPS3 input
α-HA-input
HA
NleH1
Citrobacter NleH
Y5S
N40S,T42A,T45K
A100T,A101T,M102T,I106S

for 1 h to stimulate RPS3 nuclear translocation. Infection with Δ*nleH1* EHEC failed to inhibit RPS3 nuclear translocation, whereas infection with Δ*nleH2* was not significantly different from wild type EHEC (Figure 9C). Our analysis of the Δ*nleH1*Δ*nleH2* mutant also indicated that NleH1 is the EHEC effector primarily responsible for reducing the nuclear abundance of RPS3. Complementing *nleH* mutants with corresponding NleH-FLAG plasmids confirmed the dependence of alterations in RPS3 nuclear abundance upon NleH1 (Figure 9C). Neither NleH1 nor NleH2 impaired the TNF-α or phorbol 12-myristate 13-acetate (PMA)-induced phosphorylation of IκBα, nor did they alter total IκBα concentrations (Figure 9D), suggesting that unlike OspG, NleH1 and NleH2 do not alter the degradation of the inhibitory IκBα subunit. Overall, these data support a role for NleH1, but not NleH2, in the reduction of RPS3 nuclear abundance, without significant impact on other NF-κB subunits. While the NleH1 K159 residue was non-essential for RPS3 binding, it was important to the ability of NleH1 to reduce RPS3 nuclear abundance, suggesting that other host proteins or translocated effectors may be involved.

Functional differences between NleH1 and NleH2. Because our binding studies suggested that both NleH1 and NleH2 bind to RPS3, we were somewhat surprised to observe that only NleH1, and not NleH2, reduced RPS3 nuclear abundance. To begin to elucidate the functional differences between these two effectors, we sought to generate and characterize mutations in NleH1 that would still be competent for RPS3 binding, yet would fail to alter RPS3 nuclear abundance. Because we observed that NleH binding to RPS3 is mediated by the N-terminus, we targeted this region for mutagenesis and focused on several amino acids that differ between NleH1 and NleH2.

We first confirmed that *C. rodentium* NleH, which appears to be more similar to EHEC NleH1 than NleH2, also reduced RPS3 nuclear abundance (Figure 5E–F). By transfecting individually

the N- (AAs 1–129) and C-terminal (AAs 130–293) regions of NleH1, we also determined that the N-terminus of NleH1 was sufficient to reduce RPS3 nuclear abundance. We then constructed NleH1 mutants in which residues of NleH1 were swapped for those appearing in NleH2. These point mutants (Y5S; N40S,A42T,K45T; and A100T,A101T,M102I,I106S) were expressed at similar levels as wild type NleH1 and were able to bind RPS3 (Figure 9E and 10D). We determined that mutating the N40,A42,K45 region of NleH1 to S40,T42,T45 was sufficient to prevent the NleH1-mediated inhibition of RPS3 nuclear abundance (Figure 9E–F). Mutating the A100,A101,M102,I106 region had a modest, but statistically insignificant influence on NleH1 activity, whereas we found that mutating Y5 had no impact on NleH1 activity. Since *C. rodentium* NleH appears to have similar activity to EHEC NleH1, modulating RPS3 dynamics may be a strategy employed by multiple A/E pathogens.

NleH1 and NleH2 differentially regulate NF-κB-dependent transcriptional activity. After translocating into the nucleus, RPS3 selectively alters the expression of a subset of κB-dependent gene promoters to generate specific transcriptional responses to diverse extracellular signals (Wan et al., 2007). p65 binding to κB sites in IκBα, IL-8, and IL-2 promoters is significantly reduced in RPS3-knockdown cells, whereas RPS3-independent genes (e.g. CD25 and CD69) are unaffected. This observation suggests that selective gene expression is due to differing requirements of specific promoter sites for the RPS3 subunit of NF-κB. Because NleH1 and NleH2 bind to RPS3, with NleH1 reducing its nuclear abundance, and because RPS3 regulates NF-κB activity, we hypothesized that NleH1 and/or NleH2 might also alter NF-κB dependent transcription.

To test this hypothesis, we co-transfected HeLa cells with a firefly luciferase construct driven by a consensus κB site previously demonstrated to be responsive to RPS3, to measure NF-κB

activity. For data normalization, we used a renilla luciferase plasmid. We quantified luciferase activity and then calculated the fold-induction of NF-κB activity relative to unstimulated or uninfected cells.

Treating cells with TNF-α stimulated NF-κB-dependent luciferase activity ~12-fold (Figure 11A). Transfecting RPS3 siRNA reduced RPS3 protein abundance to ~20% of native levels (Figure S6A) and reduced the effect of TNF-α stimulation ~4-fold (Figures 11A and 12B), confirming the sensitivity of the luciferase assay and importantly, the significant dependence upon RPS3 for efficient NF-κB transcription from this κB site (Figure 11A). We infected HeLa cells with wild type and T3SS-deficient ΔescN EHEC. Our findings confirmed previous observations that T3SS effectors inhibit NF-κB (Figure 6A, $p<0.001$, ANOVA; [20]). We discovered that deleting nleH1, but not nleH2, prevented EHEC from suppressing NF-κB activity ($p = 0.002$), indicating that NleH1 inhibits NF-κB-dependent transcription. By complementing the nleH mutants with corresponding NleH-FLAG plasmids, we also confirmed the dependence of alterations in RPS3/NF-κB-dependent luciferase activity upon NleH (Figure 11A).

We obtained similar data after transfecting 293T cells with NleH1 and NleH2 and stimulating these cells with TNF-α. By transfecting *nleH1*, we were able to inhibit NF-κB activity to ~45% of native levels (Figure 11B; $p<0.001$, ANOVA). In contrast, transfecting *nleH2* stimulated NF-κB activity by ~20%. We observed the differential activity of NleH1 vs. NleH2 even after we introduced additional RPS3 via transfection of RPS3-FLAG (Figure 12C). This activity was also dose-dependent with respect to the amount of transfected NleH (Figure 12D). By mutating the NleH1 K159 residue to alanine [NleH1(K159)], we eliminated NleH1-mediated NF-κB inhibition (Figure 11B).

Furthermore, neither NleH1 nor NleH2 altered CD25- or IL-2R-dependent luciferase

expression. As these reporters are known to be RPS3-independent(Wan et al., 2007), these results further demonstrate the specificity of NleH for RPS3 (Figure 11C). Transfecting NleH2 increased the activity of an AP-1-dependent luciferase reporter, suggesting a potential target for this effector.

To extend our findings and to confirm that that activity of NleH1 is restricted to specific RPS3/NF-κB promoters, we performed RT-PCR to assess NleH regulation of several genes (IL-8, NFKBIA, and TNFIAP3) that are important to the innate response to infection and whose transcription is altered by rps3 knockdown. IL-8 gene transcription was activated by infection with wild-type EHEC, as expected. This activation was further increased after infecting cells with either Δ*escN* or Δ*nleH1*, but not Δ*nleH2*, indicating that a T3SS effector, most likely NleH1, inhibits IL-8 transcription (Figure 11D). Additionally, transcription of both the NFKBIA and TNFIAP3 genes were upregulated more in Δ*escN* and Δ*nleH1*, compared with wild-type and Δ*nleH2* infections, also suggesting a role for NleH1 in transcriptional inhibition of these RPS3-

Fig. 14. NleH effectors alter host NF-κB activity. **A.** Relative NF-κB activity (compared with uninfected cells) as a function of TNF-α stimulation, siRNA transfection, and/or infection with EHEC strains possessing or lacking *nleH1* and/or *nleH2* (n≥4). HeLa cells were co-transfected with a firefly luciferase construct driven by a consensus κB site and a renilla luciferase plasmid, cultured for 36 h, and then infected with EHEC strains for 3 h in the presence or absence of TNF-α stimulation or silencing with rps3 siRNA. Asterisks indicate significantly different compared with wild-type infection ($p<0.05$, ANOVA). **B.** Relative NF-κB activity in 293T cells transfected with the indicated NleH plasmids (n = 4). After 36 h, cells were stimulated with TNF-α (100 ng/ml, 1 h). Asterisks indicate significantly different compared with HA transfection ($p<0.05$, ANOVA). **C.** Impact of NleH1 and NleH2 on CD25 (left), IL-2R (middle), and AP-1 (right)-dependent luciferase reporter activity. 293T cells were transfected with the indicated reporter plasmids and treated with either TNF-α (CD-25 and IL-2R) or PMA (AP-1) 36 h post-transfection (n = 3). Asterisks indicate significantly different compared with HA transfection ($p<0.05$, ANOVA). **D.** Relative transcript abundance, relative to uninfected cells assessed by RT-PCR analysis of 293T cells infected for 4 h with the indicated bacterial strains. IL-8, NFKBIA, and TNFIAP3 data were normalized to GAPDH expression. **E.** Relative transcript abundance in 293T cells after 48 h transfection with HA, NleH1-HA, NleH2-HA, and RPS3-specific or sequence-scrambled (ns) siRNA constructs. IL-8, PLK1, CENPE, and IRF4 data were normalized to GAPDH expression. **F.** Impact of *C. rodentium* NleH and EHEC NleH1 truncations and site-directed mutants on RPS3/NF-κB-dependent transcriptional activity. Experiments were performed as described in panel B, using the plasmids indicated on the x-axis (n = 3). Asterisks indicate significantly different compared with NleH1 transfection ($p<0.05$, ANOVA).

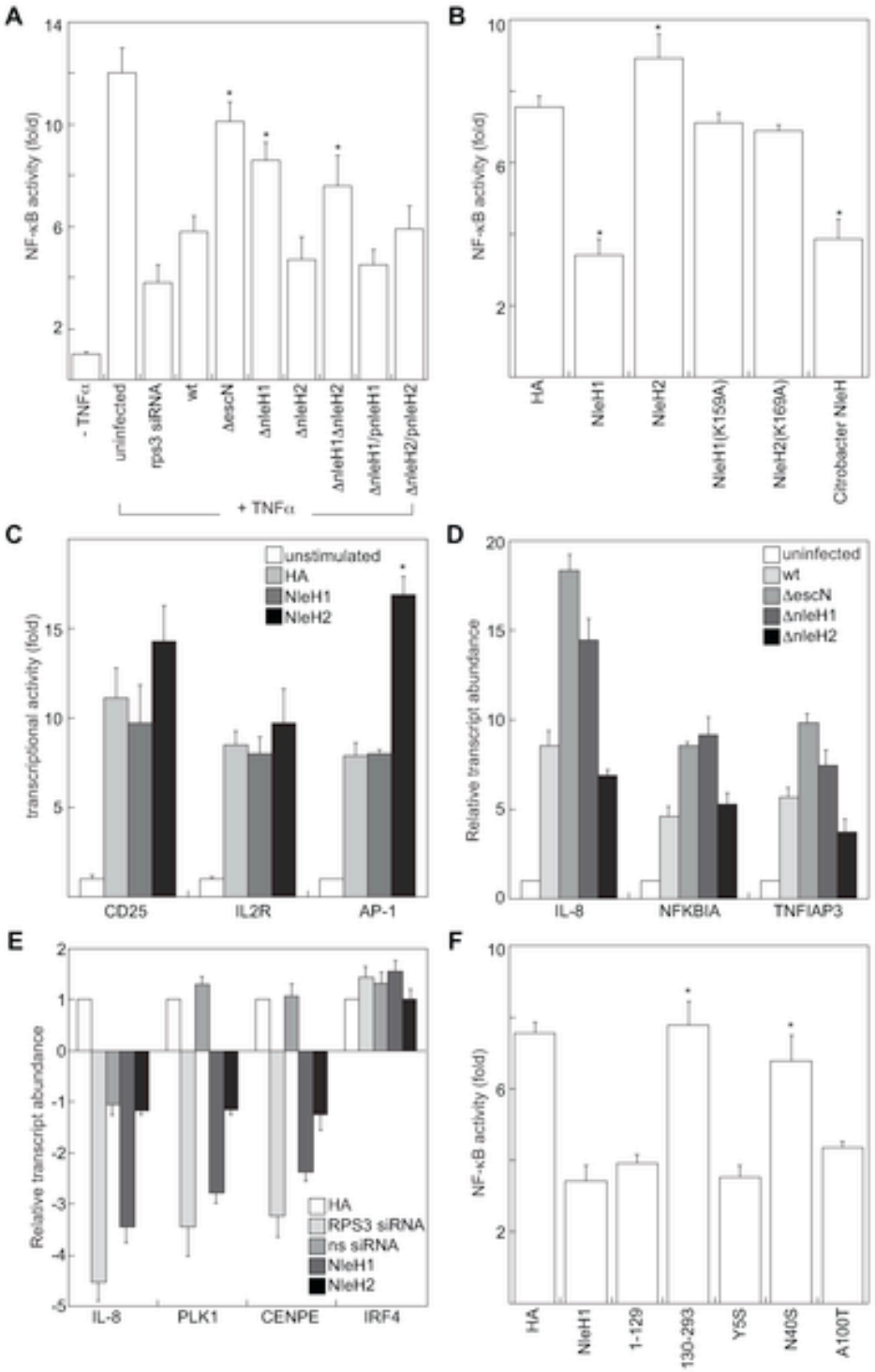
A
NF-κB activity (fold)
14
10
6
2
- TNFα
uninfected
rps3 siRNA
wt
ΔescN
ΔnleH1
ΔnleH2
ΔnleH1ΔnleH2
ΔnleH1/pnleH1
ΔnleH2/pnleH2
+ TNFα
B
NF-κB activity (fold)
10
6
2
HA
NleH1
NleH2
NleH1(K159A)
NleH2(K169A)
Citrobacter NleH
C
transcriptional activity (fold)
15
10
5
unstimulated
HA
NleH1
NleH2
CD25
IL2R
AP-1
D
Relative transcript abundance
20
15
10
5
0
uninfected
wt
ΔescN
ΔnleH1
ΔnleH2
IL-8
NFKBIA
TNFAIP3
E
Relative transcript abundance
2
1
0
-1
-2
-3
-4
-5
HA
RPS3 siRNA
ns siRNA
NleH1
NleH2
IL-8
PLK1
CENPE
IRF4
F
NF-κB activity (fold)
10
6
2
HA
NleH1
1-129
130-293
Y5S
N40S
A100T

Fig.15. Differential impact of NleH1 and NleH2 on NF-κB activity. A. Immunoblot analysis of RPS3 abundance after siRNA treatment. The numbers below the gel indicate the relative RPS3 signal intensity after normalization to tubulin. B. NF-κB activity (% activity compared to untreated samples) as a function of transfection with rps3 siRNA (open squares) and non-specific siRNA (closed squares). C. NF-κB activity as a function of transfection with RPS3-FLAG, in the presence of co-transfected HA (open circles), NleH1-HA (open squares), or NleH2-HA (closed squares). D. NF-κB activity as a function of transfection with HA (open circles), NleH1-HA (open squares), or NleH2-HA (closed squares).

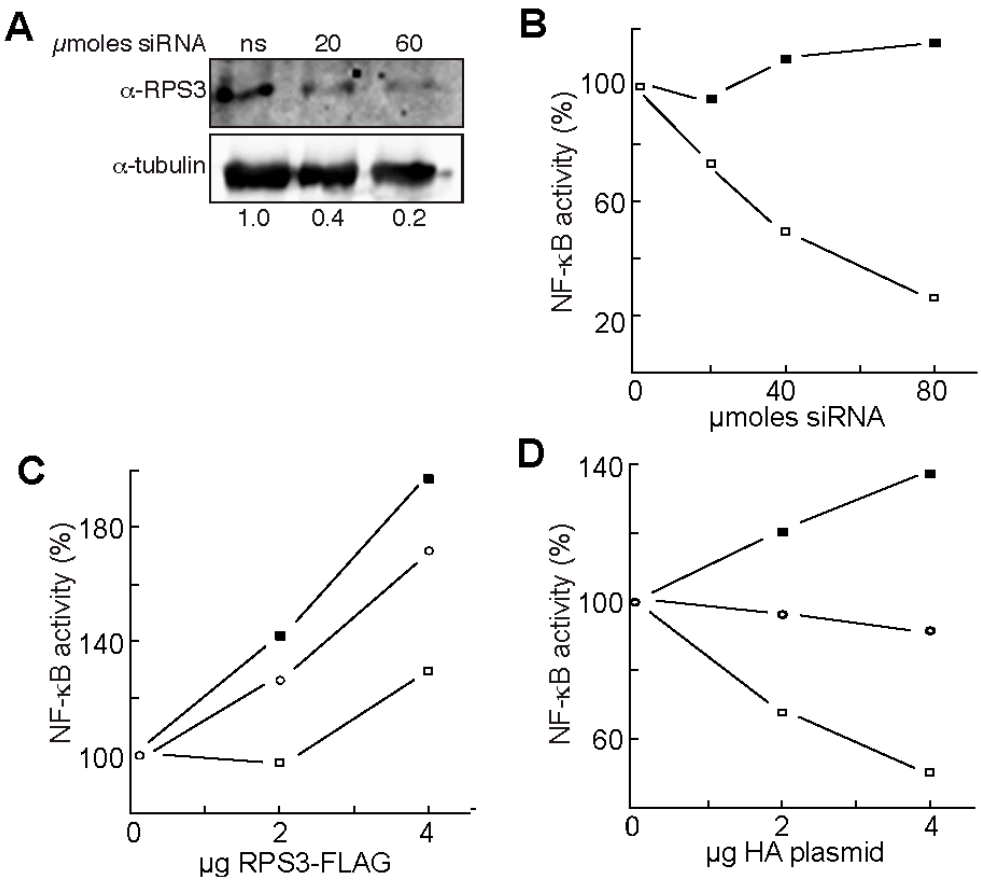
A
μmoles siRNA
ns
20
60
α-RPS3
α-tubulin
1.0
0.4
0.2
B
NF-κB activity (%)
100
60
20
0
40
80
μmoles siRNA
C
NF-κB activity (%)
180
140
100
0
2
4
μg RPS3-FLAG
D
NF-κB activity (%)
140
100
60
0
2
4
μg HA plasmid

dependent genes.

To confirm further the role of NleH1 in inhibiting RPS3-dependent gene expression, we also performed transfection experiments. Transfecting RPS3 siRNA into 293T cells inhibited IL-8 expression ~4.5-fold (Figure 11E). Transfecting NleH1, but not NleH2 reproduced this phenotype. The transcription of both PLK1 and CENPE, two genes involved in NF-κB activation (Guo et al., 2004), was also inhibited by rps3 knockdown and by NleH1, but not by a sequence-scrambled siRNA or by NleH2. In contrast, transcription of IRF4, an RPS3-indepenent gene, was unaffected. Overall, these infection and transfection experiments suggest that NleH1 specifically inhibits RPS3-dependent gene expression.

We also analyzed site-directed NleH1 mutants to extend our findings that suggest NleH1 and NleH2 have differential influence on NF-κB activity. Similar to RPS3 nuclear abundance data obtained after transfection with different NleH1 point mutants (Figure 9E–F), co-transfecting NleH1(N40S,A42T,K45T) abolished NleH1 inhibitory activity, whereas mutating either the Y5 or the A100,A101,M102,I106 region did not prevent NleH1 from inhibiting NF-κB (Figure 11F).

We wished to determine the extent to which NleH1 and NleH2 are conserved among other A/E pathogens. We first noted that *C. rodentium* NleH was also able to reduce RPS3 nuclear abundance (Figure 9E–F) and to inhibit RPS3/NF-κB luciferase activity (Figure 11B). We cloned *nleH* from other O157:H7 and O88:H25 strains and tested their ability to inhibit RPS3/NF-κB luciferase activity by transfecting them into 293T cells. NleH cloned from other O157:H7 inhibited NF-κB activity to the same magnitude as EDL933 NleH1 (92–96% of EDL933 activity; data not shown). NleH cloned from O88:H25 strains also inhibited NF-κB activity, but to a lesser extent (74–78% of EDL933). Overall, these data demonstrate that NleH-mediated inhibition of RPS3/NF-κB transcriptional activity is not restricted to EDL933, but

rather is conserved in non-O157 STEC and in *C. rodentium*.

***E. coli* O157:H7 ΔnleH1 is hypervirulent in gnotobiotic piglets.** The 1-day-old gnotobiotic pig is a robust model organism for studying human EHEC disease (Baker et al., 2007). Piglets challenged with EHEC develop diarrhea as a result of intimate bacterial attachment to the mucosal surfaces of the terminal ileum and large bowel. Infected piglets also develop fatal central nervous system (CNS) disease several days after inoculation (Francis et al., 1989)[46], an important, yet underappreciated side effect of hemolytic uremic syndrome (HUS; (Robson et al., 1991)). Anatomically and physiologically similar to human children, piglets develop CNS symptoms and intestinal lesions develop over a similar time course following the onset of diarrhea. EHEC infection of gnotobiotic piglets can be used to evaluate the contribution of virulence factors to host colonization and disease (Baker et al., 2007).

To measure the contribution of NleH1 and NleH2 to EHEC virulence *in vivo*, we orally infected gnotobiotic piglets at 24 h of age with 2*108 CFUs of wild type EHEC EDL933, Δ*nleH1*, or Δ*nleH2* (n = 5−6/group). Piglets were observed every 4 h for signs of diarrhea, dehydration, and neurological signs of disease. Piglets infected with wild-type EHEC succumbed to infection over a ~7-day period (Figure 13A, filled circles). Piglets infected with Δ*nleH1* (open circles), but not Δ*nleH2* (open squares), died more rapidly (Figure 13A; $p = 0.004$, Kruskal-Wallis test). Δ*nleH1* induced rapid and severe clinical signs of disease consistent with an inflammatory response (Figure 13B, left; $p = 0.02$), yet caused little diarrhea (Figure 13B, right; $p = 0.01$) and displayed significantly reduced colonization (Figure 13C; $p = 0.001$). In contrast, Δ*nleH2* had no effect on clinical outcome, though colonization of the piglet colon was reduced ~10-fold.

Discussion

PAMP recognition by TLRs transduces signals that activate and bind NF-κB to DNA (κB sites) within target gene promoters to regulate transcription by recruiting co-activators or co-repressors (Wan et al., 2007). Activation typically proceeds via degradation of the inhibitory NF-κB chaperone IκBα, favoring the nuclear localization of NF-κB. Bacterial pathogens inject effector proteins into host cells to inhibit the innate immune response by interfering with NF-κB activation (Bhavsar et al., 2007). For example, *Shigella* OspG is a protein kinase that binds to ubiquitinylated ubiquitin-conjugating enzymes (E2s) to block degradation of IκBα, an event that ultimately inhibits NF-κB activity. OspF is a phosphatase that targets MAPKs to prevent histone phosphorylation and dampen transcription at NF-κB-dependent promoters (Arbibe et al., 2007). OspB and OspF also interact with the retinoblastoma protein, possibly to facilitate chromatin remodelling and diminish inflammatory cytokine production (Zurawski et al., 2009). *Yersinia* YopJ inhibits the NF-κB pathway by inhibiting MAPKKs (Mukherjee et al., 2006). The *Salmonella* SseL effector is a deubiquitinating enzyme that impairs IκBα ubiquitination and degradation, thus reducing the production of NF-κB-dependent cytokines (Le Negrate et al., 2008). Mice lacking the p50 subunit of NF-κB (p50 /) do not clear a *C. rodentium* infection within the duration of the experiment (Dennis et al., 2008), indicating a critical role for NF-κB in host-defense against A/E pathogens. While the details have yet to be unravelled completely, EHEC T3SS effectors are suggested as key factors for bacterial inhibition of the host immune response.

Over a dozen ribosomal proteins that play significant roles in gene-specific transcriptional and translational regulation have been described (Lindstrom, 2009; Warner and McIntosh, 2009). For example, RPL7 binds the Vitamin D receptor to regulate gene transcription. Both RPL23 and

RPS9 interact with the nucleolar chaperone protein B23. B23, also termed NPM/nucleophosmin/NO38, is a cofactor of the zinc-finger protein Miz1, a regulator of cell proliferation (Wanzel et al., 2008). RPL11 binds directly to Myc and inhibits its transcriptional activation activity (Dai et al., 2007). Thus, the idea that ribosomal proteins also function in the nucleus to regulate transcription is well established, although until now, the targeting of these proteins by bacterial pathogens to subvert host cell functions was not.

By using several protein-interaction technologies, we determined that the translocated EHEC effectors NleH1 and NleH2 bind directly to the NF-κB non-Rel subunit, RPS3. NleH1 and NleH2 both interact with RPS3 through the binding of their N-termini to the N-terminal region of RPS3 that contains a putative nuclear localization signal (NLS). NleH1, but not NleH2, significantly reduced the nuclear abundance of RPS3, but had little influence upon other NF-κB subunits (e.g. p50 or p65). Using site-directed mutagenesis, we characterized a region of NleH1 (N40-K45) that is at least partially responsible for the inhibitory activity of this protein toward RPS3. By cloning and transfecting *nleH* from other O157 and non-O157 STEC, we demonstrated that NleH1 is present in other strains of significance to human health.

Although NleH1 and NleH2 are autophosphorylated proteins with Ser/Thr protein kinase activity, neither protein appeared to have the ability to phosphorylate RPS3. While the NleH1 K159 residue was non-essential for RPS3 binding, it was important to the ability of NleH1 to reduce RPS3 nuclear abundance, leaving open the possibility that other host proteins or translocated effectors may also be involved. Surprisingly, both the full-length and the isolated N-terminus of NleH1 (residues 1–139) inhibited RPS3 nuclear localization, while full-length NleH1 K159A site-directed mutant did not. Thus, NleH kinase activities may target another host protein with a role in RPS3 translocation, suggesting that NleH may be a multi-functional protein. We

speculate that the K159A mutant may have an altered structure or have reduced ability to bind other cellular factors that affect RPS3 activities.

Others and we have shown that NleH localizes to both host membranes and the cytosol following translocation (Garcia-Angulo et al., 2008). It is possible that the subcellular distribution of NleH may change to associate with the non-ribosomal pool of RPS3. It will be interesting to determine if mutating K159 somehow inhibits the ability of NleH to interact with a host protein needed for enrichment into the cytosol, a requirement that the isolated NleH N-terminus may not face.

The cellular factors governing the nuclear import of RPS3 are not completely understood. Its nuclear entry is thought to depend upon the phosphorylation of the T42 residue by the extracellular signal-regulated kinase (ERK)(Caamano et al., 1999). However, other reports suggest that PKCδ phosphorylates RPS3 on S6 and T221, resulting in RPS3 nuclear mobilization to participate in DNA repair activities (Kim et al., 2005b). Furthermore, the role of RPS3 phosphorylation in its interaction with NF-κB has not yet been studied in detail. As EPEC T3SS effectors have been shown to inhibit the phosphorylation-associated activation of ERK and p38 MAPK pathways (Ruchaud-Sparagano et al., 2007), it will be of interest to learn if there may be a link between NleH and ERK/MAPK pathways, some of which might also alter RPS3 function.

Despite the significant sequence identity among NleH1, NleH2 and OspG, a protein kinase which blocks degradation of IκBα, NleH1 or NleH2 did not appear to have the ability to alter IκBα degradation or to interact with the host ubiquitin machinery. However, it remains to be determined if NleH might associate with other E2 enzymes not studied in our assays. Notably, unlike NleH1 and NleH2, OspG does not possess the N-terminal region responsible for binding to RPS3, which might explain its differential activities and host targets.

Previous studies have elegantly shown that while A/E pathogens induce host IL-8 expression through both MAPK and TLR5-dependent activation of NF-κB, translocated effectors also down-regulate IL-8 at early stages of infection (Khan et al., 2008; Kim et al., 2007). However, only traditional NF-κB Rel proteins have been characterized in these studies. It is significant that these Rel proteins are associated with only ~60% of canonical- or related-κB sites (Martone et al., 2003). Thus, additional regulatory components, including RPS3, may contribute to high affinity DNA binding at various promoters (Wan et al., 2007). Our results suggest that NleH1, but not NleH2, down-regulates NF-κB activity at RPS3-dependent, but not RPS-independent promoters. We propose that NleH1-reduction of RPS3 nuclear abundance in response to PAMP detection may explain previously documented findings that IL-8 expression is suppressed at early stages of infection, even in the context of NF-κB Rel protein nuclear translocation and increased DNA-binding activity.

A *Shigella* OspG homolog in EHEC strain 11128 of *E. coli* serogroup O111 was recently described as a translocated effector (Nobe et al., 2009). This protein is somewhat distantly related (~30% identity) to NleH1 or NleH2 and lacks the N-terminal domain of NleH that is responsible for binding to RPS3. In this work, EHEC OspG was not found to inhibit significantly NF-κB activity. These authors showed that an EHEC T3SS effector, but not OspG, inhibited p65 nuclear translocation and *E. coli* strain 13369 altered IκBα degradation at 1 h post-infection. It was also previously shown that NleH2, rather than NleH1, is encoded by EHEC strains of the O111 serotype (Ogura et al., 2007). As we have shown that NleH1, but not NleH2, inhibits the contribution of RPS3 to NF-κB activity, it is perhaps not surprising that inhibition of NF-κB was not observed in the O111 strains recently examined. Consistent with these studies (Nobe et al., 2009), we also failed to observe a role for NleH in inhibiting p65 nuclear translocation. However,

Fig .16. Infection of gnotobiotic piglets with EHEC. A. Survival analysis of gnotobiotic piglets as a function of time post-inoculation with EHEC strains possessing or lacking *nleH1* or *nleH2*. B. Quantification of piglet clinical outcome (left) and extent of diarrheal disease following EHEC challenge (right). C. Quantification of EHEC colonization of piglet colonic tissue (CFUs/g colon).

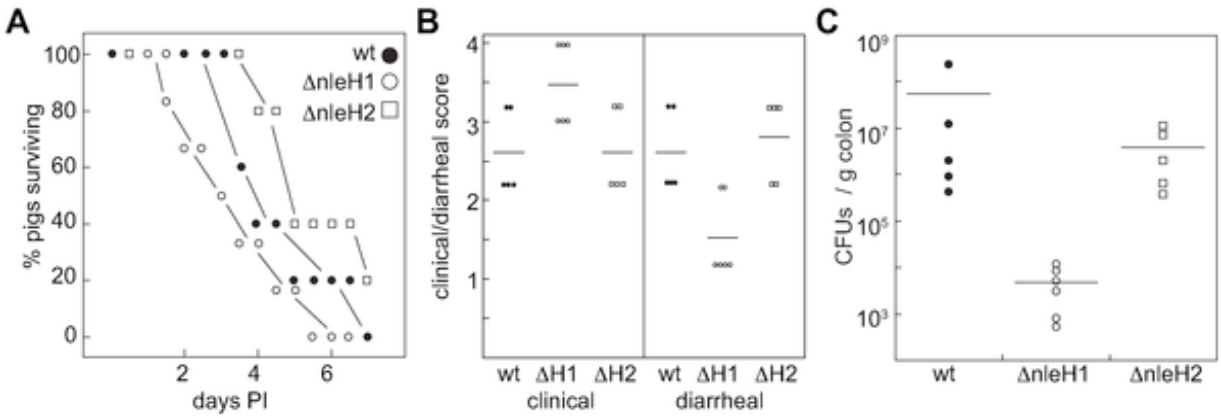
A
100
80
60
40
20
0
% pigs surviving
2
4
6
days PI
wt
ΔnleH1
ΔnleH2
B
4
3
2
1
clinical/diarrheal score
wt
ΔH1
ΔH2
clinical
wt
ΔH1
ΔH2
diarrheal
C
CFUs / g colon
wt
ΔnleH1
ΔnleH2

our analysis of NleH is limited to RPS3-dependent κB promoters and we consider it likely that other T3SS effectors will be discovered to inhibit NF-κB through other mechanisms.

While we did not observe NleH2 to inhibit RPS3 function, it may influence NF-κB through an alternative mechanism or affect other host signal transduction networks. Interestingly, NleH2 increased the activity of an AP-1-dependent luciferase reporter. EHEC infection has been shown to induce the phosphorylation of multiple MAPKs, including ERK1/2, p38, and JNK, which in turn induce AP-1 activation at later stages of infection (Dahan et al., 2002). There are multiple transcription factor binding sites in the IL-8 promoter, including both AP-1 and NF-κB (Mukaida et al., 1994). NleH1 and NleH2 may potentially target different host signal transduction pathways to contribute to the suppression of host innate responses to infection.

It was previously reported that an 'espG/orf3Δcore' EPEC mutant deficient in 'EspG/Orf3/EspH/CesF/Map/CesT/Tir/Intimin' did not differ from wild-type EPEC in its ability to inhibit IL-8 secretion from Caco-2 cells (Ruchaud-Sparagano et al., 2007). Because this mutant also lacked the chaperone CesT, it was predicted to be deficient in translocation of other effectors, including NleH. Thus, it was postulated that inhibition of IL-8 secretion might be due to a different non-LEE T3SS-dependent effector (Anantha et al., 1998). However, others reported that deletion of nleH in *C. rodentium* reduced TNF-α expression in infected mice, as compared with wild-type C. rodentium infection (Hemrajani et al., 2008). These contrasting results may also be a function of the different assay systems, cell types, and animal models employed. For example, it has been reported that the in vivo effect of NleH may be variable with respect to the host animal under investigation. Deleting both nleH1 and nleH2 from *E. coli* O157:H7 caused increased shedding compared with the parental strain in Friesian bull calves, yet had a reduced competitive advantage in mixed infections of lambs.

Our analysis of EHEC strains deleted for nleH1 and nleH2 in gnotobiotic piglets support a role for NleH1 in modulating the host innate response to infection. Previous studies have reported that severe HUS correlates with increased inflammation induced by STEC infection. Chemokines produced in response to bacterial PAMPs have been reported to lead to the stimulation and subsequent basolateral-to-apical transmigration of neutrophils, inducing concomitant translocation of Shiga-like toxins in the opposite direction (Hurley et al., 2001). Shiga toxin attachment to monocytes and macrophages can stimulate TNF-α, IL-1 and IL-6 secretion, subsequently increasing globotriaosylceramide (Gb3) expression on endothelial cell membranes (Stricklett et al., 2002). Intimin-negative STEC that lack the LEE (and thus are unlikely to translocate Nles) induce higher neutrophil migration and higher IL-8 secretion compared with intimin-positive STEC (Hurley et al., 2001). It should be noted that the primary cause of death in the gnotobiotic piglet model we employed is a manifestation of systemic intoxication, rather than diarrheal disease. As deleting nleH1 relieved the inhibition of NF-κB-dependent IL-8 gene expression in our in vitro assays, it is possible that deleting nleH1 could lead to greater neutrophil activation and Stx influx into the circulatory system.

Our findings suggest a novel mechanism for bacterial manipulation of the host response and demonstrate the direct binding of a bacterial effector to an NF-κB subunit. NF-κB is a major regulator of not only acute antimicrobial responses, but also adaptive immune responses. A growing number of cellular factors that govern the selective binding of NF-κB to different promoters (Wang et al., 2007; Wright and Duckett, 2009), combined with the discovery of novel bacterial effectors, provide us with significant opportunity to understand how pathogens subvert the host response to infection.

Experimental procedures

Ethics statement

All animal experiments were performed according to Institutional Animal Care and Use Committee-approved protocols (Animal Welfare Assurance no. A3958-01).

Materials

The TEM-1 fusion cloning vector pCX340 was a generous gift from E. Oswald. Chemicals were used according to manufacturers' recommendations and were obtained from Sigma, except for the following: myelin basic protein (New England Biolabs), Erk1 kinase (Cell Signaling), QuikChange Site-Directed Mutagenesis Kit (Stratagene), Dual-Luciferase Reporter Assay System (Promega), CCF2-AM Loading Kit (Invitrogen), Ni-NTA agarose (Qiagen), protein G agarose (Fisher), TNF-α (Genscript), RPS3 siRNA (Santa Cruz Biotechnology), and FuGene (Roche). Antibodies were obtained from the following sources: calnexin, His, FLAG, HA, β-actin, and tubulin (Sigma), phospho-Ser/Thr (Abcam), RPS3 (PrimmBiotech Inc.), RPS16 (Abnova), TEM (QED bioscience), p50/p105, p65, IκBα ubiquitin (Genscript), PARP (BD Biosciences), and phospho-IκBα (Cell Signaling).

Bacterial strains, plasmids, and oligonucleotides

The bacterial strains and plasmids used in this study are described in Table 1. The oligonucleotides used in this study are described in Table 2. The deletion of individual *nleH1* and

nleH2 genes, and the construction of a Δ*nleH1*Δ*nleH2* mutant was performed using lambda Red-mediated mutagenesis (Datsenko and Wanner, 2000) in *E. coli* O157:H7 EDL933 by replacing *nleH1* and/or *nleH2* with a kanamycin resistance marker, using plasmid pKD46 to generate the deletion cassettes. Gene replacements were confirmed with multiple PCRs and by RT-PCR. The bacterial growth kinetics, bacterial adherence to host cells, and Tir translocation into host cells did not differ significantly among *nleH* mutants and the parental strains.

Effector translocation assays

NleH-TEM fusions were constructed by cloning *nleH1 and nleH2* into pCX340. For assaying NleH-TEM translocation, plasmids were introduced into wild type and Δ*escN* EPEC and used to infect HeLa cells for 4 h in DMEM supplemented with 1 mM IPTG. Cells were washed and loaded with CCF2/AM. Fluorescence was evaluated after cells were illuminated at 409 nm (Charpentier and Oswald, 2004). NleH-FLAG fusions were constructed by cloning *nleH1* and *nleH2* into pFLAG-CTC (Sigma). HeLa cell monolayers were infected with EPEC strains (MOI ~100) for 4 h, washed, trypsinized, and resuspended in homogenization buffer (3 mM imidazole [pH 7.4], 250 mM sucrose, 0.5 mM EDTA). Cells were mechanically disrupted by vigorous passage through 22- and 27-gauge needles. Low-speed centrifugation (3,000 g, 15′) was applied to the homogenate to pellet the bacteria, unbroken HeLa cells, host nuclei, and cytoskeletal components. The supernatant was then subjected to ultracentrifugation (100,000 g, 1 h) to separate insoluble host cell membranes from soluble cytosolic proteins. The resulting fractions were resolved by SDS-PAGE (10% polyacrylamide) and transferred to nitrocellulose for Western blot analysis.

Table 1. Strains and plasmids utilized in this study.

Strain or plasmid	Description	Reference
Strains		
Escherichia coli BL21(DE3)	*E. coli* F$^-$ *ompT hsdSB* ($r_B^- m_B^-$) *gal dcm* (DE3)	Novagen
BL21(DE3)/pNleH1-pET28a	His-NleH1	This study
BL21(DE3)/pNleH2-pET28a	His-NleH2	This study
BL21(DE3)/pNleH1(K159A)-pET28a	His-NleH1 K159A mutant	This study
BL21(DE3)/pNleH2(K169A)-pET28a	His-NleH2 K169A mutant	This study
EPEC E2348/69	wild type *E. coli* O127:H6 isolate	(Levine et al., 1978)
E2348/69Δ*escN*	EPEC T3SS mutant	(Gauthier et al., 2003)
E2348/69/pNleH1-FLAG	EPEC expressing NleH1-FLAG	This study
E2348/69 Δ*escN*/pNleH1-FLAG	T3SS EPEC expressing NleH1-FLAG	This study
E2348/69/pNleH2-FLAG	EPEC expressing NleH2-FLAG	This study
E2348/69 Δ*escN*/pNleH2-FLAG	T3SS EPEC expressing NleH2-FLAG	This study
E2348/69/pNleH1-TEM	EPEC expressing NleH1-TEM	This study
E2348/69 Δ*escN*/pNleH1-TEM	T3SS EPEC expressing NleH1-TEM	This study
E2348/69/pNleH2-TEM	EPEC expressing NleH2-TEM	This study
E2348/69 Δ*escN*/pNleH2-TEM	T3SS EPEC expressing NleH2-TEM	This study
E2348/69/pNleH1(K159A)-TEM	EPEC expressing NleH1(K159A)-TEM	This study
E2348/69 Δ*escN*/pNleH1(K159A)-TEM	T3SS EPEC expressing NleH1(K159A)-TEM	This study
E2348/69/pNleH2(K169A)-TEM	EPEC expressing NleH2(K169A)-TEM	This study
E2348/69 Δ*escN*/pNleH2(K169A)-TEM	T3SS EPEC expressing NleH2(K169A)-TEM	This study
E2348/69/pTEM	EPEC expressing TEM	This study
E2348/69 Δ*escN*/pTEM	T3SS EPEC expressing TEM	This study
EPEC UMD207	EPEC *bfp-eae*-	(Donnenberg and Kaper, 1991)
EPEC UMD207/pNleH1-FLAG	UMD207 expressing NleH1-FLAG	This study
EPEC UMD207/pNleH2-FLAG	UMD207 expressing NleH2-FLAG	This study
EPEC UMD207/pNleH1(K159A)-FLAG	UMD207 expressing NleH1(K159A)-FLAG	This study
EPEC UMD207/pNleH2(K169A)-FLAG	UMD207 expressing NleH2(K169A)-FLAG	This study
EPEC UMD207/pFLAG	UMD207 expressing FLAG	This study
EPEC UMD207/pnleF-FLAG	UMD207 expressing NleF-FLAG	(Echtenkamp et al., 2008)
EHEC EDL933	wild type *E. coli* O157:H7 isolate	CDC

EDL933 Δ*escN*	EHEC T3SS mutant	J. Puente
EDL933 Δ*nleH1*	EHEC *nleH1* deletion	This study
EDL933 Δ*nleH2*	EHEC *nleH2* deletion	This study
EDL933 Δ*nleH1*Δ*nleH2*	EHEC *nleH1nleH2* deletion	This study
EDL933/pNleH1-FLAG	EHEC expressing NleH1-FLAG	This study
EDL933/pNleH2-FLAG	EHEC expressing NleH2-FLAG	This study
EDL933/pFLAG	EHEC expressing FLAG	This study
EDL933 Δ*nleH1*/pNleH1-FLAG	EHEC *nleH1* deletion expressing NleH1-FLAG	This study
EDL933 Δ*nleH2*/pNleH2-FLAG	EHEC *nleH2* deletion expressing NleH2-FLAG	This study
EDL933 Δ*nleH1*/pNleH1-FLAG(K159A)	EHEC *nleH1* deletion expressing NleH1(K159A)-FLAG	This study
EDL933 Δ*nleH2*/pNleH2-FLAG(K169A)	EHEC *nleH2* deletion expressing NleH2(K169A)-FLAG	This study

Plasmids

pCX340	TEM-1 reporter plasmid	(Charpentier and Oswald, 2004)
NleH1-TEM	NleH1-TEM	This study
NleH2-TEM	NleH2-TEM	This study
pET28a	Bacterial hexahistidine fusion expression	Novagen
NleH1-pET28a	His-NleH1	This study
NleH2-pET28a	His-NleH2	This study
NleH1(K159A)-pET28a	His-NleH1 K159A mutant	This study
NleH2(K169A)-pET28a	His-NleH2 K169A mutant	This study
pFLAG-CTC	Bacterial FLAG fusion protein expression	Sigma
NleH1-pFLAG-CTC	NleH1-FLAG	This study
NleH2-pFLAG-CTC	NleH2-FLAG	This study
NleH1(K159A)-pFLAG-CTC	NleH1(K159A)-FLAG	This study
NleH2 (K169A)-pFLAG-CTC	NleH2(K169A)-FLAG	This study
NleF-pFLAG-CTC	NleF-FLAG	(Echtenkamp et al., 2008)
p3XFLAG	Mammalian FLAG fusion expression	Sigma
RPS3-p3XFLAG	FLAG-RPS3	(Wan et al., 2007)
RPS3(1-101)-p3XFLAG	FLAG RPS3 (AAs 1-101)	(Wan et al., 2007)
RPS3(ΔKH)-p3XFLAG	FLAG RPS3 (lacking KH domain AAs 41-111)	(Wan et al., 2007)
RPS3(41-243)-p3XFLAG	FLAG RPS3 (AAs 41-243)	(Wan et al., 2007)
RPS3(112-243)-p3XFLAG	FLAG RPS3 (AAs 112-243)	(Wan et al., 2007)
κB (5X)-luc	Firefly luciferase driven by RPS3/NF-κB-dependent κB site	Promega

pTKRL-luc	Renilla luciferase	Promega
IL-2R-luc	Firefly luciferase driven by IL-2R promoter	(Wan et al., 2007)
CD25-luc	Firefly luciferase driven by CD25-promoter	(Wan et al., 2007)
AP-1-luc	Firefly luciferase driven by AP-1-promoter	(Wan et al., 2007)
pKD46	Lambda Red mediated mutagenesis	(Datsenko and Wanner, 2000)
VN	Venus fluorescence protein (AAs 1-173)	(Nagai et al., 2002)
VC	Venus fluorescence protein (AAs 155-238)	(Nagai et al., 2002)
VN-actin	Venus fluorescence protein (AAs 1-173 fused to human actin)	(Nagai et al., 2002)
VC-actin	Venus (AAs 155-238 fused to human actin	(Nagai et al., 2002)
VN-NleH1	Venus 1-173 fused to NleH1	This study
VC-NleH1	Venus 155-238 fused to NleH1	This study
VN-NleH2	Venus 1-173 fused to NleH2	This study
VC-NleH2	Venus 155-238 fused to NleH2	This study
VN-RPS3	Venus 1-173 fused to RPS3	This study
VC-RPS3	Venus 155-238 fused to RPS3	This study
VN-NleH1(1-129)	Venus 1-173 fused to NleH1 AAs 1-129AA	This study
VN-NleH1(130-293)	Venus 1-173 fused to NleH1 AAs 130-293 AA	This study
VN-NleH2(1-139)	Venus 1-173 fused to NleH2 AAs 1-139AA	This study
VN-NleH2(140-303)	Venus 1-173 fused to NleH2 AAs 140-303	This study
VN-Citro-NleH	Venus 1-173 fused to *C. rodentium* NleH	This study
VN-NleH1(Y5S)	Venus 1-173 fused to NleH1(Y5S)	This study
VN-NleH1(N40S,A42T,K45T)	Venus 1-173 fused to NleH1(N40S,A42T,K45T)	This study
VN-NleH1 (A100T,A101T,M102I,I106S)	Venus 1-173 fused to NleH1(A100T,A101T,M102I,I106S)	This study

Table 2. Oligonucleotides used in this study.

Primer	Sequence (5'-3')
NleH1 XhoI-f -FLAG/HA	$G_2CTCGAGATGT_2ATCGC_2ATAT_2CTGTA_3T_3G_3$
NleH1 BamHI-f-His	$G_4ATC_2ATGT_2ATCGC_2ATAT_2CTGTA_3T_3G_3$
NleH1 KpnI-r-FLAG	$C_2G_2TAC_2A_2T_4ACT_2A_2TAC_2ACACTA_2TA_2GATCT_2GCT_3C_2GC_2$
NleH1 XhoI-r-His	$C_3TCGAGA_2T_4ACT_2A_2TAC_2ACACTA_2TA_2GATCT_2GCT_3C_2GC_2$
NleH2 XhoI-f-FLAG/HA	$G_2CTCGAGATGT_2ATCGC_3TCT_2CTATA_3T_3G_3$
NleH2 BamHI-f-His	$G_4ATC_2ATGT_2ATCGC_3TCT_2CTATA_3T_3G_3$
NleH2 KpnI-r-FLAG	$C_2G_2TAC_2TATCT_2ACT_2A_2TACTACACTA_2TA_2GATC_2AGCT_3C_2$
NleH2 XhoI-r-His	$C_3TCGAGTATCT_2ACT_2A_2TACTACACTA_2TA_2GATC_2AGCT_3C_2$
NleH2 XmaI-r	$C_5G_3TATCT_2ACT_2A_2TACTACACTA_2TA_2GATC_2AGCT_3C_2$
NleH1 XhoI-f	$CTCGAGATGT_2ATCGC_2ATAT_2CTG$
NleH1 NdeI-f-TEM	$GCCATATGT_2ATCGC_2ATAT_2CTGTA_3T_3G_3$
NleH1 KpnI-r-TEM	$GCG_2TAC_2A_2T_4ACT_2A_2TAC_2ACACTA_2TA_2G$
NleH2 NdeI-f-TEM	$GC_2ATATGT_2ATCGC_3TCT_2CTATA_3T_3G_2$
NleH2 KpnI-r-TEM	$GCG_2TAC_2TATCT_2ACT_2A_2TACTACACTA_2TA_2G$
NleH1 K159A-f	$GCA_2CA_4GTC_2TG_2CGATGT_3ACTACATCTC$
NleH1 K159A-r	$GAGATGTAGTA_3CATCGC_2AG_2ACT_4GT_2GC$
NleH2 K169A–f	$CA_2CA_4GTGT_2G_2CGATGT_3ACTATATCTC$
NleH2 K169A–r	$GAGATATAGTA_3CATCGC_2A_2CACT_4GT_2G$
RPS3 XhoI-f-HA	$GC_2TCGAGATG_2CAGTGCA_3TATC_2A_2GA_2GAG_2$
RPS3 NotI-r-HA	$GCGCG_2C_2GCT_2ATGCTGTG_4ACTG_2CTG_4C$
NleH1 NotI-r-HA	$C_2GCG_2C_2GCT_2A_3T_4ACT_2A_2TAC_2ACACTA_2TA_2G$
NleH2 NotI-r-HA	$C_2GCG_2C_2GCT_2ATATCT_2ACT_2A_2TACTACAC$
NleH1 pKD4-f	$TGTATGT_2ATCGC_2ATAT_2CTGTA_3T_3G_3ATGT_2CTGTGTAG_2CTG_2AGCTGCT_2CG$
NleH1 pKD4-r	$GATA_4T_2ACTA_3T_4ACT_2A_2TAC_2ACACTA_2TA_2GCATATGA_2TATC_2TC_2T_2AG$
NleH2 pKD4-f	$C_2TCT_2CTATA_3T_3G_3ATGT_2CATG_2A_2T_2CT_3A_2CGTGTAG_2CTG_2AGCTGCT_2C$
NleH2 pKD4-r	$A_2TACTACACTA_2TA_2GATC_2AGCT_3C_2TC_2GTGATA_2GCATATGA_2TATC_2TC_2T_2A$
NleH1 N-term-NotI-r-HA	$GCGCG_2C_2GCT_2A_2TAGTC_2ACACTCG_2TA_2CTCTG_2CG$
NleH1 C-term-XhoI-f-HA	$GC_2TCGAGATGA_2CAG_2T_2GTCAGTAC_2TG_2TA_2TG$
NleH2 N-term-NotI-r-HA	$GCGCG_2C_2GCT_2AGT_2GCTA_2C_3TCG_2CA_2CTCTGAT_2G$
NleH2 C-term-XhoI-f-HA	$GC_2TCGAGATGA_2TA_3TCAC_3GTGC_2AG_2TA_2TG$
NleH1 Y5S-f	$ATGT_2ATCGC_2ATCT_2CTGTA_3T_3G_3ATGT_2C$

NleH1 Y5S-r	$GA_2CATC_3A_3T_3ACAGA_2GATG_2CGATA_2CAT$
NleH1 N40S-f	$GC_2GT_2CAT_2CTGATAGCG_3ACGCA_2GTA_2CG_2T_2G_2C$
NleH1 N40S-r	$GC_2A_2C_2GT_2ACT_2GCGTC_3GCTATCAGA_2TGA_2CG_2C$
NleH1 A100T-f	$CAC_2AGTGAGCACGACTATAGA_3GAG_2CTCTGT_2CAT_2CGA_2C$
NleH1 A100T-f	$GT_2CGA_2TGA_2CAGAGC_2TCT_3CTATAGTCGTGCTCACTG_2TG$
GAPDH RT-f	$AC_2AG_2TG_2TCTC_2TCTGACT_2C$
GAPDH RT-r	$GTG_2TCGT_2GAG_2GCA_2TG$
IL-8 RT-f	$CTG_2C_2GTG_2CTCTCT_2G$
IL-8 RT-r	$C_2T_2G_2CA_4CTGCAC_2T_2$
NFKBIA RT-f	$C_5TACAC_2T_2GC_2TGTG$
NFKBIA RT-r	$TCAGCAC_3A_2G_2ACAC_2A_2$
TNFIAP3 RT-f	$T_2GC_2TCATGCATGC_2ACT_2$
TNFIAP3 RT-r	$AGCA_3GC_4GT_3CA_2CA$
PLK1 RT-f	$GAG_2AG_2A_3GC_3TGACTGA$
PLK1 RT-r	$GCAGC_2A_2GCACA_2T_3GC$
CENPE RT-f	$GC_2A_2GACG_2AC_2A_2GCA$
CENPE RT-r	$TGCT_2GTAGCTGCGCT_2C_2T$
IRF4 RT-f	$TG_2T_2GC_2AG_2TGACAG_2A_2$
IRF4 RT-r	$TC_2AG_2T_2GCTG_2CGTCATA$

Protein purification

nleH1 and *nleH2* were cloned into pET-28a and expressed in *E. coli* BL21(DE3). 250 ml of bacterial culture were grown to an OD600 of 0.6, when IPTG was added to 1 mM. After 4 h additional growth, cells were pelleted and resuspended in 25 ml cold PBS. Cells were sonicated and centrifuged to clarify the supernatant. The supernatant was added to pre-equilibrated Ni-NTA agarose and incubated for 2 h. The slurry was washed 5 times with 60 mM imidazole, 500 mM NaCl, 20 mM Tris HCl pH 7.9, eluted in 1 M imidazole, 1 M NaCl, 40 mM Tris HCl pH 7.9, and analyzed on 12% SDS-PAGE.

Affinity columns

Thirty confluent 150 mM dishes of HeLa cells were washed with PBS and lysed in 20 ml of binding buffer [150 mM NaCl, 20 mM Tris (pH 8.0), 1% Triton X-100]. After centrifugation (5,000 g, 4°C, 10′), 10 ml of the supernatant was transferred to a 15 ml conical tube containing 300 µl Ni-NTA agarose in the presence or absence of 500 µg purified His-NleH1. After incubation for 1 h at 4°C, the columns were washed with binding buffer and then eluted with increasing concentrations of imidazole (0–300 mM). Fractions were analyzed by SDS-PAGE and staining with Coomassie Blue G-250.

Protein identification by LC-ESI-MS/MS

Bands excised from protein gels were digested in-gel with trypsin at 37°C overnight. The

tryptic peptide solution was transferred to a microcentrifuge tube, extracted with 1% formic acid, 2% acetonitrile in water, followed by extraction with 50% acetonitrile. Both extracts were combined, concentrated, and suspended in 3% acetonitrile, 0.1% formic acid. Peptide analysis was performed using LC-ESIMS/MS. Peptides were desalted in-line and concentrated with RP-Trap Symmetry300 C18 column, 5 μm NanoEase (Waters), and separated using a C18 RP PepMap capillary column on a CapLC (Dionex). The eluted ions were analyzed by one full precursor MS scan (400–1500 m/z), followed by four MS/MS scans of the most abundant ions detected in the MS scan. Spectra were obtained in the positive ion mode with a nano ESI-Q-Tof micro mass spectrometer (Micromass). A peak list (PKL format) was generated to identify +1 or multiple charged precursor ions from the mass spectrometry data file. Mascot server v2.2 (www.matrix-science.com) in MS/MS ion search mode was applied to conduct peptide matches (peptide masses and sequence tags) and protein searches against NCBInr v20080110.

Immunoprecipitation and immunoblotting

Bacterial strains were grown in Luria–Bertani (LB) broth, at 37°C in 5% CO2 without shaking. HeLa cells were grown in Dulbecco's minimal Eagle medium (DMEM) supplemented with 10% heat-inactivated fetal calf serum (FCS). Cell culture media was replaced with DMEM 3 h prior to infection. Overnight bacterial cultures were diluted 1:10 into DMEM, incubated 3 h at 37°C in 5% CO2 (to ‘pre-activate’ the T3SS; (Dean et al., 2006)[72]) and used to infect two 150 mm dishes of ~80% confluent HeLa cells at a multiplicity of infection of ~50. Cells were harvested after a 4 h infection by washing them 3 times with PBS to remove bacteria. Cells were scraped into PBS, pooled, centrifuged (1,500 g, 5′), resuspended in PBS, and recentrifuged. The

supernatant was removed and cells were lysed in RIPA [150 mM NaCl, 50 mM Tris pH 8.0, 0.4 mM EDTA, 10% glycerol, 1% Nonident P-40 (NP-40)], followed by brief vortexing and rotation for 30′ at 4°C. The supernatant was transferred to a tube containing protein G sepharose (prewashed in RIPA) and incubated for 1 h at 4°C. Samples were centrifuged (1,500 g, 5′), transferred to prewashed α-FLAG resin, and incubated with rotation overnight at 4°C. FLAG resin was washed with RIPA and resuspended in 500 µl RIPA (without NP-40). The resin was centrifuged (2,000 g, 5′) and the supernatant was removed with a 29-gauge needle. NleH-FLAG and associated proteins were eluted from the resin by adding 72 µg FLAG peptide (in 200 µl RIPA) and incubating with rotation for 1 h at 4°C. The resin was centrifuged (2,000 g, 5′), and the supernatant was transferred to a fresh tube, precipitated with trichloroacetic acid (TCA), and resuspended in SDS-PAGE buffer. IP samples were interrogated for the presence of NleH-FLAG and RPS3 by Western blotting.

Equal amounts of protein from cell lysates (50 µg) and IPs (5 µg) were separated by SDS-PAGE, transferred to nitrocellulose, blocked in Odyssey blocking buffer, double-probed overnight with mouse-α-FLAG and rabbit-α-RPS3 1° antibodies, washed in PBS, and then incubated for 30′ with Alexa Fluor 680/750 goat-α-rabbit and goat-α-mouse 2° antibodies at room temperature. After rinsing in PBS, blots were imaged with an Odyssey infrared imaging system (Li-Cor). For immunoprecipitation experiments with transfected RPS3 and NleH plasmids, 293T cells were incubated in 6-well plates and transfected with 1 µg total plasmid using FuGene.

Bimolecular fluorescence complementation

HeLa cells were cultured in DMEM supplemented with 10% FCS and co-transfected with a pair of BiFC plasmids (100–250 ng each) representing NleH and RPS3 truncations cloned as fusions to the N- or C-terminus of Venus eYFP (designated VN and VC). The fluorescence intensities derived from BiFC (due to effector-host protein binding) were measured after 48 h incubation using appropriate filters (excitation: 500/20 nm; emission: 535/30 nm).

Immunofluorescence microscopy

HeLa and 293T cells were grown on glass coverslips in 24-well tissue culture plates and infected for 4 h with overnight cultures of indicated bacterial strains (MOI~20–50). After infection, cells were washed 3 times in PBS containing Ca2+/Mg2+ and fixed in 2.5% paraformaldehyde. Cells were permeabilized in 0.1% saponin in PBS, blocked with 5% goat serum, and incubated with α-FLAG (1:1,000), and α-RPS3 (1:200) primary antibodies for 1 h at room temperature. The cells were washed with PBS and probed with Alexa Fluor 488- and 594-conjugated secondary antibodies (1:1,000, 1 h) and DAPI (1 μg/ml, 2′). For experiments involving transfection, 1 μg total plasmid suspended in Fugene was used and cells were typically immunostained 48 h post-transfection. Coverslips were mounted in Mowiol and samples were visualized using a LSM 510 Laser Scanning Microscope (Carl Zeiss).

In vitro kinase assays

Kinase assays were performed by incubating His-NleH proteins (10 ng/μl) with myelin basic protein (MBP, 100 ng/μl) in 50 mM Tris-HCl, pH 7.6, 5 mM MgCl2, 1 mM DTT, 1 mM ATP, at

30°C for 1 h. Phosphorylation was monitored by separating the samples by SDS-PAGE and Western blotting with an a-phospho-Ser/Thr-specific antibody [40] and Pro-Q staining. As a positive control in the assay, ERK1 was used at a concentration of 5 ng/μl, as it is known to phosphorylate MBP.

RPS3 nuclear translocation

Cytosolic and nuclear protein extracts were prepared from HeLa or 293T cells transfected with NleH plasmids or infected with *nleH* mutants as previously described (Wan et al., 2007). TNF-α stimulation (1 h, 100 ng/ml) was used to promote RPS3 translocation into the nucleus. Data were analyzed by Western blotting for nuclear RPS3. PARP and tubulin were used to normalize the protein concentrations of nuclear and cytoplasmic fractions, respectively.

Luciferase assays

HeLa or 293T cells were co-transfected at a ratio of 10:1 (1.0 μg total DNA) with a firefly luciferase construct driven by a consensus κB site, together with the renilla luciferase pTKRL plasmid (Promega), cultured for 36–48 h, and then infected with EHEC strains for 3 h, in the presence or absence of TNF-α stimulation (κB, CD25, IL-2R reporters) or PMA (AP-1 reporter) or silencing with rps3 siRNA. Cells were lysed with passive lysis buffer and lysates were analyzed by using the Dual-Luciferase Kit (Promega) with firefly fluorescence units (FU) normalized to renilla FU. The fold-induction was calculated as [relative FU stimulated)/(relative FU unstimulated] samples. Luciferase assays were performed in triplicate with at least three

independently transfected cell populations.

RT-PCR

cDNA was prepared from 1 μg RNA by using the Superscript First Strand System (Invitrogen) with oligo (dT) primer. Real-time PCR was performed in triplicate using a SYBR Green PCR Master Mix (Ambion) in a Fast 7500 sequence-detection system (Applied Biosystems). Relative transcription levels were calculated by using the ΔΔCt method.

Gnotobiotic piglet infections

Gnotobiotic piglets were delivered into germ-free incubators through sterile closed hysterotomy of pregnant sows. Piglets were separated into individual compartments without regard to sex, fed individually with a sterile commercial piglet formula (SPF-Lac; PetAg, Inc.), and inoculated at 24 h of age with 3 ml tryptic soy broth containing 1*108 CFUs of wild type, *Δnle1*, or *Δnle2 E. coli* O157:H7 EDL933. Piglets were observed every 4 h for signs of diarrhea, dehydration, and neurological signs of disease (head tilt, circling, lethargy, inability to stand, lateral recumbency and paddling). When piglets developed severe dehydration, lethargy or CNS disease, they were euthanized and subjected to postmortem examination. Animals that did not become lethargic or dehydrated were euthanized after 8 d. Spiral colon specimens were collected at necropsy, split longitudinally, rinsed in PBS to remove feces, diluted 1:10 (*w/v*) in PBS, ground, normalized to tissue weight, serially diluted, and cultured to quantify the extent of intestinal colonization. Data were normalized by tissue weight.

Statistical analyses

NleH translocation, BiFC, RPS3 immunoblotting, luciferase, and RT-PCR assays were analyzed statistically using one-way ANOVA. RPS3 immunofluorescence data were analyzed with t-tests. Gnotobiotic piglet data were analyzed with the Kruskal-Wallis Test. p-values<0.05 were considered significant.

ACKNOWLEDGEMENTS

Dr. Fengyi Wan and Dr. Michael Lenardo performed experiments identifying IKKβ-mediated RPS3 phosphorylation and conducted functional analysis of RPS3 phosphorylation in NF-κB activation.

Chapter III: IKK phosphorylation regulates RPS3 nuclear translocation and NF-κB function during infection with *Escherichia coli* strain O157:H7

Abstract

NF-κB is a major gene regulator in immune responses, and ribosomal protein S3 (RPS3) is an NF-κB subunit that directs specific gene transcription. However, it is unknown how nuclear translocation of RPS3 is regulated. Here we report that phosphorylation of RPS3 Ser209 by the kinase IKKβ was crucial for nuclear localization of RPS3 in response to activating stimuli. Moreover, virulence protein NleH1 of the foodborne pathogen *Escherichia coli* strain O157:H7 specifically inhibited phosphorylation of RPS3 Ser209 and blocked RPS3 function, thereby promoting bacterial colonization and diarrhea but resulting in less mortality in a gnotobiotic piglet-infection model. Thus, the IKKβ-dependent modification of a specific amino acid in RPS3 promoted specific NF-κB functions that underlie the molecular pathogenetic mechanisms of *E. coli* O157:H7.

Introduction

The pleiotropic transcription factor NF-κB regulates crucial cellular functions, and diverse stimuli activate NF-κB, which in turn regulates a vast array of genetic targets (Lenardo and Baltimore, 1989; Vallabhapurapu and Karin, 2009). The best-known mammalian NF-κB subunits are the Rel proteins, including RelA (p65), RelB, c-Rel, p50 and p52 (Chen and Greene, 2004; Rothwarf and Karin, 1999). However, ribosomal protein S3 (RPS3) has been shown to be a key non-Rel subunit of certain native NF-κB complexes (Wan et al., 2007). RPS3 is defined as a 'specifier' subunit of NF-κB, because it facilitates high-affinity binding of DNA and thus determines the regulatory specificity of NF-κB for selected target genes (Wan and Lenardo, 2009). The regulation of NF-κB by RPS3 governs key physiological processes, including expression of the immunoglobulin-κ light-chain gene and receptor editing in B cells (Cadera et al., 2009; Mukherjee et al., 2006), cytokine production in T cells (Mukherjee et al., 2006), and host defense against enterohemorrhagic *Escherichia coli* (Gao et al., 2009). In particular, the type III secretion system effector protein NleH1 of *E. coli* strain O157:H7 selectively blocks the transcription of NF-κB target genes by attenuating nuclear translocation of RPS3 without affecting p65 localization (Gao et al., 2009). Nonetheless, how specific NF-κB-activating signals induce the nuclear translocation of RPS3 is unknown.

Extraribosomal functions have been ascribed to ribosomal proteins(Warner and McIntosh, 2009). In addition to binding RNA in the 40S ribosomal subunit, RPS3 participates in transcription (Wan et al., 2007), DNA repair (Hegde et al., 2004; Kim et al., 1995) and apoptosis (Jang et al., 2004). Whether or not RPS3 is phosphorylated has been controversial (Abe et al., 1998; Kim et al., 2005b; Kim et al., 2009; Leader, 1980; Shin et al., 2009). As kinase cascades have a critical role in NF-κB regulation, we assessed whether RPS3 is phosphorylated in the

context of NF-κB activation and sought to identify the responsible kinase (Karin and Ben-Neriah, 2000). Additionally, we aimed to define a regulatory role for the C-terminal tail of RPS3, whose function was unknown.

Here we show that the kinase IKKβ (inhibitor of κB (IκB) kinase-β) phosphorylated RPS3 at Ser209. This phosphorylation enhanced the association of RPS3 with importin-α, which mediated the entry RPS3 into the karyopherin pathway for nuclear translocation. Furthermore, the *E. coli* NleH1 effector protein specifically inhibited RPS3 Ser209, which shows how *E. coli* O157:H7 inhibits this important innate immune response mechanism.

Results

RPS3 phosphorylation in response to NF-κB activation. To determine whether RPS3 is phosphorylated during NF-κB activation, we did ^{32}P-labeling experiments with human embryonic kidney HEK293T cells stimulated with tumor necrosis factor (TNF). Whereas RPS3 was scarcely phosphorylated at all in unstimulated cells, we observed a considerable increase in the incorporation of ^{32}P after TNF stimulation despite no increase in RPS3 protein (Fig. 14a). To determine which RPS3 residues were phosphorylated, we immunoprecipitated RPS3 from either resting or stimulated cells, followed by immunoblot analysis with phosphorylation-specific antibodies. Both TNF and phorbol myristate acetate (PMA) plus ionomycin stimulated rapid phosphorylation and degradation of IκBα within 5 min, accompanied by phosphorylation of serine residues of RPS3 (Fig. 14b and data not shown), similar to the in vivo labeling. We did not detect phosphorylation of tyrosine or threonine residues of RPS3 (Fig. 14b).

RPS3-IKKβ interaction. Activation of IKK, which consists of a regulatory subunit (IKKγ)

Fig. 17. RPS3 is phosphorylated and associates with IKKβ in response to NF-κB activation. (**a**) ^{32}P-labeling assay of HEK293T cells stimulated for 0–30 min (above lanes) with TNF (20 ng/ml), followed by immunoprecipitation (IP) of whole-cell lysates with antibody to RPS3 (anti-RPS3) and autoradiography (top) or immunoblot analysis with anti-RPS3 (bottom). (**b**) Immunoassay of whole-cell lysates of Jurkat cells stimulated for 0–15 min (above lanes) with TNF and analyzed by immunoblot for total or phosphorylated (p-) proteins directly (Input) or after immunoprecipitation with anti-RPS3. (**c**) Immunoprecipitation and immunoblot analysis of the interaction between hemagglutinin (HA)-tagged RPS3 and Flag-tagged IKKβ in HEK293T cells. (**d**) Immunoassay of whole-cell lysates of Jurkat cells stimulated as in **b** and analyzed by immunoblot for IKKα, IKKβ or RPS3 directly or after immunoprecipitation with anti-RPS3. Data are representative of at least two independent experiments.

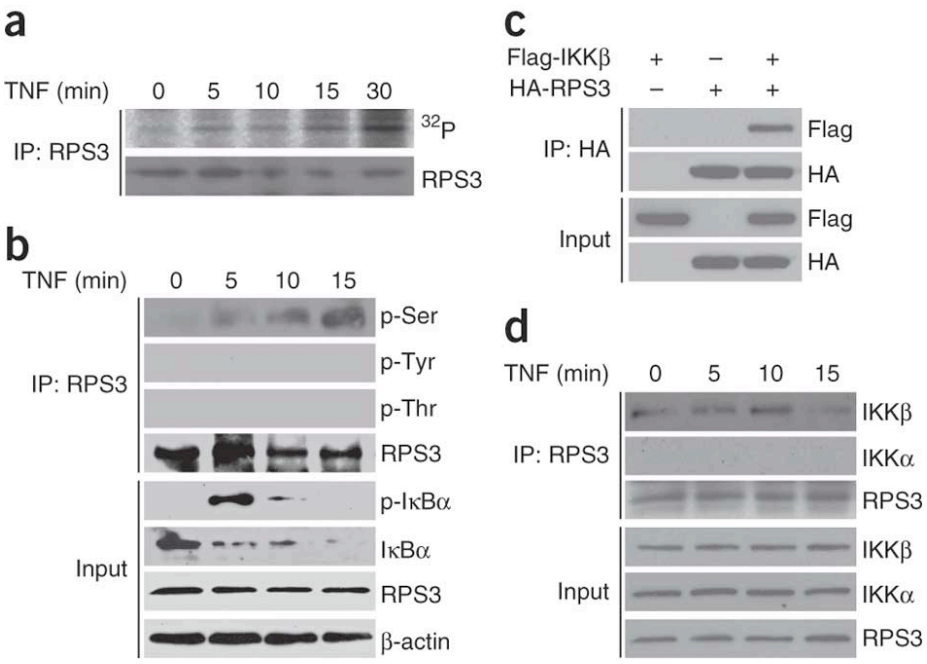
a
TNF (min) 0 5 10 15 30
IP: RPS3
32P
RPS3
b
TNF (min) 0 5 10 15
IP: RPS3
p-Ser
p-Tyr
p-Thr
RPS3
Input
p-IκBα
IκBα
RPS3
β-actin
c
Flag-IKKβ + − +
HA-RPS3 − + +
IP: HA
Flag
HA
Input
Flag
HA
d
TNF (min) 0 5 10 15
IP: RPS3
IKKβ
IKKα
RPS3
Input
IKKβ
IKKα
RPS3

and two catalytic subunits (IKKα and IKKβ), is critical for the phosphorylation and dispatch of the inhibitory IκB proteins and the liberation of NF-κB (Israel, 2000; Karin, 1999; Scheidereit, 2006). Given that RPS3 can be found in the cytoplasmic p65-p50-IκBα inhibitory complex in resting cells (Wan et al., 2007), we hypothesized that activated IKKβ might also bind to and phosphorylate RPS3. First, we found that ectopically expressed IKKβ and RPS3 interacted (Fig. 14c). We next examined resting Jurkat human T lymphocyte cells and detected modest interaction of endogenous IKKβ and RPS3 (Fig. 14d), which potentially accounted for the basal transcription of NF-κB required for cell proliferation and survival. The RPS3-IKKβ association was augmented after TNF stimulation, peaking at 10 min (Fig. 14d), with kinetics similar to those of serine phosphorylation of RPS3 (Fig. 14b). In contrast, there was no detectable interaction between RPS3 and IKKα (Fig. 14d).

Nuclear translocation of RPS3 requires IKK. To determine whether the RPS3-IKKβ interaction was required for nuclear translocation of RPS3, we knocked down expression of IKKα or IKKβ with small interfering RNA (siRNA; Fig. 15) and then monitored stimulation-induced nuclear migration of RPS3 by confocal microscopy. Both TNF and PMA plus ionomycin triggered nuclear translocation of RPS3 in Jurkat cells transfected with a nonspecific siRNA with a scrambled sequence6 (Fig. 16a). Nuclear translocation of RPS3 was impaired only slightly, if at all, by silencing of IKKα. Conversely, knockdown of IKKβ attenuated 60–70% of the nuclear accumulation of RPS3 after stimulation (Fig. 16a). Immunoblot analysis of nuclear fractions confirmed that full expression of IKKβ, but not of IKKα, was necessary for activation-induced nuclear translocation of RPS3 (Fig. 16b). Control immunoblot analysis showed that nuclear translocation of p65 was blocked under the same conditions (Fig. 16b).

We next examined the nuclear translocation of RPS3 in cells ectopically expressing either

'kinase-dead' (SSAA) or constitutively active (SSEE) mutant IKKβ proteins. As expected, the SSEE IKKβ mutant induced NF-κB-dependent luciferase reporter activity, but the SSAA IKKβ mutant did not (Fig. 16c, left). Although RPS3 remained cytosolic in cells expressing the SSAA IKKβ mutant (Fig. 16c, right), a substantial proportion of RPS3 translocated to the nucleus in cells expressing the SSEE IKKβ mutant (Fig. 16c, right). There were five times as many cells containing detectable nuclear RPS3 in populations expressing the SSEE IKKβ mutant as in populations expressing the SSAA IKKβ mutant (Fig. 16d and Fig. 17). Thus, IKKβ activity is necessary and sufficient for nuclear translocation of RPS3 in response to NF-κB-activating stimuli.

IκBα degradation and nuclear translocation of RPS3. Importin-α regulates the nuclear importation of NF-κB Rel subunits (Fagerlund et al., 2005; Fagerlund et al., 2008). RPS3 has a nuclear-localization signal sequence, and its nuclear translocation occurs in parallel to but independently of p65 translocation (Wan et al., 2007). We envisioned that RPS3 could also use the importin-α–importin-β pathway. Consistent with our hypothesis, the association of RPS3 with importin-α was enhanced in TNF-stimulated cells, but its association with importin-β was not (Fig. 18a). Therefore, we assessed whether the binding of RPS3 to importin-α was essential for nuclear translocation during NF-κB activation.

As IκBα degradation is a prerequisite for unmasking of the nuclear-localization signal of p65, and both RPS3 and IκBα bind to p65 in the cytoplasmic inhibitory complex, we assessed whether IκBα degradation was required for the liberation of RPS3. We measured the association of RPS3 with importin-α in HEK293T cells overexpressingwild-type IκBα or an IκBα mutant (SSAA) that is resistant to IKKβ-induced phosphorylation and degradation. In cells transfected with wild-type IκBα, TNF stimulation augmented the interaction of RPS3 and importin-α to a

Fig. 18. Knockdown of IKKα and IKKβ in Jurkat cells. Immunoblot for IKKα, IKKβ, IκBα and β-actin in Jurkat cells transfected with scrambled nonspecific (NS), IKKα, or IKKβ siRNAs. The data represent four independent experiments.

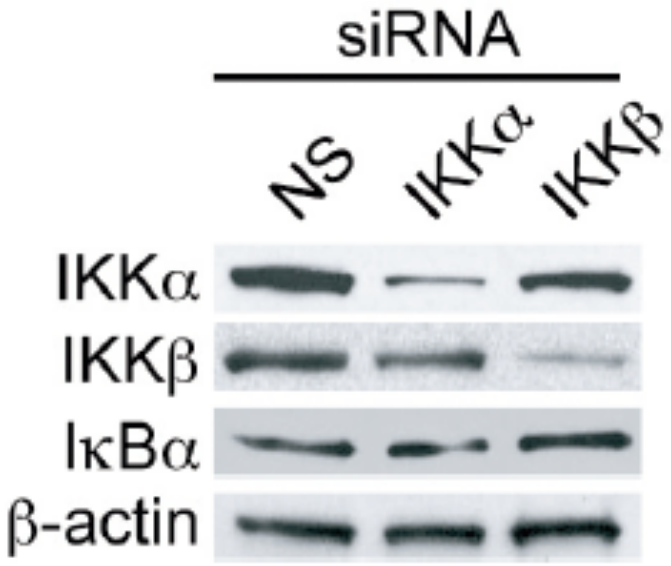
siRNA
NS
IKKα
IKKβ
IKKα
IKKβ
IκBα
β-actin

Fig. 19. RPS3 nuclear translocation requires IKK. (**a**) Confocal microscopy (left) of RPS3 (red) and counterstained nuclei (blue) in Jurkat cells transfected for 72 h with siRNA specific for IKKα or IKKβ or scrambled nonspecific siRNA (NSp), then left untreated (Unstim) or stimulated with TNF (50 ng/ml) or with PMA (50 ng/ml) plus ionomycin (1.5 mM; PMA+I). Original magnification, ×630. Right, quantification of cells with nuclear RPS3. (**b**) Immunoblot analysis of whole-cell lysates (WCL) or nuclear subcellular fractions (Nuc) of Jurkat cells transfected with siRNA (top) and then left unstimulated (−) or stimulated for 30 min with TNF (T) or PMA plus ionomycin (P). (**c**) NF-κB luciferase assay (left) of Jurkat cells transfected with empty vector (Vec) or plasmid encoding Flag-tagged SSAA or SSEE IKKβ mutant together with a luciferase reporter driven by 5× immunoglobulin κB sites, and immunoblot analysis (right) of cytosolic (C) and nuclear (N) subcellular fractions of Jurkat cells overexpressing Flag-tagged IKKβ constructs. Heat-shock protein 90 (hsp90) and poly(ADP-ribose) (PARP) serve as cytosolic and nuclear markers, respectively, and/or loading controls throughout. (**d**) Quantification of Jurkat cells with nuclear RPS3 with ($Flag^+$) or without ($Flag^-$) expression of Flag-tagged IKKβ, assessed by confocal microscopy after fixation and staining for RPS3, Flag and nuclei. Data are representative of three (**a**,**d**), two (**b**) or four (**c**) independent experiments with at least 200 cells each (mean and s.d. in **a**,**d**; mean and s.d. of triplicates in **c**).

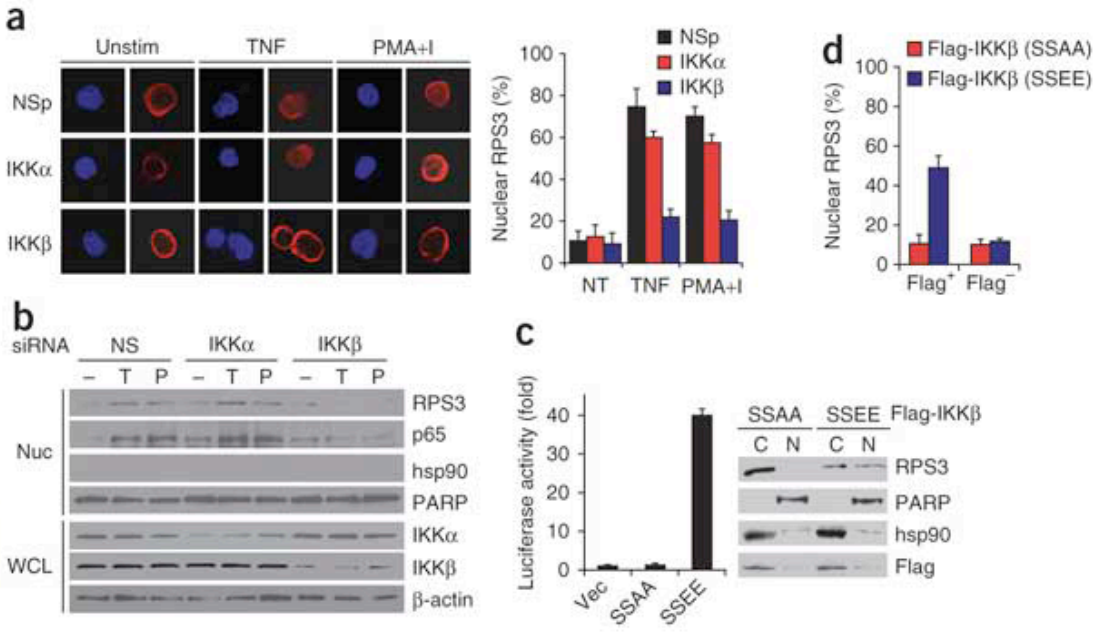
a
Unstim
TNF
PMA+I
NSp
IKKα
IKKβ
Nuclear RPS3 (%)
NSp
IKKα
IKKβ
NT
TNF
PMA+I
d
Flag-IKKβ (SSAA)
Flag-IKKβ (SSEE)
Nuclear RPS3 (%)
Flag+
Flag−
b
siRNA
NS
IKKα
IKKβ
– T P – T P – T P
Nuc
WCL
RPS3
p65
hsp90
PARP
IKKα
IKKβ
β-actin
c
Luciferase activity (fold)
Vec
SSAA
SSEE
SSAA
SSEE
Flag-IKKβ
C N C N
RPS3
PARP
hsp90
Flag

Fig. 20. Representative immunofluorescence images of Jurkat cells overexpressing constructive active (SSEE) or kinase-dead (SSAA) IKKβ construct. Jurkat cells overexpressing indicated Flag-IKKβ constructs were analyzed by confocal microscopy following fixation and staining for RPS3, Flag, and nuclei. Representative Flag positive (top) and Flag negative (bottom) cells from at least 200 cells in two independent experiments were shown, respectively.

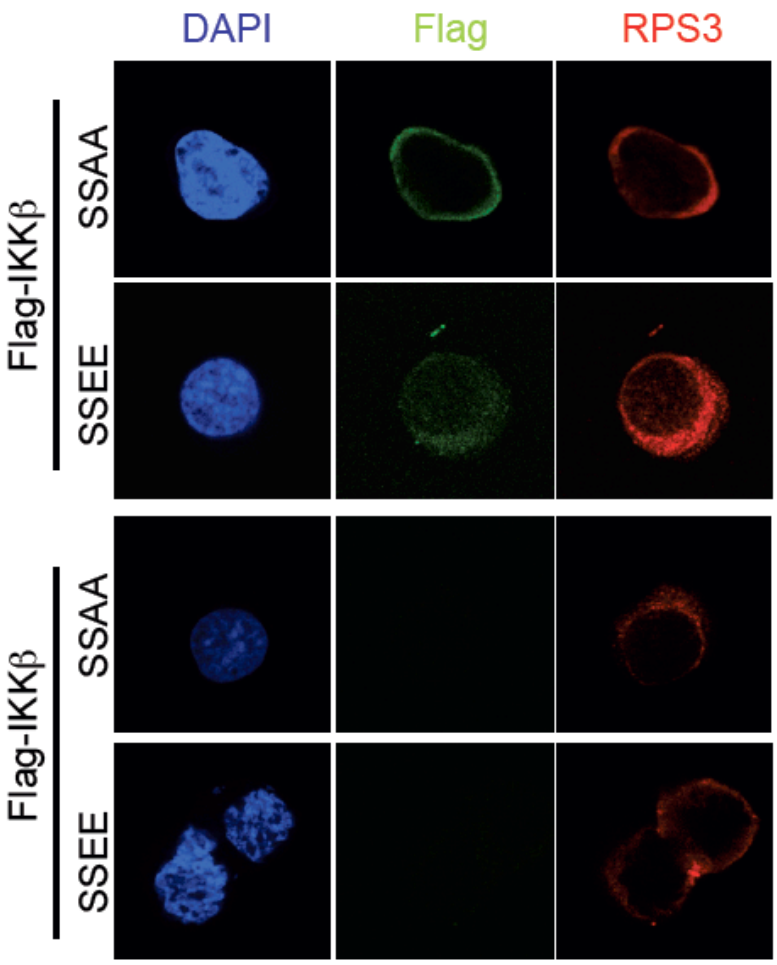
DAPI
Flag
RPS3
Flag-IKKβ
SSAA
SSEE
Flag-IKKβ
SSAA
SSEE

Fig. 21. Importin-α-mediated nuclear translocation of RPS3 is dependent on degradation of IκBα. (**a**) Immunoassay of whole-cell lysates of Jurkat cells stimulated for 0–15 min with TNF and analyzed by immunoblot for importin-α (Imp-α), importin-β (Imp-β) or RPS3 directly or after immunoprecipitation with anti-RPS3. (**b**) Immunoprecipitation and immunoblot analysis of the association of endogenous importin-α or importin-β with RPS3 in Jurkat cells overexpressing hemagglutinin-tagged wild-type IκBα or SSAA IκBα mutant and stimulated for 0–45 min with TNF. (**c**) Immunoassay of whole-cell lysates of Jurkat cells transfected for 72 h with nonspecific or IκBα-specific siRNA, then analyzed by immunoblot for importin-α or RPS3 directly or after immunoprecipitation with anti-RPS3. (**d**) Immunoblot analysis of cytosolic (Cyt) and nuclear (Nuc) subcellular fractions of Jurkat cells transfected with nonspecific or IκBα-specific siRNA. (**e**) Immunoassay of whole-cell lysates of Jurkat cells given no pretreatment (−) or pretreated for 2 h (+) with 800 mM sodium pervanadate (Pv), followed by no stimulation or 30 min of TNF stimulation, then analyzed by immunoblot directly or after immunoprecipitation with anti-RPS3. Data are representative of at least two experiments.

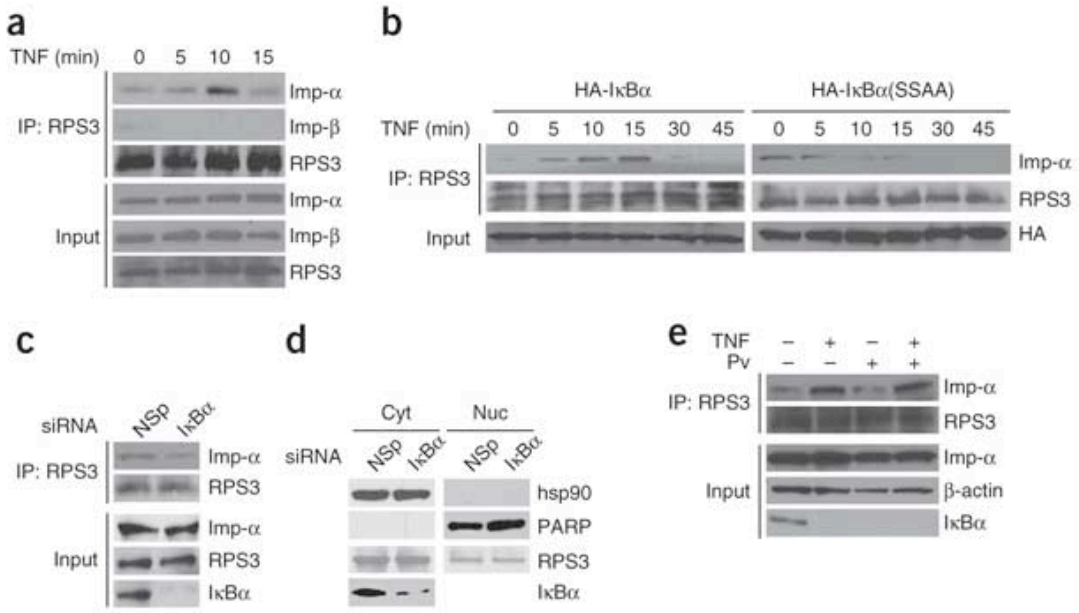
a
TNF (min) 0 5 10 15
IP: RPS3
Imp-α
Imp-β
RPS3
Input
Imp-α
Imp-β
RPS3
b
HA-IκBα
HA-IκBα(SSAA)
TNF (min) 0 5 10 15 30 45 0 5 10 15 30 45
IP: RPS3
Imp-α
RPS3
Input
HA
c
siRNA NSp IκBα
IP: RPS3
Imp-α
RPS3
Input
Imp-α
RPS3
IκBα
d
Cyt Nuc
siRNA NSp IκBα NSp IκBα
hsp90
PARP
RPS3
IκBα
e
TNF − + − +
Pv − − + +
IP: RPS3
Imp-α
RPS3
Input
Imp-α
β-actin
IκBα

degree similar to that in untransfected cells. In contrast, we observed that the RPS3–importin-α association was abolished by the presence of nondegradable IκBα (Fig. 18b).

To determine whether IκBα is the only cytoplasmic barrier that precludes the nuclear translocation of RPS3, we measured both the RPS3–importin-α association and nuclear RPS3 after diminishing IκBα expression. In contrast to nonspecific siRNA, siRNA targeting IκBα resulted in complete depletion of IκBα in Jurkat cells (Fig. 18c, Input). Nevertheless, the RPS3–importin-α association was not augmented (Fig. 18c), nor did we detect substantial nuclear RPS3 (Fig. 18d). Moreover, cells treated with sodium pervanadate to induce IκBα degradation through an IKK-independent mechanism25–27 did not show more association between RPS3 and importin-α (Fig. 18e and Fig. 19b) or nuclear accumulation of RPS3, despite complete degradation of IκBα (Fig. 19c). We further determined whether a subsequent NF-κB-activation signal independently promoted the association of importin-α with RPS3 and nuclear transport of RPS3 after IκBα degradation. We found that TNF stimulation after sodium pervanadate treatment was required for the RPS3–importin-α association, similar to TNF stimulation alone (Fig. 18e). Thus, phosphorylation and degradation of IκBα itself is required but not sufficient for the association of RPS3 with importin-α followed by nuclear translocation of RPS3. Instead, an additional signal, possibly phosphorylation of RPS3 by IKKβ, is required.

IKKβ phosphorylates RPS3 at Ser209. Although originally defined as the kinase that phosphorylates IκB (Karin, 1999), IKKβ also phosphorylates unrelated substrates, including 14-3-3β and Bcl-10, which lack the IKK consensus motif (DpSGΨXpS/T, where ‘pS’ indicates a phosphorylated serine residue, ‘Ψ’ indicates a hydrophobic residue, ‘X’ indicates any residue, and ‘pS/T’ indicates a phosphorylated serine or threonine residue) (Wegener et al., 2006). We therefore hypothesized that IKKβ might directly phosphorylate RPS3. By in vitro kinase assays

with recombinant IKK and RPS3 proteins, we observed considerable incorporation of ^{32}P into autophosphorylated IKKα and IKKβ (Fig. 20a, lanes 2–7), as well as a phosphorylated glutathione S-transferase (GST)-tagged IκBα peptide of amino acids 1–54 (Fig. 21), but not into GST protein alone (Fig. 20a, lanes 3 and 6), when we used either IKKα or IKKβ. We discovered that GST-RPS3 was phosphorylated by IKKβ but not by IKKα in vitro (Fig. 20a, lanes 4 and 7).

To identify the RPS3 amino acid residue (or residues) phosphorylated by IKKβ, we analyzed in vitro–phosphorylated RPS3 by liquid chromatography–tandem mass spectrometry. The results indicated that IKKβ phosphorylated Ser209, located in the C terminus of RPS3 (Fig. 20b). Amino acid sequence alignment of RPS3 showed that Ser209 is conserved in many species throughout phylogeny, except *Caenorhabditis elegans* and *Schizosaccharomyces pombe*, two organisms that do not have the NF-κB signaling pathway (Fig. 22).

To verify biochemically that Ser209 is an IKKβ substrate, we did ^{32}P-labeling in vitro kinase assays with recombinant wild-type RPS3 or a mutant RPS3 with substitution of the serine at position 209 with alanine (S209A). This RPS3(S209A) mutant had less IKKβ-mediated phosphorylation than did wild-type RPS3 (Fig. 20c). There might have been alternative phosphorylation sites under these conditions, given the modest residual phosphorylation of RPS3 (Fig. 20c). RPS3 Ser209 is not in a conventional IKK recognition motif but is instead in a sequence motif (XXXpS/TXXE) that is potentially recognized by casein kinase II (CK2). Although IKKβ kinase can show CK2-like phosphorylation specificity, no CK2 protein contaminant was detectable in our recombinant IKK protein preparations (Fig. 23). Thus, the than to any trace amount of CK2 bound to IKK proteins. To determine whether Ser209 is the critical site at which IKKβ phosphorylates RPS3 in living cells, we transfected Flag-tagged wild-type RPS3 or RPS3(S209A) into cells alone or together with IKKβ. Indeed, we observed that

Fig. 22. Sodium pervanadate (Pv) treatment induces IκBα degradation, but not nuclear phosphorylation of RPS3 Ser209 was due to the alternative specificity of the IKKβ kinase rather translocation of RPS3 in Jurkat cells. (a) Jurkat cells were treated with indicated concentration of Pv for 2 h, and whole-cell lysates were immunoblotted as indicated. β-actin was used as a loading control. (b) Jurkat cells were treated with or without 800 μM sodium pervanadate (Pv) for 2 h, and wholecell lysates were immunoblotted directly or after immunoprecipitation (IP) with anti-RPS3 antibody for importin-α (imp-α), RPS3 and IκBα. (c) Immunoblotting of cytosolic (Cyto) and nuclear (Nuc) subcellular fractions derived from Jurkat cells treated with or without 800 μM sodium pervanadate (Pv) for 2 h. Hsp90 and PARP served as the cytosolic and nuclear markers and loading controls, respectively. The data represent at least two independent experiments.

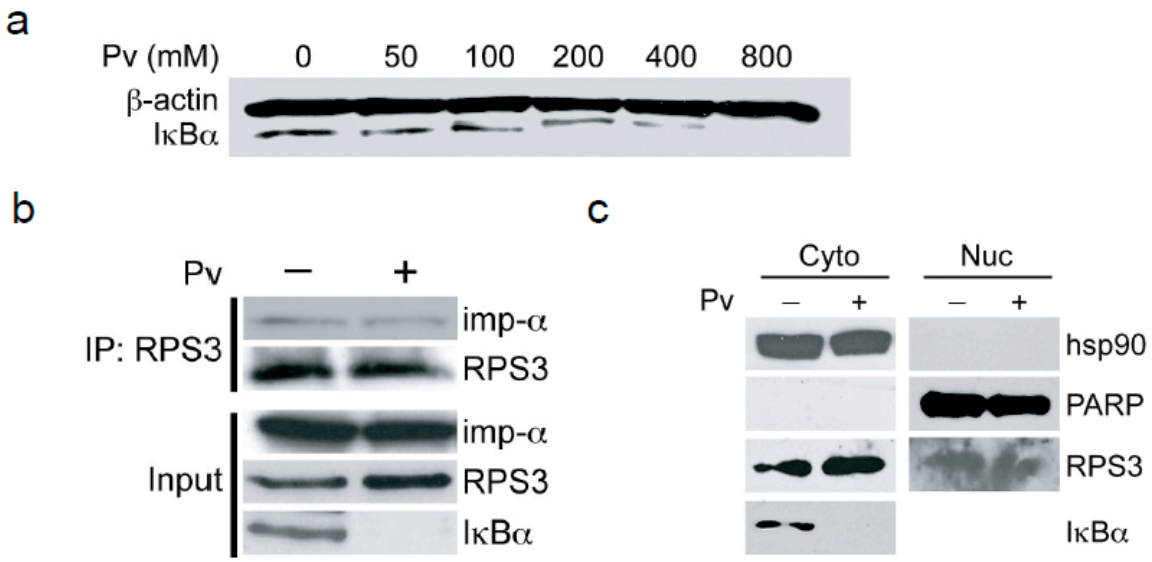
a
Pv (mM)
0
50
100
200
400
800
β-actin
IκBα
b
Pv
–
+
IP: RPS3
imp-α
RPS3
Input
imp-α
RPS3
IκBα
c
Cyto
Nuc
Pv
–
+
–
+
hsp90
PARP
RPS3
IκBα

Fig. 23. IKKβ phosphorylates RPS3 at Ser209. (**a**) Autoradiography (above) and Coomassie blue staining (below) of *in vitro* kinase assays with recombinant GST or GST-RPS3 plus recombinant human IKKα (rIKKα) or IKKβ (rIKKβ); p-IKKα and p-IKKβ (right) indicate autophosphorylated IKK proteins, and p-RPS3 indicates phosphorylated RPS3. (**b**) *In vitro* kinase assay of recombinant RPS3 protein with recombinant human IKKβ; after digestion, samples were enriched for phosphorylated peptides by TiO_2 and were fragmented by a mass spectrometer; intensity of ions is presented relative to the tallest peak in the spectrum, set as 100%. The spectrum of the 1+ fragment ion displays indicative of KPLPDHVpSIVEPK, based on a Mascot algorithm database search. The y6 ion (red) shows incorporation of the site of phosphorylation (the sixth amino acid from the C terminus of the fragment), further confirmed by the loss of H_3PO_4 from several ions. Top, RPS3 with characterized domains (NLS, nuclear localization signal; KH, K homology) and the IKKβ Ser209 phosphorylation site in red. (**c**) Autoradiography (above) and Coomassie blue staining (below) of *in vitro* kinase assays with GST-tagged recombinant wild-type RPS3 or RPS3(S209A) plus recombinant human IKKβ. (**d**) Immunoprecipitation and immunoblot analysis of the serine phosphorylation of ectopically expressed RPS3 in HEK293T cells transfected with a plasmid expressing Flag-tagged wild-type RPS3 or RPS3(S209A) with or without a plasmid expressing IKKβ. (**e**) Immunoblot analysis (below) of phosphorylated and total RPS3 in whole-cell lysates or Jurkat cells stimulated for 0–30 min with TNF; above, densitometry, normalized as the intensity of each phosphorylated RPS3 band to the corresponding total RPS3 band and presented as the ratio of phosphorylated RPS3 to RPS3 relative to that of unstimulated cells. Data are representative of four (**a**,**e**) or two (**b**–**d**) independent experiments.

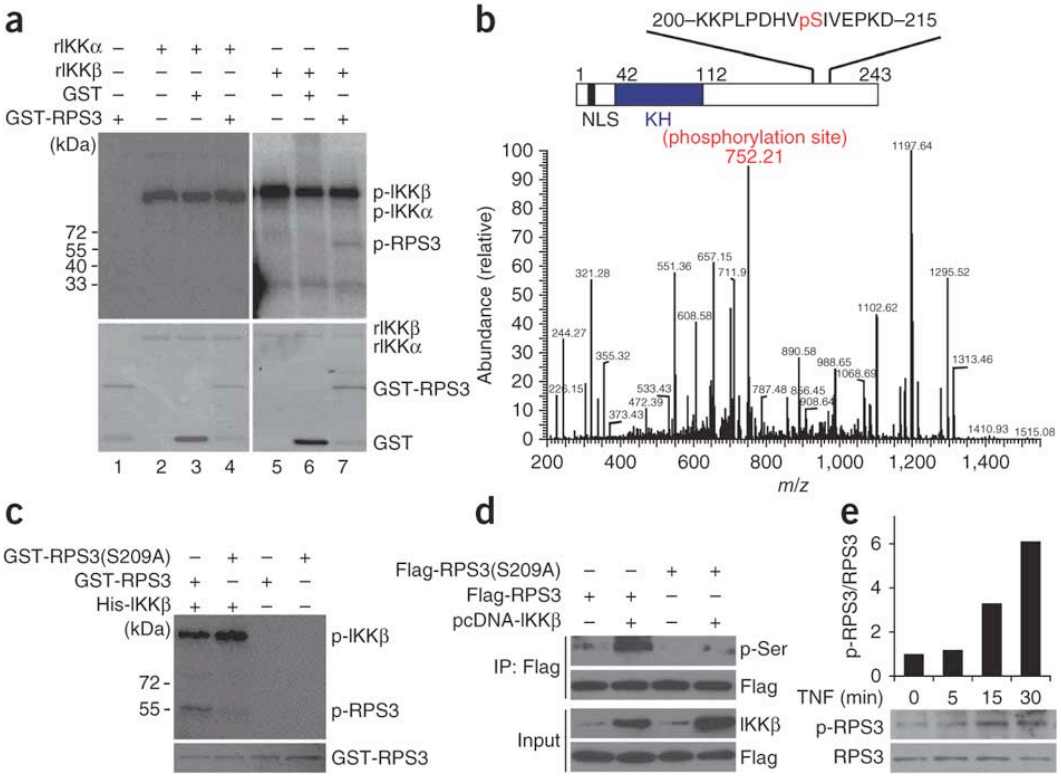
a
rIKKα
rIKKβ
GST
GST-RPS3
(kDa)
72
55
40
33
p-IKKβ
p-IKKα
p-RPS3
rIKKβ
rIKKα
GST-RPS3
GST
1 2 3 4 5 6 7
b
200–KKPLPDHVpSIVEPKD–215
1 42 112 243
NLS KH
(phosphorylation site)
752.21
Abundance (relative)
m/z
c
GST-RPS3(S209A)
GST-RPS3
His-IKKβ
(kDa)
72
55
p-IKKβ
p-RPS3
GST-RPS3
d
Flag-RPS3(S209A)
Flag-RPS3
pcDNA-IKKβ
IP: Flag
p-Ser
Flag
Input
IKKβ
Flag
e
p-RPS3/RPS3
TNF (min) 0 5 15 30
p-RPS3
RPS3

Fig. 24. The recombinant IKKβ phosphorylates IκBα (1-54) in vitro. Autoradiograph (top) and Coomassie blue-stained gel (bottom) of *in vitro* kinase assays performed with recombinant GST or GST- IκBα (1-54) protein using recombinant human IKKβ as kinase. Filled and open symbols indicate autophosphorylated IKKα and phosphorylated IκBα, respectively. The data represent three independent experiments.

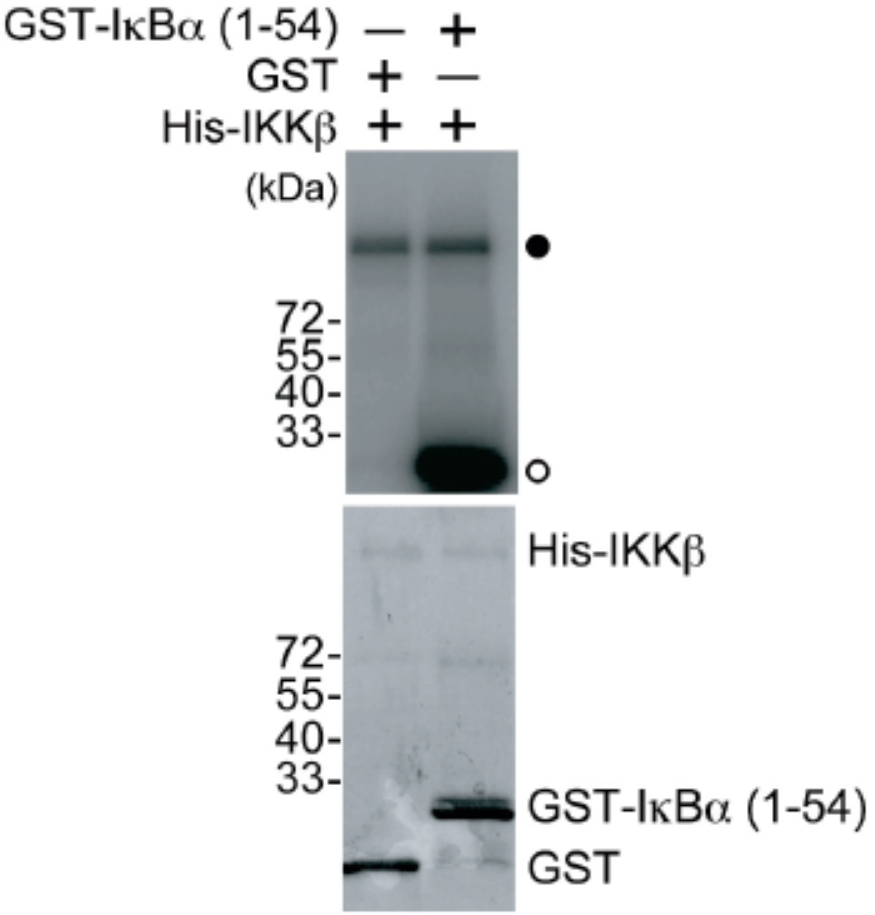
GST-IκBα (1-54) — +
GST + —
His-IKKβ + +
(kDa)
72-
55-
40-
33-
His-IKKβ
72-
55-
40-
33-
GST-IκBα (1-54)
GST

Fig. 25. Serine 209 of RPS3 is conserved in many species. Alignment of the C-terminal tail region of RPS3 from different species. The serine 209 residue conserved in many species is indicated in red.


Homo sapiens QGVLGIKVKIMLPWDPTGKIGPKKPLPDHVSIVEPKDEILPTTP---ISEQKGGKPEPPA 235
Bos taurus QGVLGIKVKIMLPWDPTGKIGPKKPLPDHVSIVEPKDEILPTTP---ISEQKGGKPEPPA 235
Mus musculus QGVLGIKVKIMLPWDPSGKIGPKKPLPDHVSIVEPKDEILPTTP---ISEQKGGKPEPPA 235
Rattus norvegicus QGVLGIKVKIMLPWDPSGKIGPKKPLPDHVSIVEPKDEILPTTP---ISEQKGGKPEPPA 235
Canis familiar QGVLGIKVKIMLPWDPSGKIGPKKPLPDHVSIVEPKDEILPTTP---ISEQKGGKPEPPA 235
Gallus gallus QGVLGIKVKIMLPWDTSGKIGPKKPLPDHVSIVEPKEEILPTTTH--ISEQKGGKPEQPA 236
Pan troglodytes QGVLGIKVKFMLPWDPTGKTGPKKPLPDHVSVVEPKDEILPTTP---ISEQKGGKPEPSA 235
Danio rerio QGVLGIKVKIMLPWDPSGKIGPKKPLPDHVSIVEPKEEVLSTTP---VSEQKGAKPEVPV 235
Drosophila melanogaster QGVLGIKVKVMLPYDPKNKIGPKKPLPDNVSVVEPKEEKIYETP---ETEYKIPPPSKPL 237
Caenorhabditis elegans QGVIGIKVKIMLPYDPRGQNGPRNALPDHVQIVEPQEEVLPKEP---HSQHKEEKKD-VQ 236
Schizosaccharomyces pombe QGVLGVKVKIMLP-EP--KTRQKKSLPDIVVVLDPKEEEPITKPYTVINQPVEAAAAAGQ 237

overexpression of IKKβ enhanced the phosphorylation of Flag-tagged RPS3, but phosphorylation was effectively eliminated by the S209A substitution (Fig. 20d), which indicated that Ser209 is the main target site for IKKβ phosphorylation. We next generated an antibody to RPS3 phosphorylated at Ser209 and confirmed that endogenous RPS3 was phosphorylated at Ser209 in a time-dependent manner after TNF stimulation (Fig. 20e). Thus, the C-terminal tail of RPS3 potentially contains an important regulatory site.

Phosphorylation of RPS3 and its NF-κB function. We next assessed whether Ser209 phosphorylation has a role in the nuclear translocation of RPS3 during NF-κB activation. We prepared subcellular fractions of cells transfected with wild-type RPS3 or RPS3(S209A) and analyzed them by immunoblot for heat-shock protein 90 (a cytoplasmic protein) and poly(ADP-ribose) polymerase (a nuclear protein); the results confirmed clean separation (Fig. 21a). As expected, stimulation with PMA plus ionomycin triggered nuclear translocation of Flag-tagged wild-type RPS3 (Fig. 21a). However, nuclear translocation of RPS3(S209A) was attenuated (Fig. 21a). We also tested the effect of activating NF-κB via overexpression of IKKβ on the nuclear translocation of RPS3. IKKβ overexpression activated NF-κB, as measured by luciferase assay (Fig. 24), and also induced the nuclear translocation of wild-type RPS3 but not of RPS3(S209A) (Fig. 21b). These data suggest that phosphorylation of Ser209 is critical for the nuclear translocation of RPS3 induced by activation of NF-κB.

To examine the role of phosphorylation of RPS3 Ser209 in its NF-κB function (Ruchaud-Sparagano et al., 2011; Wan et al., 2007; Wan and Lenardo, 2010), we silenced endogenous RPS3 expression with siRNA targeting the 3' untranslated region (3' UTR) of RPS3 mRNA, followed by complementation with either wild-type RPS3 or RPS3(S209A) via transfection. As expected, RPS3-specific siRNA resulted in a much lower abundance of endogenous RPS3 than

did nonspecific siRNA, but it did not affect the robust expression of Flag-tagged RPS3 expressed from a transfected construct lacking the 3' UTR (Fig. 21c). We also found that knockdown of RPS3 resulted in less TNF-induced expression of a luciferase construct driven by immunoglobulin κB sites6 (Fig. 21d). The impaired luciferase signal caused by RPS3 deficiency was completely restored by transfection of wild-type RPS3 but not by transfection of RPS3(S209A) (Fig. 21d), despite their equivalent expression (Fig. 21c). Moreover, the failure of RPS3(S209A) to restore luciferase activity did not result from defective translation, as green fluorescent protein, produced normally from a transiently transfected expression construct, was similar in cells complemented with wild-type or RPS3(S029A) (Fig. 25). Together these data suggest that phosphorylation of RPS3 Ser209 is critical for NF-κB activity involving the canonical immunoglobulin κB site.

We next used chromatin immunoprecipitation to determine whether phosphorylation of Ser209 affected the recruitment of RPS3 and p65 to specific κB sites in intact chromatin during NF-κB activation. In cells in which RPS3 was knocked down, PMA plus ionomycin stimulated the recruitment of ectopically expressed, Flag-tagged wild-type RPS3, but not of RPS3(S209A), to the κB sites of the promoters of the genes encoding IκBα (NFKBIA) and interleukin 8 (IL8; Fig. 21e). Although expression of RPS3(S209A) had no effect on the nuclear translocation of p65, it substantially attenuated the recruitment of p65 (Fig. 21e). Additional experiments showed that the attraction of p65 to the promoters of RPS3-independent NF-κB target genes such as CD25 was greater (Fig. 26), consistent with published observations6. There was not much recruitment of Flag-tagged RPS3 or p65 to the β-actin (ACTB) promoter, which lacks κB sites (Fig. 21e), which suggested the recruitment was specific for the κB site. Thus, the recruitment of RPS3 as well as the contingent recruitment of p65 to key promoters depended on Ser209.

Secretion of IL-8 induced by stimulation with a T cell antigen receptor (TCR) agonist or with PMA plus ionomycin was diminished as a consequence of less recruitment of RPS3 and/or p65 to the κB sites of IL8 in the presence of RPS3(S209A) than in the presence of wild-type RPS3 (Fig. 27). However, cell surface expression of CD25 was similar in cells transfected with wild-type RPS3 or RPS3(S209A) (Fig. 28). Therefore, phosphorylation of RPS3 Ser209 by IKKβ is apparently required by RPS3 in directing NF-κB to a specific subset of target genes.

NleH1 inhibits RPS3 phosphorylation in vitro. Enterohemorrhagic *E. coli* pathogens are important causative agents of both food-borne disease and pediatric renal failure (Sears and Kaper, 1996). These pathogens use type III secretion systems to inject effector proteins directly into intestinal epithelial cells (Cornelis, 2010); a subset of the injected effector proteins inhibit NF-κB-dependent innate responses (Baruch et al., 2011; Nadler et al., 2010; Newton et al., 2010; Royan et al., 2010; Vossenkamper et al., 2010; Yen et al., 2010). The effector protein NleH1 of *E. coli* strain O157:H7 EDL933 binds to RPS3 and attenuates the nuclear translocation of RPS3, thus impairing RPS3-dependent NF-κB signaling (Gao et al., 2009). We therefore hypothesized that NleH1 may function by inhibiting phosphorylation of RPS3 Ser209. As expected, transfection of increasing amounts of plasmid encoding hemagglutinin-tagged NleH1 blocked TNF-induced activation of NF-κB in a dose-dependent manner9 (Fig. 29a,b). Notably, NleH1 decreased both TNF-induced and basal phosphorylation of RPS3 to roughly 20% of the phosphorylation obtained with vehicle control (Fig. 29c). Expression of NleH1 did not interfere with either TNF-induced activation of IKK or degradation IκBα (Fig. 29c), consistent with the lack of effect of NleH1 on p65 nuclear translocation9.

To determine if NleH1 inhibits RPS3 phosphorylation, we infected HeLa human cervical cancer cells with *E. coli* O157:H7 with or without the gene encoding NleH1 (ΔnleH1) or with *E.*

coli O157:H7 lacking a functional type III secretion system unable to inject NleH1 into mammalian cells (ΔescN). In uninfected cells, TNF treatment stimulated a sevenfold increase in phosphorylation of RPS3 Ser209 that peaked at 30 min (Fig. 29d). In contrast, phosphorylation of RPS3 Ser209 was substantially impaired in cells infected with wild-type *E. coli* O157:H7 (Fig. 29d). However, TNF-induced phosphorylation of RPS3 Ser209 was unimpaired in cells infected with either ΔnleH1 or ΔescN *E. coli* O157:H7 (Fig. 29d). Wild-type *E. coli* O157:H7 substantially attenuates TNF-induced nuclear translocation of RPS3, but ΔnleH1 and ΔescN *E. coli* O157:H7 do not (Sekiya et al., 2001). The parallel between RPS3 phosphorylation and its nuclear translocation during *E. coli* infection provides evidence in the context of an NF-κB-dependent disease process that phosphorylation of RPS3 Ser209 is important for nuclear translocation.

Our discovery that NleH1 inhibited the phosphorylation of RPS3 Ser209 suggested that it should also blocks RPS3-dependent transcription of NF-κB target genes (such as IL8, NFKBIA and TNFAIP3). Indeed, these genes were only modestly upregulated in cells infected with wild-type *E. coli* O157:H7 but were substantially induced in cells infected with either ΔnleH1 or ΔescN *E. coli* O157:H7 (Fig. 29e). In contrast, deleting NleH1 had no effect on the expression of RPS3-independent genes, including CD25 and TNFSF13B (Fig. 30). Together these results demonstrate that NleH1 specifically inhibits the protective immune response by directly blocking phosphorylation of RPS3 Ser209 and thereby impairing critical RPS3-dependent NF-κB target genes.

NleH1 inhibits phosphorylation of RPS3 Ser209 in vivo. A gnotobiotic piglet-infection model has been used before to show that piglets infected with ΔnleH1 *E. coli* O157:H7 die more rapidly than do those infected with wild-type *E. coli* O157:H7. Piglets infected with ΔnleH1

Fig. 26. No CK2 contaminant in the recombinant IKK proteins. IKKα or IKKβ recombinant proteins (1 μg each), and 15 μg of whole-cell lysate from HEK 293T cells (293WCL) were separated by SDS-PAGE, followed by immunoblotted with antibodies specific for IKKα/β or CK2α. The data represent two independent experiments.

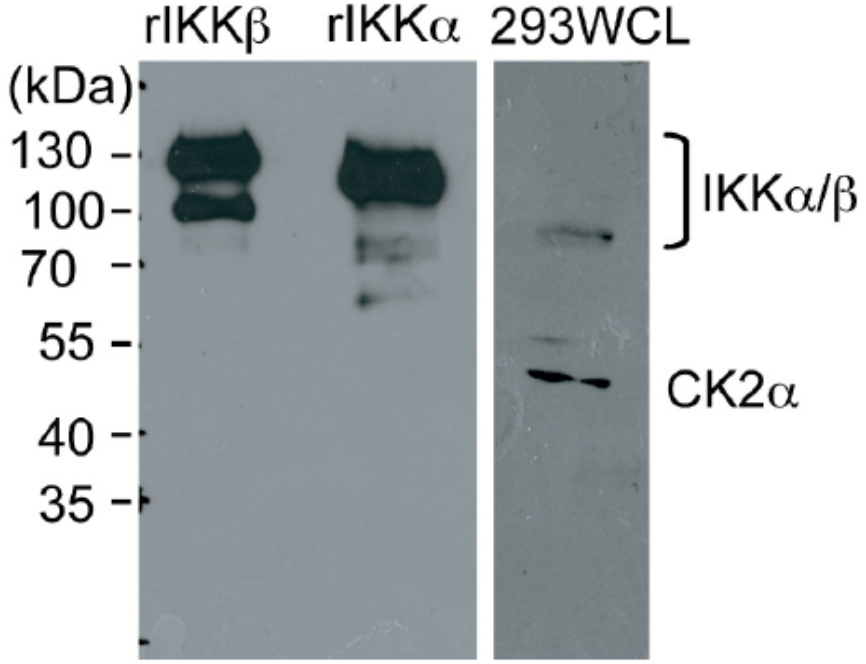
rIKKβ
rIKKα
293WCL
(kDa)
130
100
70
55
40
35
IKKα/β
CK2α

Fig. 27. Activation of NF-κB by IKKβ overexpression. NF-κB luciferase assay (mean and s.d., n=3) using Jurkat cells transfected with empty vector pcDNA or pcDNAIKKβ plasmids together with a 5 x *Ig* κB sites-driven luciferase reporter gene. Representative results from at least four independent experiments were shown.

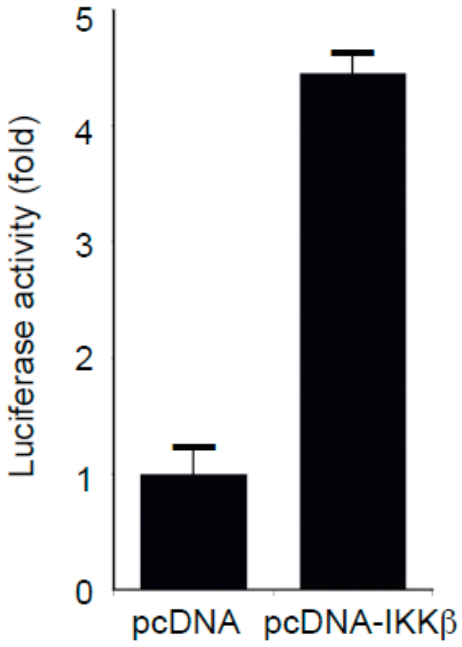
Luciferase activity (fold)
5
4
3
2
1
0
pcDNA
pcDNA-IKKβ

Fig. 28. The S209A mutation of RPS3 does not impair translation. Jurkat cells, transfected with siRNA specifically targeting the 3' untranslated region of RPS3 mRNA for 48 h, were transfected again with the same siRNA plus wild-type or S209A mutant Flag-RPS3 constructs together with pEGFP plasmid. 24 h later, GFP expression was assessed by flow cytometer. Numbers indicate the percentage of GFP-positive cells, gated on living cells. Representative plots from three independent experiments were shown.

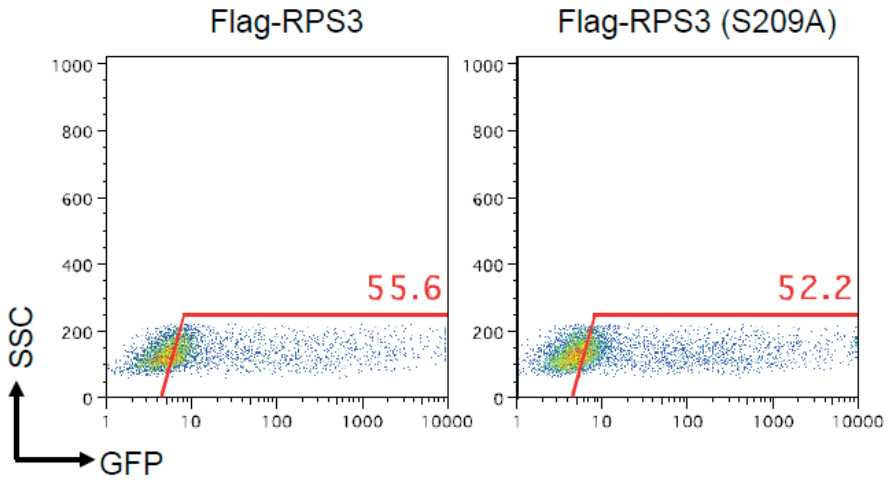
Flag-RPS3
Flag-RPS3 (S209A)
SSC
GFP
55.6
52.2
1000
800
600
400
200
0
1
10
100
1000
10000

Fig. 29. The S209A mutation of RPS3 does not attenuate the recruitment of endogenous p65 to the RPS3-independent CD25 κB promoter. Jurkat cells transfected with RPS3-3' UTR siRNA and Flag-tagged wild-type (WT) or S209A mutant RPS3 constructs were left untreated or stimulated with 50 ng/ml PMA plus 1.5 μM ionomycin (PMA+I) for 2 h. The cell extracts were analyzed by chromatin immunoprecipitation assays of the recruitment of endogenous p65 to the κB region of *CD25* promoter. p65-bound DNA was analyzed by quantitative real-time PCR (primers, above diagrams) and normalized to the input DNA, and the cells transfected with Flag-tagged WT RPS3 construct and untreated (mean and S.D., n=3). Data are from one representative of two independent experiments. * $P < 0.05$, Student's *t*-test.

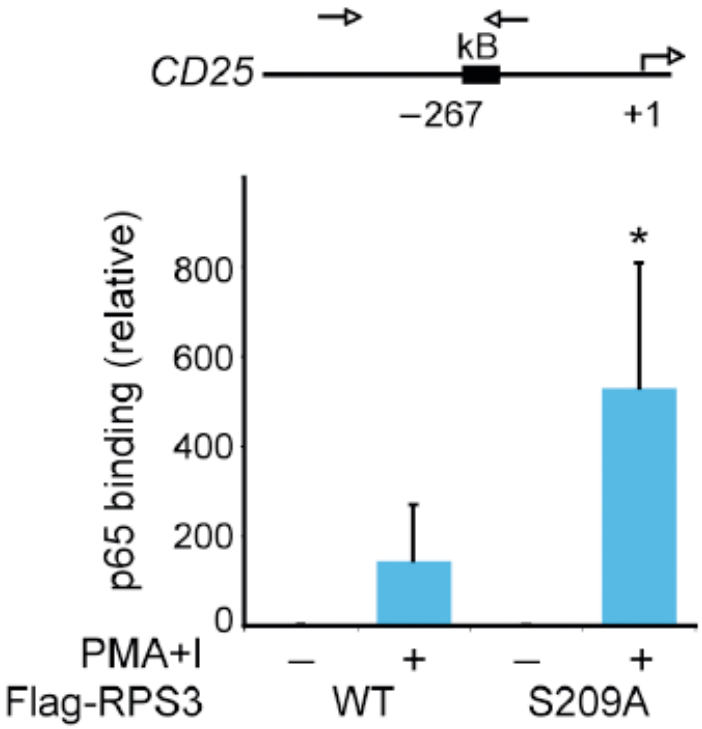
CD25
kB
−267
+1
p65 binding (relative)
800
600
400
200
0
*
PMA+I
–
+
–
+
Flag-RPS3
WT
S209A

Fig. 30. The S209A mutation of RPS3 attenuates the T cell receptor engagement-induced IL-8 expression in Jurkat cells. Jurkat cells transfected with RPS3-3' UTR siRNA and Flag-tagged wild-type (WT) or S209A mutant RPS3 constructs were left unstimulated (Unstim) or stimulated with 1 μg/ml of anti-CD3/CD28, or 50 ng/ml PMA plus 1.5 μM ionomycin (PMA+I) for 24 h. The IL-8 in the supernatant was measured by ELISA (mean and s.d., n=3). ND, not detected. The data represent two independent experiments.

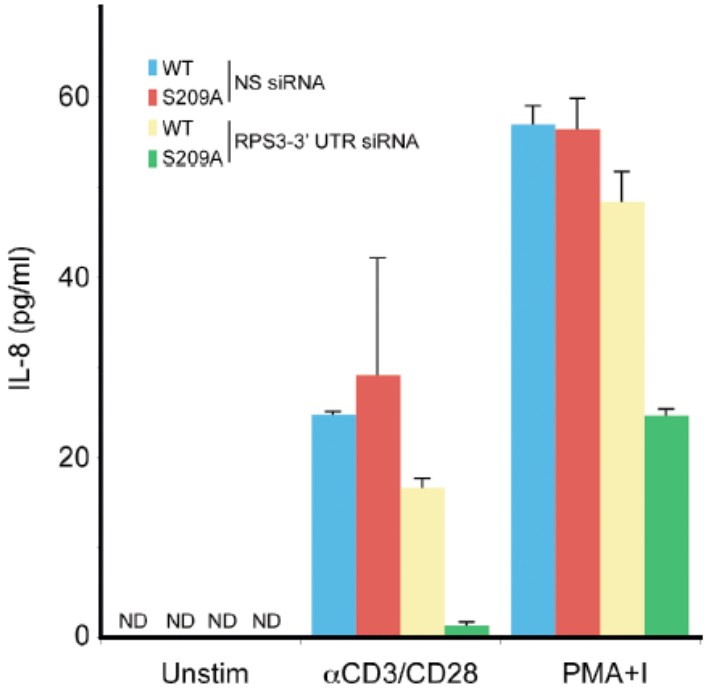
WT
S209A
NS siRNA
WT
S209A
RPS3-3' UTR siRNA
IL-8 (pg/ml)
60
40
20
0
ND ND ND ND
Unstim
αCD3/CD28
PMA+I

Fig. 31. The S209A mutation of RPS3 does not attenuate the T cell receptor engagement-induced CD25 expression in Jurkat cells. Jurkat cells transfected with RPS3-3' UTR siRNA and Flag-tagged wild-type (WT) or S209A mutant RPS3 constructs were left unstimulated (Unstim) or stimulated with 1 μg/ml of anti-CD3/CD28, or 50 ng/ml PMA plus 1.5 μM ionomycin (PMA/I) for 12 h. The induced CD25 expression on the cell surface was stained with PE-conjugated anti-CD25 antibody and analyzed by flow cytometer. The percentage of viable cells with CD25 positive were shown (mean and s.d., n=3).

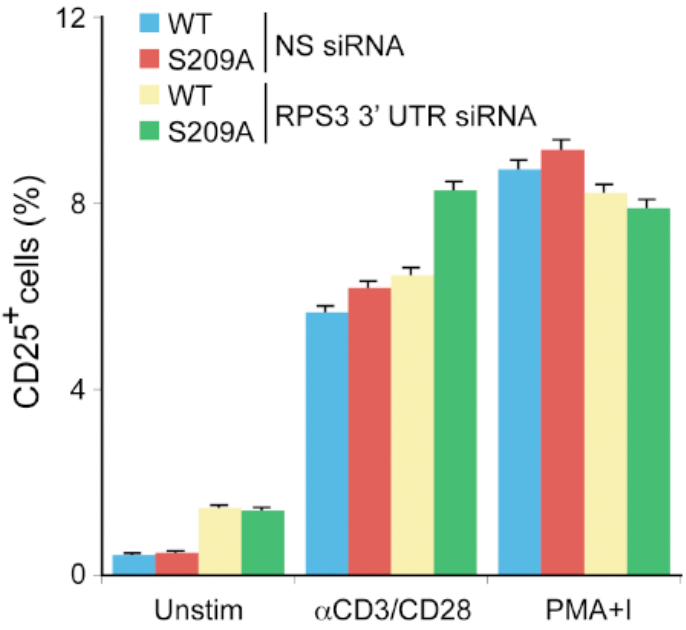
12
8
4
0
CD25+ cells (%)
WT
S209A
NS siRNA
WT
S209A
RPS3 3' UTR siRNA
Unstim
αCD3/CD28
PMA+I

develop clinical disease consistent with a robust inflammatory response, but with less bacterial colonization and little diarrhea (Sekiya et al., 2001). Although it seemed paradoxical on the basis of our cell culture data (Fig. 29d), we hypothesized that NleH1 blocks phosphorylation of RPS3 Ser209 *in vivo*, thereby preventing nuclear translocation of RPS3 in infected piglets. We isolated piglet colons at necropsy and analyzed them by immunohistochemistry with our antibody to phosphorylated RPS3. Consistent with in vitro data, piglets infected with wild-type *E. coli* O157:H7 showed diffuse and low-intensity staining of phosphorylated RPS3, whereas in piglets infected with ΔnleH1 *E. coli* O157:H7, phosphorylated RPS3 expression was florid and intense (Fig. 29f). These data demonstrate that NleH1 inhibits phosphorylation of RPS3 Ser209 both in vitro and in vivo, which might benefit the bacterium in colonization and transmission.

NleH1 steers IKKβ substrate specificity. NleH1 is an autophosphorylated serine-threonine kinase that depends on its lysine residue at position 159 (Sekiya et al., 2001). To explore the mechanism by which NleH1 inhibits phosphorylation of RPS3 Ser209, we first did an *in vitro* kinase assay with purified wild-type histidine-tagged NleH1 and mutant histidine-tagged NleH1 with substitution of the lysine at position 159 with alanine (NleH1(K159A)); our results confirmed that NleH1 was autophosphorylated and that NleH1(K159A) was a 'kinase-dead' mutant (Fig. 31a). To determine whether its kinase activity was required for NleH1 to inhibit IKKβ phosphorylation of RPS3 on Ser209, we ectopically expressed wild-type NleH1or NleH1(K159A) in HEK293T cells. Expression of wild-type NleH1 resulted in much less TNF-induced phosphorylation of RPS3 Ser209, whereas expression of NleH1(K159A) failed to do so (Fig. 31b). Thus, the kinase activity of NleH1 is needed to protect RPS3 from IKKβ-mediated phosphorylation.

Citrobacter rodentium is a mouse pathogen that shares pathogenic strategies with *E. coli* (Deng et al., 2003); most notably for our investigation, *C. rodentium* NleH inhibits the nuclear translocation of RPS3 and RPS3-dependent NF-κB luciferase activity to an extent equivalent to that of *E. coli* NleH1 (Gao et al., 2009). We assayed phosphorylation of RPS3 Ser209 in HeLa cells infected with various *C. rodentium* strains. In uninfected cells, cells stimulated with TNF had three- to fivefold more phosphorylation of RPS3 Ser209 than did unstimulated cells (Fig. 31c). Such augmentation of RPS3 phosphorylation was about 60% lower after infection with wild-type *C. rodentium* (Fig. 31c). However, RPS3 phosphorylation was enhanced in cells infected with a *C. rodentium* strain lacking NleH (ΔnleH; Fig. 31c). We further examined the role of NleH1 kinase activity using the *C. rodentium* ΔnleH strain as a background on which to express either wild-type NleH1 or NleH1(K159A). Complementation of the ΔnleH mutant with wild-type NleH1 almost completely abolished TNF-induced phosphorylation of RPS3 Ser209, whereas complementation with NleH1(K159A) failed to inhibit RPS3 phosphorylation (Fig. 31c). Collectively, these results demonstrate that the kinase activity of NleH1 is needed to block the phosphorylation of RPS3 Ser209.

We next assessed whether the inhibitory activity of NleH1 was sufficiently robust to impair the substantial nuclear translocation of RPS3 trigged by the constitutively active SSEE IKKβ mutant (Fig. 16d). We found that ectopic expression of either wild-type or SSEE IKKβ triggered more nuclear translocation of RPS3 than did the kinase-dead SSAA IKKβ mutant (Fig. 31d). The nuclear accumulation of RPS3 was substantially retarded by infection of cells with wild-type *E. coli* O157:H7 (Fig. 31d). In contrast, infection with either ΔnleH1 or ΔescN *E. coli* O157:H7 impaired the nuclear translocation of RPS3 only slightly in cells expressing either wild-type IKKβ or the SSEE IKKβ mutant (Fig. 31d). As expected, infection with *E. coli* did not affect the

nuclear translocation of RPS3 in cells expressing the SSAA IKKβ mutant, in which NF-κB signaling was low (Fig. 31d). Thus, during infection, NleH1 is sufficiently potent to inhibit the nuclear translocation of RPS3 even in cells expressing constitutively activate IKKβ.

We assessed whether NleH1 directly phosphorylated IKKβ, thus inhibiting IKKβ-mediated phosphorylation of RPS3 Ser209. We did *in vitro* kinase assays with immunoprecipitated Flag-tagged IKKβ with substitution of the lysine at position 44 with alanine as the substrate and recombinant histidine-tagged NleH1 as kinase, so that autophosphorylation of IKKβ would not obscure NleH1-induced phosphorylation. However, we did not observe any detectable incorporation of ^{32}P into IKKβ (Fig. 32), which thus ruled out this possibility.

We then tested the hypothesis that NleH1 might alter IKKβ substrate specificity. For this we did in vitro kinase assays with both CK2 and IKK substrates for IKKβ. As expected, IKKβ phosphorylated RPS3 (Fig. 31e, lane 7) and a GST-tagged IκBα peptide of amino acids 1–54 (Fig. 31e, lane 9), which demonstrated that it has substrate specificity for either CK2 or IKK. Preincubation of IKKβ with NleH1 resulted in less IKKβ-mediated phosphorylation of RPS3 (CK2 kinase specificity) but not IKKβ-mediated phosphorylation of GST-IκBα (IKK kinase specificity; Fig. 31e). Control experiments showed no NleH1-mediated phosphorylation or autophosphorylation of RPS3 or GST-IκBα (Fig. 31e). Together these results indicate that NleH1 blocks the CK2 substrate specificity of IKKβ, thus inhibiting IKKβ-mediated phosphorylation of RPS3 Ser209. This represents a previously unknown strategy by which *E. coli* O157:H7 alters the host innate immune response.

Discussion

RPS3 functions as an associated subunit that confers regulatory specificity on NF-κB (Wan et al.,

2007). Here we sought to elucidate how NF-κB-activation signaling triggers RPS3 to translocate and participate in NF-κB function in the nucleus. We have demonstrated that IKKβ-mediated phosphorylation of RPS3 Ser209 represents a critical determinant in governing its nuclear import and have thus identified a previously unknown mechanism behind the regulatory specificity of NF-κB. IKKβ is the main kinase that phosphorylates IκB proteins in the classical NF-κB pathway, leading to their subsequent degradation (Hacker and Karin, 2006). Notably, RPS3 has no consensus IKK motif; instead, Ser209 is centered on a consensus CK2 motif. The observation that human IKKβ has CK2-like phosphorylation specificity (Shaul et al., 2008) coincides with our evidence that recombinant IKKβ phosphorylated RPS3, but IKKα did not. We found that this phosphorylation was a critical modulation for the nuclear translocation of RPS3 (via importin-α) and engagement in specific NF-κB transcription. CK2 is known to phosphorylate p65 and to bind to and phosphorylate IKKβ (Chantome et al., 2004; Wang et al., 2000; Yu et al., 2006); however, we ruled out the possibility that the IKKβ-bound CK2 accounted for the observed RPS3 phosphorylation because we detected no CK2 in the IKKβ preparations used for the in vitro kinase assay. Because RPS3 has only the CK2 motif and does not have a traditional IKK motif, this regulatory function of RPS3 could explain why IKK has the ability to phosphorylate alternative substrates.

More notably, we have elucidated how RPS3 is biochemically integrated into NF-κB-activation signaling in a manner that is pivotal for the pathogenesis of food-borne pathogen *E. coli* O157:H7. IKKβ-mediated phosphorylation of RPS3 Ser209 is a critical signaling event modulated by this pathogen to subvert host NF-κB signaling. The bacterial effector NleH1 specifically binds to RPS3 once it is injected into host cells and profoundly suppresses NF-κB and its attendant protective immune responses (Gao et al., 2009). Our data have now shown that

Fig. 32. The bacterial effector protein NleH1 blocks RPS3 S209 phosphorylation. (**a**) 293T cells were transfected with control VN-HA or NleH1-HA plasmids and whole cell lysates were derived and immunoblotted for HA and β-actin as a loading control. (**b**) NF-κB luciferase assay (mean and s.d., n = 3) using 293T cells transfected with control VN-HA or NleH1-HA plasmids together with a 5 × Ig κB site-driven luciferase reporter gene. (**c**) 293T cells were stimulated with (+) or without (-) 50 ng/ml of TNF for 15 min. The derived whole cell lysates were immunoblotted for S209 phosphorylated RPS3 (p-RPS3) and indicated proteins. β-actin served as a loading control. (**d**) HeLa cells were left uninfected (Uninf) or infected for 3 h with wild-type (WT) *E. coli* O157:H7 or strains with isogenic deletions in the escN (ΔescN) or nleH1 (ΔnleH1) genes, followed by TNF treatment for the indicated periods. Whole cell lysates were extracted and immunoblotted with antibodies specific for normal RPS3 or S209 phosphorylated RPS3 (left). Densitometry of all bands was performed, and the intensity of each p-RPS3 band was normalized to corresponding RPS3 band. The fold change of p-RPS3/RPS3 was further normalized to the 0-min samples (set as 1.0) in cells infected with the indicated E. coli O157:H7 strains (right). (**e**) Transcript abundance relative to uninfected cells assessed by RT-PCR analysis of HeLa cells infected for 3 h with *E. coli* O157:H7 strains as in (d). The relative mRNA abundance of IL8, TNFAIP3, and NFKBIA were normalized to GAPDH expression (mean and s.d., n = 3). (f) Immunohistochemistry for S209 phosphorylated RPS3 in paraffin-embedded piglet colons derived from gnotobiotic piglets infected with *E. coli* O157:H7 EDL933 strains possessing (WT) or lacking NleH1 (ΔnleH1), using phospho-RPS3 antibody and 3,3′-diaminobenzidine as a substrate (brown). Nuclei were counterstained with hematoxylin (blue). Size bar represents 25 μm. Representative images from two piglets are shown. Data are representative of two (a, c), four (b), three (d, e), and six (f) independent experiments.

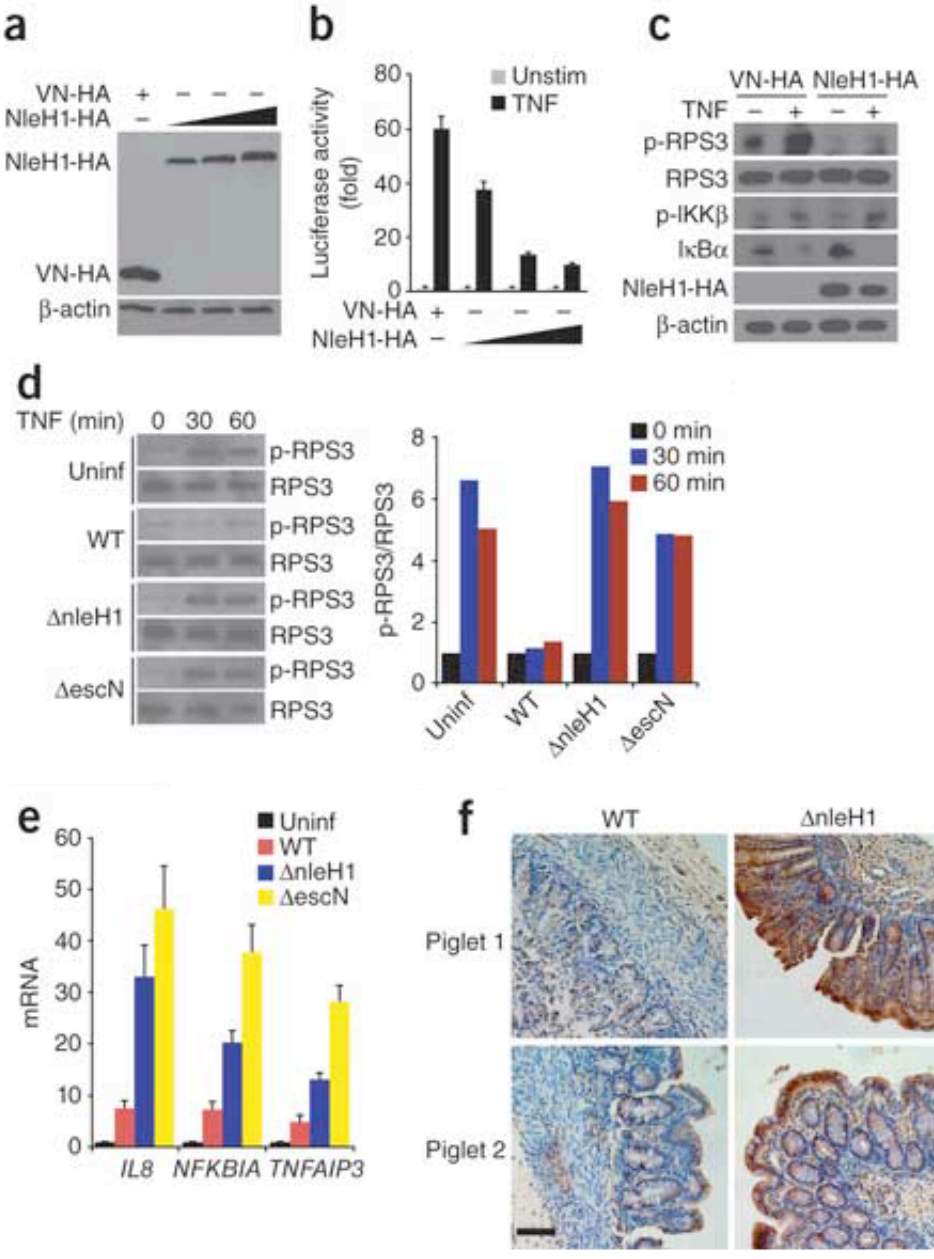
a
VN-HA + – – –
NleH1-HA – ▲
NleH1-HA
VN-HA
β-actin
b
Luciferase activity (fold)
80
60
40
20
0
Unstim
TNF
VN-HA + – – –
NleH1-HA – ▲
c
VN-HA NleH1-HA
TNF – + – +
p-RPS3
RPS3
p-IKKβ
IκBα
NleH1-HA
β-actin
d
TNF (min) 0 30 60
Uninf
WT
ΔnleH1
ΔescN
p-RPS3
RPS3
p-RPS3/RPS3
8
6
4
2
0
0 min
30 min
60 min
Uninf
WT
ΔnleH1
ΔescN
e
mRNA
60
50
40
30
20
10
0
Uninf
WT
ΔnleH1
ΔescN
IL8
NFKBIA
TNFAIP3
f
WT
ΔnleH1
Piglet 1
Piglet 2

Fig. 33. A subset of certain NF-κB target gene transcription is not impaired by NleH1. HeLa cells were left uninfected (Uninf) or infected for 3 h with wildtype (WT) *E. coli* O157:H7 or stains isogenic deletions in the *escN* (ΔescN) or *nleH1* (ΔnleH1) genes. Transcript abundance of *TNFSF13B*, *IFNGR2*, and *CD25* relative to uninfected cells assessed by RT-PCR analysis. The relative mRNA abundance were normalized to *GAPDH* expression (mean and s.d., n=3). The data represent two independent experiments.

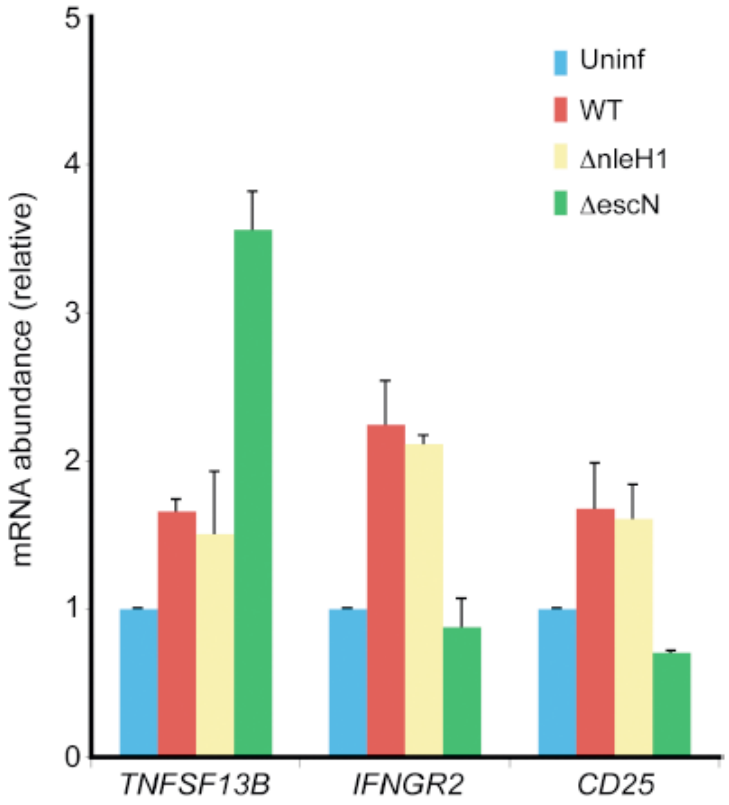
5
4
3
2
1
0
mRNA abundance (relative)
Uninf
WT
ΔnleH1
ΔescN
TNFSF13B
IFNGR2
CD25

Fig. 34. NleH1 alters the substrate specificity of IKKβ to block IKKβ-mediated phosphorylation of RPS3. (**a**) Autoradiography (left) and Coomassie blue staining (right) of *in vitro* kinase assays with recombinant histidine-tagged (His-) NleH1 or NleH1(K159A), showing autophosphorylated NleH1 (p-NleH1) and total NleH1 (right margin). (**b**) Immunoblot analysis (above) of whole-cell lysates of HeLa cells overexpressing hemagglutinin-tagged control protein (−), wild-type NleH1 or NleH1(K159A), left unstimulated (−) or stimulated for 30 min (+) with TNF (50 ng/ml). Below, densitometry, normalized and presented as in Figure 20d (c) Immunoblot analysis (above) of whole-cell lysates of HeLa cells left uninfected or infected for 3 h with wild-type or ΔnleH *C. rodentium* or with ΔnleH *C. rodentium* complemented with wild-type NleH1 (ΔnleH+nleH1) or NleH1(K159A) (ΔnleH+nleH1(K159A)), followed by TNF treatment for 30 min. Below, densitometry, normalized as in Figure 20d and presented as the ratio of phosphorylated RPS3 to RPS3 relative to that in untreated cells without infection, set as 1. (**d**) Immunoblot analysis (above) of nuclear proteins from HeLa cells transfected for 48 h with Flag-tagged IKKβ constructs (top), then left uninfected (Mock) or infected for 3 h with wild-type, ΔescN or ΔnleH1 *E. coli* O157:H7. Below, densitometry, normalized as the intensity of each RPS3 band to the corresponding PARP band and presented as the change in nuclear RPS3 relative to that in mock-infected cells, set as 1. (**e**) Autoradiography (left) and Coomassie blue staining (right) of *in vitro* kinase assays with recombinant RPS3 or GST-tagged IκBα peptide of amino acids 1–54 (GST-IκBα (1–54)) as the substrate and recombinant NleH1 or human IKKβ as the kinase. Data are representative of at least of two experiments.

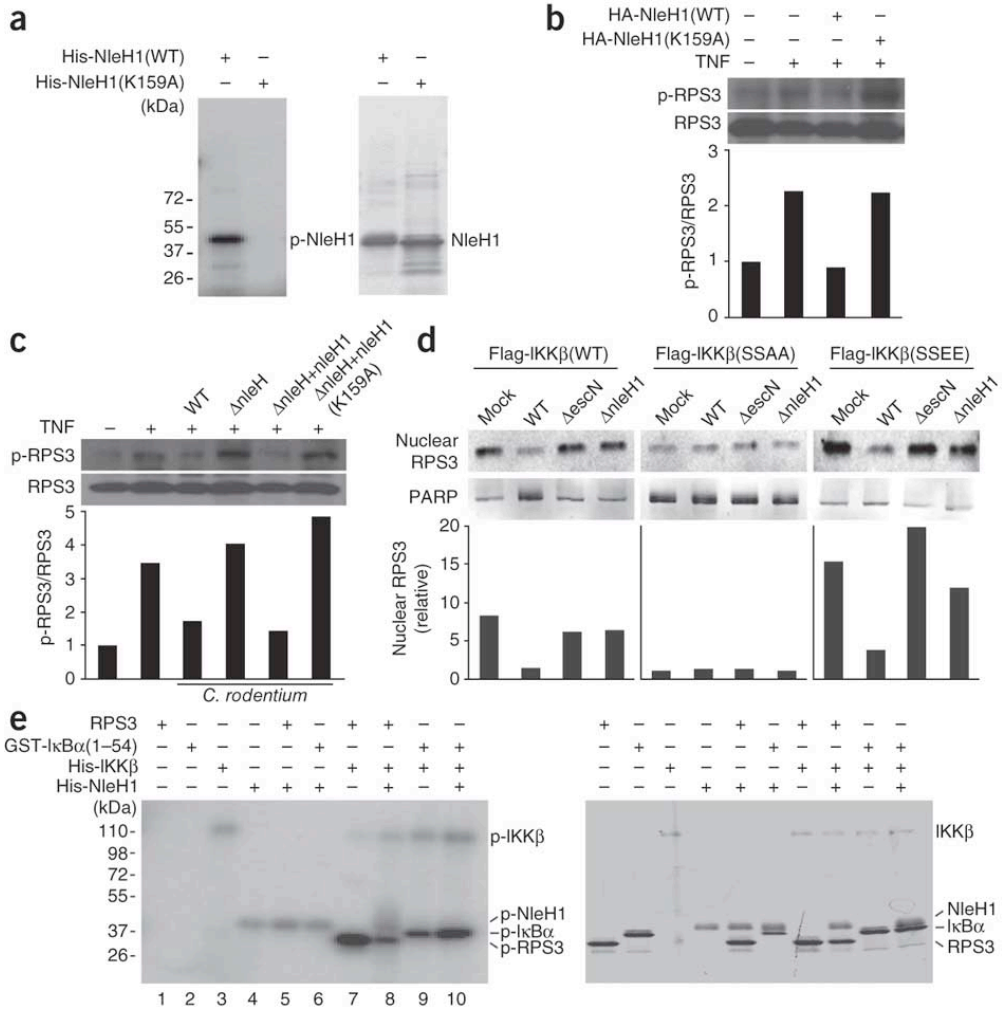
a
His-NleH1(WT)
His-NleH1(K159A)
(kDa)
72-
55-
37-
26-
p-NleH1
NleH1
b
HA-NleH1(WT)
HA-NleH1(K159A)
TNF
p-RPS3
RPS3
p-RPS3/RPS3
c
WT
ΔnleH
ΔnleH+nleH1
ΔnleH+nleH1 (K159A)
TNF
p-RPS3
RPS3
p-RPS3/RPS3
C. rodentium
d
Flag-IKKβ(WT)
Flag-IKKβ(SSAA)
Flag-IKKβ(SSEE)
Mock
WT
ΔescN
ΔnleH1
Nuclear RPS3
PARP
Nuclear RPS3 (relative)
e
RPS3
GST-IκBα(1–54)
His-IKKβ
His-NleH1
(kDa)
110-
98-
72-
55-
37-
26-
p-IKKβ
p-NleH1
p-IκBα
p-RPS3
IKKβ
NleH1
IκBα
RPS3
1 2 3 4 5 6 7 8 9 10

Fig. 35. NleH1 does not phosphorylate IKKβ in vitro. HEK 293T cells were transfected with IKKβ (K44A)-Flag construct. In 24 h, the cells were lysed and followed by an immunoprecipitation with anti-Flag or isotype control (iso) antibodies. The immunoprecipitants were used as substrate in *in vitro* kinase assays with either wild-type or kinase dead (K159A) NleH1 proteins as kinases. The proteins were separated by SDS-PAGE and followed by autoradiograph (top). The expression and immunoprecipitated IKKβ (K44A)-Flag proteins were immunoblotted with anti-Flag antibody (bottom). The data represent two independent experiments.

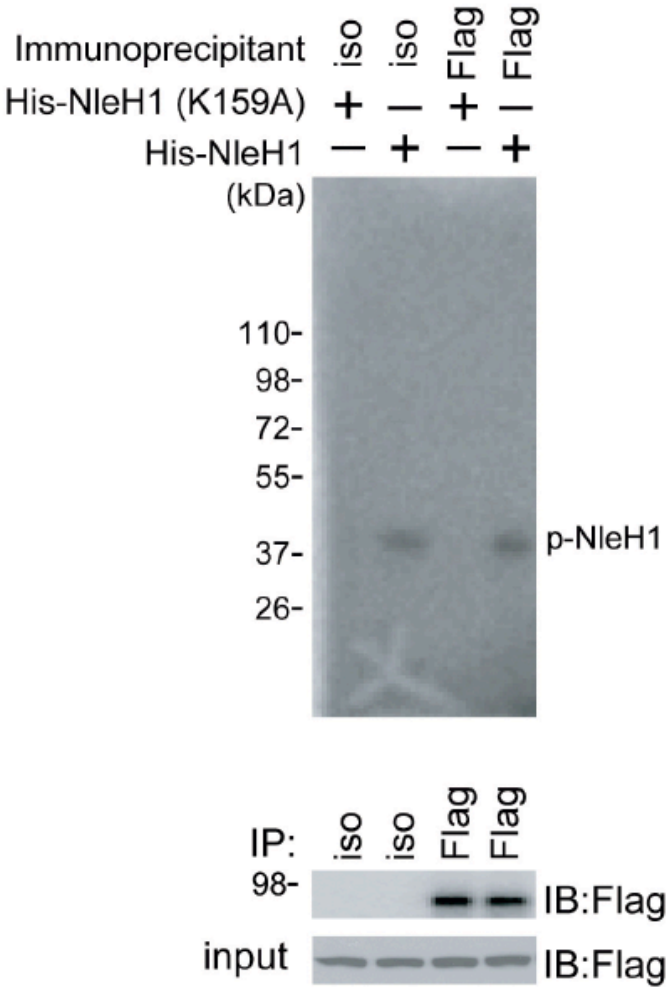
Immunoprecipitant
iso
iso
Flag
Flag
His-NleH1 (K159A)
+
—
+
—
His-NleH1
—
+
—
+
(kDa)
110-
98-
72-
55-
37-
26-
p-NleH1
IP:
iso
iso
Flag
Flag
98-
IB:Flag
input
IB:Flag

NleH1 selectively inhibited RPS3 phosphorylation, thus retarding its nuclear translocation and subsequent NF-κB function without altering other NF-κB signaling. Although NleH1 did not directly phosphorylate IKKβ, its kinase activity was needed to inhibit IKKβ-mediated phosphorylation of RPS3 Ser209. Many bacterial pathogens have products that target key kinases to inactivate the kinases in host cells, whereas *E. coli* O157:H7 used NleH1 to steer the substrate specificity of IKKβ, thus specifically fine-tuning host NF-κB signaling. This could represent a previously unknown strategy for fine-tuning host NF-κB signaling that could be shared by other pathogens. Our data have provided new insight into the poorly understood action mechanism of most type III secretion system effectors.

NleH1 attenuated the transcription of RPS3-dependent target genes but not all NF-κB target genes, in particular those genes associated with acute proinflammatory responses, including IL8 and TNF. In contrast, NleH1 did not block nuclear translocation of NF-κB p65, which suggests that certain p65-dependent but RPS3-independent NF-κB target genes might thus be beneficial for the replication and dissemination of *E. coli* O157:H7 in the host. By selectively inhibiting RPS3 and its attendant NF-κB function with NleH1, the pathogen achieves the ability to increase colonization and diarrhea while limiting the mortality of the host. This seemingly paradoxical combination of effects make sense given that the greater bacterial load and diarrhea together with survival of the infected host would promote the spreading of the bacteria among a population of susceptible organisms. Such complex and paradoxical pathological effects that influence the spread of disease are often poorly understood at the molecular level. We have elucidated how alterations in selective NF-κB function, achieved by impeding RPS3 but not altering the nuclear translocation of p65, can influence specific cytokines that affect bacterial colonization, diarrheal disease and mortality. It may be fruitful while attempting to understand other infectious and

autoimmune diseases involving NF-κB to consider selective effects of subunits such as RPS3 in addition to global inhibition of NF-κB.

Experimental procedures

Cells and reagents

Jurkat E6.1, HEK293T and HeLa cells were cultured in RPMI-1640 medium and DMEM supplemented with 10% (vol/vol) FCS and 2 mM glutamine, plus penicillin and streptomycin (100 U/ml each). Anti-IκBα (C-21; sc-371), anti-p65 (C-20; sc-372) and antibody to phosphoryalted threonine (H-2; sc-5267) were from Santa Cruz Biotechnology; anti-β-actin (AC-15; A5441), anti-Flag (M2; F3165), anti-hemagglutinin (HA-7; H3663), anti-importin-α (IM-75; I1784) and anti-importin-β (31H4, I2534) were from Sigma; anti-PARP (C2-10; 556362), anti-IKKα (B78-1; 556532) and anti-IKKβ (24; 611254) were from BD Pharmingen; anti-CK2α (31; 611610) and anti-hsp90 (68; 610418) were from BD Transduction Laboratories; antibody to phosphorylated IκBα (5A5; 9246S) and antibody to phosphorylated IKKα-IKKβ (16A6; 2697S) were from Cell Signaling Technology; antibody to phosphorylated serine (AB1603) and antibody to phosphorylated tyrosine (4G10; 05-777) were from Millipore. Rabbit polyclonal antiserum to RPS3 has been described6. Rabbit polyclonal antibody specific for RPS3 phosphorylated at Ser209 was generated and affinity-purified by Primm Biotech with the peptide NH2-CKPLPDHV(Sp)IVE-COOH.

Plasmid constructs.

The constructs for Flag-tagged SSEE and SSAA IKKβ mutants and the hemagglutinin-tagged SSAA IκBα mutant were provided by C. Wu and U. Siebenlist, respectively. The plasmids for hemagglutinin-tagged IκBα and Flag-tagged IKKβ with the K44A substitution were from Addgene44, 45. The plasmids for Flag-tagged RPS3, GST-tagged RPS3 and hemagglutinin-tagged RPS3, control VN protein and NleH1 have been described6, 9. RPS3(S209A) was generated by site-directed mutagenesis with the Quick Change Kit (Stratagene) with primers 5′-CTGCCTGACCACGTGGCCATTGTGGAACCCAAA-3′ (forward) and 5′-TTTGGGTTCC-ACAATGGCCACGTGGTCAGGCAG-3′ (reverse). All mutants were verified by DNA sequencing.

^{32}P *in vivo* labeling.

HEK293T cells were labeled for 2 h with [^{32}P]orthophosphate (2 mCi/ml; PerkinElmer) in phosphate-free medium (Invitrogen). Cells were then left untreated or were treated for the appropriate time with TNF (50 ng/ml; R&D Systems). Cell lysates were prepared and used for immunoprecipitation with anti-RPS3.

In vitro kinase assay.

Kinase-active recombinant IKKβ and IKKα proteins were from Active Motif and Millipore, respectively. Bacterially purified GST, GST-IκBα (amino acids 1–54), wild-type GST-RPS3, mutant GST-RPS3 or RPS3 from which the tag was cleaved served as substrates. In vitro kinase

assays were done as described29. Enzyme (100 ng) and substrate (2 μg) were incubated together in IKK reaction buffer (25 mM Tris-HCl, pH 8.0, 50 mM KCl, 10 mM MgCl2, 1 mM dithiothreitol, 1 mM Na3VO4 and 1 mM ATP) or NleH1 reaction buffer (50 mM Tris-HCl, pH 7.6, 5 mM MgCl2, 1 mM dithiothreitol and 1 mM ATP), with 0.5 μCi [γ-^{32}P]ATP (GE Healthcare) added for 30 min at 37 °C. Reactions were resolved by SDS–PAGE and visualized by autoradiography.

Liquid chromatography–tandem mass spectrometry.

GST or GST-RPS3 was incubated with recombinant IKKβ protein as described above in in vitro kinase assay reactions without [γ-^{32}P]ATP labeling. Reactions were separated by SDS-PAGE and gels were stained with colloidal blue (Invitrogen). The corresponding protein fragments were excised and digested with trypsin, followed by liquid chromatography–tandem mass spectrometry at the Yale Cancer Center Mass Spectrometry Resource.

RNA-mediated interference and transfection.

The siRNA sense-strand sequences were as follows: IKKα, 5′-AUGACAGAGAAU-GAUCAUGUUCUGC-3′; IKKβ, 5′-GCAGCAAGGAGAACAGAGGUUAAUA-3′; IκBα, 5′-GAGCUCCGAGACUUUCGAGGAAAUA-3′; RPS3-3′ UTR, 5′-GGAUGUUGCUCUCUA-AAGACC-3′ (Invitrogen). Transient transfection of siRNA and DNA constructs into Jurkat cells and HEK293T cells has been described (Wan et al., 2007).

Subcellular fractionation.

Differential centrifugation was used for subcellular fractionation as described (Wan et al., 2007). Cells were resuspended for 5 min at 4 °C in ice-cold buffer A (10 mM HEPES, pH 7.9, 10 mM KCl, 1.5 mM MgCl2, 0.1 mM EDTA, 0.5 mM dithothreitol, 0.4% (vol/vol) NP-40, 0.5 mM phenylmethyl sulfonyl fluoride and complete protease inhibitor 'cocktail'). Lysates were centrifuged for 3 min at 500g and 4 °C, and supernatants were collected as cytosolic fractions. Pellets were incubated for 10 min at 4 °C in buffer C (20 mM HEPES, pH 7.9, 420 mM NaCl, 1.5 mM MgCl2, 25% (vol/vol) glycerol, 0.5 mM PMSF, 0.2 mM EDTA, 0.5 mM dithiothreitol and complete protease inhibitor 'cocktail'). Supernatants were collected as nuclear fractions after centrifugation for 10 min at 13,800g and 4 °C.Luciferase reporter gene assays.

These assays were done as described (Wan et al., 2007). Cells were cotransfected with firefly luciferase constructs driven by various promoters and the renilla luciferase plasmid pTKRL at a ratio of 10:1, together with the appropraite plasmid. Cells were cultured for 1–2 d and then were stimulated (in triplicate) before being collected. Lysates were analyzed with a Dual-Luciferase kit (Promega).

Chromatin immunoprecipitation.

These assays were done as described (Wan et al., 2007). The primers used to amplify the promoter region adjacent to the κB sites of IL8 and NFKBIA, as well as ACTB have been described (Wan et al., 2007).

Immunofluorescence microscopy.

Confocal microscopy was done as described (Wan et al., 2007). Cells were fixed with 4% (vol/vol) paraformaldehyde in PBS and then mounted with Cellspin onto slides. Fixed cells were then made permeable with 0.05% (vol/vol) Triton X-100 in PBS and were stained for 40 min with fluorescein isothiocyanate–conjugated donkey antibody to rabbit immunoglobin G (711-096-152; Jackson Laboratory) and rabbit anti-RPS3 (Primm Biotech) or Alexa Fluor 594–conjugated goat antibody to mouse immunoglobin G1 (A21125; Invitrogen) and anti-Flag (M2; F3165; Sigma) and were incubated for 5 min at 25 °C together with Hoechst 33342 (1 μg/ml; Sigma). Slides were then rinsed three times with PBS and were mounted with covers for fluorescence microscopy.

Immunoprecipitation and immunoblot analysis.

Cells were lysed for 30 min on ice by 0.4 ml modified radioimmunoprecipitation assay buffer (50 mM Tris-HCl, pH 7.4, 1% (vol/vol) Nonidet-P40, 0.25% (wt/vol) sodium deoxycholate, 150 mM NaCl, 1 mM EDTA, 1 mM phenylmethyl sulfonyl fluoride, 1 mM Na3VO4 and 1 mM NaF) supplemented with 1× protease inhibitor 'cocktail' (Roche) and 1× phosphatase inhibitor 'cocktail' set I (EMD Biosciences). Lysates were centrifuged for 10 min at 10,000g and 4 °C for removal of insoluble material. After normalization of protein concentrations, lysates were subjected to immunoprecipitation by the addition of the appropriate antibody (10 mg/ml) plus 30 ml of protein G–agarose (Roche), followed by rotation for at least 2 h at 4 °C. Precipitates were washed at least five times with cold lysis buffer, followed by separation by SDS-PAGE under

reducing and denaturing conditions. Nitrocellulose membranes were blocked in 5% (wt/vol) nonfat milk in 0.1% (vol/vol) Tween 20 in PBS, then were probed with the appropriate antibodies as described6. For immunoblot analysis of phosphorylated proteins, gels were transferred to methanol-treated polyvinylidene chloride membranes, retreated with methanol and dried for 30 min. Blots were blocked in 5% (wt/vol) bovine serum albumin in 0.1% (vol/vol) Tween 20 in Tris-buffered saline and were probed with the appropriate antibodies as described46. Bands were imaged by the Super Signaling system (Pierce) according to the manufacturer's instructions.

Enzyme-linked immunosorbent assay.

Interleukin 8 in supernatants of Jurkat cell cultures was measured with a Human IL-8 ELISA Ready-SET-Go! kit according to the manufacturer's instructions (eBioscience).

Cell Infection.

HeLa cells were infected with *E. coli* O157:H7 or *C. rodentium* as described (Gao et al., 2009).

Immunohistochemistry.

Gnotobiotic piglets were infected with *E. coli* O157:H7 as described (Gao et al., 2009). Spiral colon specimens collected at necropsy were embedded in paraffin. Paraffin sectioning and immunohistochemical staining with antibody to phosphorylated RPS3 were done by Histoserv.

Chapter IV: Bacterial effector glycosyltransferase activity reveals an integral role for GAPDH in innate immunity

Abstract

Here we studied the mechanism of how the T3SS effector NleB targets the NF--κB signaling pathway. We identified the host glycolytic protein GAPDH as a eukaryotic interaction partner for NleB, which lead us to identify an integral role for GAPDH in the NF-κB signaling pathway. GAPDH interacts with TRAF2 and co-activates TRAF2 under stess conditions. We further demonstrated that NleB is an O-GlcNAc transferase and O-GlcNAclates GAPDH during bacterial infection. The NleB-mediated O-GlcNAcylation of GAPDH disrupts the formation of the GAPDH-TRAF2 complex resulting in the attenuation of TRAF2 polyubiquitination and NF-κB activation. Eliminating the O-GlcNAc transferase activity abolishes the inhibitory effect of NleB on NF-κB activation and reduces the bacterial colonization ability in the host.

Introduction

Infectious diarrhea constitutes a major endemic health threat and an increasingly frequent and deadly source of food- and water-borne illness. The Shiga toxin-producing *Escherichia coli* (STEC), a type of enterohemorrhagic *E. coli* (EHEC) are especially significant because they cause a type of renal failure (hemolytic uremic syndrome; HUS) for which therapy is limited. Furthermore, these infections are difficult to treat because antibiotics are contraindicated. A related attaching/effacing (A/E) pathogen, enteropathogenic *E. coli* (EPEC), is an important cause of infantile diarrhea.

These human pathogens, as well as *C. rodentium*, a mouse pathogen that shares virulence strategies with *E. coli* (Deng et al., 2003), adhere to intestinal enterocytes and translocate virulence proteins (effectors) directly into intestinal epithelial cells through a type III secretion system (T3SS, (Cornelis, 2010)). Translocated T3SS effectors subvert host cell function by disrupting epithelial barrier function, altering ion channel/water pump activity, degrading absorptive microvilli, and suppressing innate immune responses.

The knowledge of how T3SS effectors modulate the innate immune system, especially pathways regulated by the transcription factor NF-κB, has been expanded during past decades (Rahman and McFadden, 2011). In A/E pathogens, we have reported NleH1 from EPEC/EHEC specifically targets IKKβ-mediated non-Rel subunit Ribosomal protein S3 (RPS3) phosphorylation and subsequently blocks RPS3 nucleular translocation (Gao et al., 2009; Wan et al., 2011). The reduction of RPS3 nucleular translocation during cytokine stimulation or bacterial infection impairs NF-κB activation. Recently, NleC is a Zn-dependent protease that specifically cleaves the N-termini of RelA and inhibits RelA nucleular translocation upon stimulation

(Pearson et al., 2011; Shames et al., 2010; Yen et al., 2010). The latest studies showed that NleE is a methyltransferase that specifically methylates zinc-coordinating cysteines 673/692 in Npl4 zinc finger (NZF) domains of TAB2/TAB3 (Zhang et al., 2012). The methylated NZF domains of TAB2/3 show a defect in binding zinc ions as well as binding with ubiquitin chains to impair the signalling of the NF-κB pathway.

NleB is a T3SS-translocated effector that is highly conserved among the A/E pathogens. NleB-deficient *C. rodentium* do not cause mortality (Wickham et al., 2007b) or significant colonic hyperplasia (Kelly et al., 2006) in mice. These bacteria also suffer drastically reduced colonization, indicating the importance of NleB to *C. rodentium* virulence. While the function of NleB is unclear, the presence of NleB is a signature of STEC strains with high virulence in humans (Bugarel et al., 2010). NleB is strongly associated with human STEC outbreaks and the subsequent development of HUS (Wickham et al., 2006). Additionally, the presence of NleB in atypical EPEC strains is associated with diarrheal disease (Bugarel et al., 2010). Thus, it is clear that NleB plays an important role in the virulence of A/E pathogens. While NleB is not similar to proteins of known function and no functional domains in NleB have been identified, two recent studies suggest that a function of NleB may be to suppress NF-κB activation (Nadler et al., 2010; Newton et al., 2010). Here, we demonstrate that NleB is an O-GlcNAc transferase that utilizes UDP-GlcNAc (Uridine diphosphate N-acetylglucosamine) from the host hexamine biosynthesis pathway (HBP) to target GAPDH. We provide the evidence that GAPDH is a co-activator of TRAF2 and the O-GlcNAcylation of GAPDH mediated by NleB prevents its function in TRAF2 activation and alter NF-κB signalling.

Results

NleB inhibits NF-κB activation by inhibiting TRAF2 polyubiquitination. Recent studies have identified NleB as a virulence factor required for bacterial colonization and transmission (Kelly et al., 2006; Wickham et al., 2007a). In agreement with previous studies, we found that the colonization of C57BL/6J mice by wild-type (WT) *C. rodentium* is significantly greater than that of either *ΔescN* or *ΔnleB C. rodentium* (Fig. 36A). Complementing the *ΔnleB* C. *rodentium* strain (*ΔnleB*/p*nleB*) restored bacterial colonization to a magnitude comparable to the wild-type strain. Additionally, TNF concentrations in sera are significantly higher in mice infected with wild-type *C. rodentium*, as compared with mice infected with *ΔnleB* (Fig. 36B), which indicates that NleB contributes to bacterial-induced inflammation in the host. NleB has been suggested to inhibit TNF-induced NF-κB activation, but the mechanism is unclear (Nadler et al., 2010; Newton et al., 2010). To confirm these data, we transfected HeLa cells with NleB-HA or an HA-epitope control plasmid and then stimulated these cells with TNF and subsequently examined the extent of IκBα degradation. Consistent with previous studies (Nadler et al., 2010; Newton et al., 2010), we found that NleB prevents TNF-induced IκBα degradation and the subsequent translocation of the NF-kB p65 subunit to the nucleus (Fig. 37A).

After stimulation with TNF, the cytosolic death domain of the TNF receptor-1 (TNF-R1) recruits molecules such as the TNFR-associated death domain protein (TRADD), the TNFR associated factor 2 (TRAF2) and receptor-interacting protein 1 (RIP1) to form multiple protein complexes that subsequently activate the NF-κB pathway (Chen and Goeddel, 2002). During this process, TRAF2, an E3 ubiquitin ligase, quickly becomes polyubiquitinated and activates the kinase RIP1. As NleB has been proposed to target the initial events of TNF-NF-κB signaling, we therefore examined whether NleB affects TRAF2 polyubiquitination. Because of the difficulty in

detecting endogenous TRAF2 in HeLa cells, we co-transfected a TRAF2-FLAG expression plasmid with *C. rodentium* NleB-HA or an HA-epitope control plasmid. TRAF2 polyubiquitination was strongly induced by TNF in control cells (Fig. 37D). By contrast, cells transfected with NleB-HA exhibited significantly reduced TRAF2 polyubiquitination (Fig. 37D). Surprisingly, TRADD was still recruited to TRAF2 in the presence of NleB (Fig. 37D), indicating the molecular target of NleB might instead be a co-activator of TRAF2 polyubiquitination

To assess the impact of NleB on TRAF2 stability, we transfected HeLa cells with TRAF2-FLAG and then infected these cells with *C. rodentium* strains possessing or lacking NleB. Infecting cells with *ΔnleB C. rodentium* strain quickly induced TRAF2 protein degradation (Fig. 37B), with almost complete TRAF2 degradation observed after 3 h infection. By contrast, TRAF2 was stable in cells infected with either wild-type (WT) or *ΔnleB*/p*nleB C. rodentium* (Fig. 37B). The dynamics of TRAF2 protein degradation was synergized with the NF-κB inhibitor, IκBα protein degradation (Fig. 37B). *ΔnleB C. rodentium* failed to induce TRAF2 degradtion in cells transfected with TRAF2 ΔRING mutant, which can not become polyubiquitinated (Fig. 37C, (Chen, 2005; Shi and Kehrl, 2003)). The 26S proteasome inhibitor MG-132 stabilized TRAF2 during bacterial infection (Fig. 37E). Therefore, our data suggested TRAF2 degradation induced by the bacterial infection is clearly dependent on the host ubiquitin-26S proteasome system, which is consistent with previous studies (Brown et al., 2001). As we expected, TRAF2 polyubiquitination is prevented in cells infected by WT or *ΔnleB*/p*nleB C. rodentium* but not *ΔnleB* C. *rodentium* strain (Fig. 37E). Taken together, our results suggested NleB might target a missing co-activator(s) of TRAF2 to prevent its polyubiquitination upon TNF stimulation or bacterial infection, which subsequently results in the attenuation of NF-κB

activation.

NleB interacts with GAPDH. As we did not obtain evidence that NleB binds TRAF2 (Fig. 37D), we conducted a proteomic screen to identify NleB interaction partner(s). By using an NleB-FLAG affinity column, we identified a HeLa cell protein of ~ 37 kDa that specifically interacted with immobilized NleB (Fig. 38A). By using mass spectrometry, we identified this protein as glyceraldehyde 3-phosphate dehydrogenase (GAPDH; Fig. 38B), an integral component of the glycolysis pathway.

We confirmed the association of NleB with endogenous GAPDH by performing immunoprecipitation assays. Infecting HeLa cells with *C. rodentium* strains expressing either NleB-FLAG or NleC-FLAG showed that NleB, but not NleC immunoprecipitates with GAPDH (Fig. 38C). GAPDH also co-immunoprecipitates with ectopically-expressed NleB-HA, but not with an HA-epitope control (Fig. 38D). Our *in vitro* pulldown assay with recombinant proteins showed that NleB-FLAG but not NleC-FLAG binds directly to GAPDH (Fig. 38E).

GAPDH converts glyceraldehyde-3-phosphate to D-glycerate 1,3-bisphospate and generates NADH from NAD^+ in the sixth step of glycolysis (Sirover, 1999; Tristan et al., 2011). Besides its glycolytic function, GAPDH is also involved in a broad range of biological events (Sirover, 2011; Tristan et al., 2011). Over-expressing GAPDH induces apoptosis and results in GAPDH localization to the nucleus (Dastoor and Dreyer, 2001; Tajima et al., 1999). GAPDH can bind to and protect telomere DNA from degradation in the presence of DNA damaging agents (Sundararaj et al., 2004). GAPDH also accumulates in the mitochondria of cells with DNA damage, where it induces a pro-apoptotic mitochondrial membrane permeabilization (Tarze et al., 2007).

Some apoptotic stimuli generate nitric oxide, which causes GAPDH S-nitrosylation on its

catalytic cysteine residue (Chen and Goeddel, 2002). Nitrosylated GAPDH (SNO-GAPDH) binds the E3 ubiquitin-protein ligase Siah1, allowing both proteins to enter the nucleus. While Siah1 binding and GAPDH S-nitrosylation do not have a significant impact on overall glycolytic activity (Chen and Goeddel, 2002), elevated glucose concentrations increase Siah1 expression and promote its binding to GAPDH (Yego et al., 2009). Nuclear GAPDH can also function as a trans-nitrosylase, with targets that include the histone deacetylating enzymes SIRT1 and HDAC2 (Kornberg et al., 2010).

To test whether Cys 150 (C150) is essential for NleB-GAPDH binding, we performed an *in vitro* pulldown assay. Our data showed that both GAPDH WT and C150S, which replaces cysteine with serine, are both able to interact with NleB *in vitro* (Fig. 38F). Likewise, treatment with iodoacetate (IA), which modifies the SH-group of the active-site GAPDH cysteine and prevents disulfide bond formation, also does not interrupt GAPDH-NleB interaction *in vitro* (Fig. 38G). In addition, NleB does not alter GAPDH enzymatic activity or the total ATP level in cells (data not shown), which indicates that this NleB-GAPDH interaction is unlikely to alter host metabolism. Taken together, our data strongly suggested GAPDH is the eukaryotic interaction partner for NleB.

GAPDH is required for TNF-induced NF-κB activation. The involvement of GAPDH in stress-responsive pathways has been identified in eukaryotic cells (Colell et al., 2009; Hara et al., 2005; Mookherjee et al., 2009; Morigasaki et al., 2008). Interestingly, GAPDH is also predicted to participate in the NF-κB signaling pathway (Bouwmeester et al., 2004; Mookherjee et al., 2009). We therefore hypothesized GAPDH might be important for NF-κB activation. We first performed a "Loss-of-Function" assay by knocking down endogenous GAPDH protein.

Fig.36 NleB is a bacterial virulence factor. A. Colonization (CFUs / 100mg mouse feces) of indicated *C. rodentium* strains (7 d post-gavage) in C57BL/6J mice (n = 6/group). B. TNF-α concentration in serum samples from mice uninfected or infected with different *C.rodentium* strains.

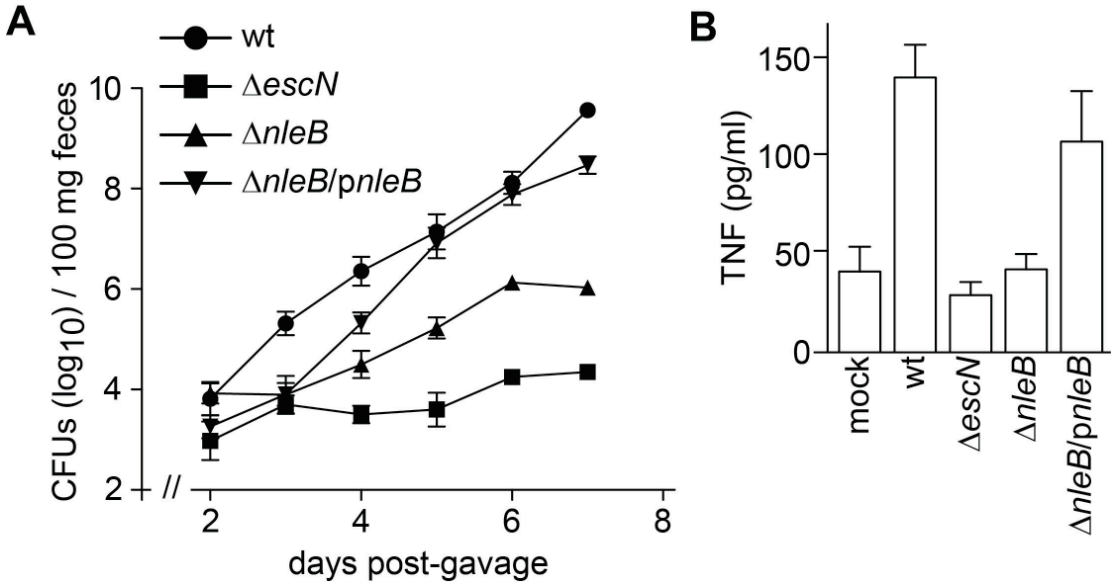
A
wt
ΔescN
ΔnleB
ΔnleB/pnleB
CFUs (log10) / 100 mg feces
10
8
6
4
2
//
2
4
6
8
days post-gavage
B
TNF (pg/ml)
150
100
50
0
mock
wt
ΔescN
ΔnleB
ΔnleB/pnleB

Fig. 37. NleB inhibits NF-κB activation by inhibiting TRAF2 polyubiquitination. A. Western-blot analysis of IκBα degradation and p65 nuclear translocation stimulated by TNF with or without the presence of NleB. B. Stabilization of TRAF2 during infection. HeLa cells were transfected with 1 μg of TRAF2-FLAG expression plasmids and infected with different *C. rodentium* strains for 1 or 3 h. The amount of NleB protein translocated into the cytosol of host cells is indicated as NleB-FLAG. C. Effect of TRAF2 RING domain on TRAF2 protein stabilization during bacterial infection. HeLa cells transfected with either TRAF2-FLAG or ΔRING TRAF2-FLAG expression plasmid were infected with *C. rodentium* for 3 h. D. Immunoprecipitation of TRAF2-FLAG was performed to assess whether NleB targets TRAF2. Samples were immunoprecipitated by α-FLAG antibody to capture TRAF2 and immunoblotted for TRADD, FLAG to detect TRAF2, ubiquitin to detect polyubiquitin chain and HA to detect NleB. The bottom panel depicts the expression levels of the TRADD, TRAF2, NleB and Actin. E. Polyubiquitination of TRAF2 during the bacterial infection. HeLa cells transfected with TRAF2-FLAG were pre-treated with MG-132 for 2 h and infected with *C. rodentium* strains as indicated for 1 or 3 h. TRAF2 was immunoprecipitated and subjected to western-blot analysis for TRAF2 polyubiquitination.

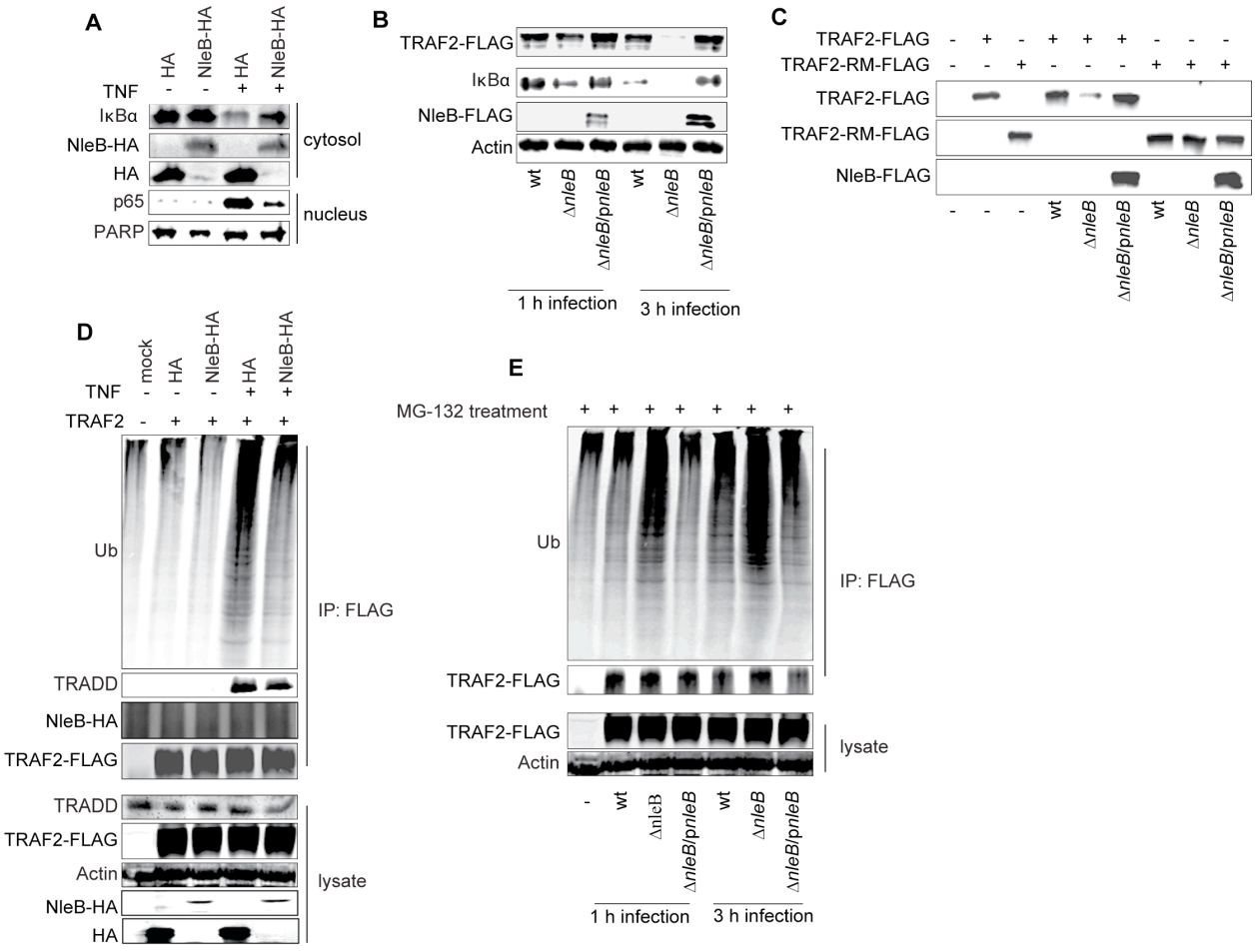
A
HA
NleB-HA
+ HA
+ NleB-HA
TNF
IκBα
NleB-HA
HA
cytosol
p65
PARP
nucleus
B
TRAF2-FLAG
IκBα
NleB-FLAG
Actin
wt
ΔnleB
ΔnleB/pnleB
1 h infection
3 h infection
C
TRAF2-FLAG
TRAF2-RM-FLAG
NleB-FLAG
D
mock
TNF
TRAF2
Ub
IP: FLAG
TRADD
NleB-HA
TRAF2-FLAG
lysate
Actin
HA
E
MG-132 treatment
ΔnleB

Fig. 38. NleB interacts with host glycolytic protein GAPDH. A. Affinity enrichment of HeLa proteins with NleB-FLAG. Upper panel: HeLa cell lysates were incubated with purified NleB-FLAG pre-bound to FLAG M2 beads and analyzed by SDS-PAGE. Samples included M2 beads (lane 1), NleB-FLAG + M2 beads (lane 2), HeLa lysate + M2 beads (lane 3) and HeLa lysate + NleB-FLAG + M2 beads (Lane 4). Protein band cut for mass spectrometry was indicated with Asterisk. Lower pannel: samples from the affinity column assay were analyzed by western-blot with α-GAPDH antibody. B. GAPDH amino acid sequence. Tryptic peptides identified by mass spectrometry are indicated in red. C. Immunoprecipitation of GAPDH from HeLa cells by translocated NleB-FLAG or NleC-FLAG by *C. rodentium* infection for 1 or 3 h. Samples were immunoprecipitated with α-GAPDH antibody and immunoblotted with FLAG and GAPDH. D. Co-immunoprecipitation of GAPDH with HA or NleB-HA plasmids. Samples were immunoprecipitated with α-GAPDH antibody to capture endogenous GAPDH and immunoblotted for HA to detect NleB. E. *In vitro* pulldown assay was conducted to examine the interaction between NleB and GAPDH. The FLAG-tagged NleB or NleC proteins were coupled to M2 beads and incubated with GAPDH. The bound proteins and flow-through (F.T) were analyzed by SDS-PAGE and subjected to IRDye Blue protein stain (LI-COR Bioscience). F. GAPDH enzymatic activity of HeLa cells treated or non-treated with GAPDH inhibitor IA was measured as described in experimental procedures. G. The effect of IA on the interaction binding between GAPDH and NleB-FLAG was measured by *in vitro* pulldown assay. GAPDH proteins were incubated with M2 beads alone or M2 beads pre-binding with NleB-FLAG. GAPDH protein treated with IA was indicated.

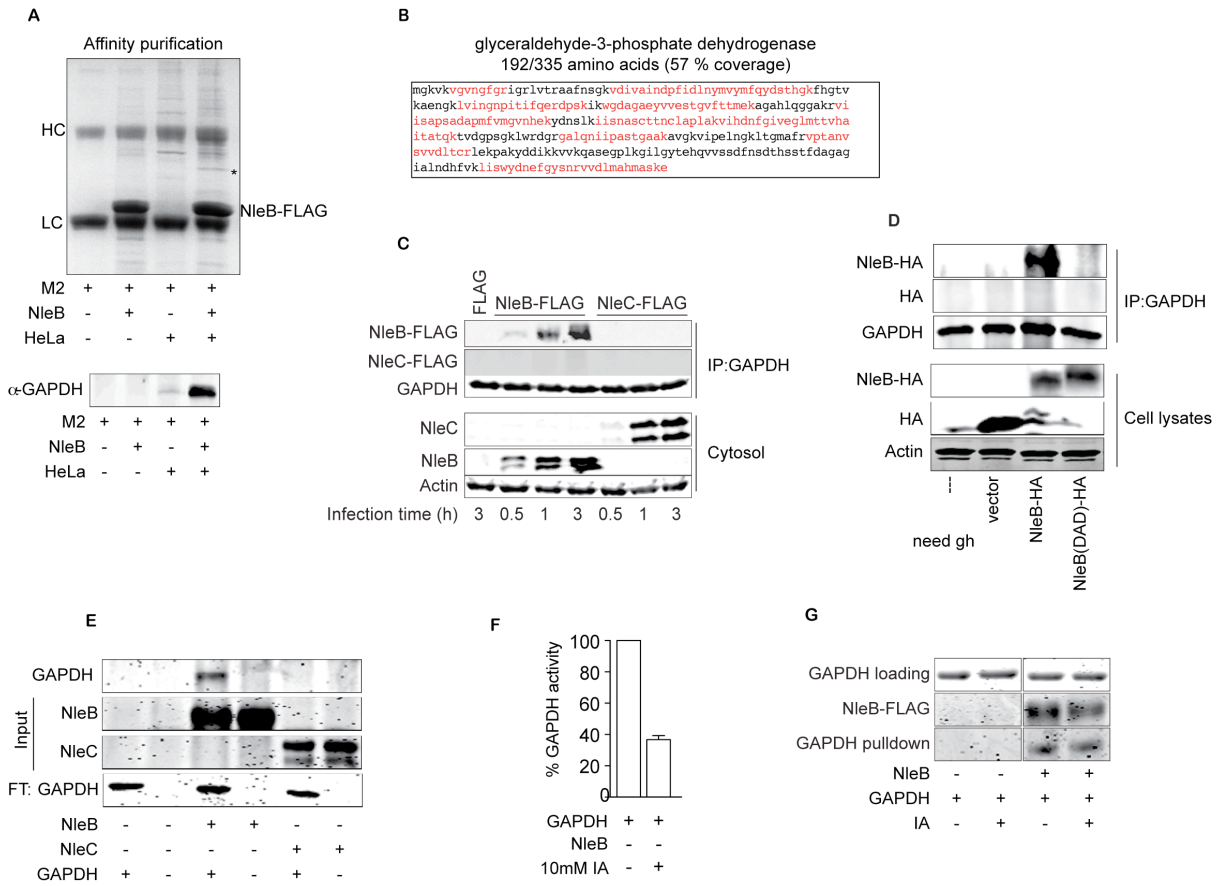
A
Affinity purification
HC
LC
NleB-FLAG
M2 + + + +
NleB - + - +
HeLa - - + +
αGAPDH
M2 + + + +
NleB - + - +
HeLa - - + +
B
glyceraldehyde-3-phosphate dehydrogenase
192/335 amino acids (57 % coverage)
mgkvkvgvngfgrigrlvtraafnsgkvdivaindpfidlnymvymfqydsthgkfhgtv
kaengklvingnpitifqerdpskikwgdagaeyvvestgvfttmekagahlqggakrvi
isapsadapmfvmgvnhekydnslkiisnascttnclaplakvihdnfgiveglmttvha
itatqktvdgpsgklwrdgrgalqniipastgaakavgkvipelngkltgmafrvptanv
svvdltcrlekpakyddikkvvkqasegplkgilgytehqvvssdfnsdthsstfdagag
ialndhfvkliswydnefgysnrvvdlmahmaske
C
FLAG
NleB-FLAG
NleC-FLAG
NleB-FLAG
NleC-FLAG
GAPDH
IP:GAPDH
NleC
NleB
Actin
Cytosol
Infection time (h) 3 0.5 1 3 0.5 1 3
D
NleB-HA
HA
GAPDH
IP:GAPDH
NleB-HA
HA
Actin
Cell lysates
-
vector
NleB-HA
NleB(DAD)-HA
need gh
E
GAPDH
Input
NleB
NleC
FT: GAPDH
NleB - - + + - -
NleC - - - - + +
GAPDH + - + - + -
F
% GAPDH activity
100
80
60
40
20
0
GAPDH + +
NleB - -
10mM IA - +
G
GAPDH loading
NleB-FLAG
GAPDH pulldown
NleB - - + +
GAPDH + + + +
IA - + - +

The depletion of GAPDH activates multiple stress-induced signaling pathways (Fig. 39A). This is likely due to the production of reactive oxygen species (ROS) and the release of cytochrome *c* from mitochondria (Fig. 39B and C). These data indicated that the presence of GAPDH is required to keep cellular homeostasis possibly by maintaining mitochondria membrane integrity (Tarze et al., 2007). Moreover, in GAPDH knocking-down cells, complementing with either GAPDH WT or C150S prevents the release of cytochrome *c* and reduces the activation of stress-responsive pathways (Fig. 39C and D). Knocking down endogenous GAPDH in cells as well as complementing these cells with GAPDH C150S results in 30 % decrease in cellular ATP amount, whereas complementing with GAPDH WT and another mutant K160R slightly increase the ATP amount compared to the control (Fig. 39E). This is likely due to the role of GAPDH in glycolysis. Thus, our "Loss-of-Function" experiments did not indicate a specific role for GAPDH in the NF-κB pathway other than keeping cellular homeostasis. However, we found complementation with the GAPDH C150S expression plasmid specifically attenuates TNF-induced IκBα degradation and NF-κB activation (Fig. 40A). We therefore hypothesized that the C150 of GAPDH might be required for NF-κB activation upon TNF stimulation.

To test this hypothesis, we pre-treated HeLa cells with GAPDH inhibitor IA for 20' followed by TNF stimulation. To evaluate the effect of glycolysis on TNF-induced NF-κB activation, we also pre-treated cells with hexokinase inhibitor 2-deoxy-D-glucose (2-DG) or the pyruvate kinase (PK) inhibitor potassium oxalate (P.Ox). As shown in Fig. 40D, treatment with P.Ox or 2DG results in over 80 % ATP depletion in cells, whereas a 40 % decrease in ATP amount was seen in IA-treated cells. However, treatment of IA leads to a significant inhibition on GAPDH enzymatic activity compared to that in P.Ox or 2-DG-treated cells (Fig. 40B). After TNF treatment, cell samples were collected and subjected to microarray and real-time PCR (RT-

PCR) analysis. Both our microarray (data not shown) and real-time PCR results showed that all NF-κB-mediated genes induced by TNF are significantly inhibited by the treatment of IA (Fig. 41A). Inhibition of glycolysis by 2-DG or P.Ox leads to a moderate inhibition of NF-κB activation but not as significant as that with IA treatment (Fig. 41A). Similar results were also observed in our luciferase assays (Fig. 40C).

To exclude the possibility of off-target effects, we further performed luciferase analysis and RT-PCR in cells complemented with GAPDH WT or C150S. Our luciferase data showed that complementing with GAPDH C150S plasmid attenuates NF-κB activation induced by TNF whereas complementation with GAPDH WT plasmid slightly enhances NF-κB activation if there is any (Fig. 41B). In contrast, AP-1 luciferase activity stimulated by TNF is affected by neither GAPDH (Fig. 41B).

We further found TNF-induced phosphorylation of IKKβ but not p38 is attenuated by GAPDH C150S (Fig. 41C). This is consistent with our results that complementation with GAPDH C150S attenuates TNF-induced IκBα degradation (Fig. 40A). Likewise, TNF fails to induce IκBα degradation and IKKβ phosphorylation in IA-treated cells but not in P.Ox- or non-treated cells, whereas phosphorylation of p38 and JNK is not affected (Fig. 41D). Taken together, our results suggest that GAPDH has a non-glycolytic role in regulating the NF-κB signaling pathway.

GAPDH interacts with and activates TRAF2. TRAF2 shares significant structure similarity with Siah1 (Reed and Ely, 2002). Siah1, an E3 ligase belonging to the

Fig. 39. Knockdown of GAPDH disrupts cellular homeostasis. A. Luciferase activities as a function of GAPDH knockdown. ns: non-specific. B. ROS production after GAPDH knockdown was evaluated as described in experimental procedures. C. Western-blot analysis of the release of cytochrome *C*. HeLa cells were co-transfected with GAPDH 3'-UTR siRNAs and GAPDH-Myc or GAPDH-C150S-Myc. Cell lysates were harvested and subjected to mitochondria fractionation. The amount of cytochrome *C* in the cytosol fraction was analyzed by monoclonal α-cytochrome *C* antibody. D. NF-κB luciferase activities as the function of GAPDH complementary. E. ATP levels in GAPDH knockdown HeLa cells with or without complementation of different GAPDH expression plasmids.

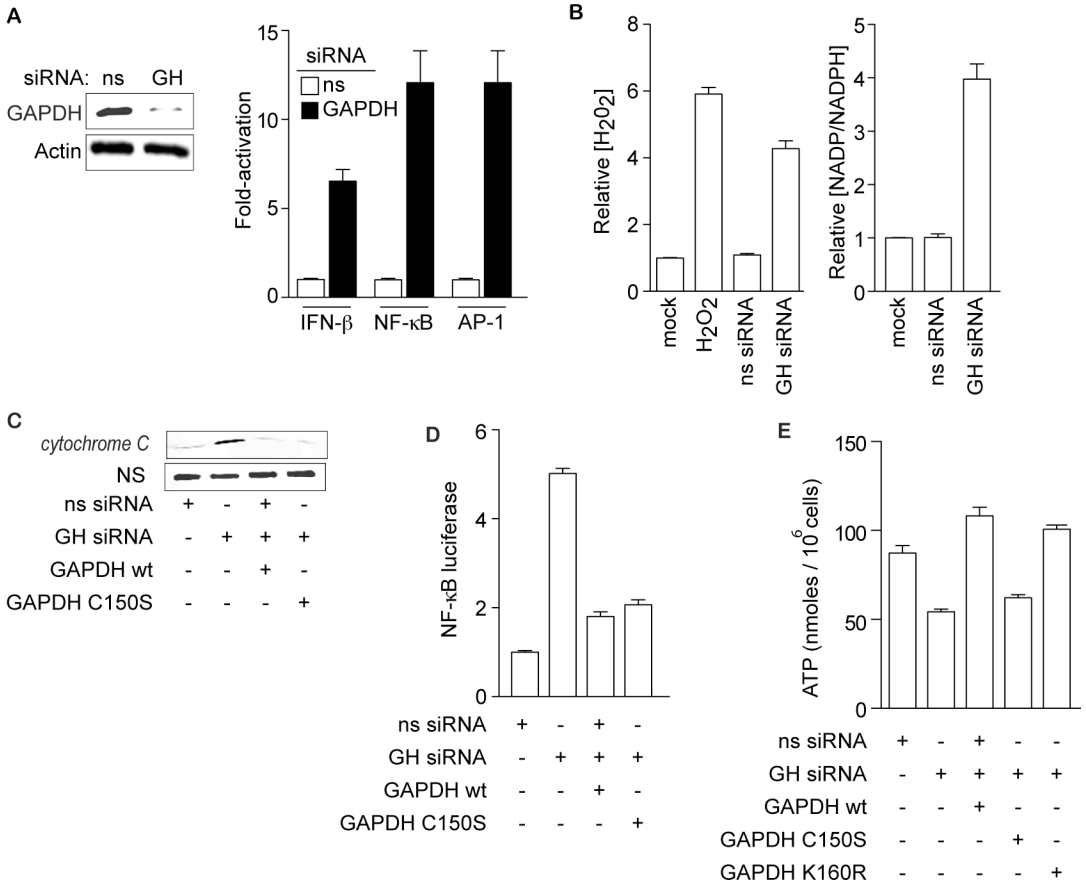
A
siRNA: ns GH
GAPDH
Actin
siRNA
ns
GAPDH
Fold-activation
IFN-β
NF-κB
AP-1
B
Relative [H2O2]
mock
H2O2
ns siRNA
GH siRNA
Relative [NADP/NADPH]
C
cytochrome C
NS
ns siRNA
GH siRNA
GAPDH wt
GAPDH C150S
D
NF-κB luciferase
E
ATP (nmoles / 10^6 cells)
GAPDH K160R

Fig. 40. GAPDH C150 residue is important for NF-κB activation. A. IκBα degradation in HeLa cells induced by TNF. Endogenous GAPDH was knocked down in HeLa cells, and complemented with indicated GAPDH plasmids. Cells were stimulated with TNF and analyzed by western-blot for protein expression as indicated. B-C. ATP levels, GAPDH activities and NF-κB luciferase activities in HeLa cells treated different drugs as indicated.

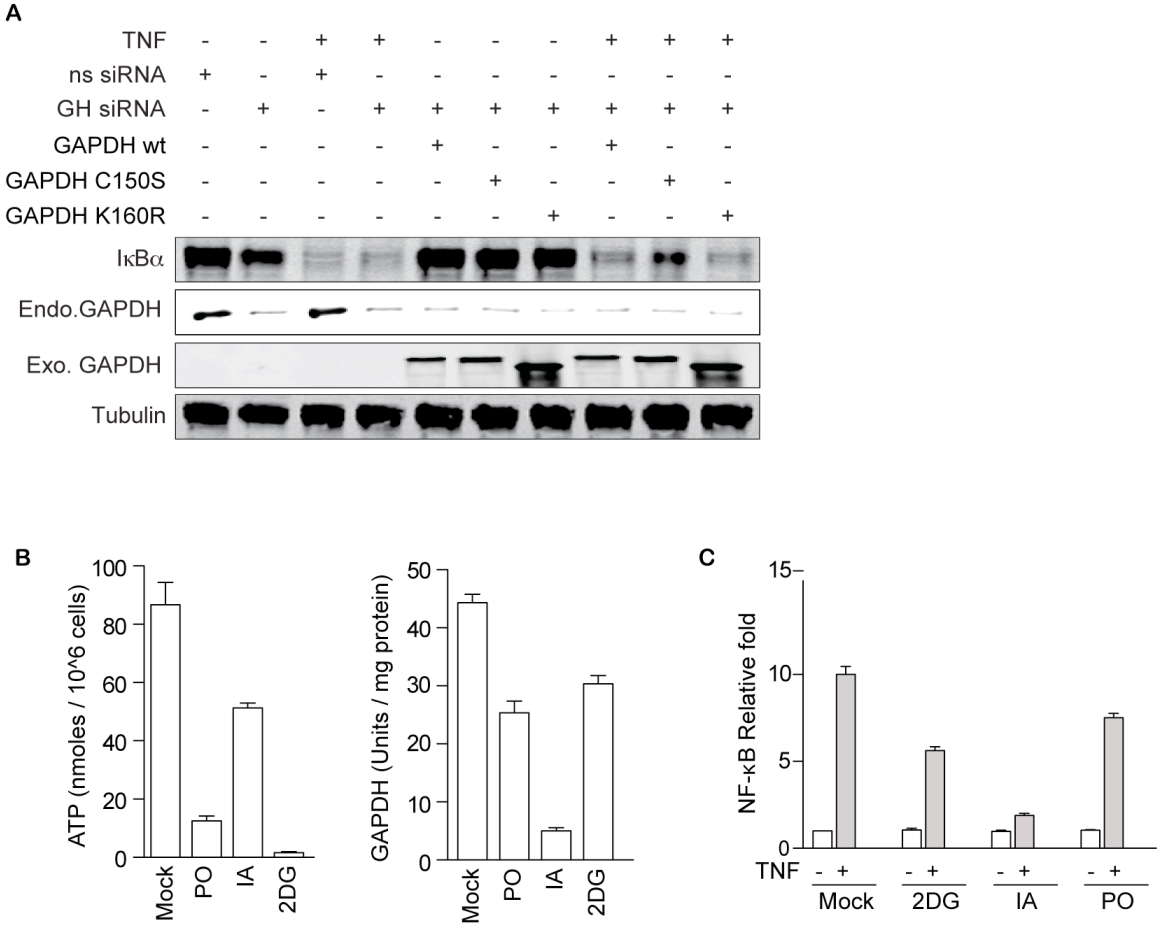
A
TNF - - + + - - - + + +
ns siRNA + - + - - - - - - -
GH siRNA - + - + + + + + + +
GAPDH wt - - - - + - - + - -
GAPDH C150S - - - - - + - - + -
GAPDH K160R - - - - - - + - - +
IκBα
Endo.GAPDH
Exo. GAPDH
Tubulin
B
ATP (nmoles / 10^6 cells)
100
80
60
40
20
0
Mock
PO
IA
2DG
GAPDH (Units / mg protein)
50
40
30
20
10
0
Mock
PO
IA
2DG
C
NF-κB Relative fold
15
10
5
0
TNF - + - + - + - +
Mock
2DG
IA
PO

Fig. 41. GAPDH is essential for TNF-induced NF-κB activation. A. Heatmap showing results of RT-PCR analysis measruing the expression of NF-κB dependent or independent genes after different treatments. Hela cells were treated with indicated drugs before stimulation with TNF (10 ng/ml, 20'). Data are presented as mean + SEM, n = 3. B. NF-κB and AP-1 luciferase activities as the function of GAPDH or GAPDH C150S complementation. Data are presented as mean + SEM, n = 3. $^{*}P < 0.05$. C. Analysis of IKKβ phosphorylation in GAPDH knockdown cells complemented with GAPDH or GAPDH C150S. HeLa cells were co-transfected with or without GAPDH siRNA. Meanwhile, IKKβ-FLAG with GAPDH-Myc or GAPDH-C150S-Myc plasmids were also introduced into the GAPDH knockdown cells before stimulated with TNF. D. Effects of the drugs on multiple cellular signaling pathways. HeLa cells were treated with indicated drugs before stimulated with TNF. Cell lysates were analyzed by SDS-PAGE and immunoblotted for indicated antibodies.

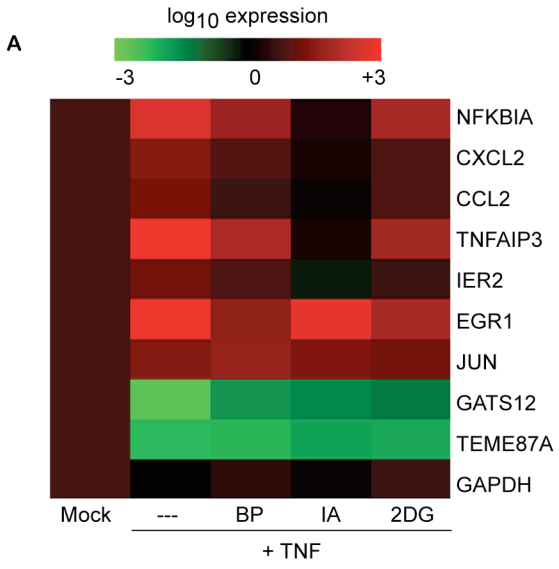
A
log10 expression
-3
0
+3
NFKBIA
CXCL2
CCL2
TNFAIP3
IER2
EGR1
JUN
GATS12
TEME87A
GAPDH
Mock

BP
IA
2DG
+ TNF

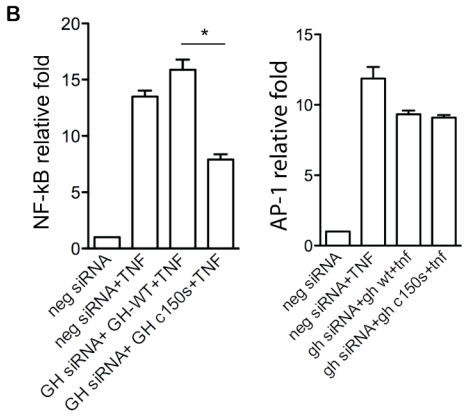
B
NF-kB relative fold
AP-1 relative fold
*
neg siRNA
neg siRNA+TNF
GH siRNA+ GH-WT+TNF
GH siRNA+ GH c150s+TNF
neg siRNA
neg siRNA+TNF
gh siRNA+gh wt+tnf
gh siRNA+gh c150s+tnf

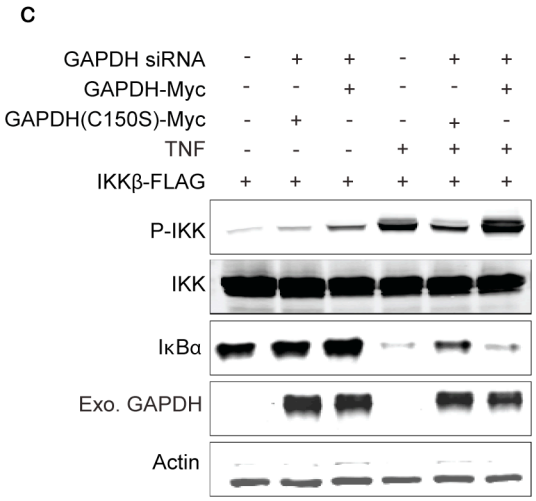
C
GAPDH siRNA
GAPDH-Myc
GAPDH(C150S)-Myc
TNF
IKKβ-FLAG
P-IKK
IKK
IκBα
Exo. GAPDH
Actin

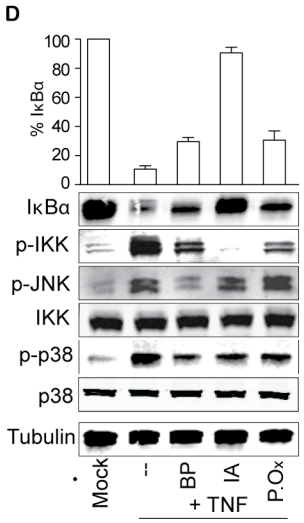
D
% IκBα
IκBα
p-IKK
p-JNK
IKK
p-p38
p38
Tubulin
Mock
BP
IA
P.Ox
+ TNF

Siah/Sina family, interacts with and is stabilized by GAPDH under stress (Hara et al., 2005). Interestingly, Siah1 and TRAF2 can both interact with the Peg3/Pw1 protein to activate NF-κB (Relaix et al., 1998). Therefore, we hypothesized that GAPDH interacts with TRAF2 under stress conditions. Co-transfection of TRAF2 with GAPDH plasmids showed that TRAF2 is associated with GAPDH WT (Fig. 42A). This association is enhanced upon TNF stimulation and is interrupted by treatment with IA (Fig. 43A). Endogenous GAPDH was also immunoprecipitated by TRAF2 upon TNF stimulation (Fig. 42B). Our *in vitro* pulldown assays showed that only TRAF2 interacts directly with GAPDH and not NleB, which is consistent with our previous data (Fig. 42C and 37D). The ΔRING domain of TRAF2 is not required for this interaction as ΔRING TRAF2 is still able to immunoprecipitate GAPDH (Fig. 42D). GAPDH C150S appears to be important for GAPDH-TRAF2 interaction as GAPDH C150S fails to immunoprecipitate TRAF2 in our co-transfection experiments (Fig. 42A and D). To our surprise, not even a basal level of interaction between TRAF2 and GAPDH C150S could be detected (Fig. 42A). To further investigate whether GAPDH C150S can interact with TRAF2, we conducted an *in vitro* pulldown assay. We replaced the His-Tag on GAPDH and its mutant C150S with different epitope tags for use in our *in vitro* pulldown assay with TRAF2-His protein. However, we did not get proteins expressed in our hands. We therefore deciced to employ an alternative strategy by using GAPDH inhibitor IA based on the fact that both IA treatment and the C150S mutant block GAPDH-TRAF2 interaction *in vivo*. GAPDH proteins treated with different concentration of IA are still able to interact with TRAF2 *in vitro* (Fig. 43B). Therefore, our data suggested that C150 is crucial for the interaction of GAPDH with TRAF2 *in vivo*. There might be additional domain(s) on GAPDH responsible for the binding with TRAF2. We are currently mapping the domains on TRAF2 respobsible for the interaction.

We next investigated whether this GAPDH-TRAF2 interaction is important for TRAF2 activation in response to TNF stimulation. We knocked down the endogenous GAPDH level by siRNAs and complemented with TRAF2-FLAG plus GAPDH WT or C150S plasmids. TNF stimulation, TRAF2 polyubiquitination is significantly induced in groups with GAPDH WT and the control group following TNF stimulation (Fig. 42E). In contrast, TNF-induced TRAF2 polyubiquitination in cells complemented with GAPDH C150S or treated with IA is significantly attenuated (Fig. 42E). This is not related to the alteration of the cellular energy level, as treatment with P.Ox does not impair TRAF2 polyubiquitination. Therefore, our results indicate that GAPDH physically interacts with TRAF2 and the recruitment of GAPDH is dependent upon its C150 *in vivo* and is enhanced by TNF stimulation.

NleB is a glycosyltransferase and O-GlcNAcylates GAPDH. Bioinformatic prediction suggested NleB is a glycosyltransferase (GT) belonging to the GT-A clan, GT-8 family. This group of glycosyltransferases is characterized by a DXD motif critical for the binding of a catalytic divalent cation such as Mn^{2+} (Liu and Mushegian, 2003). In addition, this group of glycosyltransferase also employs the Rossmann-like fold responsible for the nucleotide sugar binding. NleB contains multiple Rossman-like folds localizing at its N-terminus followed by a DXD motif ($_{221}$DAD$_{223}$) (Fig. 44A). This DAD motif is conserved in NleB homologs within enteropathogenic bacteria (Fig. 44B). Therefore, we hypothesized that NleB is a glycosyltransferase.

In eukaryotic cells, O-linked-N-acetylglucosamine (O-GlcNAc) is involved in regulating cellular signaling network including the NF-κB signalling pathway (Yang et al., 2008; Zachara and Hart, 2006). O-GlcNAcylation is highly regulated by two enzymes, O-GlcNAc transferase

Fig. 42. GAPDH physically interacts with TRAF2. A-B. HeLa cells were transfected with TRAF2-FLAG or co-transfected with TRAF2-FLAG and GAPDH-Myc. HeLa cells was immunoprecipitated by α-FLAG antibody to capture TRAF2-FLAG and immunoblotted for α-Myc antibody to detect GAPDH-Myc or α-GAPDH antibody to detect endogenous GAPDH. TNF stimulation was indicated at the top of each figure. C. In vitro pulldown assay for the interaction between TRAF2 and GAPDH. TRAF2-His protein was coupled with Ni-NTA agarose and incubated with GAPDH or NleB-FLAG + 1mM UDP-GlcNAc. D. Immunoprecipitation of TRAF2- or ΔRING TAF2-FLAG was performed with the α-FLAG antibody. Samples were analyzed by SDS-PAGE and immunoblotted for α-Myc for detecting GAPDH-Myc. E. GAPDH activates TRAF2 polyubiquitination. HeLa cells were introduced a combination of plasmids and siRNAs as indicated. After 60 h incubation, cells were treated with or without indicated drugs. Cell lysate aliquots were subjected to different immunoprecipitation analysis. Cell lysates was immunoprecipitated by the α-FLAG antibody and immunoblotted for ubiquitin and GAPDH-Myc. Another immunoprecipitation was conducted by α-Myc antibody and immunoblotted for O-GlcNAc and OGT. The endogenous GAPDH and OGT expression was also showed for protein expression controls.

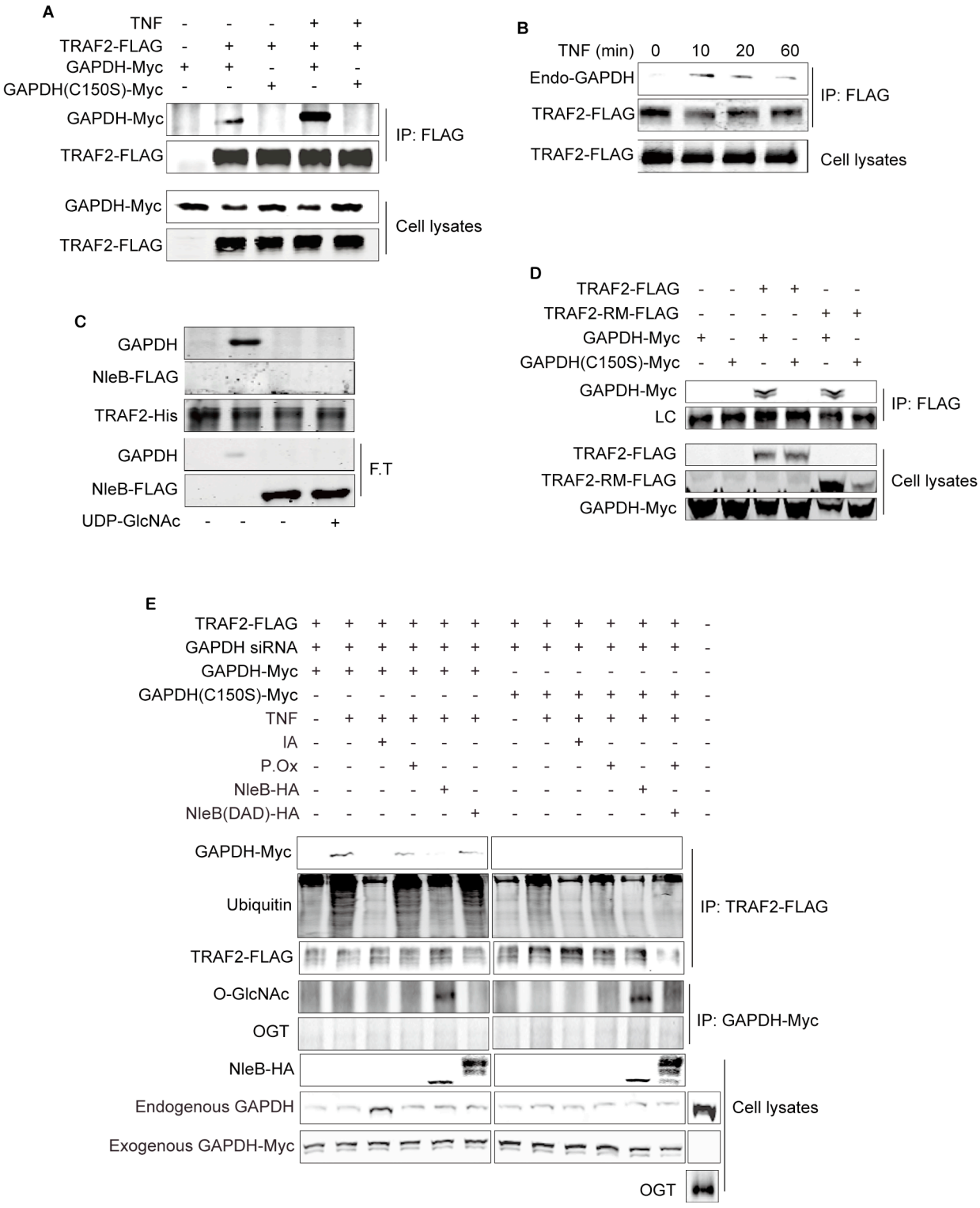
A
TNF - - - + +
TRAF2-FLAG - + + + +
GAPDH-Myc + + - + -
GAPDH(C150S)-Myc - - + - +
GAPDH-Myc
TRAF2-FLAG
IP: FLAG
GAPDH-Myc
TRAF2-FLAG
Cell lysates
B
TNF (min) 0 10 20 60
Endo-GAPDH
TRAF2-FLAG
IP: FLAG
TRAF2-FLAG
Cell lysates
C
GAPDH
NleB-FLAG
TRAF2-His
GAPDH
NleB-FLAG
F.T
UDP-GlcNAc - - - +
D
TRAF2-FLAG - - + + - -
TRAF2-RM-FLAG - - - - + +
GAPDH-Myc + - + - + -
GAPDH(C150S)-Myc - + - + - +
GAPDH-Myc
LC
IP: FLAG
TRAF2-FLAG
TRAF2-RM-FLAG
GAPDH-Myc
Cell lysates
E
TRAF2-FLAG + + + + + + + + + + + + -
GAPDH siRNA + + + + + + + + + + + + -
GAPDH-Myc + + + + + + - - - - - - -
GAPDH(C150S)-Myc - - - - - - + + + + + + -
TNF - + + + + + - + + + + + -
IA - - + - - - - - + - - - -
P.Ox - - - + - - - - - + - + -
NleB-HA - - - - + - - - - - + - -
NleB(DAD)-HA - - - - - + - - - - - + -
GAPDH-Myc
Ubiquitin
IP: TRAF2-FLAG
TRAF2-FLAG
O-GlcNAc
OGT
IP: GAPDH-Myc
NleB-HA
Endogenous GAPDH
Exogenous GAPDH-Myc
Cell lysates
OGT

Fig. 43. IA impairs TRAF2-GAPDH interaction in vivo but not in vitro. **A.** HeLa cells were treated with IA or P.Ox before TNF stimulation for indicated time. Cells were then subjected to TRAF2-FLAG immunoprecipitation and detected for the endogenous GAPDH by the α-GAPDH antibody. **B.** In vitro pulldown assay for assessing the effect of IA on the interaction between GAPDH and TRAF2. TRAF2-His was pre-bound with Ni-NTA agarose and incubated with GAPDH. The bound proteins were analyzed by SDS-PAGE and protein gel staining. The amount of IA added to the reaction is indicated.

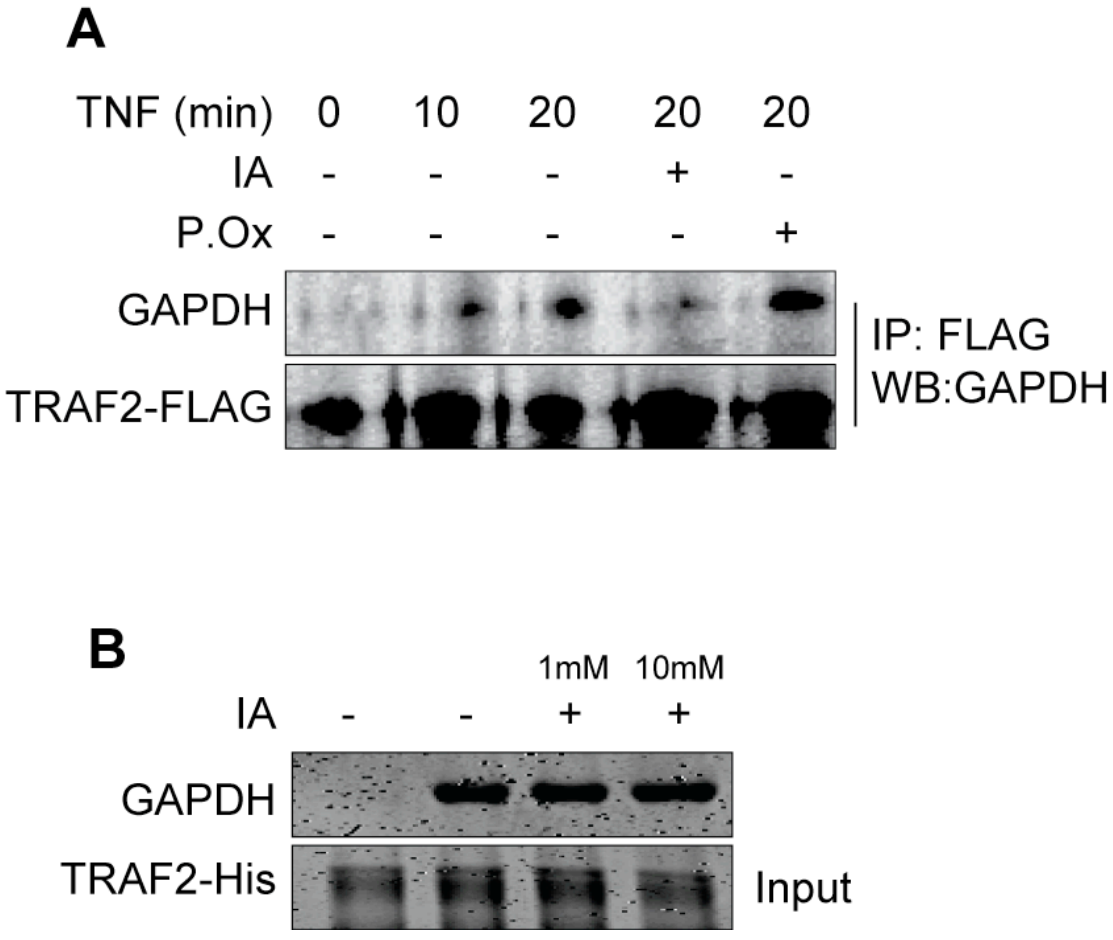
A
TNF (min) 0 10 20 20 20
IA - - - + -
P.Ox - - - - +
GAPDH
TRAF2-FLAG
IP: FLAG
WB:GAPDH
B
1mM 10mM
IA - - + +
GAPDH
TRAF2-His
Input

Fig. 44. Bioinformatic analysis of NleB. A. Predicted motifs on the NleB protein. B. Sequence alignment of NleB from *C. rodentium*, EHEC, EPEC and *Salmonella* by using Clustal W. The red box indicates the conserved DAD motif in NleB with its homologues.

A

B

```
        EHEC EDL933 --------------MLSSLN--VLQSSFRGKTALSNS-TLLQKVSFAGKEYPLEPIDEKTPILFQWFEARPERYEKGEVPILNTKEHPYLSNIINAAKIENERIIGVLVDGNFTYEQKK
          EHEC Sakai --------------MLSSLN--VLQSSFRGKTALSNS-TLLQKVSFAGKEYPLEPIDEKTPILFQWFEARPERYEKGEVPILNTKEHPYLSNIINAAKIENERIIGVLVDGNFTYEQKK
         EPEC 2348/69 --------------MLSSLN--VLQSSFRGKTALSNS-TLLQKVSFAGKEYSLEPIDERTPILFQWFEARPERYEKGEVPILNTKEHPYLSNIINAAKIENERIIGVLVDGNFTYEQKK
C. rodentium DBS100 --------------MLSPLN--VLQFNFRGETALSDS-APLQTVSFAGKDYSMEPIDEKTPILFQWFEARPERYGKGEVPILNTKEHPYLSNIINAAKIENERVIGVLVDGDFTYEQRK
   S.enterica SseK1 --------------MIPPLNRYVPALSKNELVKTVTN-RDIQFTSFNGKDYPLCFLDEKTPLLFQWFERNPARFGKNDIPIINTEKNPYLNNIIKAATIEKERLIGIFVDGDFFPGQKD
   S.enterica SseK2 MARFNAAFTRIKIMFSRIRGLISCQSNTQTIAPTLSPPSSGHVSFAGIDYPLLPLNHQTPLVFQWFERNPDRFGQNEIPIINTQKNPYLNNIINAAIIEKERIIGIFVDGDFSKGQRK

        EHEC EDL933 EFLSLENEYQNIKIIYRADVDFSMYDKKLSDIYLENIHKQESYPASERDNYLLGLLREELKNIPEGK--DSLIESYAEKREHTWFDFFRNLAMLKAGSLFTETGKTGCHNISPCSGCI
          EHEC Sakai EFLSLENEYQNIKIIYRADVDFSMYDKKLSDIYLENIHKQESYPASERDNYLLGLLREELKNIPEGK--DSLIESYAEKREHTWFDFFRNLAMLKAGSLFTETGKTGCHNISPCSGCI
         EPEC 2348/69 EFLNLENEHQNIKIIYRADVDFSMYDKKLSDIYLENIHKQESYPASERDNYLLGLLREELKNIPEGK--DSLIESYAEKREHTWFDFFRNLAILKAGSLFTETGKTGCHNISPCSGCI
C. rodentium DBS100 EFLSLEDEHQNIKIIYRENVDFSMYDKKLSDIYLENIHEQESYPASERDNYLLGLLREELKNIPYGK--DSLIESYAEKRGHTWFDFFRNLAVLKGGGLFTETGKTGCHNISPCGGCI
   S.enterica SseK1 AFSKLEYDYENIKVIYRNDIDFSMYDKKLSEIYMENISKQESMPEEKRDCHLLQLLKKELSDIQEGN--DSLIKSYLLDKGHGWFDFYRNMAMLKAGQLFLEADKVGCYDLSTNSGCI
   S.enterica SseK2 ALGKLEQNYRNIKVIYNSDLNYSMYDKKLTTIYLENITKLEAQSASERDEVLLNGVKKSLEDVLKNNPEETLISSHNKDKGHLWFDFYRNLFLLKGSDAFLEAGKPGCHHLQPGGGCI

        EHEC EDL933 YLDADMIITDKLGVLYAPDGIAVHVDCNDEIKSLENGAIVVNRSNHPALLAGLDIMKSKVDAHPYYDGLGKGIKRHFNYSSLHDYNAFCDFIEFKHENIIPNTSMYTCSSW----- 329
          EHEC Sakai YLDADMIITDKLGVLYAPDGIAVHVDCNDEIKSLENGAIVVNRSNHPALLAGLDIMKSKVDAHPYYDGLGKGIKRHFNYSSLHDYNAFCDFIEFKHENIIPNTSMYTCSSW----- 329
         EPEC 2348/69 YLDADMIITDKLGVLYAPDGIAVHVDCNDEIKSLENGAIVVNRSNHPALLAGLDIMKSKVDAHPYYDGLGKGIKRHFNYSSLHNYNAFCDFIEFKHENIIPNTSMYTSSSW----- 329
C. rodentium DBS100 YLDADMIITDKLGVLYAPDGIAVYVDCNDR-KSLENGAIVVNRSNHPALLAGLDIMKSKVDAHPYYDGVGKGLKRHFNYSSLQDYNVFCNFIEFKHKNIIPNTSMYTNSSW----- 328
   S.enterica SseK1 YLDADMIITEKLGGIYIPDGIAVHVERIDGRASMENGIIAVDRNNHPALLAGLEIMHTKFDADPYSDGVCNGIRKHFNYSLNEDYNSFCDFIEFKHDNIIMNTSQFTQSSWARHVQ 336
   S.enterica SseK2 YLDADMLLTDKLGTLYLPDGIAIHVSRKDNHVSLENGIIAVNRSEHPALIKGLEIMHSKPYGDPYNDWLSKGLRHYFDGSHIQDYDAFCDFIEFKHENIIMNTSSLTASSW-R--- 348
```

(OGT) and O-GlcNAcase (OGA) (Hart et al., 2007). OGT catalyzes the transfer of *N*-acetylglucosamine from UDP-GlcNAc to the hydroxyl oxygen of serine or threonine, whereas OGA removes O-GlcNAc from targeted proteins. As targeting for similar sites on serine or threonine, O-GlcNAcylation is found to compete with phosphorylation, which often leads to the function switch of proteins. By using O-GlcNAc enzymatic *in vitro* labeling system, we found recombinant NleB-FLAG protein strongly O-GlcNAcylate GAPDH protein (Fig. 45A). We confirmed this result by using antibodies specifically recognizing O-GlcNAcylation sites on proteins (Fig. 45B). Notably, the intensity of NleB-mediated O-GlcNAcylation on GAPDH is correlated with the concentration of UDP-GlcNAc, which further indicates NleB is an O-GlcNAc transferase (Fig. 45C). To investigate whether NleB is able to O-GlcNAcylate GAPDH during bacterial infection, we performed a time-course infection experiment by using *C. rodentium* strains. At 3 h post infection, we found O-GlcNAcylation of GAPDH is strongly induced only in cells with WT *C.rodentium* infection, whereas no significant O-GlcNAcylation signal on GAPDH can be detected in the group infected with the *ΔnleB C.rodentium* (Fig. 45D). Moreover, while TNF alone does not induce GAPDH O-GlcNAcylation, GAPDH from cells transfected with NleB plasmid is clearly O-GlcNAcylated (Fig. 45E). Although GAPDH O-GlcNAcylation has been reported before (Park et al., 2009), we could not detect any significant O-GlcNAcylation signal from GAPDH without NleB in our experimental systems. Notably, immunoprecipitation of GAPDH does not pull down the host OGT protein in our hands, which indicates that GAPDH O-GlcNAcylation is specifically mediated by NleB (Fig. 45E). We also found NleB is able to O-GlcNAcylate the GAPDH C150S mutant, which is consistent with our previous results that C150 residue is not required for the interaction of GAPDH with NleB (Fig. 45E).

To confirm NleB is an O-GlcNAc transferase, we mutated the predicted catalytic site $_{221}$DAD$_{223}$ on NleB to $_{221}$AAA$_{223}$ (NleB DAD→AAA). We found the NleB DAD→AAA mutant fails to O-GlcNAcylate GAPDH both *in vitro* and *in vivo* (Fig. 45E and 46A). Intriguingly, mutating $_{221}$DAD$_{223}$ to $_{221}$AAA$_{223}$ causes a slower mobililty of the protein on SDS-PAGE (Fig. 45E and 46A). As we expected, disruption of Rossmann-like folds of NleB (Δ202 NleB) prevents O-GlcNAcylation of GAPDH (Figure 45E). OGA catalyzes the cleavage of O-GlcNAc from modified proteins (Hart et al., 2007). Treatment of cells with an OGA enzyme inhibitor thiamet G (TMG) blocks the cleavage and significantly increases the O-GlcNAcylation level of cellular proteins (Fig. 46A). We therefore decided to test whether O-GlcNAcylation of GAPDH by NleB is enhanced by the treatment with TMG. We found O-GlcNAcylation of GAPDH mediated by NleB is significantly increased with the TMG treatment (Fig. 46A). In contrast, the NleB DAD→AAA mutant does not O-GlcNAcylate GAPDH in cells treated with TMG, which indicates that this DAD motif is essential for the O-GlcNAc transferase activity of NleB. Taken together, our data strongly suggests NleB is an O-GlcNAc transferase and uses UDP-GlcNAc sugars to modify GAPDH protein in the host.

NleB disrupts the interaction between GAPDH and TRAF2 through its O-GlcNAc transferase activity. Our *in vitro* data showed that the addition of UDP-GlcNAc molecules increases the interaction between GAPDH and NleB, which indicates O-GlcNAc transferase activity might promote the interaction between NleB and GAPDH (Fig. 47A). Immunoprecipitation of GAPDH also showed that the amount of NleB associated with GAPDH is increased by the TMG treatment (Fig. 46A). Interestingly, in our *in vitro* pulldown assay by which NleB-FLAG, GAPDH and TRAF-His proteins were incubated together, we found that

NleB-FLAG is pulled down by TRAF2-His without the presence of UDP-GlcNAc (Fig. 46C). As NleB does not interact with TRAF2 even in the presence of UDP-GlcNAc, this association of NleB with TRAF2 in vitro must be through GAPDH (Fig. 42C). In contrast, when UDP-GlcNAc is present, decreased amount of NleB-FLAG and GAPDH is able to be pulled down by TRAF2-His and an increased amount of NleB and GAPDH proteins can be detected in the flow-through. Remarkably, only disassociated GAPDH shows a strong signal of O-GlcNAcylation compared to the GAPDH bound to TRAF2. Therefore, we hypothesized that NleB might interact with GAPDH to disrupt the formation of TRAF2-GAPDH complex through its O-GlcNAc transferase activity. In our TRAF2 immunoprecipitation assay, we found that much less GAPDH is associated with TRAF2 in the presence of NleB compared to the control, which is consistent with our *in vitro* data (Fig. 42E). The interaction between GAPDH and TRAF2 is not interrupted by the presence of the NleB DAD→AAA mutant, which is likely due to the disassociation of the NleB DAD→AAA mutant with GAPDH (Fig. 42E). Interestingly, the NleB DAD→AAA mutant displays a significantly different intracellular localization pattern compared to the NleB WT and does not co-localize with GAPDH (Fig. 46B). Therefore, our results indicated NleB prevents GAPDH-TRAF2 interaction through its O-GlcNAc transferase activity. Meanwhile, we are investigating whether NleB will have a more significant phenotype upon disrupting the interaction between TRAF2 and GAPDH by the treatment with TMG *in vivo*, which we believe can further support our results.

The O-GlcNAc transferase activity is required for the function of NleB on NF-κB. To evaluate whether O-GlcNAc transferase activity of NleB is important for its virulence in the host, we infected mice with the *ΔnleB*/p*nleB C. rodentium* strain or the *ΔnleB*/pNleB-DAD→AAA *C. rodentium* strain. Mice infected with the *ΔnleB*/pNleB-DAD→AAA *C. rodentium* strain shows

Fig. 45. NleB O-GlcNAcylates GAPDH. A-B. Detection of GAPDH O-GlcNAcylation of NleB through the Click-iT^{Tm} O-GlcNAcylation system or α-GlcNAc antibody as described in experimental procedures. C. Detection of GAPDH O-GlcNAcylation by NleB with an increased amount of UDP-GlcNAc. NleB- and NleC-FLAG proteins were incubated with GAPDH protein with the indicated amount of UDP-GlcNAc. Proteins were analyzed by SDS-PAGE and immunoblotted for the O-GlcNAcylation by the α-GlcNAc antibody. D. Analysis of GAPDH O-GlcNAcylation during the bacterial infection. HeLa cells were infected with *C. rodentium* WT or *ΔnleB* strain for 1 or 3 h. Cell lysates were immunoprecipitated with α-GAPDH antibody and analyzed for the O-GlcNAcylation level. E. Analysis of GAPDH O-GlcNAcylation by NleB mutants. FLAG-NleB WT and mutants were purified and incubated with GAPDH. The incubated proteins were analyzed by SDS-PAGE and immunobloted with α-GlcNAc, α-FLAG and α-GAPDH antibodies.

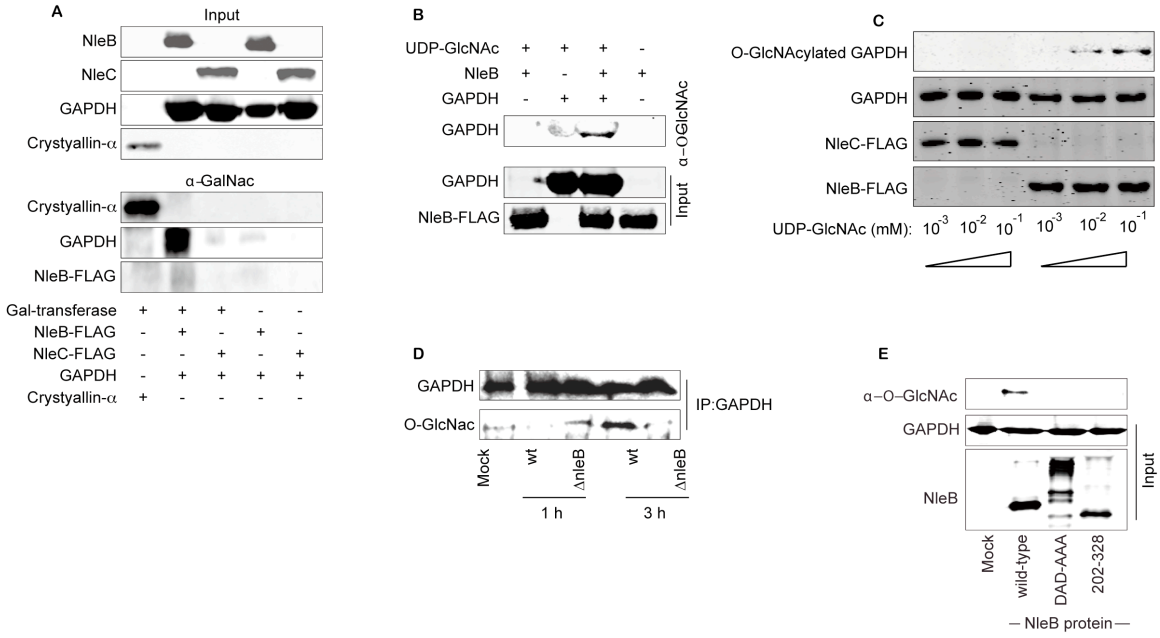
A
Input
NleB
NleC
GAPDH
Crystyallin-α
α-GalNac
Crystyallin-α
GAPDH
NleB-FLAG
Gal-transferase + + + - -
NleB-FLAG - + - + -
NleC-FLAG - - + - +
GAPDH - + + + +
Crystyallin-α + - - - -
B
UDP-GlcNAc + + + -
NleB + - + +
GAPDH - + + -
GAPDH
α-OGlcNAc
GAPDH
Input
NleB-FLAG
C
O-GlcNAcylated GAPDH
GAPDH
NleC-FLAG
NleB-FLAG
UDP-GlcNAc (mM): 10-3 10-2 10-1 10-3 10-2 10-1
D
GAPDH
IP:GAPDH
O-GlcNac
Mock
wt
ΔnleB
wt
ΔnleB
1 h
3 h
E
α-O-GlcNAc
GAPDH
NleB
Input
Mock
wild-type
DAD-AAA
202-328
— NleB protein —

Fig. 46. The The O-GlcNAc transferase activity is essential for the function of NleB on NF-κB. **A.** HeLa cells were co-transfected with NleB-HA, TRAF2-FLAG and GAPDH-Myc expression plasmids for 60 h and treated with TMG for 8 h before stimulated with or without TNF. Cell lysates were immunoprecipitated for TRAF2-FLAG or GAPDH-Myc to detect TRAF2 polyubiquitination or GAPDH O-GlcNAcylation and NleB-HA individually. Cell lysates were also immunoblotted for the global O-GlcNAc level and other protein levels as indicated. **B.** NleB(DAD) mutant does not colocalize with GAPDH. HeLa cells were transfected with NleB-GFP plasmids (green) and stained with α-GAPDH antibody (red). **C.** *In vitro* pulldown were performed to assess whether NleB prevents the interaction between GAPDH and TRAF2 through its O-GlcNAc transferase activity. TRAF2-His was coupled with Ni-NTA beads and incubated with NleB-FLAG and GAPDH proteins. UDP-GlcNAc was added at the final concentration of 1mM in the indicated group. The bound and flow-through protein were analyzed by SDS-PAGE and subjected for both gel staining and O-GlcNAcylation with the α-GlcNAc antibody. **D.** Colonization (CFUs / g mouse colon) of indicated *C. rodentium* strains (7 d post-gavage) in C57BL/6J mice. **E.** Analysis of AP-1 luciferase activity in the presence of NleB with the treatment of TMG. HeLa cells were co-transfected with luciferase reporters and NleB-HA or control plasmids for 60 h, and treated with TMG for 8 h before the stimulation of TNF for 20’.

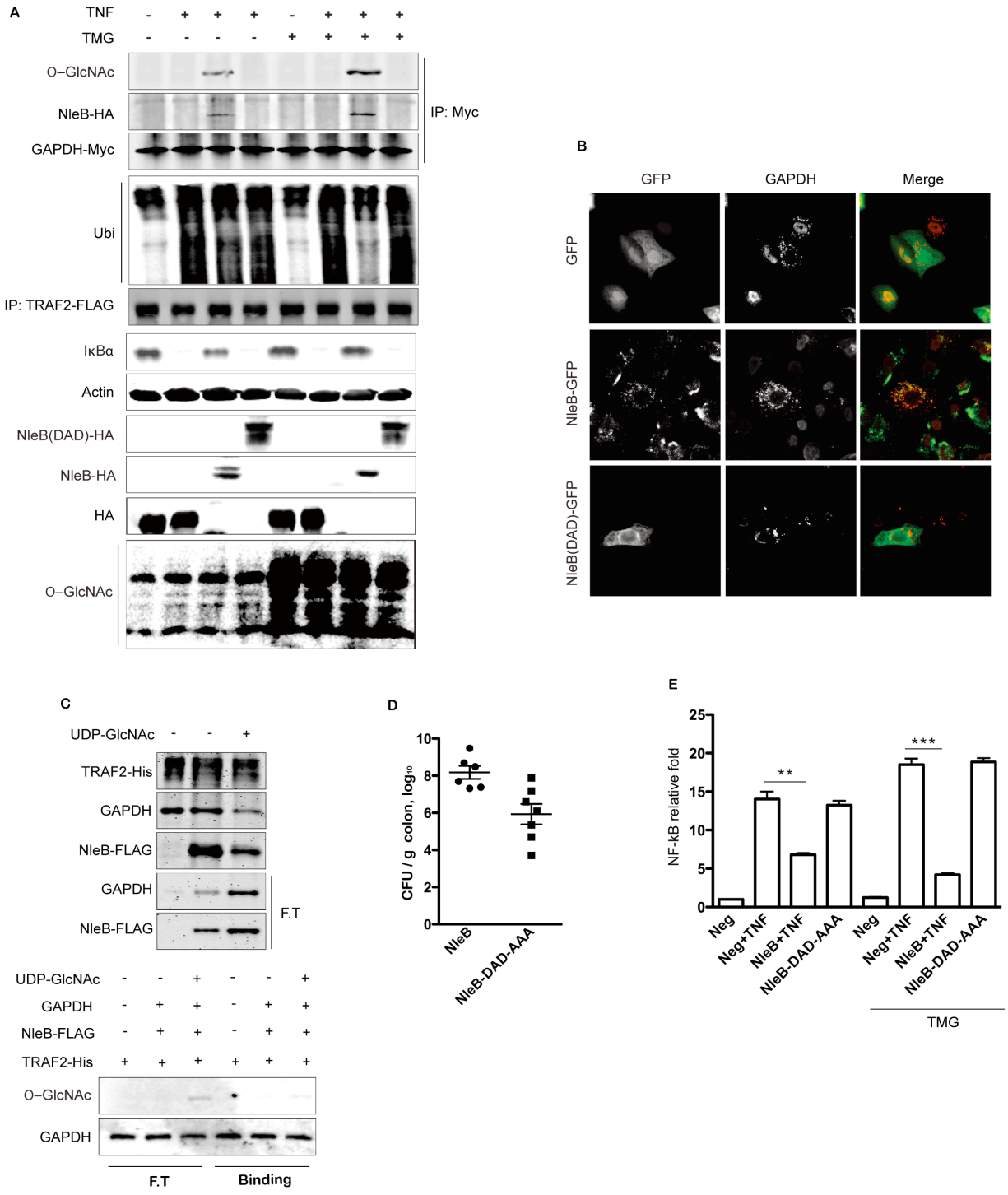
A
TNF
TMG
O–GlcNAc
NleB-HA
GAPDH-Myc
IP: Myc
Ubi
IP: TRAF2-FLAG
IκBα
Actin
NleB(DAD)-HA
NleB-HA
HA
O–GlcNAc
B
GFP
GAPDH
Merge
GFP
NleB-GFP
NleB(DAD)-GFP
C
UDP-GlcNAc
TRAF2-His
GAPDH
NleB-FLAG
GAPDH
NleB-FLAG
F.T
UDP-GlcNAc
GAPDH
NleB-FLAG
TRAF2-His
O–GlcNAc
GAPDH
F.T
Binding
D
CFU / g colon, log10
NleB
NleB-DAD-AAA
E
NF-kB relative fold
**
***
Neg
Neg+TNF
NleB+TNF
NleB-DAD-AAA
Neg
Neg+TNF
NleB+TNF
NleB-DAD-AAA
TMG

more than a 2 log reduction in bacterial colonization number compared to mice infected with the *ΔnleB*/pNleB *C. rodentium* strain (Fig. 46D). Therefore, the O-GlcNAc transferase activity of NleB enhaces bacterial virulence in the host.

We next examined whether this NleB-mediated O-GlcNAcylation of GAPDH is essential for the effect of NleB on NF-κB activation. In contrast to WT, the NleB DAD→AAA mutant does not prevent IκBα degradation or NF-κB activation stimulated by TNF (Fig. 46A). Disruption of Rossmann-like folds also fails to block IκBα degradation and p65 nuclear translocation (Fig. 47B). TRAF2 polyubiquitination is not impaired by the NleB DAD-AAA mutant upon TNF stimulation, which is in contrast with NleB WT (Fig. 42E). Furthermore, NleB WT completely abolishes TRAF2 polyubiquitination induced by TNF in TMG-treated cells whereas the DAD→AAA mutant does not show any effect (Fig. 46A). We next found that although TMG treatment alone does not prevent IκBα degradation and NF-κB activation, it stabilizes IκBα in the presence of NleB but not the NleB DAD-AAA mutant (Fig. 46A). Our luciferase assays also showed that NleB exhibits an augmented inhibitory effect on NF-κB activation in cells treated with TMG (Fig. 46E). We observed an increased NF-κB activity promoted by TMG treatment, which is in consistent with previous reports (Kawauchi et al., 2008; Yang et al., 2008). In contrast, neither NleB nor TMG can alter the TNF-induced AP-1 activation (Fig. 47C). Therefore, our data suggest the O-GlcNAc transferase activity is essential for NleB to inhibit NF-κB activation and enhances its virulence in the host.

Discussion

In this study, we have shown that the bacterial T3SS effector NleB physically interacts

Fig. 47. The O-GlcNAc transferase activity promotes the interaction between NleB and GAPDH. **A.** *In vitro* analysis of the interaction between NleB and GAPDH in the presence of UDP-GlcNAc. NleB-FLAG protein was pre-bound with M2 beads and incubated with GAPDH. The addition of 1mM UDP-GlcNAc in the reaction was indicated. The bound and flow-through proteins were analyzed by SDS-PAGE and gel staining. **B.** Western-blot analysis of IκBα degradation and p65 nuclear translocation stimulated by TNF with Δ202 NleB deletion mutant. **C.** Analysis of AP-1 luciferase activity in the presence of NleB with the treatment of TMG

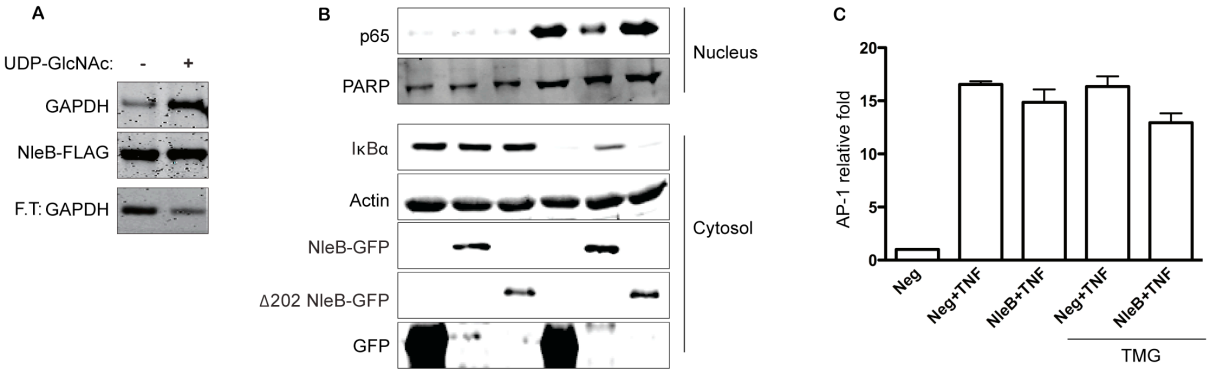
A
UDP-GlcNAc: - +
GAPDH
NleB-FLAG
F.T: GAPDH
B
p65
PARP
Nucleus
IκBα
Actin
NleB-GFP
Δ202 NleB-GFP
GFP
Cytosol
C
AP-1 relative fold
20
15
10
5
0
Neg
Neg+TNF
NleB+TNF
Neg+TNF
NleB+TNF
TMG

with the host glycolytic protein GAPDH. This observation lead us to identify an integral role for GAPDH in the NF--κB signaling pathway. GAPDH directly interacts with TRAF2 and serves as a co-activator of TRAF2 upon TNF stimulation and bacterial infection. We further demonstrated that NleB possesses O-GlcNAc transferase activity and O-GlcNAcylates GAPDH during the infection. This NleB-mediated GAPDH GlcNAcylation disrupts GAPDH-TRAF2 interaction resulting in the attenuation of TRAF2 polyubiquitination and NF-κB activation. Loss of its O-GlcNAc tranferase activity eliminates the inhibitory effect of NleB on NF-κB activation and reduces the bacterial colonization ability in hosts (**Fig. 48**).

Instead of being considered as separate components in the glycolytic pathway, multiple glycolytic proteins have been found to participate in non-metabolic cellular events (Kim and Dang, 2005). Previous studies have indicated GAPDH is involved in a wide range of biological events such as transcriptional regulation, vesicle trafficking and cell survival (Tristan et al., 2011). Several recent studies have also shown that GAPDH might be involved in immune signaling pathways. By screening cellular factors involved in the TNF/NF-κB pathway, Bouwmeester *et* al reported that GAPDH is associated with NF-κB family member C-Rel and NF-κB signaling molecules (Bouwmeester et al., 2004). In another study, Mookherjee *et* al also predicted GAPDH interacts with molecules involved in the NF-κB signaling pathway. Recently, Hara *et* al reported that C150 residue of GAPDH becomes S-nitrosylated under stress conditions, which enables GAPDH to interact with an E3 ligase Siah1 (Hara et al., 2005). The GAPDH-Siah1 complex then translocates into the nucleus, where Siah1 is stabilized and induces apoptosis in cells. Polekhina *et* al reported the substrate binding domains (SBD) from TRAF proteins share significant structure similarity with Siah/Sina-family proteins (Polekhina et al., 2002). Both Siah1 and TRAF2 can interact with Peg3/Pw1 to induce NF-κB activation (Relaix et al., 2000).

Fig. 48. Working model for the role of GAPDH in the NF-κB signaling pathway and how NleB targets GAPDH to attenuate the activation of TRAF2. GAPDH is recruited to TRAF2 through an as-yet-unknown mechanism, which might be dependent upon the modification of C150 residue.

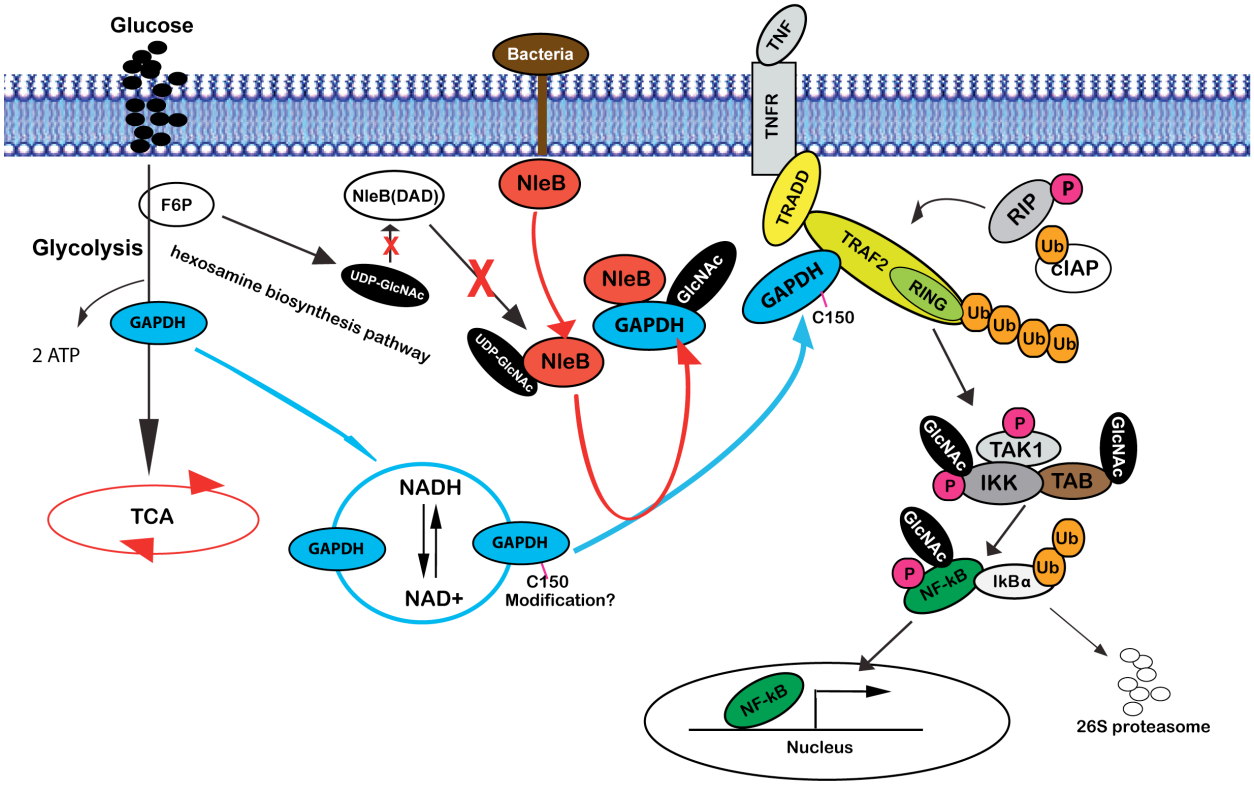
Glucose
Bacteria
TNF
TNFR
NleB
NleB(DAD)
F6P
Glycolysis
hexosamine biosynthesis pathway
UDP-GlcNAc
GAPDH
2 ATP
TCA
NADH
NAD+
C150
Modification?
TRADD
TRAF2
RING
RIP
P
Ub
cIAP
C150
GlcNAc
TAK1
IKK
TAB
NF-kB
IkBα
Nucleus
26S proteasome

In our study, we demonstrated an interaction between GAPDH and TRAF2, which further suggests that Siah1 and TRAF2 might share common biochemical features (Polekhina et al., 2002). The binding of GAPDH to TRAF2 is enhanced under stress conditions, which is similar to the interaction between Siah1 and GAPDH. As blocking the interaction between GAPDH-TRAF2 does not impair the recruitment of TRADD to TRAF2, our data therefore suggest that GAPDH is a co-activator of TRAF2. We are currently investigating whether binding of TRAF2 by TRADD is required for GAPDH-TRAF2 interaction through "loss of function" assays. The other important experiment we are conducting now is the *in vitro* TRAF2 ubiquitination assay, which will allow us to directly evaluate the role of GAPDH and/or NleB on TRAF2 polyubiquitination. Nevertheless, our data suggest that there might be a hierarchical network of multiple factor recruitment to TRAF2 upon stimulation, which is essential for the regulation of TRAF2 activation.

Our studies demonstrated that the C150 residue is essential for promoting the GAPDH and TRAF2 interaction. This is consistent with previous studies, which also showed the cysteine residue in the catalytic center is important for non-glycolytic function of GAPDH (Colell et al., 2007; Hara et al., 2005). Although it is still not clear how this cysteine contributes to GAPDH involvement in these processes, the catalytic residue is redox-sensitive and often modified under stress conditions. Hara *et* al showed that nitric oxide synthase (NOS) S-nitrosylates GAPDH at C150 (Hara et al., 2005). The nitrosylated C150 promotes the interaction between GAPDH and Siah1. In yeast, the oxidation of C152 residue in the GAPDH homologue Tdh1 enhances its interaction with Mcs4 (Morigasaki et al., 2008). Complementation with the Tdh1 C152S mutant fails to repeat the oxdative modification and impairs the phosphorelay signaling in the stress-responsive pathways. These modifications generally have a mild effect in glycolysis, but are

essential for non-metabolic functions of GAPDH. It will be interesting to study whether the C150 undergoes any specific modification under our experimental conditions.

Different studies have shown that cellular signaling and metabolism are tightly linked (Wellen and Thompson, 2012). Metabolite-modification such as glycosylation and acetylation is known to regulate different cellular signaling pathways. O-GlcNAcylation is one of the major glycosylations mediated by UDP-GlcNAc, which is the final product of the hexosamine biosynthetic pathway (Hart et al., 2011). Evidences that O-GlcNAcylation is important in regulating immune signaling pathways are emerging. It has been demonstrated that enhanced glucose metabolism induces O-GlcNAcylation of NF-κB components and increases NF-κB activity (Kawauchi et al., 2008, 2009; Yang et al., 2008). Recently, Pathak *et* al reported an increased O-GlcNAcylation on TAB1 upon IL-1β stimulation, which is essential for TAK1 kinase activation (Pathak et al., 2012). In an agreement with previous studies, we also found that a high glucose concentration (data not shown) or increasing the O-GlcNAcylation level of cellular proteins by the treatment with TMG enhances NF-κB activity in response to TNF stimulation. Most importantly, we demonstrated here that GAPDH is O-GlcNAcylated by NleB. The O-GlcNAcylated GAPDH shows decreased binding ability with TRAF2. The O-GlcNAcylation of GAPDH mediated by OGT at the Thr 227 residue has been reported before (Park et al., 2009). This modification is required for GAPDH nuclear translocation by disrupting GAPDH homo-tetramer formation. Thus, this O-GlcNAcylation might induce a protein conformational change in GAPDH and regulate its function. Although we did not detect OGT-mediated GAPDH O-GlcNAcylation, it is possibly due to the variation in experimental conditions. Therefore, the O-GlcNAcylation of GAPDH is likely to be only mediated by NleB in our experiments. Moreover, treatment with the OGA inhibitor TMG enhances O-GlcNAcylation

of GAPDH by NleB, which indicates O-GlcNAcylation of GAPDH is dynamically regulated by NleB and OGA in host cells. Several evidences suggest the effect of NleB on NF-κB is tightly linked with its O-GlcNAc transferase activity on GAPDH. First, a less amount of GAPDH proteins are able to bind with TRAF2 in the presence of NleB, which attenuates TRAF2 polyubiquitination. This is similar with GAPDH C150S, which we found fails to bind with TRAF2 and facilitate its polyubiquitination *in vivo*. Also, an increased inhibition of TRAF2 polyubiquitination is associated with an enhanced GAPDH O-GlcNAcylation by NleB under the treatment with TMG. Second, neither the NleB DAD→AAA mutant nor Δ202 NleB is able to O-GlcNAcylate GAPDH and both are not capable of inhibiting NF-κB activation. Of note, there is another DXD motif $_{93}$DGD$_{95}$ in NleB. However, this motif is unlikely to be essential for NleB function as a mutant with the deletion of 120 amino acids from the N-terminus still can O-GlcNAcylate GAPDH and blocks NF-κB activation (data not shown). Current efforts are also focusing on the identification of NleB-mediated O-GlcNAcylation site(s) on GAPDH, which can help us further elucidate not only how NleB functions with GAPDH, but also the mechanism of how GAPDH and TRAF2 interact.

So far, several bacterial toxins have been demonstrated as glycosyltransfeases (Belyi and Aktories, 2010). Clostridial toxins glucosylate GTPases of the Rho and Ras superfamily at threonine residues and inhibit GTPase activation (Kelly and LaMont, 2008). Notably, α-toxin from *C. novyi* uses UDP-GlcNAc as the sugar donor and O-GlcNAcylates Rho subfamily proteins at Thr 35 or 37 depending on the target (Selzer et al., 1996). Lgt proteins from *Legionella pneumophila* are also glucosylating toxins and glucosylate eukaryotic elongation factor 1A (eEF1A) at serine 53, which leads to the interruption of protein biosynthesis and cell death (Belyi et al., 2006). These toxins all belong to the GT-A family of glycosyltransferases

(Belyi and Aktories, 2010). Typical characteristics of these toxins include at least one Rossmann-like fold and DXD motif. Replacing these residues results in significant reduction in transferase activities, which is also consistent with our observation on NleB. Surprisingly, mutating $_{221}$DAD$_{223}$ on NleB to $_{221}$AAA$_{223}$ causes slower protein mobility on SDS-PAGE compared to WT, which indicates the mutation of the DAD motif might accompany with the alteration in protein structures.

In A/E pathogens, multiple Nle proteins have been reported to modulate the NF-κB signaling pathway (Wong et al., 2011). Our discovery that NleB utilizes the host metabolic product UDP-GlcNAc to disrupt the formation of TRAF2 complex suggested a novel mechanism for T3SS effectors to dampen the host immune signaling pathways. As the flux of hexamine biosynthesis is closely related to the cellular glucose concentration, it will be interesting to determine whether the virulence of NleB can be associated with host metabolic switches. However, metabolic switches in the host usually lead to a complicated change in the both host immune system and the intestinal microbiota community (Kau et al., 2011). Therefore, better animal models are required to further evaluate the function of NleB and other effectors in different physiological conditions.

Experimental procedures

All animal experiments were performed according to Institutional Animal Care and Use Committee-approved protocols.

Bacterial strains and plasmids

C. Rodentium and *ΔnleB C. Rodentium* strains were described in previous studies (Gao et al., 2009). FLAG-TRAF2 expression plasmid was obtained from Addgene (plasmid #20229). FLAG-ΔRING-TRAF2 expression plasmid was a gift from Dr. Francis Chan (University of Massachusetts). Myc-GAPDH, Myc-GAPDH-C150S and HA-GAPDH-K160R expression plasmids were kindly provided by Dr. Akira Sawa (Johns Hopkins Univerisity).

Reagents

Chemicals were used according to manufacturers' recommendations and were obtained from Sigma, except for the following: QuikChange Site-Directed Mutagenesis Kit (Stratagene), Dual-Luciferase Reporter Assay System (Promega), Ni-NTA agarose (Qiagen), protein G agarose (Fisher), TNF (Cell Signaling), FuGene (Roche), lipofectamine 2000 (Invitrogen). Antibodies were obtained from the following sources: His, FLAG, HA (Sigma), Ubiquitin, β-actin, tubulin, GAPDH, O-GlcNAc CTD110.6 (Santa Cruz Biotechnology), p65, IκBα, TRADD, PARP, Myc (Cell Signaling). Purified TRAF2-His (ab84725) and GAPDH (ab77109) proteins were obtained from Abcam. OGA inhibitor TMG was kindly provided by Dr. Chad Slawson (University of Kansas Medical Center).

Protein purification

For the purification of NleB fusion proteins, 500 ml of the *C.rodentium* containing the FLAG-CTC plasmid encoding NleB or its mutation or truncations was induced by IPTG at the

final concentration of 1mM. After 4 h additional growth, cells were pelleted. The protein extraction was following step 1 and 2 of the protocol from the protein solubilization and renaturation Kit (Cell Biolabs, AKR-110). After renaturation, 100 µl FLAG M2 beads (Sigma, A2220) were added into the supernatant and proteins were purified according to the protocol offered by Sigma (A2220).

RNA interference

For RNA interference (RNAi), 3 pmol of scramble siRNAs or siRNAs against GAPDH were transfected into HeLa cells by lipofectamine 2000 (Invitrogen). The transfection mixture was replaced with complete growth media after 6 hr and cells were incubated for a further 60 h (37 °C, 5 % CO_2) prior to the harvest. Specificity of knockdown was confirmed by western-blot with specific antibodies. The siRNA sense-strand sequences were as follows: GAPDH 3' UTR-1: 5'-AGCACAAGAGGAAGAGA- GAGACCCU-3', GAPDH 3' UTR-2: 5'- CAUGUACCAUCA-AUAAAGUACCCUG, GAPDH 3' UTR-3: CUCCUCACAGUUGCCAUGUAGACCC.

Immunoprecipitation and immunoblotting.

Immunoprecipitation was performed as described before (Gao et al., 2009). Cell lysates were analyzed by SDS-PAGE and immunoblotted with monoclonal anti-O-GlcNAc antibody (CTD110.6) or monoclonal anti-GAPDH antibody at room temperature for 2 h. For TMG treatment, cells were treated with TMG for 8 h and were harvested for immunoprecipitation or immunoblotting. After rinsing in PBS, blots were imaged with an Odyssey infrared imaging

system (Li-Cor).

Immunofluorescence microscopy.

HeLa cells were grown on glass coverslips in 24-well tissue culture plates. Cells were transfected with 1μg NleB-GFP plasmids and incubated for 60 h. After that, cells were permeabilized in 0.1 % saponin in PBS, blocked with 5 % goat serum, and incubated with α-GAPDH (1:1,000) primary antibodies for 1 h at room temperature. The cells were washed with PBS and probed with 594-conjugated secondary antibodies (1:1,000, 1 h) and DAPI (1 μg/ml, 2'). Coverslips were mounted in Mowiol and samples were visualized using a LSM 510 Laser Scanning Microscope (Carl Zeiss).

Affinity columns and Protein identification by LC-ESI-MS/MS

Both affinity columns and LC-ESI-MS/MS were conducted as described before (Gao et al., 2009). Briefly, bands excised from protein gels were digested in-gel with trypsin at 37°C overnight. The tryptic peptide solution was transferred to a microcentrifuge tube, extracted with 1% formic acid, 2% acetonitrile in water, followed by extraction with 50% acetonitrile. Both extracts were combined, concentrated, and suspended in 3% acetonitrile, 0.1% formic acid. Peptide analysis was performed using LC-ESIMS/MS. Peptides were desalted in-line and concentrated with RP-Trap Symmetry300 C18 column, 5 μm NanoEase (Waters), and separated using a C18 RP PepMap capillary column on a CapLC (Dionex). The eluted ions were analyzed by one full precursor MS scan (400–1500 m/z), followed by four MS/MS scans of the most

abundant ions detected in the MS scan. Spectra were obtained in the positive ion mode with a nano ESI-Q-Tof micro mass spectrometer (Micromass). A peak list (PKL format) was generated to identify +1 or multiple charged precursor ions from the mass spectrometry data file. Mascot server v2.2 in MS/MS ion search mode was applied to conduct peptide matches (peptide masses and sequence tags) and protein searches against NCBInr v20080110.

In vitro O-GlcNAc assay

0.5 μg of purified NleB-FLAG or NleC-FLAG proteins with 0.5 μg of GAPDH protein were pre-incubated in 4 °C for O/N in the presence of 1mM UDP-GlcNAc. The O-GlcNAcylated proteins were detected by click-iT™ O-GlcNAc Enzymatic Labeling System (mp 33368) and Click-iT™ Tetramethylrhodamine (TAMRA) Protein Analysis Detection Kit (mp 33370). For the alternative *in vitro* O-GlcNAcylation assay, same amount of proteins were pre-incubated in the reaction buffer (50 mM Tris–HCl, pH 7.5, 1 mM DTT, 10 mM $MnCl_2$) for 4 h at room temperature with UDP-GlcNAc. After that, reactions were stopped by adding 2 x SDS–PAGE sample buffer, resolved by SDS-PAGE and probed with appropriate antibodies.

Measurement of GAPDH enzymatic activity

GAPDH activity was measured by using fluorescence-based assay kit (KDalert™ GAPDH, Ambion). Briefly, 10^4 cells were treated with or without 10 mM GAPDH inhibitor IA for 40 mins. Cells were resuspended in ice-cold Cell Lysis Buffer and incubated for 20 mins. 10 μl aliquots of each sample were transferred to each well of the 96-well plate containing 90 μl of the master mix. The change of fluorescence was measured every 4 mins by using a fluorescence

reader. The GAPDH activity of the samples was determined compared to the standard curve. The relative fold was determined by comparing with negative control samples.

RT-PCR

We performed real-time PCR assays in a Power SYBR Green PCR Master Mix (Applied Biosystems).

Luciferase assay

Luciferase assays were conducted as described (Gao et al., 2009). Briefly, HeLa cells were co-transfected at a ratio of 10:1 (1.0 μg total DNA) with a luciferase reporter construct together with the renilla luciferase pTKRL plasmid (Promega), cultured for 48 h, in the presence or absence of TNF. Cells were lysed with passive lysis buffer and lysates were analyzed according to the protocol from Dual-Luciferase Kit (Promega). The fold-induction was calculated as [relative FU stimulated)/(relative FU unstimulated] samples. Luciferase assays were performed in triplicate with at least three independently transfected cell populations.

Measurement of ROS production

HeLa cells transfected with scramble or GAPDH 3'UTR siRNAs were harvested and analyzed for the concentration of H_2O_2 (STA-343, Cell Biolabs) and the ratio of $NADP^+$/NADPH (NC9531485, Fisher Scientific) by the individual kit according to

manufactures' protocols.

Mitochondria fractionation

HeLa cells were cotransfected with 3 pmol scramble or GAPDH 3'UTR siRNAs with GAPDH expression plasmids for 60 h. After that, cells were harvested and a total number of 10^7 cells were subjected to the mitochondria fractionation by the Mitochondria Isolation Kit (#89874, Thermo Scientific). Cell extracts were analyzd by SDS-PAGE and immunoblotted with appropriate antibodies.

Enzyme-linked immunosorbent assay.

TNF-alpha concentration in mice serum samples were measured with a mouse TNF-alpha Quantikine ELISA Kit from R&D according to the manufacturer's instructions (MTA00B).

Statistical analyses.

RT-PCR results were analyzed statistically using one-way ANOVA. Luciferase assay data was analyzed with t-tests.

Chapter V: Conclusions

To survive and grow in the host, A/E pathogens employ T3SS effectors to inhibit host innate immune responses. However, which T3SS effectors contribute to this process have not yet been identified. In this thesis, we discovered the mechanism of how the T3SS effectors NleH1 and NleB modulate the host NF-κB signaling pathway to inhibit host innate immune responses.

There are two copies of NleH (NleH1 and NleH2) in EPEC and EHEC, whereas only one copy of NleH has been discovered in *C. rodentium* and it is more closely related to NleH1 based on sequence similarity. The C-terminal of NleH proteins share similarity in amino acid sequence with the *Shigella* T3SS effector OspG. OspG targets ubiquitin E2 enzymes and prevents IκBα degradation. Through proteomic screening, we found that NleH proteins interact with the non-Rel NF-κB subunit RPS3. The binding of NleH1 with RPS3 prevents RPS3 nuclear translocation upon TNF stimulation or bacterial infection. Targeting RPS3 by NleH1 subsequently leads to the inactivation of NF-κB. The modulation of NleH on NF-κB has also been identified from other studies (Royan et al., 2010). In these studies, NleH proteins were found to stabilize IκBα degradation induced by EPEC. Although our studies did not produce similar results, this might be due to different experimental conditions. Therefore, NleH might target different steps in NF-κB signaling pathway to inhibit its activation. In addition, NleH proteins are Ser/Thr kinases and the kinase activity is important for NleH1 to inhibit RPS3 nuclear translocation. However, there is no evidence from our experiments suggesting that NleH proteins are able to phosphorylate RPS3 protein. Therefore, there might be other unidentified host proteins serving as NleH kinase substrates. Although the activation of RPS3 is dependent upon IKKβ-mediated phosphorylation at Ser 209, other eukaryotic factors may also contribute to RPS3 activation. Thus, identifying

these proteins will be important not only for a better understanding of NleH working mechanism, but also for further understanding of how RPS3 is involved in NF-κB signaling pathway.

Targets for NleH are not limited to RPS3. During the course of this study, others reported that several other eukaryotic proteins are associated with NleH effectors. NleH proteins physically interact with Bax inhibitor-1 (Bl-1) by binding with the N-terminal 40 amino acids of Bl-1 (Hemrajani et al., 2010). Bl-1 is an evolutionarily conserved apoptosis inhibitor, which targets the apoptotic proteins Bcl-2 and Bcl-xL (Robinson et al., 2011). The binding of Bl-I enables NleH proteins to inhibit procaspase-3 cleavage and apoptosis during EPEC infection. Therefore, this study suggested NleH proteins have cytoprotective function in host cells, which can facilitate EPEC colonization. In contrast to our results, it appears that the kinase activity is not essential for NleH anti-apoptotic activity. This difference indicates that the kinase activity of NleH might determine their various functions in host cells. The anti-apoptosis function of NleH was also reported in another study, in which they found that expression of NleH prevents cells from apoptosis induced by *C. difficile* toxin B (TcdB) (Robinson et al., 2010).

NleH1 also interacts with host membrane protein Na^+/H^+ exchanger regulatory factor 2 (NHERF2) (Martinez et al., 2010). NHERF2 belongs to NHERF protein family, which contains NHERF1-4 (Donowitz et al., 2005). NHERFs are plasma membrane proteins found abundantly in the mammalian small intestine and colon. Interestingly, two other T3SS effectors, Map and EspI, also interact with NHERF2. This interaction is dependent upon the C-terminal class I PSD-95/Disc Large/ZO-1 (PDZ)-binding motif, which is found on all three T3SS effectors. NHERF2 serves as a scaffold protein on the plasma membrane to regulate effector protein function. Specifically, overexpression of NleH1 attenuates the anti-apoptotic activity of NleH1, which indicates there might be a complex regulatory mechanism of NleH in host cells.

In the second part of this thesis, we tried to understand the mechanism of how NleB targets the NF-κB signaling pathway. These studies lead us to identify the integral role of GAPDH in the NF-κB signaling pathway. GAPDH is a glycolytic protein that catalyzes the sixth step of glycolysis. However, the non-glycolytic role of GAPDH has also been explored during last decade. In our studies, we found GAPDH directly interacts with the TRAF2 protein and facilitates its polyubiquitinaton under stress conditions. The participation of GAPDH in the NF-κB signaling pathway has been predicted before. Although we demonstrated here that GAPDH is involved in the TNF-NF-κB signaling pathway through TRAF2, we also have preliminary results showing GAPDH is able to interact with TRAF6 (data not presented). As TRAF proteins are critical signaling molecules regulating multiple innate signaling pathways in host cells, it will be interesting to examine whether GAPDH possesses high binding affinities with different TRAF proteins and how this will contribute to different roles of GAPDH in host immune system.

Our *in vivo* data suggested that GAPDH C150 is crucial for the recruitment of GAPDH to TRAF2, although not likely to be essential for the binding of two proteins. The modification of C150 has been reported in different studies and appears to be important for GAPDH's non-glycolytic functions. It also will be interesting to determine whether there is a modification on C150 after TNF stimulation or bacterial infection and how this modification regulates the GAPDH recruitment to TRAF2.

In this study, we also demonstrated NleB is an O-GlcNAc transferase. We found NleB is able to O-GlcNAcylate GAPDH to interrupt the interaction of GAPDH with TRAF2, which subsequently results in the inactivation of TRAF2 upon TNF stimulation or bacterial infection. To our knowledge, NleB is the first T3SS effector identified with O-GlcNAc transferase activity. Unfortunately, we have not identified the O-GlcNAc site(s) on GAPDH by NleB here. As O-

GlcNAc is able to compete with phosphorylation on Ser/Thr residue, it will also be interesting to test how the addition of sugars on the residue(s) is able to disrupt GAPDH-TRAF2 interaction. This deserves further efforts as it will greatly advance our knowledge on the virulence mechanism of NleB.

By the time we reported the function of NleH1 on NF-κB in 2009, we were the first group to identify a T3SS effector in A/E pathogens targeting the NF-κB signaling pathway. Since then, other T3SS effectors in A/E pathogens, which target NF-κB signaling pathway, have also been identified. In this thesis, we provided two novel mechanisms from T3SS effectors NleH1 and NleB for the manipulation of the host response. We hope these studies will benefit us to understand the virulence of A/E pathogens and contribute to the development of any potential therapy in the future.

References:

Abe, A., Heczko, U., Hegele, R.G., and Brett Finlay, B. (1998). Two enteropathogenic Escherichia coli type III secreted proteins, EspA and EspB, are virulence factors. The Journal of experimental medicine *188*, 1907-1916.

Abreu, M.T., Fukata, M., and Arditi, M. (2005). TLR signaling in the gut in health and disease. J Immunol *174*, 4453-4460.

Abul-Milh, M., Wu, Y., Lau, B., Lingwood, C.A., and Barnett Foster, D. (2001). Induction of epithelial cell death including apoptosis by enteropathogenic Escherichia coli expressing bundle-forming pili. Infection and immunity *69*, 7356-7364.

Akeda, Y., and Galan, J.E. (2005). Chaperone release and unfolding of substrates in type III secretion. Nature *437*, 911-915.

Akira, S. (2003). Mammalian Toll-like receptors. Current opinion in immunology *15*, 5-11.

Anantha, R.P., Stone, K.D., and Donnenberg, M.S. (1998). Role of BfpF, a member of the PilT family of putative nucleotide-binding proteins, in type IV pilus biogenesis and in interactions between enteropathogenic Escherichia coli and host cells. Infection and immunity *66*, 122-131.

Arbibe, L., Kim, D.W., Batsche, E., Pedron, T., Mateescu, B., Muchardt, C., Parsot, C., and Sansonetti, P.J. (2007). An injected bacterial effector targets chromatin access for transcription factor NF-kappaB to alter transcription of host genes involved in immune responses. Nature immunology *8*, 47-56.

Ashida, H., Kim, M., Schmidt-Supprian, M., Ma, A., Ogawa, M., and Sasakawa, C. (2010). A bacterial E3 ubiquitin ligase IpaH9.8 targets NEMO/IKKgamma to dampen the host NF-kappaB-mediated inflammatory response. Nature cell biology *12*, 66-73; sup pp 61-69.

Baker, D.R., Moxley, R.A., Steele, M.B., Lejeune, J.T., Christopher-Hennings, J., Chen, D.G., Hardwidge, P.R., and Francis, D.H. (2007). Differences in virulence among Escherichia coli O157:H7 strains isolated from humans during disease outbreaks and from healthy cattle. Applied and environmental microbiology *73*, 7338-7346.

Baruch, K., Gur-Arie, L., Nadler, C., Koby, S., Yerushalmi, G., Ben-Neriah, Y., Yogev, O., Shaulian, E., Guttman, C., Zarivach, R.*, et al.* (2011). Metalloprotease type III effectors that specifically cleave JNK and NF-kappaB. The EMBO journal *30*, 221-231.

Baumler, A.J., Tsolis, R.M., and Heffron, F. (1996). The lpf fimbrial operon mediates adhesion of Salmonella typhimurium to murine Peyer's patches. Proceedings of the National Academy of Sciences of the United States of America *93*, 279-283.

Beg, A.A., and Baldwin, A.S., Jr. (1993). The I kappa B proteins: multifunctional regulators of Rel/NF-kappa B transcription factors. Genes & development *7*, 2064-2070.

Belyi, Y., and Aktories, K. (2010). Bacterial toxin and effector glycosyltransferases. Biochimica et biophysica acta *1800*, 134-143.

Belyi, Y., Niggeweg, R., Opitz, B., Vogelsgesang, M., Hippenstiel, S., Wilm, M., and Aktories, K. (2006). Legionella pneumophila glucosyltransferase inhibits host elongation factor 1A. Proceedings of the National Academy of Sciences of the United States of America *103*, 16953-16958.

Bhavsar, A.P., Guttman, J.A., and Finlay, B.B. (2007). Manipulation of host-cell pathways by bacterial pathogens. Nature *449*, 827-834.

Bieber, D., Ramer, S.W., Wu, C.Y., Murray, W.J., Tobe, T., Fernandez, R., and Schoolnik, G.K. (1998). Type IV pili, transient bacterial aggregates, and virulence of enteropathogenic Escherichia coli. Science *280*, 2114-2118.

Blattner, F.R., Plunkett, G., 3rd, Bloch, C.A., Perna, N.T., Burland, V., Riley, M., Collado-Vides, J., Glasner, J.D., Rode, C.K., Mayhew, G.F., *et al.* (1997). The complete genome sequence of Escherichia coli K-12. Science *277*, 1453-1462.

Bouwmeester, T., Bauch, A., Ruffner, H., Angrand, P.O., Bergamini, G., Croughton, K., Cruciat, C., Eberhard, D., Gagneur, J., Ghidelli, S., *et al.* (2004). A physical and functional map of the human TNF-alpha/NF-kappa B signal transduction pathway. Nature cell biology *6*, 97-105.

Brodsky, I.E., and Medzhitov, R. (2008). Reduced secretion of YopJ by Yersinia limits in vivo cell death but enhances bacterial virulence. PLoS pathogens *4*, e1000067.

Brown, K., Gerstberger, S., Carlson, L., Franzoso, G., and Siebenlist, U. (1995). Control of I kappa B-alpha proteolysis by site-specific, signal-induced phosphorylation. Science *267*, 1485-1488.

Brown, K.D., Hostager, B.S., and Bishop, G.A. (2001). Differential signaling and tumor necrosis factor receptor-associated factor (TRAF) degradation mediated by CD40 and the Epstein-Barr virus oncoprotein latent membrane protein 1 (LMP1). The Journal of experimental medicine *193*, 943-954.

Brunder, W., Schmidt, H., Frosch, M., and Karch, H. (1999). The large plasmids of Shiga-toxin-producing Escherichia coli (STEC) are highly variable genetic elements. Microbiology *145 (Pt 5)*, 1005-1014.

Bugarel, M., Beutin, L., and Fach, P. (2010). Low-density macroarray targeting non-locus of enterocyte effacement effectors (nle genes) and major virulence factors of Shiga toxin-producing Escherichia coli (STEC): a new approach for molecular risk assessment of STEC isolates. Appl Environ Microbiol *76*, 203-211.

Caamano, J., Alexander, J., Craig, L., Bravo, R., and Hunter, C.A. (1999). The NF-kappa B family member RelB is required for innate and adaptive immunity to Toxoplasma gondii. J Immunol *163*, 4453-4461.

Cadera, E.J., Wan, F., Amin, R.H., Nolla, H., Lenardo, M.J., and Schlissel, M.S. (2009). NF-kappaB activity marks cells engaged in receptor editing. The Journal of experimental medicine *206*, 1803-1816.

Campellone, K.G., Robbins, D., and Leong, J.M. (2004). EspFU is a translocated EHEC effector that interacts with Tir and N-WASP and promotes Nck-independent actin assembly. Developmental cell *7*, 217-228.

Celli, J., Olivier, M., and Finlay, B.B. (2001). Enteropathogenic Escherichia coli mediates antiphagocytosis through the inhibition of PI 3-kinase-dependent pathways. The EMBO journal *20*, 1245-1258.

Chantome, A., Pance, A., Gauthier, N., Vandroux, D., Chenu, J., Solary, E., Jeannin, J.F., and Reveneau, S. (2004). Casein kinase II-mediated phosphorylation of NF-kappaB p65 subunit enhances inducible nitric-oxide synthase gene transcription in vivo. The Journal of biological chemistry *279*, 23953-23960.

Charpentier, X., and Oswald, E. (2004). Identification of the secretion and translocation domain of the enteropathogenic and enterohemorrhagic Escherichia coli effector Cif, using TEM-1 beta-lactamase as a new fluorescence-based reporter. Journal of bacteriology *186*, 5486-5495.

Chen, G., and Goeddel, D.V. (2002). TNF-R1 signaling: a beautiful pathway. Science *296*, 1634-1635.

Chen, L.F., and Greene, W.C. (2004). Shaping the nuclear action of NF-kappaB. Nature reviews Molecular cell biology *5*, 392-401.

Chen, Z.J. (2005). Ubiquitin signalling in the NF-kappaB pathway. Nature cell biology *7*, 758-765.

Cheng, H.C., Skehan, B.M., Campellone, K.G., Leong, J.M., and Rosen, M.K. (2008). Structural mechanism of WASP activation by the enterohaemorrhagic E. coli effector EspF(U). Nature *454*, 1009-1013.

Clarke, S.C. (2001). Diarrhoeagenic Escherichia coli--an emerging problem? Diagnostic microbiology and infectious disease *41*, 93-98.

Colell, A., Green, D.R., and Ricci, J.E. (2009). Novel roles for GAPDH in cell death and carcinogenesis. Cell death and differentiation *16*, 1573-1581.

Colell, A., Ricci, J.E., Tait, S., Milasta, S., Maurer, U., Bouchier-Hayes, L., Fitzgerald, P., Guio-Carrion, A., Waterhouse, N.J., Li, C.W.*, et al.* (2007). GAPDH and autophagy preserve survival after apoptotic cytochrome c release in the absence of caspase activation. Cell *129*, 983-997.

Collier-Hyams, L.S., Zeng, H., Sun, J., Tomlinson, A.D., Bao, Z.Q., Chen, H., Madara, J.L., Orth, K., and Neish, A.S. (2002). Cutting edge: Salmonella AvrA effector inhibits the key proinflammatory, anti-apoptotic NF-kappa B pathway. J Immunol *169*, 2846-2850.

Cornelis, G.R. (2006). The type III secretion injectisome. Nature reviews Microbiology *4*, 811-825.

Cornelis, G.R. (2010). The type III secretion injectisome, a complex nanomachine for intracellular 'toxin' delivery. Biological chemistry *391*, 745-751.

Crane, J.K., McNamara, B.P., and Donnenberg, M.S. (2001). Role of EspF in host cell death induced by enteropathogenic Escherichia coli. Cellular microbiology *3*, 197-211.

Dahan, S., Busuttil, V., Imbert, V., Peyron, J.F., Rampal, P., and Czerucka, D. (2002). Enterohemorrhagic Escherichia coli infection induces interleukin-8 production via activation of

mitogen-activated protein kinases and the transcription factors NF-kappaB and AP-1 in T84 cells. Infection and immunity *70*, 2304-2310.

Dai, M.S., Arnold, H., Sun, X.X., Sears, R., and Lu, H. (2007). Inhibition of c-Myc activity by ribosomal protein L11. The EMBO journal *26*, 3332-3345.

Daniell, S.J., Takahashi, N., Wilson, R., Friedberg, D., Rosenshine, I., Booy, F.P., Shaw, R.K., Knutton, S., Frankel, G., and Aizawa, S. (2001). The filamentous type III secretion translocon of enteropathogenic Escherichia coli. Cellular microbiology *3*, 865-871.

Darnay, B.G., and Aggarwal, B.B. (1999). Signal transduction by tumour necrosis factor and tumour necrosis factor related ligands and their receptors. Annals of the rheumatic diseases *58 Suppl 1*, I2-I13.

Dasanayake, D., Richaud, M., Cyr, N., Caballero-Franco, C., Pittroff, S., Finn, R.M., Ausio, J., Luo, W., Donnenberg, M.S., and Jardim, A. (2011). The N-terminal amphipathic region of the Escherichia coli type III secretion system protein EspD is required for membrane insertion and function. Molecular microbiology *81*, 734-750.

Dastoor, Z., and Dreyer, J.L. (2001). Potential role of nuclear translocation of glyceraldehyde-3-phosphate dehydrogenase in apoptosis and oxidative stress. Journal of cell science *114*, 1643-1653.

Datsenko, K.A., and Wanner, B.L. (2000). One-step inactivation of chromosomal genes in Escherichia coli K-12 using PCR products. Proceedings of the National Academy of Sciences of the United States of America *97*, 6640-6645.

Dean-Nystrom, E.A., Bosworth, B.T., Moon, H.W., and O'Brien, A.D. (1998). Escherichia coli O157:H7 requires intimin for enteropathogenicity in calves. Infection and immunity *66*, 4560-4563.

Dean, P., and Kenny, B. (2009). The effector repertoire of enteropathogenic E. coli: ganging up on the host cell. Current opinion in microbiology *12*, 101-109.

Dean, P., Maresca, M., Schuller, S., Phillips, A.D., and Kenny, B. (2006). Potent diarrheagenic mechanism mediated by the cooperative action of three enteropathogenic Escherichia coli-injected effector proteins. Proceedings of the National Academy of Sciences of the United States of America *103*, 1876-1881.

Demchenko, Y.N., Glebov, O.K., Zingone, A., Keats, J.J., Bergsagel, P.L., and Kuehl, W.M. (2010). Classical and/or alternative NF-kappaB pathway activation in multiple myeloma. Blood *115*, 3541-3552.

Deng, W., Puente, J.L., Gruenheid, S., Li, Y., Vallance, B.A., Vazquez, A., Barba, J., Ibarra, J.A., O'Donnell, P., Metalnikov, P.*, et al.* (2004). Dissecting virulence: systematic and functional analyses of a pathogenicity island. Proceedings of the National Academy of Sciences of the United States of America *101*, 3597-3602.

Deng, W., Vallance, B.A., Li, Y., Puente, J.L., and Finlay, B.B. (2003). Citrobacter rodentium translocated intimin receptor (Tir) is an essential virulence factor needed for actin condensation, intestinal colonization and colonic hyperplasia in mice. Molecular microbiology *48*, 95-115.

Dennis, A., Kudo, T., Kruidenier, L., Girard, F., Crepin, V.F., MacDonald, T.T., Frankel, G., and Wiles, S. (2008). The p50 subunit of NF-kappaB is critical for in vivo clearance of the noninvasive enteric pathogen Citrobacter rodentium. Infection and immunity *76*, 4978-4988.

DeVinney, R., Gauthier, A., Abe, A., and Finlay, B.B. (1999a). Enteropathogenic Escherichia coli: a pathogen that inserts its own receptor into host cells. Cellular and molecular life sciences : CMLS *55*, 961-976.

DeVinney, R., Stein, M., Reinscheid, D., Abe, A., Ruschkowski, S., and Finlay, B.B. (1999b). Enterohemorrhagic Escherichia coli O157:H7 produces Tir, which is translocated to the host cell membrane but is not tyrosine phosphorylated. Infection and immunity *67*, 2389-2398.

Dong, N., Liu, L., and Shao, F. (2010). A bacterial effector targets host DH-PH domain RhoGEFs and antagonizes macrophage phagocytosis. The EMBO journal *29*, 1363-1376.

Donnenberg, M.S., and Kaper, J.B. (1991). Construction of an eae deletion mutant of enteropathogenic Escherichia coli by using a positive-selection suicide vector. Infect Immun *59*, 4310-4317.

Donnenberg, M.S., Kaper, J.B., and Finlay, B.B. (1997). Interactions between enteropathogenic Escherichia coli and host epithelial cells. Trends in microbiology *5*, 109-114.

Donnenberg, M.S., Tzipori, S., McKee, M.L., O'Brien, A.D., Alroy, J., and Kaper, J.B. (1993). The role of the eae gene of enterohemorrhagic Escherichia coli in intimate attachment in vitro and in a porcine model. The Journal of clinical investigation *92*, 1418-1424.

Donowitz, M., Cha, B., Zachos, N.C., Brett, C.L., Sharma, A., Tse, C.M., and Li, X. (2005). NHERF family and NHE3 regulation. The Journal of physiology *567*, 3-11.

Ea, C.K., and Baltimore, D. (2009). Regulation of NF-kappaB activity through lysine monomethylation of p65. Proceedings of the National Academy of Sciences of the United States of America *106*, 18972-18977.

Echtenkamp, F., Deng, W., Wickham, M.E., Vazquez, A., Puente, J.L., Thanabalasuriar, A., Gruenheid, S., Finlay, B.B., and Hardwidge, P.R. (2008). Characterization of the NleF effector protein from attaching and effacing bacterial pathogens. FEMS microbiology letters *281*, 98-107.

Egan, L.J., Eckmann, L., Greten, F.R., Chae, S., Li, Z.W., Myhre, G.M., Robine, S., Karin, M., and Kagnoff, M.F. (2004). IkappaB-kinasebeta-dependent NF-kappaB activation provides

radioprotection to the intestinal epithelium. Proceedings of the National Academy of Sciences of the United States of America *101*, 2452-2457.

Erhardt, M., Namba, K., and Hughes, K.T. (2010). Bacterial nanomachines: the flagellum and type III injectisome. Cold Spring Harbor perspectives in biology *2*, a000299.

Fagerlund, R., Kinnunen, L., Kohler, M., Julkunen, I., and Melen, K. (2005). NF-{kappa}B is transported into the nucleus by importin {alpha}3 and importin {alpha}4. The Journal of biological chemistry *280*, 15942-15951.

Fagerlund, R., Melen, K., Cao, X., and Julkunen, I. (2008). NF-kappaB p52, RelB and c-Rel are transported into the nucleus via a subset of importin alpha molecules. Cellular signalling *20*, 1442-1451.

Finlay, B.B., Rosenshine, I., Donnenberg, M.S., and Kaper, J.B. (1992). Cytoskeletal composition of attaching and effacing lesions associated with enteropathogenic Escherichia coli adherence to HeLa cells. Infection and immunity *60*, 2541-2543.

Fitzgerald, K.A., McWhirter, S.M., Faia, K.L., Rowe, D.C., Latz, E., Golenbock, D.T., Coyle, A.J., Liao, S.M., and Maniatis, T. (2003). IKKepsilon and TBK1 are essential components of the IRF3 signaling pathway. Nature immunology *4*, 491-496.

Francis, D.H., Moxley, R.A., and Andraos, C.Y. (1989). Edema disease-like brain lesions in gnotobiotic piglets infected with Escherichia coli serotype O157:H7. Infection and immunity *57*, 1339-1342.

Gao, X., Wan, F., Mateo, K., Callegari, E., Wang, D., Deng, W., Puente, J., Li, F., Chaussee, M.S., Finlay, B.B.*, et al.* (2009). Bacterial effector binding to ribosomal protein s3 subverts NF-kappaB function. PLoS pathogens *5*, e1000708.

Garcia-Angulo, V.A., Deng, W., Thomas, N.A., Finlay, B.B., and Puente, J.L. (2008). Regulation of expression and secretion of NleH, a new non-locus of enterocyte effacement-encoded effector in Citrobacter rodentium. Journal of bacteriology *190*, 2388-2399.

Garmendia, J., Frankel, G., and Crepin, V.F. (2005). Enteropathogenic and enterohemorrhagic Escherichia coli infections: translocation, translocation, translocation. Infection and immunity *73*, 2573-2585.

Gauthier, A., Puente, J.L., and Finlay, B.B. (2003). Secretin of the enteropathogenic Escherichia coli type III secretion system requires components of the type III apparatus for assembly and localization. Infect Immun *71*, 3310-3319.

Ghosh, S., and Karin, M. (2002). Missing pieces in the NF-kappaB puzzle. Cell *109 Suppl*, S81-96.

Ghosh, S., May, M.J., and Kopp, E.B. (1998). NF-kappa B and Rel proteins: evolutionarily conserved mediators of immune responses. Annual review of immunology *16*, 225-260.

Gilmore, T.D. (2006). Introduction to NF-kappaB: players, pathways, perspectives. Oncogene *25*, 6680-6684.

Gohda, J., Matsumura, T., and Inoue, J. (2004). Cutting edge: TNFR-associated factor (TRAF) 6 is essential for MyD88-dependent pathway but not toll/IL-1 receptor domain-containing adaptor-inducing IFN-beta (TRIF)-dependent pathway in TLR signaling. J Immunol *173*, 2913-2917.

Griffin, F.M., Jr. (1981). Roles of macrophage Fc and C3b receptors in phagocytosis of immunologically coated Cryptococcus neoformans. Proceedings of the National Academy of Sciences of the United States of America *78*, 3853-3857.

Gruenheid, S., Sekirov, I., Thomas, N.A., Deng, W., O'Donnell, P., Goode, D., Li, Y., Frey, E.A., Brown, N.F., Metalnikov, P.*, et al.* (2004). Identification and characterization of NleA, a

non-LEE-encoded type III translocated virulence factor of enterohaemorrhagic Escherichia coli O157:H7. Molecular microbiology *51*, 1233-1249.

Guo, G., Wang, T., Gao, Q., Tamae, D., Wong, P., Chen, T., Chen, W.C., Shively, J.E., Wong, J.Y., and Li, J.J. (2004). Expression of ErbB2 enhances radiation-induced NF-kappaB activation. Oncogene *23*, 535-545.

Hacker, H., and Karin, M. (2006). Regulation and function of IKK and IKK-related kinases. Science's STKE : signal transduction knowledge environment *2006*, re13.

Hacker, J., Blum-Oehler, G., Muhldorfer, I., and Tschape, H. (1997). Pathogenicity islands of virulent bacteria: structure, function and impact on microbial evolution. Molecular microbiology *23*, 1089-1097.

Hagemann, T., Lawrence, T., McNeish, I., Charles, K.A., Kulbe, H., Thompson, R.G., Robinson, S.C., and Balkwill, F.R. (2008). "Re-educating" tumor-associated macrophages by targeting NF-kappaB. The Journal of experimental medicine *205*, 1261-1268.

Hara, M.R., Agrawal, N., Kim, S.F., Cascio, M.B., Fujimuro, M., Ozeki, Y., Takahashi, M., Cheah, J.H., Tankou, S.K., Hester, L.D.*, et al.* (2005). S-nitrosylated GAPDH initiates apoptotic cell death by nuclear translocation following Siah1 binding. Nature cell biology *7*, 665-674.

Hardwidge, P.R., Deng, W., Vallance, B.A., Rodriguez-Escudero, I., Cid, V.J., Molina, M., and Finlay, B.B. (2005). Modulation of host cytoskeleton function by the enteropathogenic Escherichia coli and Citrobacter rodentium effector protein EspG. Infection and immunity *73*, 2586-2594.

Hart, G.W., Housley, M.P., and Slawson, C. (2007). Cycling of O-linked beta-N-acetylglucosamine on nucleocytoplasmic proteins. Nature *446*, 1017-1022.

Hart, G.W., Slawson, C., Ramirez-Correa, G., and Lagerlof, O. (2011). Cross talk between O-GlcNAcylation and phosphorylation: roles in signaling, transcription, and chronic disease. Annual review of biochemistry *80*, 825-858.

Hauf, N., and Chakraborty, T. (2003). Suppression of NF-kappa B activation and proinflammatory cytokine expression by Shiga toxin-producing Escherichia coli. J Immunol *170*, 2074-2082.

Hayden, M.S., and Ghosh, S. (2008). Shared principles in NF-kappaB signaling. Cell *132*, 344-362.

Hegde, V., Wang, M., and Deutsch, W.A. (2004). Characterization of human ribosomal protein S3 binding to 7,8-dihydro-8-oxoguanine and abasic sites by surface plasmon resonance. DNA repair *3*, 121-126.

Hemrajani, C., Berger, C.N., Robinson, K.S., Marches, O., Mousnier, A., and Frankel, G. (2010). NleH effectors interact with Bax inhibitor-1 to block apoptosis during enteropathogenic Escherichia coli infection. Proceedings of the National Academy of Sciences of the United States of America *107*, 3129-3134.

Hemrajani, C., Marches, O., Wiles, S., Girard, F., Dennis, A., Dziva, F., Best, A., Phillips, A.D., Berger, C.N., Mousnier, A.*, et al.* (2008). Role of NleH, a type III secreted effector from attaching and effacing pathogens, in colonization of the bovine, ovine, and murine gut. Infection and immunity *76*, 4804-4813.

Hicks, S., Frankel, G., Kaper, J.B., Dougan, G., and Phillips, A.D. (1998). Role of intimin and bundle-forming pili in enteropathogenic Escherichia coli adhesion to pediatric intestinal tissue in vitro. Infection and immunity *66*, 1570-1578.

Holmes, A., Muhlen, S., Roe, A.J., and Dean, P. (2010). The EspF effector, a bacterial pathogen's Swiss army knife. Infection and immunity *78*, 4445-4453.

Hsu, H., Xiong, J., and Goeddel, D.V. (1995). The TNF receptor 1-associated protein TRADD signals cell death and NF-kappa B activation. Cell *81*, 495-504.

Hu, C.D., Chinenov, Y., and Kerppola, T.K. (2002). Visualization of interactions among bZIP and Rel family proteins in living cells using bimolecular fluorescence complementation. Molecular cell *9*, 789-798.

Hu, C.D., Grinberg, A.V., and Kerppola, T.K. (2005). Visualization of protein interactions in living cells using bimolecular fluorescence complementation (BiFC) analysis. Current protocols in protein science / editorial board, John E Coligan [et al] *Chapter 19*, Unit 19 10.

Hu, C.D., Grinberg, A.V., and Kerppola, T.K. (2006). Visualization of protein interactions in living cells using bimolecular fluorescence complementation (BiFC) analysis. Current protocols in cell biology / editorial board, Juan S Bonifacino [et al] *Chapter 21*, Unit 21 23.

Hu, C.D., and Kerppola, T.K. (2003). Simultaneous visualization of multiple protein interactions in living cells using multicolor fluorescence complementation analysis. Nature biotechnology *21*, 539-545.

Huang, D.B., Huxford, T., Chen, Y.Q., and Ghosh, G. (1997). The role of DNA in the mechanism of NFkappaB dimer formation: crystal structures of the dimerization domains of the p50 and p65 subunits. Structure *5*, 1427-1436.

Huang, D.B., Vu, D., and Ghosh, G. (2005). NF-kappaB RelB forms an intertwined homodimer. Structure *13*, 1365-1373.

Hueck, C.J. (1998). Type III protein secretion systems in bacterial pathogens of animals and plants. Microbiology and molecular biology reviews : MMBR *62*, 379-433.

Huguet, C., Crepieux, P., and Laudet, V. (1997). Rel/NF-kappa B transcription factors and I kappa B inhibitors: evolution from a unique common ancestor. Oncogene *15*, 2965-2974.

Hurley, B.P., Thorpe, C.M., and Acheson, D.W. (2001). Shiga toxin translocation across intestinal epithelial cells is enhanced by neutrophil transmigration. Infection and immunity *69*, 6148-6155.

Iguchi, A., Thomson, N.R., Ogura, Y., Saunders, D., Ooka, T., Henderson, I.R., Harris, D., Asadulghani, M., Kurokawa, K., Dean, P.*, et al.* (2009). Complete genome sequence and comparative genome analysis of enteropathogenic Escherichia coli O127:H6 strain E2348/69. Journal of bacteriology *191*, 347-354.

Iizumi, Y., Sagara, H., Kabe, Y., Azuma, M., Kume, K., Ogawa, M., Nagai, T., Gillespie, P.G., Sasakawa, C., and Handa, H. (2007). The enteropathogenic E. coli effector EspB facilitates microvillus effacing and antiphagocytosis by inhibiting myosin function. Cell host & microbe *2*, 383-392.

Israel, A. (2000). The IKK complex: an integrator of all signals that activate NF-kappaB? Trends in cell biology *10*, 129-133.

Jacobs, M.D., and Harrison, S.C. (1998). Structure of an IkappaBalpha/NF-kappaB complex. Cell *95*, 749-758.

Jang, C.Y., Lee, J.Y., and Kim, J. (2004). RpS3, a DNA repair endonuclease and ribosomal protein, is involved in apoptosis. FEBS letters *560*, 81-85.

Jerse, A.E., Yu, J., Tall, B.D., and Kaper, J.B. (1990). A genetic locus of enteropathogenic Escherichia coli necessary for the production of attaching and effacing lesions on tissue culture cells. Proceedings of the National Academy of Sciences of the United States of America *87*, 7839-7843.

Jiang, Y., Woronicz, J.D., Liu, W., and Goeddel, D.V. (1999). Prevention of constitutive TNF receptor 1 signaling by silencer of death domains. Science *283*, 543-546.

Johnson, T.J., and Nolan, L.K. (2009). Pathogenomics of the virulence plasmids of Escherichia coli. Microbiology and molecular biology reviews : MMBR *73*, 750-774.

Jones, R.M., Wu, H., Wentworth, C., Luo, L., Collier-Hyams, L., and Neish, A.S. (2008). Salmonella AvrA Coordinates Suppression of Host Immune and Apoptotic Defenses via JNK Pathway Blockade. Cell host & microbe *3*, 233-244.

Kabelitz, D., and Medzhitov, R. (2007). Innate immunity--cross-talk with adaptive immunity through pattern recognition receptors and cytokines. Current opinion in immunology *19*, 1-3.

Kaisho, T., and Akira, S. (2001). Dendritic-cell function in Toll-like receptor- and MyD88-knockout mice. Trends in immunology *22*, 78-83.

Kaper, J.B., Nataro, J.P., and Mobley, H.L. (2004). Pathogenic Escherichia coli. Nature reviews Microbiology *2*, 123-140.

Karin, M. (1999). How NF-kappaB is activated: the role of the IkappaB kinase (IKK) complex. Oncogene *18*, 6867-6874.

Karin, M., and Ben-Neriah, Y. (2000). Phosphorylation meets ubiquitination: the control of NF-[kappa]B activity. Annual review of immunology *18*, 621-663.

Karmali, M.A. (1989). Infection by verocytotoxin-producing Escherichia coli. Clinical microbiology reviews *2*, 15-38.

Kau, A.L., Ahern, P.P., Griffin, N.W., Goodman, A.L., and Gordon, J.I. (2011). Human nutrition, the gut microbiome and the immune system. Nature *474*, 327-336.

Kawauchi, K., Araki, K., Tobiume, K., and Tanaka, N. (2008). p53 regulates glucose metabolism through an IKK-NF-kappaB pathway and inhibits cell transformation. Nature cell biology *10*, 611-618.

Kawauchi, K., Araki, K., Tobiume, K., and Tanaka, N. (2009). Loss of p53 enhances catalytic activity of IKKbeta through O-linked beta-N-acetyl glucosamine modification. Proceedings of the National Academy of Sciences of the United States of America *106*, 3431-3436.

Kelly, C.P., and LaMont, J.T. (2008). Clostridium difficile--more difficult than ever. The New England journal of medicine *359*, 1932-1940.

Kelly, M., Hart, E., Mundy, R., Marches, O., Wiles, S., Badea, L., Luck, S., Tauschek, M., Frankel, G., Robins-Browne, R.M.*, et al.* (2006). Essential role of the type III secretion system effector NleB in colonization of mice by Citrobacter rodentium. Infection and immunity *74*, 2328-2337.

Kenny, B., DeVinney, R., Stein, M., Reinscheid, D.J., Frey, E.A., and Finlay, B.B. (1997). Enteropathogenic E. coli (EPEC) transfers its receptor for intimate adherence into mammalian cells. Cell *91*, 511-520.

Kenny, B., and Finlay, B.B. (1995). Protein secretion by enteropathogenic Escherichia coli is essential for transducing signals to epithelial cells. Proceedings of the National Academy of Sciences of the United States of America *92*, 7991-7995.

Kenny, B., and Jepson, M. (2000). Targeting of an enteropathogenic Escherichia coli (EPEC) effector protein to host mitochondria. Cellular microbiology *2*, 579-590.

Kenny, B., Lai, L.C., Finlay, B.B., and Donnenberg, M.S. (1996). EspA, a protein secreted by enteropathogenic Escherichia coli, is required to induce signals in epithelial cells. Molecular microbiology *20*, 313-323.

Kerppola, T.K. (2006). Visualization of molecular interactions by fluorescence complementation. Nature reviews Molecular cell biology *7*, 449-456.

Khan, M.A., Bouzari, S., Ma, C., Rosenberger, C.M., Bergstrom, K.S., Gibson, D.L., Steiner, T.S., and Vallance, B.A. (2008). Flagellin-dependent and -independent inflammatory responses following infection by enteropathogenic Escherichia coli and Citrobacter rodentium. Infection and immunity *76*, 1410-1422.

Khan, M.A., Ma, C., Knodler, L.A., Valdez, Y., Rosenberger, C.M., Deng, W., Finlay, B.B., and Vallance, B.A. (2006). Toll-like receptor 4 contributes to colitis development but not to host defense during Citrobacter rodentium infection in mice. Infection and immunity *74*, 2522-2536.

Kim, D.W., Lenzen, G., Page, A.L., Legrain, P., Sansonetti, P.J., and Parsot, C. (2005a). The Shigella flexneri effector OspG interferes with innate immune responses by targeting ubiquitin-conjugating enzymes. Proceedings of the National Academy of Sciences of the United States of America *102*, 14046-14051.

Kim, H.D., Lee, J.Y., and Kim, J. (2005b). Erk phosphorylates threonine 42 residue of ribosomal protein S3. Biochemical and biophysical research communications *333*, 110-115.

Kim, J., Chubatsu, L.S., Admon, A., Stahl, J., Fellous, R., and Linn, S. (1995). Implication of mammalian ribosomal protein S3 in the processing of DNA damage. The Journal of biological chemistry *270*, 13620-13629.

Kim, J., Thanabalasuriar, A., Chaworth-Musters, T., Fromme, J.C., Frey, E.A., Lario, P.I., Metalnikov, P., Rizg, K., Thomas, N.A., Lee, S.F*., et al.* (2007). The bacterial virulence factor NleA inhibits cellular protein secretion by disrupting mammalian COPII function. Cell host & microbe *2*, 160-171.

Kim, J.W., and Dang, C.V. (2005). Multifaceted roles of glycolytic enzymes. Trends in biochemical sciences *30*, 142-150.

Kim, T.S., Kim, H.D., and Kim, J. (2009). PKCdelta-dependent functional switch of rpS3 between translation and DNA repair. Biochimica et biophysica acta *1793*, 395-405.

Kimbrough, T.G., and Miller, S.I. (2002). Assembly of the type III secretion needle complex of Salmonella typhimurium. Microbes and infection / Institut Pasteur *4*, 75-82.

Knutton, S., Rosenshine, I., Pallen, M.J., Nisan, I., Neves, B.C., Bain, C., Wolff, C., Dougan, G., and Frankel, G. (1998). A novel EspA-associated surface organelle of enteropathogenic Escherichia coli involved in protein translocation into epithelial cells. The EMBO journal *17*, 2166-2176.

Kodama, T. (2002). [Mechanism of A/E lesion formation produced by enterohemorrhagic Escherichia coli: O157--role of EspB, Tir and cortactin]. Nihon rinsho Japanese journal of clinical medicine *60*, 1101-1107.

Kornberg, M.D., Sen, N., Hara, M.R., Juluri, K.R., Nguyen, J.V., Snowman, A.M., Law, L., Hester, L.D., and Snyder, S.H. (2010). GAPDH mediates nitrosylation of nuclear proteins. Nature cell biology *12*, 1094-1100.

Lai, L.C., Wainwright, L.A., Stone, K.D., and Donnenberg, M.S. (1997). A third secreted protein that is encoded by the enteropathogenic Escherichia coli pathogenicity island is required for transduction of signals and for attaching and effacing activities in host cells. Infection and immunity *65*, 2211-2217.

Law, D., and Kelly, J. (1995). Use of heme and hemoglobin by Escherichia coli O157 and other Shiga-like-toxin-producing E. coli serogroups. Infection and immunity *63*, 700-702.

Le Negrate, G., Faustin, B., Welsh, K., Loeffler, M., Krajewska, M., Hasegawa, P., Mukherjee, S., Orth, K., Krajewski, S., Godzik, A.*, et al.* (2008). Salmonella secreted factor L deubiquitinase of Salmonella typhimurium inhibits NF-kappaB, suppresses IkappaBalpha ubiquitination and modulates innate immune responses. J Immunol *180*, 5045-5056.

Leader, D.P. (1980). Phosphorylated and other modified forms of eukaryotic ribosomal protein S3 analysed by two-dimensional gel electrophoresis. The Biochemical journal *189*, 241-245.

Legarda-Addison, D., Hase, H., O'Donnell, M.A., and Ting, A.T. (2009). NEMO/IKKgamma regulates an early NF-kappaB-independent cell-death checkpoint during TNF signaling. Cell death and differentiation *16*, 1279-1288.

Lenardo, M.J., and Baltimore, D. (1989). NF-kappa B: a pleiotropic mediator of inducible and tissue-specific gene control. Cell *58*, 227-229.

Levine, M.M., Bergquist, E.J., Nalin, D.R., Waterman, D.H., Hornick, R.B., Young, C.R., and Sotman, S. (1978). Escherichia coli strains that cause diarrhoea but do not produce heat-labile or heat-stable enterotoxins and are non-invasive. Lancet *1*, 1119-1122.

Li, X., Yang, Y., and Ashwell, J.D. (2002). TNF-RII and c-IAP1 mediate ubiquitination and degradation of TRAF2. Nature *416*, 345-347.

Li, Z., and Nabel, G.J. (1997). A new member of the I kappaB protein family, I kappaB epsilon, inhibits RelA (p65)-mediated NF-kappaB transcription. Molecular and cellular biology *17*, 6184-6190.

Lindstrom, M.S. (2009). Emerging functions of ribosomal proteins in gene-specific transcription and translation. Biochemical and biophysical research communications *379*, 167-170.

Ling, H., Boodhoo, A., Hazes, B., Cummings, M.D., Armstrong, G.D., Brunton, J.L., and Read, R.J. (1998). Structure of the shiga-like toxin I B-pentamer complexed with an analogue of its receptor Gb3. Biochemistry *37*, 1777-1788.

Littman, D.R., and Pamer, E.G. (2011). Role of the commensal microbiota in normal and pathogenic host immune responses. Cell host & microbe *10*, 311-323.

Liu, J., and Mushegian, A. (2003). Three monophyletic superfamilies account for the majority of the known glycosyltransferases. Protein science : a publication of the Protein Society *12*, 1418-1431.

Louise, C.B., and Obrig, T.G. (1991). Shiga toxin-associated hemolytic-uremic syndrome: combined cytotoxic effects of Shiga toxin, interleukin-1 beta, and tumor necrosis factor alpha on human vascular endothelial cells in vitro. Infection and immunity *59*, 4173-4179.

Ma, W., Dong, F.F., Stavrinides, J., and Guttman, D.S. (2006). Type III effector diversification via both pathoadaptation and horizontal transfer in response to a coevolutionary arms race. PLoS genetics *2*, e209.

Malek, S., Huang, D.B., Huxford, T., Ghosh, S., and Ghosh, G. (2003). X-ray crystal structure of an IkappaBbeta x NF-kappaB p65 homodimer complex. The Journal of biological chemistry *278*, 23094-23100.

Marches, O., Covarelli, V., Dahan, S., Cougoule, C., Bhatta, P., Frankel, G., and Caron, E. (2008). EspJ of enteropathogenic and enterohaemorrhagic Escherichia coli inhibits opsono-phagocytosis. Cellular microbiology *10*, 1104-1115.

Marches, O., Ledger, T.N., Boury, M., Ohara, M., Tu, X., Goffaux, F., Mainil, J., Rosenshine, I., Sugai, M., De Rycke, J.*, et al.* (2003). Enteropathogenic and enterohaemorrhagic Escherichia

coli deliver a novel effector called Cif, which blocks cell cycle G2/M transition. Molecular microbiology *50*, 1553-1567.

Marches, O., Wiles, S., Dziva, F., La Ragione, R.M., Schuller, S., Best, A., Phillips, A.D., Hartland, E.L., Woodward, M.J., Stevens, M.P.*, et al.* (2005). Characterization of two non-locus of enterocyte effacement-encoded type III-translocated effectors, NleC and NleD, in attaching and effacing pathogens. Infection and immunity *73*, 8411-8417.

Martinez-Argudo, I., Sands, C., and Jepson, M.A. (2007). Translocation of enteropathogenic Escherichia coli across an in vitro M cell model is regulated by its type III secretion system. Cellular microbiology *9*, 1538-1546.

Martinez, E., Schroeder, G.N., Berger, C.N., Lee, S.F., Robinson, K.S., Badea, L., Simpson, N., Hall, R.A., Hartland, E.L., Crepin, V.F.*, et al.* (2010). Binding to Na(+) /H(+) exchanger regulatory factor 2 (NHERF2) affects trafficking and function of the enteropathogenic Escherichia coli type III secretion system effectors Map, EspI and NleH. Cellular microbiology *12*, 1718-1731.

Martone, R., Euskirchen, G., Bertone, P., Hartman, S., Royce, T.E., Luscombe, N.M., Rinn, J.L., Nelson, F.K., Miller, P., Gerstein, M.*, et al.* (2003). Distribution of NF-kappaB-binding sites across human chromosome 22. Proceedings of the National Academy of Sciences of the United States of America *100*, 12247-12252.

Mason, N., Aliberti, J., Caamano, J.C., Liou, H.C., and Hunter, C.A. (2002). Cutting edge: identification of c-Rel-dependent and -independent pathways of IL-12 production during infectious and inflammatory stimuli. J Immunol *168*, 2590-2594.

Matsuzawa, T., Kuwae, A., Yoshida, S., Sasakawa, C., and Abe, A. (2004). Enteropathogenic Escherichia coli activates the RhoA signaling pathway via the stimulation of GEF-H1. The EMBO journal *23*, 3570-3582.

McDaniel, T.K., Jarvis, K.G., Donnenberg, M.S., and Kaper, J.B. (1995). A genetic locus of enterocyte effacement conserved among diverse enterobacterial pathogens. Proceedings of the National Academy of Sciences of the United States of America *92*, 1664-1668.

McKee, M.L., and O'Brien, A.D. (1995). Investigation of enterohemorrhagic Escherichia coli O157:H7 adherence characteristics and invasion potential reveals a new attachment pattern shared by intestinal E. coli. Infection and immunity *63*, 2070-2074.

McWhirter, S.M., Fitzgerald, K.A., Rosains, J., Rowe, D.C., Golenbock, D.T., and Maniatis, T. (2004). IFN-regulatory factor 3-dependent gene expression is defective in Tbk1-deficient mouse embryonic fibroblasts. Proceedings of the National Academy of Sciences of the United States of America *101*, 233-238.

Medzhitov, R., and Janeway, C., Jr. (2000a). Innate immune recognition: mechanisms and pathways. Immunological reviews *173*, 89-97.

Medzhitov, R., and Janeway, C., Jr. (2000b). Innate immunity. The New England journal of medicine *343*, 338-344.

Meyers, K.E., and Kaplan, B.S. (2000). Many cell types are Shiga toxin targets. Kidney international *57*, 2650-2651.

Mise-Omata, S., Kuroda, E., Sugiura, T., Yamashita, U., Obata, Y., and Doi, T.S. (2009). The NF-kappaB RelA subunit confers resistance to Leishmania major by inducing nitric oxide synthase 2 and Fas expression but not Th1 differentiation. J Immunol *182*, 4910-4916.

Mookherjee, N., Lippert, D.N., Hamill, P., Falsafi, R., Nijnik, A., Kindrachuk, J., Pistolic, J., Gardy, J., Miri, P., Naseer, M.*, et al.* (2009). Intracellular receptor for human host defense peptide LL-37 in monocytes. J Immunol *183*, 2688-2696.

Morigasaki, S., Shimada, K., Ikner, A., Yanagida, M., and Shiozaki, K. (2008). Glycolytic enzyme GAPDH promotes peroxide stress signaling through multistep phosphorelay to a MAPK cascade. Molecular cell *30*, 108-113.

Mukaida, N., Okamoto, S., Ishikawa, Y., and Matsushima, K. (1994). Molecular mechanism of interleukin-8 gene expression. Journal of leukocyte biology *56*, 554-558.

Mukherjee, S., Keitany, G., Li, Y., Wang, Y., Ball, H.L., Goldsmith, E.J., and Orth, K. (2006). Yersinia YopJ acetylates and inhibits kinase activation by blocking phosphorylation. Science *312*, 1211-1214.

Mundy, R., MacDonald, T.T., Dougan, G., Frankel, G., and Wiles, S. (2005). Citrobacter rodentium of mice and man. Cellular microbiology *7*, 1697-1706.

Nadler, C., Baruch, K., Kobi, S., Mills, E., Haviv, G., Farago, M., Alkalay, I., Bartfeld, S., Meyer, T.F., Ben-Neriah, Y.*, et al.* (2010). The type III secretion effector NleE inhibits NF-kappaB activation. PLoS pathogens *6*, e1000743.

Nagai, T., Ibata, K., Park, E.S., Kubota, M., Mikoshiba, K., and Miyawaki, A. (2002). A variant of yellow fluorescent protein with fast and efficient maturation for cell-biological applications. Nat Biotechnol *20*, 87-90.

Nenci, A., Becker, C., Wullaert, A., Gareus, R., van Loo, G., Danese, S., Huth, M., Nikolaev, A., Neufert, C., Madison, B.*, et al.* (2007). Epithelial NEMO links innate immunity to chronic intestinal inflammation. Nature *446*, 557-561.

Newton, H.J., Pearson, J.S., Badea, L., Kelly, M., Lucas, M., Holloway, G., Wagstaff, K.M., Dunstone, M.A., Sloan, J., Whisstock, J.C.*, et al.* (2010). The type III effectors NleE and NleB from enteropathogenic E. coli and OspZ from Shigella block nuclear translocation of NF-kappaB p65. PLoS pathogens *6*, e1000898.

Ninomiya-Tsuji, J., Kishimoto, K., Hiyama, A., Inoue, J., Cao, Z., and Matsumoto, K. (1999). The kinase TAK1 can activate the NIK-I kappaB as well as the MAP kinase cascade in the IL-1 signalling pathway. Nature *398*, 252-256.

Nobe, R., Nougayrede, J.P., Taieb, F., Bardiau, M., Cassart, D., Navarro-Garcia, F., Mainil, J., Hayashi, T., and Oswald, E. (2009). Enterohaemorrhagic Escherichia coli serogroup O111 inhibits NF-(kappa)B-dependent innate responses in a manner independent of a type III secreted OspG orthologue. Microbiology *155*, 3214-3225.

O'Brien, A.D., Tesh, V.L., Donohue-Rolfe, A., Jackson, M.P., Olsnes, S., Sandvig, K., Lindberg, A.A., and Keusch, G.T. (1992). Shiga toxin: biochemistry, genetics, mode of action, and role in pathogenesis. Current topics in microbiology and immunology *180*, 65-94.

Ogura, Y., Ooka, T., Asadulghani, Terajima, J., Nougayrede, J.P., Kurokawa, K., Tashiro, K., Tobe, T., Nakayama, K., Kuhara, S.*, et al.* (2007). Extensive genomic diversity and selective conservation of virulence-determinants in enterohemorrhagic Escherichia coli strains of O157 and non-O157 serotypes. Genome biology *8*, R138.

Orth, K., Palmer, L.E., Bao, Z.Q., Stewart, S., Rudolph, A.E., Bliska, J.B., and Dixon, J.E. (1999). Inhibition of the mitogen-activated protein kinase kinase superfamily by a Yersinia effector. Science *285*, 1920-1923.

Oswald, I.P. (2006). Role of intestinal epithelial cells in the innate immune defence of the pig intestine. Veterinary research *37*, 359-368.

Pahl, H.L. (1999). Activators and target genes of Rel/NF-kappaB transcription factors. Oncogene *18*, 6853-6866.

Papatheodorou, P., Domanska, G., Oxle, M., Mathieu, J., Selchow, O., Kenny, B., and Rassow, J. (2006). The enteropathogenic Escherichia coli (EPEC) Map effector is imported into the mitochondrial matrix by the TOM/Hsp70 system and alters organelle morphology. Cellular microbiology *8*, 677-689.

Park, J., Han, D., Kim, K., Kang, Y., and Kim, Y. (2009). O-GlcNAcylation disrupts glyceraldehyde-3-phosphate dehydrogenase homo-tetramer formation and mediates its nuclear translocation. Biochimica et biophysica acta *1794*, 254-262.

Pathak, S., Borodkin, V.S., Albarbarawi, O., Campbell, D.G., Ibrahim, A., and van Aalten, D.M. (2012). O-GlcNAcylation of TAB1 modulates TAK1-mediated cytokine release. The EMBO journal *31*, 1394-1404.

Pearson, J.S., Riedmaier, P., Marches, O., Frankel, G., and Hartland, E.L. (2011). A type III effector protease NleC from enteropathogenic Escherichia coli targets NF-kappaB for degradation. Molecular microbiology *80*, 219-230.

Phillips, N., Hayward, R.D., and Koronakis, V. (2004). Phosphorylation of the enteropathogenic E. coli receptor by the Src-family kinase c-Fyn triggers actin pedestal formation. Nature cell biology *6*, 618-625.

Pineda, G., Ea, C.K., and Chen, Z.J. (2007). Ubiquitination and TRAF signaling. Advances in experimental medicine and biology *597*, 80-92.

Polekhina, G., House, C.M., Traficante, N., Mackay, J.P., Relaix, F., Sassoon, D.A., Parker, M.W., and Bowtell, D.D. (2002). Siah ubiquitin ligase is structurally related to TRAF and modulates TNF-alpha signaling. Nature structural biology *9*, 68-75.

Pupo, G.M., Karaolis, D.K., Lan, R., and Reeves, P.R. (1997). Evolutionary relationships among pathogenic and nonpathogenic Escherichia coli strains inferred from multilocus enzyme electrophoresis and mdh sequence studies. Infection and immunity *65*, 2685-2692.

Quitard, S., Dean, P., Maresca, M., and Kenny, B. (2006). The enteropathogenic Escherichia coli EspF effector molecule inhibits PI-3 kinase-mediated uptake independently of mitochondrial targeting. Cellular microbiology *8*, 972-981.

Rahman, M.M., and McFadden, G. (2011). Modulation of NF-kappaB signalling by microbial pathogens. Nature reviews Microbiology *9*, 291-306.

Rasko, D.A., Rosovitz, M.J., Myers, G.S., Mongodin, E.F., Fricke, W.F., Gajer, P., Crabtree, J., Sebaihia, M., Thomson, N.R., Chaudhuri, R.*, et al.* (2008). The pangenome structure of Escherichia coli: comparative genomic analysis of E. coli commensal and pathogenic isolates. Journal of bacteriology *190*, 6881-6893.

Reber, L., Vermeulen, L., Haegeman, G., and Frossard, N. (2009). Ser276 phosphorylation of NF-kB p65 by MSK1 controls SCF expression in inflammation. PloS one *4*, e4393.

Reed, J.C., and Ely, K.R. (2002). Degrading liaisons: Siah structure revealed. Nature structural biology *9*, 8-10.

Relaix, F., Wei, X., Li, W., Pan, J., Lin, Y., Bowtell, D.D., Sassoon, D.A., and Wu, X. (2000). Pw1/Peg3 is a potential cell death mediator and cooperates with Siah1a in p53-mediated apoptosis. Proceedings of the National Academy of Sciences of the United States of America *97*, 2105-2110.

Relaix, F., Wei, X.J., Wu, X., and Sassoon, D.A. (1998). Peg3/Pw1 is an imprinted gene involved in the TNF-NFkappaB signal transduction pathway. Nature genetics *18*, 287-291.

Rickert, R.C., Jellusova, J., and Miletic, A.V. (2011). Signaling by the tumor necrosis factor receptor superfamily in B-cell biology and disease. Immunological reviews *244*, 115-133.

Robinson, K.S., Clements, A., Williams, A.C., Berger, C.N., and Frankel, G. (2011). Bax inhibitor 1 in apoptosis and disease. Oncogene *30*, 2391-2400.

Robinson, K.S., Mousnier, A., Hemrajani, C., Fairweather, N., Berger, C.N., and Frankel, G. (2010). The enteropathogenic Escherichia coli effector NleH inhibits apoptosis induced by Clostridium difficile toxin B. Microbiology *156*, 1815-1823.

Robson, W.L., Leung, A.K., and Montgomery, M.D. (1991). Causes of death in hemolytic uremic syndrome. Child nephrology and urology *11*, 228-233.

Rosqvist, R., Magnusson, K.E., and Wolf-Watz, H. (1994). Target cell contact triggers expression and polarized transfer of Yersinia YopE cytotoxin into mammalian cells. The EMBO journal *13*, 964-972.

Rothwarf, D.M., and Karin, M. (1999). The NF-kappa B activation pathway: a paradigm in information transfer from membrane to nucleus. Science's STKE : signal transduction knowledge environment *1999*, RE1.

Royan, S.V., Jones, R.M., Koutsouris, A., Roxas, J.L., Falzari, K., Weflen, A.W., Kim, A., Bellmeyer, A., Turner, J.R., Neish, A.S.*, et al.* (2010). Enteropathogenic E. coli non-LEE encoded effectors NleH1 and NleH2 attenuate NF-kappaB activation. Molecular microbiology *78*, 1232-1245.

Ruchaud-Sparagano, M.H., Maresca, M., and Kenny, B. (2007). Enteropathogenic Escherichia coli (EPEC) inactivate innate immune responses prior to compromising epithelial barrier function. Cellular microbiology *9*, 1909-1921.

Ruchaud-Sparagano, M.H., Muhlen, S., Dean, P., and Kenny, B. (2011). The enteropathogenic E. coli (EPEC) Tir effector inhibits NF-kappaB activity by targeting TNFalpha receptor-associated factors. PLoS pathogens *7*, e1002414.

Sadikot, R.T., Zeng, H., Joo, M., Everhart, M.B., Sherrill, T.P., Li, B., Cheng, D.S., Yull, F.E., Christman, J.W., and Blackwell, T.S. (2006). Targeted immunomodulation of the NF-kappaB pathway in airway epithelium impacts host defense against Pseudomonas aeruginosa. J Immunol *176*, 4923-4930.

Sallee, N.A., Rivera, G.M., Dueber, J.E., Vasilescu, D., Mullins, R.D., Mayer, B.J., and Lim, W.A. (2008). The pathogen protein EspF(U) hijacks actin polymerization using mimicry and multivalency. Nature *454*, 1005-1008.

Sandvig, K., Garred, O., Prydz, K., Kozlov, J.V., Hansen, S.H., and van Deurs, B. (1992). Retrograde transport of endocytosed Shiga toxin to the endoplasmic reticulum. Nature *358*, 510-512.

Sason, H., Milgrom, M., Weiss, A.M., Melamed-Book, N., Balla, T., Grinstein, S., Backert, S., Rosenshine, I., and Aroeti, B. (2009). Enteropathogenic Escherichia coli subverts phosphatidylinositol 4,5-bisphosphate and phosphatidylinositol 3,4,5-trisphosphate upon epithelial cell infection. Molecular biology of the cell *20*, 544-555.

Savkovic, S.D., Koutsouris, A., and Hecht, G. (1997). Activation of NF-kappaB in intestinal epithelial cells by enteropathogenic Escherichia coli. The American journal of physiology *273*, C1160-1167.

Saxena, S.K., O'Brien, A.D., and Ackerman, E.J. (1989). Shiga toxin, Shiga-like toxin II variant, and ricin are all single-site RNA N-glycosidases of 28 S RNA when microinjected into Xenopus oocytes. The Journal of biological chemistry *264*, 596-601.

Scheidereit, C. (2006). IkappaB kinase complexes: gateways to NF-kappaB activation and transcription. Oncogene *25*, 6685-6705.

Schmidt, H., Beutin, L., and Karch, H. (1995). Molecular analysis of the plasmid-encoded hemolysin of Escherichia coli O157:H7 strain EDL 933. Infection and immunity *63*, 1055-1061.

Schmidt, M.A. (2010). LEEways: tales of EPEC, ATEC and EHEC. Cellular microbiology *12*, 1544-1552.

Sears, C.L., and Kaper, J.B. (1996). Enteric bacterial toxins: mechanisms of action and linkage to intestinal secretion. Microbiological reviews *60*, 167-215.

Sekiya, K., Ohishi, M., Ogino, T., Tamano, K., Sasakawa, C., and Abe, A. (2001). Supermolecular structure of the enteropathogenic Escherichia coli type III secretion system and its direct interaction with the EspA-sheath-like structure. Proceedings of the National Academy of Sciences of the United States of America *98*, 11638-11643.

Selyunin, A.S., Sutton, S.E., Weigele, B.A., Reddick, L.E., Orchard, R.C., Bresson, S.M., Tomchick, D.R., and Alto, N.M. (2011). The assembly of a GTPase-kinase signalling complex by a bacterial catalytic scaffold. Nature *469*, 107-111.

Selzer, J., Hofmann, F., Rex, G., Wilm, M., Mann, M., Just, I., and Aktories, K. (1996). Clostridium novyi alpha-toxin-catalyzed incorporation of GlcNAc into Rho subfamily proteins. The Journal of biological chemistry *271*, 25173-25177.

Sen, R., and Baltimore, D. (1986). Multiple nuclear factors interact with the immunoglobulin enhancer sequences. Cell *46*, 705-716.

Sha, W.C., Liou, H.C., Tuomanen, E.I., and Baltimore, D. (1995). Targeted disruption of the p50 subunit of NF-kappa B leads to multifocal defects in immune responses. Cell *80*, 321-330.

Shames, S.R., Deng, W., Guttman, J.A., de Hoog, C.L., Li, Y., Hardwidge, P.R., Sham, H.P., Vallance, B.A., Foster, L.J., and Finlay, B.B. (2010). The pathogenic E. coli type III effector EspZ interacts with host CD98 and facilitates host cell prosurvival signalling. Cellular microbiology *12*, 1322-1339.

Shaul, J.D., Farina, A., and Huxford, T. (2008). The human IKKbeta subunit kinase domain displays CK2-like phosphorylation specificity. Biochemical and biophysical research communications *374*, 592-597.

Shi, C.S., and Kehrl, J.H. (2003). Tumor necrosis factor (TNF)-induced germinal center kinase-related (GCKR) and stress-activated protein kinase (SAPK) activation depends upon the E2/E3 complex Ubc13-Uev1A/TNF receptor-associated factor 2 (TRAF2). The Journal of biological chemistry *278*, 15429-15434.

Shin, H.S., Jang, C.Y., Kim, H.D., Kim, T.S., Kim, S., and Kim, J. (2009). Arginine methylation of ribosomal protein S3 affects ribosome assembly. Biochemical and biophysical research communications *385*, 273-278.

Sirover, M.A. (1999). New insights into an old protein: the functional diversity of mammalian glyceraldehyde-3-phosphate dehydrogenase. Biochimica et biophysica acta *1432*, 159-184.

Sirover, M.A. (2011). On the functional diversity of glyceraldehyde-3-phosphate dehydrogenase: biochemical mechanisms and regulatory control. Biochimica et biophysica acta *1810*, 741-751.

Spears, K.J., Roe, A.J., and Gally, D.L. (2006). A comparison of enteropathogenic and enterohaemorrhagic Escherichia coli pathogenesis. FEMS microbiology letters *255*, 187-202.

Stone, K.D., Zhang, H.Z., Carlson, L.K., and Donnenberg, M.S. (1996). A cluster of fourteen genes from enteropathogenic Escherichia coli is sufficient for the biogenesis of a type IV pilus. Molecular microbiology *20*, 325-337.

Stricklett, P.K., Hughes, A.K., Ergonul, Z., and Kohan, D.E. (2002). Molecular basis for up-regulation by inflammatory cytokines of Shiga toxin 1 cytotoxicity and globotriaosylceramide expression. The Journal of infectious diseases *186*, 976-982.

Sundararaj, K.P., Wood, R.E., Ponnusamy, S., Salas, A.M., Szulc, Z., Bielawska, A., Obeid, L.M., Hannun, Y.A., and Ogretmen, B. (2004). Rapid shortening of telomere length in response to ceramide involves the inhibition of telomere binding activity of nuclear glyceraldehyde-3-phosphate dehydrogenase. The Journal of biological chemistry *279*, 6152-6162.

Tajima, H., Tsuchiya, K., Yamada, M., Kondo, K., Katsube, N., and Ishitani, R. (1999). Over-expression of GAPDH induces apoptosis in COS-7 cells transfected with cloned GAPDH cDNAs. Neuroreport *10*, 2029-2033.

Tampakaki, A.P., Fadouloglou, V.E., Gazi, A.D., Panopoulos, N.J., and Kokkinidis, M. (2004). Conserved features of type III secretion. Cellular microbiology *6*, 805-816.

Tarze, A., Deniaud, A., Le Bras, M., Maillier, E., Molle, D., Larochette, N., Zamzami, N., Jan, G., Kroemer, G., and Brenner, C. (2007). GAPDH, a novel regulator of the pro-apoptotic mitochondrial membrane permeabilization. Oncogene *26*, 2606-2620.

Taylor, K.A., O'Connell, C.B., Luther, P.W., and Donnenberg, M.S. (1998). The EspB protein of enteropathogenic Escherichia coli is targeted to the cytoplasm of infected HeLa cells. Infection and immunity *66*, 5501-5507.

Tobe, T., Beatson, S.A., Taniguchi, H., Abe, H., Bailey, C.M., Fivian, A., Younis, R., Matthews, S., Marches, O., Frankel, G.*, et al.* (2006). An extensive repertoire of type III secretion effectors in Escherichia coli O157 and the role of lambdoid phages in their dissemination. Proceedings of the National Academy of Sciences of the United States of America *103*, 14941-14946.

Tobe, T., Hayashi, T., Han, C.G., Schoolnik, G.K., Ohtsubo, E., and Sasakawa, C. (1999). Complete DNA sequence and structural analysis of the enteropathogenic Escherichia coli adherence factor plasmid. Infection and immunity *67*, 5455-5462.

Tristan, C., Shahani, N., Sedlak, T.W., and Sawa, A. (2011). The diverse functions of GAPDH: views from different subcellular compartments. Cellular signalling *23*, 317-323.

Trosky, J.E., Li, Y., Mukherjee, S., Keitany, G., Ball, H., and Orth, K. (2007). VopA inhibits ATP binding by acetylating the catalytic loop of MAPK kinases. The Journal of biological chemistry *282*, 34299-34305.

Vallabhapurapu, S., and Karin, M. (2009). Regulation and function of NF-kappaB transcription factors in the immune system. Annual review of immunology *27*, 693-733.

Vallance, B.A., Deng, W., De Grado, M., Chan, C., Jacobson, K., and Finlay, B.B. (2002). Modulation of inducible nitric oxide synthase expression by the attaching and effacing bacterial pathogen citrobacter rodentium in infected mice. Infection and immunity *70*, 6424-6435.

Vermeulen, L., De Wilde, G., Van Damme, P., Vanden Berghe, W., and Haegeman, G. (2003). Transcriptional activation of the NF-kappaB p65 subunit by mitogen- and stress-activated protein kinase-1 (MSK1). The EMBO journal *22*, 1313-1324.

Vossenkamper, A., Marches, O., Fairclough, P.D., Warnes, G., Stagg, A.J., Lindsay, J.O., Evans, P.C., Luong le, A., Croft, N.M., Naik, S.*, et al.* (2010). Inhibition of NF-kappaB signaling in human dendritic cells by the enteropathogenic Escherichia coli effector protein NleE. J Immunol *185*, 4118-4127.

Wachter, C., Beinke, C., Mattes, M., and Schmidt, M.A. (1999). Insertion of EspD into epithelial target cell membranes by infecting enteropathogenic Escherichia coli. Molecular microbiology *31*, 1695-1707.

Wan, F., Anderson, D.E., Barnitz, R.A., Snow, A., Bidere, N., Zheng, L., Hegde, V., Lam, L.T., Staudt, L.M., Levens, D.*, et al.* (2007). Ribosomal protein S3: a KH domain subunit in NF-kappaB complexes that mediates selective gene regulation. Cell *131*, 927-939.

Wan, F., and Lenardo, M.J. (2009). Specification of DNA binding activity of NF-kappaB proteins. Cold Spring Harbor perspectives in biology *1*, a000067.

Wan, F., and Lenardo, M.J. (2010). The nuclear signaling of NF-kappaB: current knowledge, new insights, and future perspectives. Cell research *20*, 24-33.

Wan, F., Weaver, A., Gao, X., Bern, M., Hardwidge, P.R., and Lenardo, M.J. (2011). IKKbeta phosphorylation regulates RPS3 nuclear translocation and NF-kappaB function during infection with Escherichia coli strain O157:H7. Nature immunology *12*, 335-343.

Wang, C., Deng, L., Hong, M., Akkaraju, G.R., Inoue, J., and Chen, Z.J. (2001). TAK1 is a ubiquitin-dependent kinase of MKK and IKK. Nature *412*, 346-351.

Wang, D., Westerheide, S.D., Hanson, J.L., and Baldwin, A.S., Jr. (2000). Tumor necrosis factor alpha-induced phosphorylation of RelA/p65 on Ser529 is controlled by casein kinase II. The Journal of biological chemistry *275*, 32592-32597.

Wang, J., An, H., Mayo, M.W., Baldwin, A.S., and Yarbrough, W.G. (2007). LZAP, a putative tumor suppressor, selectively inhibits NF-kappaB. Cancer cell *12*, 239-251.

Wanzel, M., Russ, A.C., Kleine-Kohlbrecher, D., Colombo, E., Pelicci, P.G., and Eilers, M. (2008). A ribosomal protein L23-nucleophosmin circuit coordinates Mizl function with cell growth. Nature cell biology *10*, 1051-1061.

Warner, J.R., and McIntosh, K.B. (2009). How common are extraribosomal functions of ribosomal proteins? Molecular cell *34*, 3-11.

Wegener, E., Oeckinghaus, A., Papadopoulou, N., Lavitas, L., Schmidt-Supprian, M., Ferch, U., Mak, T.W., Ruland, J., Heissmeyer, V., and Krappmann, D. (2006). Essential role for IkappaB kinase beta in remodeling Carma1-Bcl10-Malt1 complexes upon T cell activation. Molecular cell *23*, 13-23.

Weih, F., Carrasco, D., Durham, S.K., Barton, D.S., Rizzo, C.A., Ryseck, R.P., Lira, S.A., and Bravo, R. (1995). Multiorgan inflammation and hematopoietic abnormalities in mice with a targeted disruption of RelB, a member of the NF-kappa B/Rel family. Cell *80*, 331-340.

Welch, R.A. (1991). Pore-forming cytolysins of gram-negative bacteria. Molecular microbiology *5*, 521-528.

Wellen, K.E., and Thompson, C.B. (2012). A two-way street: reciprocal regulation of metabolism and signalling. Nature reviews Molecular cell biology *13*, 270-276.

Whiteside, S.T., Epinat, J.C., Rice, N.R., and Israel, A. (1997). I kappa B epsilon, a novel member of the I kappa B family, controls RelA and cRel NF-kappa B activity. The EMBO journal *16*, 1413-1426.

Wickham, M.E., Brown, N.F., Boyle, E.C., Coombes, B.K., and Finlay, B.B. (2007a). Virulence is positively selected by transmission success between mammalian hosts. Current biology : CB *17*, 783-788.

Wickham, M.E., Lupp, C., Mascarenhas, M., Vazquez, A., Coombes, B.K., Brown, N.F., Coburn, B.A., Deng, W., Puente, J.L., Karmali, M.A.*, et al.* (2006). Bacterial genetic determinants of non-O157 STEC outbreaks and hemolytic-uremic syndrome after infection. J Infect Dis *194*, 819-827.

Wickham, M.E., Lupp, C., Vazquez, A., Mascarenhas, M., Coburn, B., Coombes, B.K., Karmali, M.A., Puente, J.L., Deng, W., and Brett Finlay, B. (2007b). Citrobacter rodentium virulence in

mice associates with bacterial load and the type III effector NleE. Microbes and infection / Institut Pasteur *9*, 400-407.

Wong, A.R., Pearson, J.S., Bright, M.D., Munera, D., Robinson, K.S., Lee, S.F., Frankel, G., and Hartland, E.L. (2011). Enteropathogenic and enterohaemorrhagic Escherichia coli: even more subversive elements. Molecular microbiology *80*, 1420-1438.

Wright, C.W., and Duckett, C.S. (2009). The aryl hydrocarbon nuclear translocator alters CD30-mediated NF-kappaB-dependent transcription. Science *323*, 251-255.

Xia, Z.P., Sun, L., Chen, X., Pineda, G., Jiang, X., Adhikari, A., Zeng, W., and Chen, Z.J. (2009). Direct activation of protein kinases by unanchored polyubiquitin chains. Nature *461*, 114-119.

Xu, L.G., Li, L.Y., and Shu, H.B. (2004). TRAF7 potentiates MEKK3-induced AP1 and CHOP activation and induces apoptosis. The Journal of biological chemistry *279*, 17278-17282.

Xu, M., Skaug, B., Zeng, W., and Chen, Z.J. (2009). A ubiquitin replacement strategy in human cells reveals distinct mechanisms of IKK activation by TNFalpha and IL-1beta. Molecular cell *36*, 302-314.

Yacoub, A., Augeri, L., Kelley, M.R., Doetsch, P.W., and Deutsch, W.A. (1996). A Drosophila ribosomal protein contains 8-oxoguanine and abasic site DNA repair activities. The EMBO journal *15*, 2306-2312.

Yadavilli, S., Hegde, V., and Deutsch, W.A. (2007). Translocation of human ribosomal protein S3 to sites of DNA damage is dependant on ERK-mediated phosphorylation following genotoxic stress. DNA repair *6*, 1453-1462.

Yamada, H., Mizuno, S., Reza-Gholizadeh, M., and Sugawara, I. (2001). Relative importance of NF-kappaB p50 in mycobacterial infection. Infection and immunity *69*, 7100-7105.

Yamamoto, M., Sato, S., Hemmi, H., Sanjo, H., Uematsu, S., Kaisho, T., Hoshino, K., Takeuchi, O., Kobayashi, M., Fujita, T.*, et al.* (2002). Essential role for TIRAP in activation of the signalling cascade shared by TLR2 and TLR4. Nature *420*, 324-329.

Yamamoto, T., Fujita, K., and Yokota, T. (1990). Adherence characteristics to human small intestinal mucosa of Escherichia coli isolated from patients with diarrhea or urinary tract infections. The Journal of infectious diseases *162*, 896-908.

Yang, W.H., Park, S.Y., Nam, H.W., Kim do, H., Kang, J.G., Kang, E.S., Kim, Y.S., Lee, H.C., Kim, K.S., and Cho, J.W. (2008). NFkappaB activation is associated with its O-GlcNAcylation state under hyperglycemic conditions. Proceedings of the National Academy of Sciences of the United States of America *105*, 17345-17350.

Yego, E.C., Vincent, J.A., Sarthy, V., Busik, J.V., and Mohr, S. (2009). Differential regulation of high glucose-induced glyceraldehyde-3-phosphate dehydrogenase nuclear accumulation in Muller cells by IL-1beta and IL-6. Investigative ophthalmology & visual science *50*, 1920-1928.

Yen, H., Ooka, T., Iguchi, A., Hayashi, T., Sugimoto, N., and Tobe, T. (2010). NleC, a type III secretion protease, compromises NF-kappaB activation by targeting p65/RelA. PLoS pathogens *6*, e1001231.

Yoshida, S., Handa, Y., Suzuki, T., Ogawa, M., Suzuki, M., Tamai, A., Abe, A., Katayama, E., and Sasakawa, C. (2006). Microtubule-severing activity of Shigella is pivotal for intercellular spreading. Science *314*, 985-989.

Yoshida, S., Katayama, E., Kuwae, A., Mimuro, H., Suzuki, T., and Sasakawa, C. (2002). Shigella deliver an effector protein to trigger host microtubule destabilization, which promotes Rac1 activity and efficient bacterial internalization. The EMBO journal *21*, 2923-2935.

Yu, M., Yeh, J., and Van Waes, C. (2006). Protein kinase casein kinase 2 mediates inhibitor-kappaB kinase and aberrant nuclear factor-kappaB activation by serum factor(s) in head and neck squamous carcinoma cells. Cancer research *66*, 6722-6731.

Yuhan, R., Koutsouris, A., Savkovic, S.D., and Hecht, G. (1997). Enteropathogenic Escherichia coli-induced myosin light chain phosphorylation alters intestinal epithelial permeability. Gastroenterology *113*, 1873-1882.

Zachara, N.E., and Hart, G.W. (2006). Cell signaling, the essential role of O-GlcNAc! Biochimica et biophysica acta *1761*, 599-617.

Zarivach, R., Vuckovic, M., Deng, W., Finlay, B.B., and Strynadka, N.C. (2007). Structural analysis of a prototypical ATPase from the type III secretion system. Nature structural & molecular biology *14*, 131-137.

Zhang, L., Ding, X., Cui, J., Xu, H., Chen, J., Gong, Y.N., Hu, L., Zhou, Y., Ge, J., Lu, Q.*, et al.* (2012). Cysteine methylation disrupts ubiquitin-chain sensing in NF-kappaB activation. Nature *481*, 204-208.

Zheng, Y., Lilo, S., Brodsky, I.E., Zhang, Y., Medzhitov, R., Marcu, K.B., and Bliska, J.B. (2011). A Yersinia effector with enhanced inhibitory activity on the NF-kappaB pathway activates the NLRP3/ASC/caspase-1 inflammasome in macrophages. PLoS pathogens *7*, e1002026.

Zhong, H., Voll, R.E., and Ghosh, S. (1998). Phosphorylation of NF-kappa B p65 by PKA stimulates transcriptional activity by promoting a novel bivalent interaction with the coactivator CBP/p300. Molecular cell *1*, 661-671.

Zhou, H., Monack, D.M., Kayagaki, N., Wertz, I., Yin, J., Wolf, B., and Dixit, V.M. (2005). Yersinia virulence factor YopJ acts as a deubiquitinase to inhibit NF-kappa B activation. The Journal of experimental medicine *202*, 1327-1332.

Zurawski, D.V., Mumy, K.L., Faherty, C.S., McCormick, B.A., and Maurelli, A.T. (2009). Shigella flexneri type III secretion system effectors OspB and OspF target the nucleus to downregulate the host inflammatory response via interactions with retinoblastoma protein. Molecular microbiology *71*, 350-368.